Computer Analysis of Foundations

Theory for the calculation of shallow foundations by *ELPLA*

Preface

The purpose of this text is to present the methods, equations, procedures, and techniques used in the formulation and development of the *ELPLA* function. It is of value to be familiar with this information when using the software.

An understanding of these concepts will be of great benefit in applying the software, resolving difficulties and judging the acceptability of the results.

Two familiar types of subsoil models are considered, *Winkler*'s model and Continuum model. In addition, the simple assumption model is also considered. The model assumes linear contact pressure on the base of the foundation.

Finite elements-method is used to analyze both of the raft and grid foundations (or the ribbed raft). In which plate bending elements represent the raft according to the two-dimensional nature of foundation, while grid elements represent the grid.

The development of the finite element equations for plate elements and grid elements is well documented in standard textbooks and consequently it is not duplicated in this User's Guide.

Contents

Page

Chapter 1

Mathematical Models

Contents

1.1   Symbols used in chapter 1

i Node number
k Field number
j Iteration cycle number
N_w Band width number of the matrix
N Sum of all vertical applied loads on the foundation [kN]
q_i Contact pressure at node i [kN/m^2]
x_i Coordinate of node i from the centroidal axis x [m]
y_i Coordinate of node i from the centroidal axis y [m]
A_f Foundation area [m²]
M_x Moment due to N about the x-axis [kN.m]
M_y Moment due to N about the y-axis [kN.m]
I_x Moment of inertia of the foundation about the x-axis [m^4]
I_y Moment of inertia of the foundation about the y-axis [m^4]
I_{xy} Product of inertia [m^4]
e_x Eccentricity measured from the centroidal axis x [m]
e_y Eccentricity measured from the centroidal axis y [m]
a_i Side of contact area around node i parallel to x-axis [m]
b_i Side of contact area around node i parallel to y-axis [m]
E_b Modulus of elasticity of the plate element [kN/m^2]
ν_b *Poisson*'s ratio of the plate element [1]
d Thickness of the plate element [m]
D Flexural rigidity of the plate element $D = E_b\ d^3/(12(1-\nu_b{}^2))$
Q_i Contact force at node i [kN]
$E_s{}^l$ Modulus of compressibility of the layer l [kN/m^2]
F^l Settlement coefficients f for the system of all layers until layer l, which have been
           replaced by a material from layer l
$f^{(l-1)}$ Settlement coefficients f for the system of all layers until layer l - 1, which have been
           replaced by a material from layer l
Δf^l Difference of settlement coefficients f^l - $f^{(l-1)}$
w_i Displacement at node i [m]
s_i Soil settlement at node i [m]
k_{si} Modulus of subgrade reaction at node i [kN/m^3]
k_i Spring stiffness (Modification of modulus of subgrade reaction by iteration) [kN/m]
$c_{k,i}$ Flexibility coefficient of point k due to a unit load at point i [m/kN]
w_o Rigid body translation of the raft w_o at the centroid [m]
s_{Wi} Settlement of point i due to load from 0 to q_v [m]
           with modulus of compressibility W_s (part of reloading)
s_{Ei} Settlement of point i due to load from q_v to q_o [m]
           with modulus of compressibility E_s (part of primary loading)
q_v Overburden pressure [kN/m^2]
H_{mi} Foundation level of raft i above the specified datum [m]
t_{fi} Foundation level of raft i from the ground surface [m]
z_{il} z-value of flexibility coefficient from the ground surface [m]
z_{ikl} z-value of flexibility coefficient of raft (or node) i due to load from raft (or node) k [m]
θ_{xi} Rotation of node i about the x-direction [Rad]
θ_{yi} Rotation of node i about the y-direction [Rad]

ε   Tolerance of accuracy [m]

θ_{xo} Rigid body rotation of the raf about the *x*-axis of geometry centroid [Rad]

θ_{yo} Rigid body rotation of the raft about the *y*-axis of geometry centroid [Rad]

$\{F\}$ Vector of total external forces due to applied loads and the soil reactions

$\{N\}$ Vector of the resultant force *N* and moments M_y and M_x

$\{P\}$ Vector of applied loads

$\{Q\}$ Vector of soil reactions

$\{Q_w\}$ Vector of groundwater forces

$\{s\}$ Vector of nodal settlements

$\{s_W\}$ Vector of settlements due to reloading

$\{s_E\}$ Vector of settlements due to primary loading

$\{s_T\}$ Vector of displacement due to temperature difference

$\{Q_E\}$ Vector of contact pressures for loading part

$\{Q_v\}$ Vector of contact pressures for reloading part

$\{Q_w\}$ Vector of water pressure forces

$[c]$ Flexibility matrix of the soil

$[k_s]$ Soil stiffness matrix

$[k_p]$ Plate stiffness matrix

$[k_g]$ Grid stiffness matrix

$[X]$ Vector of coordinates *x* and *y*

$[c_W]$ Flexibility matrix which is determined by modulus W_s

$[c_E]$ Flexibility matrix which is determined by modulus E_s

$[k_{s.E}]$ Soil stiffness matrix which is determined by modulus E_s

$[k_{s.w}]$ Soil stiffness matrix which is determined by modulus W_s

$\{\delta\}$ Nodal displacements of the foundation, each nodal displacement has deflection *w* and two rotations θ_x and θ_y about *x*- and *y*-axis, respectively

$\{\Delta\}$ Vector of translation w_o and rotations $\tan\theta_{xo}$ and $\tan\theta_{yo}$

1.2   Introduction

This chapter describes the most common practical models used in the analysis of foundations.

Foundation is the base of the structure that transmits its loads to the soil. It must include often considerable moments and forces. Although every structure is founded on soil, most of the practical analyses of the structure and its foundation do not take into account the influence of the subsoil behavior below or around the foundation.

In times, when there no computers were available, simplified methods were used considering as low as possible computation effort to receive the results with acceptable accuracy. In some publications, such as that of *Ohde* (1942), extensive and refined calculation methods were proposed and applied only for few cases in the practice.

The computers whose programming and memory possibilities are developed increasingly caused a revolution of the calculation practice. Now the programming and extensive computation effort can expand considerably to achieve the results as perfect as possible to the reality. These methods are considered particularly for the analysis of mostly deformation sensitive large structures.

By determination of contact pressures, internal forces and deformations of foundations, distinguishing between the calculation methods used in the analysis of strip foundations and those of rafts is important. Where by strip foundations a linear or uniform distribution of contact pressures in long direction may be assumed, while for rafts the contact pressures are examined in both directions.

Strip foundations may be analyzed using classical subsoil models. Such as *Winkler*'s model according to *Winkler* (1867), *Graßhoff* (1978) and *Wölfer* (1978) and Continuum model according to *Ohde* (1942), *Graßhoff* (1978) and *Kany* (1974). In addition, cases of small and irregular foundations can be analyzed by fewer extensive methods using tables and charts.

For determination of internal forces and deformations of rafts, Finite differences-method or Finite elements-method is applied. *Deninger* (1964) developed a computer program to determine the contact pressures and deformation of rectangular rafts on elastic layer using the Finite differences-method. The earliest application of the Finite elements-method for the investigation of the soil foundation interaction was that of *Cheung/ Zienkiewicz* (1965). These authors considered the analysis of rectangular plate resting on *Winkler*'s medium and on isotropic elastic half-space soil medium.

The subsoil models for analysis of foundations (standard models) can be divided into three main groups:

A   Simple assumption model
B   *Winkler*'s model
C   Continuum model

Simple assumption model does not consider the interaction between the foundation and the soil. The model assumes a linear distribution of contact pressures beneath the foundation. *Winkler*'s model is the oldest and simplest one that considers the interaction between the foundation and the soil. The model represents the soil as elastic springs. Continuum model is the complicated one. The model considers also the interaction between the foundation and soil. It represents the soil as a layered continuum medium or isotropic elastic half-space soil medium.

Although Continuum model provides a better physical representation of the supporting soil, it has remained unfamiliar, because of its mathematical difficulties where an application of this model requires extensive calculations. Practical application for this model is only possible if a computer program or appropriate tables or charts are available. For this aim *Wölfer* (1978), *Graßhoff* (1978), *Kany* (1974), *Sherif/ König* (1975), *Hahn* (1971) and *El Kadi* (1968) presented series of tables and charts that can be used for determining contact pressures, moments, shear forces and deflections, but using these tables and charts is limited to certain problems.

For this purpose, a general computerized mathematical solution based on Finite elements-method was developed to represent an analysis for foundations on the real subsoil model. The solution can analyze foundations of any shape considering holes within the foundation and the interaction of external foundations. This mathematical solution is coded in the program *ELPLA* (2001).

The developed computer program *ELPLA* also can analyze different types of subsoil models, especially the three dimensional Continuum model that considers any number of irregular layers.

Additionally, the program can be used to represent the effect of structural rigidity on the foundation-soil system and the influence of temperature change on the foundation.

In this book, the three standard soil models are described through nine different numerical calculation methods. The methods graduate from the simplest one to more complicated one covering the analysis of most common foundation problems that may be found in the practice.

1.3   Description of the numerical calculation methods

According to the three standard soil models (simple assumption model - *Winkler*'s model - Continuum model), nine numerical calculation methods are considered to analyze the raft as shown in Figure 1.1 and Table 1.1.

Table 1.1   Numerical calculation methods

Method No.	Method
1	Linear contact pressure (Simple assumption model)
2	Constant modulus of subgrade reaction (*Winkler*'s model)
3	Variable modulus of subgrade reaction (*Winkler*'s model)
4	Modification of modulus of subgrade reaction by iteration (*Winkler*'s model/ Continuum model)
5	Modulus of compressibility method for elastic raft on half-space soil medium (Isotropic elastic half-space soil medium - Continuum model)
6	Modulus of compressibility method for elastic raft on layered soil medium (Solving system of linear equations by iteration) (Layered soil medium - Continuum model)
7	Modulus of compressibility method for elastic raft on layered soil medium (Solving system of linear equations by elimination) (Layered soil medium - Continuum model)
8	Modulus of compressibility method for rigid raft on layered soil medium (Layered soil medium - Continuum model)
9	Modulus of compressibility method for flexible foundation on layered soil medium (Layered soil medium - Continuum model)
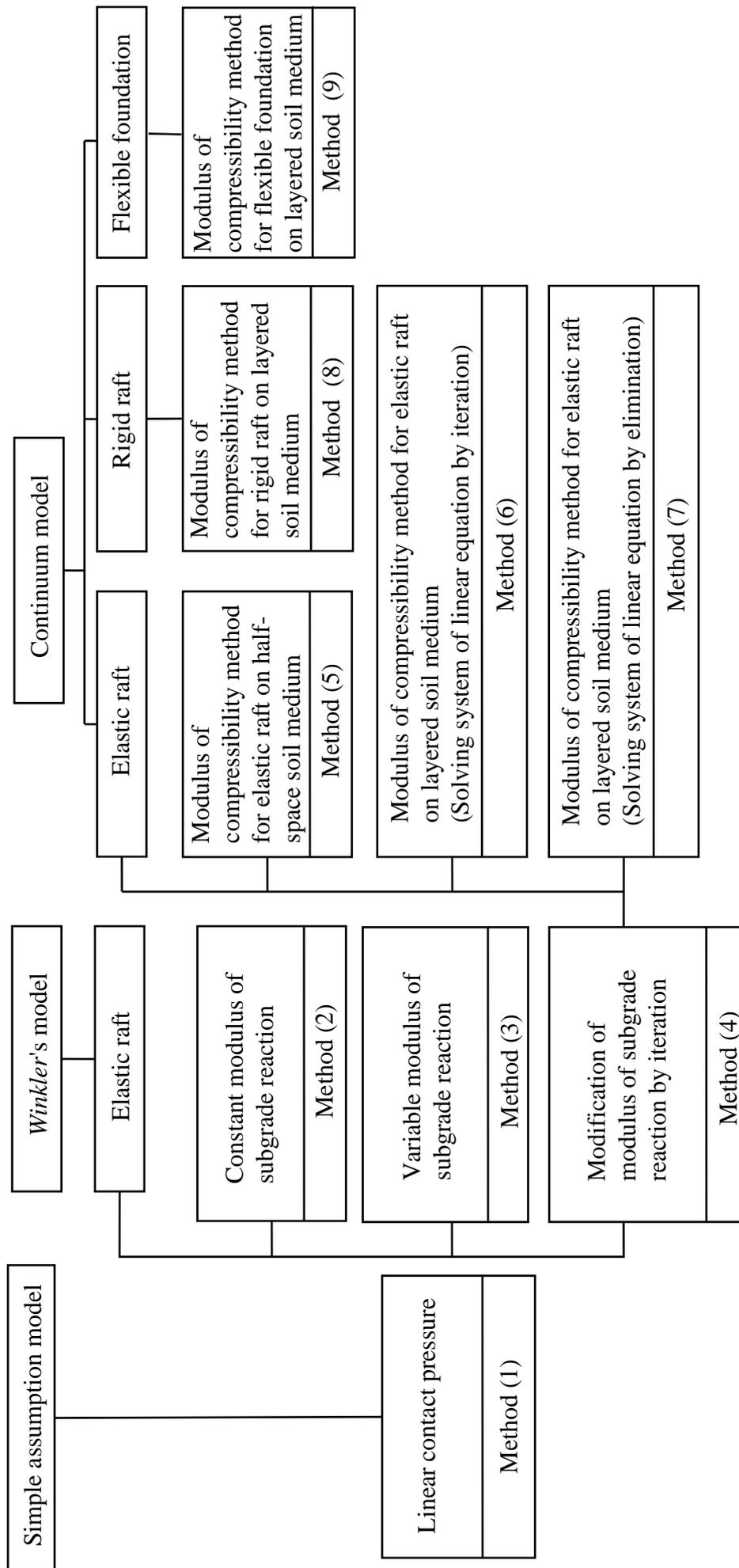
Figure 1.1   Numerical calculation methods of rafts (methods 1 - 9)

Today, The Finite elements-method is the most powerful procedure available in many complex problems. It can be applied to nearly all engineering problems, especially in structure analysis problems. In this book, the Finite elements-method is used to analyze the raft for all numerical calculation methods except Modulus of compressibility method for rigid raft on layered soil medium (method 8), which does not obey the elasticity rules. In the Finite elements-analysis, the raft is represented by rectangular plate bending elements according to the two dimensional nature of foundation. Grid elements are selected to represent the presence of ribs in the ribbed raft or grid foundations. Each node of plate or grid elements has three degrees of freedom, vertical displacement w and two rotations θ_x and θ_y about x- and y-axis, respectively. The development of the finite element equations is well documented in standard textbooks. Consequently, it is not duplicated in this book. The reader can see as an example that of *Zienkiewicz/ Cheung* (1970) or *Schwarz* (1984) for further information on the development of finite element equations.

To formulate the equations of the numerical calculation methods both the raft and the contact area of the supporting medium are divided into rectangular elements as shown in Figure 1.2. Compatibility between the raft and the soil medium in vertical direction is considered for all methods except Linear contact pressure method (method 1).

The fundamental formulation of equilibrium equation for the raft can be described in general form through the following Equation 1.1

$$[k_p]\{\delta\} = \{F\} \tag{1.1}$$

where the vector of forces $\{F\}$ contains the action and reaction forces acting on the raft. In principle for all calculation methods, the action forces are known and equal to the applied forces on the raft while the reaction forces (contact forces) are required to be found according to each soil model.

It is assumed that the contact pressure qi can be replaced by equivalent force Q_i at the various nodal points. The contact pressure around the node i is given by $q_i = Q_i/ (a_i \times b_i)$ over an appropriate area $a_i \times b_i$ corresponding to the nodal contact i. It should be noticed that the contact area contributing to the nodal reactive force is variable from a node to another according to its location. Figure 1.2 shows some examples for the different nodal areas (nodes 34, 36, 38, 39 and 61).

According to subsoil models (Simple assumption model - *Winkler*'s model - Continuum model), eight numerical calculation methods are considered to find the contact pressures q_i, and hence to analyze the raft. The next pages describe the interaction between the raft and subsoil medium in these methods.
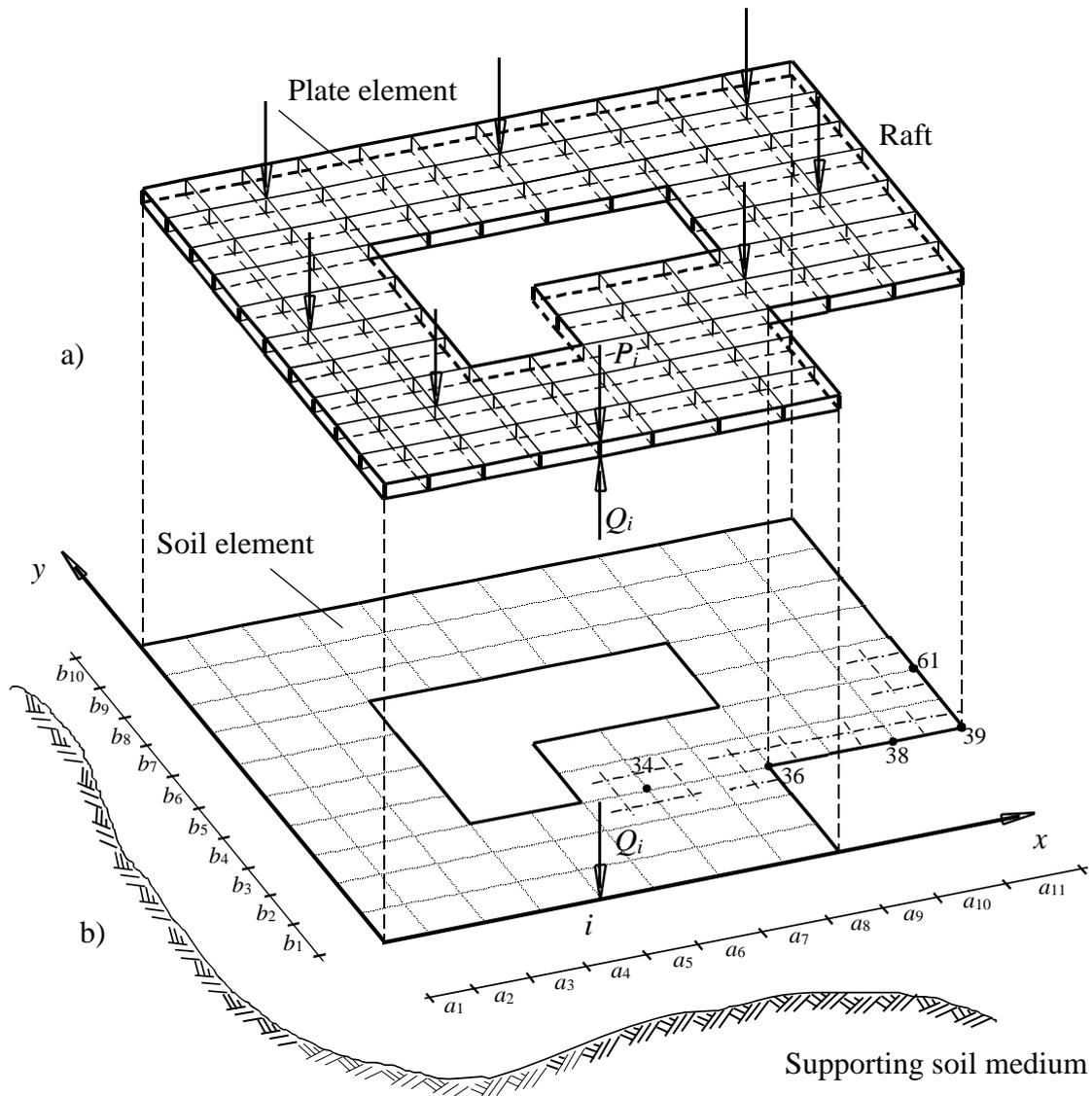
Figure 1.2   Nodal action between raft and soil
              a) Raft foundation
              b) Nodal action on soil

1.3.1   Linear contact pressure (method 1 - Simple assumption model)

This method is the simplest one for determination of the contact pressure distribution under foundations. The assumption of this method is that there is no compatibility between the foundation deflection and the soil settlement. In the method, it is assumed that the contact pressures are distributed linearly on the bottom of the foundations (statically determined) as shown in Figure 1.3, in which the resultant of soil reactions coincides with the resultant of applied loads.
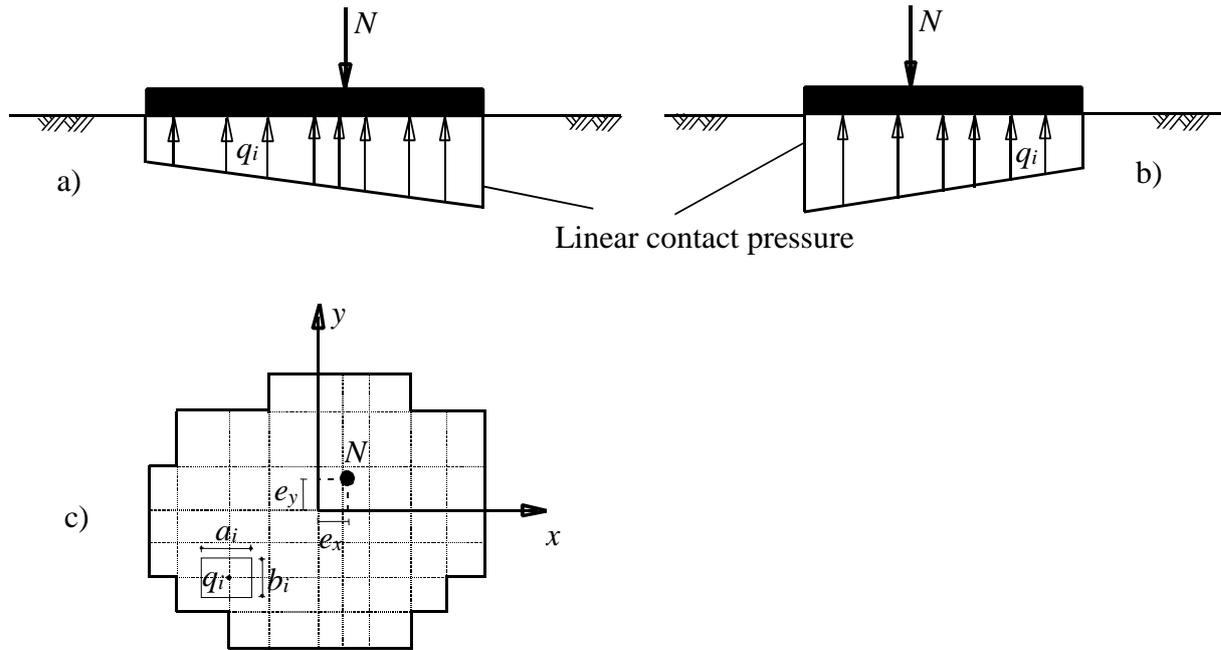
Figure 1.3   Contact pressure distribution for Simple assumption model
               a) Section parallel to x-direction
               b) Section parallel to y-direction
               c) Foundation plan

In the general case of a foundation with an arbitrary unsymmetrical shape and loading, based on *Navier*'s solution the contact pressure q_i at any point (x_i, y_i) from the geometry centroid on the bottom of the foundation is given by

$$q_i = \frac{N}{A_f} + \frac{M_y\,I_x - M_x\,I_{xy}}{I_x\,I_y - I_{xy}^{\,2}}\,x_i + \frac{M_x\,I_y - M_y\,I_{xy}}{I_x\,I_y - I_{xy}^{\,2}}\,y_i \qquad \text{[kN/m}^2\text{]} \quad (1.2)$$

For a foundation of rectangular shape, there are two axes of symmetry and $I_{xy} = 0$. Therefore, the contact pressure q_i of Equation 1.2 reduces to

$$q_i = \frac{N}{A_f} + \frac{M_y}{I_y}\,x_i + \frac{M_x}{I_x}\,y_i \qquad\qquad (1.3)$$

while for a foundation without moments or without eccentricity about both axes the contact pressure q_i will be uniform under the foundation and is given by

$$q_i = \frac{N}{A_f} \qquad\qquad (1.4)$$

System of equations of Linear contact pressure method

The foundation can be analyzed by working out the soil reactions at the different nodal points of the Finite elements-mesh. This is done by obtaining the contact pressure q_i from Equation 1.2. Then, the contact force Q_i at node i is given by

$$Q_i = q_i \, a_i \, b_i \tag{1.5}$$

Considering the entire foundation, the foundation will deflect under the action of the total external forces $\{F\}$ due to known applied loads $\{P\}$ and the known soil reactions $\{Q\}$, where

$$\{F\} = \{P\} - \{Q\} \tag{1.6}$$

The equilibrium of the system is expressed by the following matrix equation

$$\left[k_p\right] \{\delta\} = \{P\} - \{Q\} \tag{1.7}$$

Equation solver of Linear contact pressure method

As the plate stiffness matrix $[k_p]$ in Equation 1.7 is a diagonal matrix, the system of linear equations 1.7 is solved by Banded coefficients-technique. The unknown variables are the nodal displacements w_i and the nodal rotations θ_{xi} and θ_{yi} about the x- and y-directions.

1.3.2   Modulus of subgrade reaction (methods 2 and 3 - *Winkler*'s model)

The oldest method for the analysis of foundation on elastic medium is the modulus of subgrade reaction, which was proposed by *Winkler* (1867). The assumption of this method is that the soil model is represented by elastic springs as shown in Figure 1.4. The settlement s_i of the soil medium at any point i on the surface is directly proportional to the contact pressure q_i at that point and is mathematically expressed as

$$q_i = k_{si} \, s_i \tag{1.8}$$

The ratio between the contact pressure q_i [kN/m^2] and the corresponding settlement s_i [m] is termed the modulus of subgrade reaction k_{si} [kN/m^3].
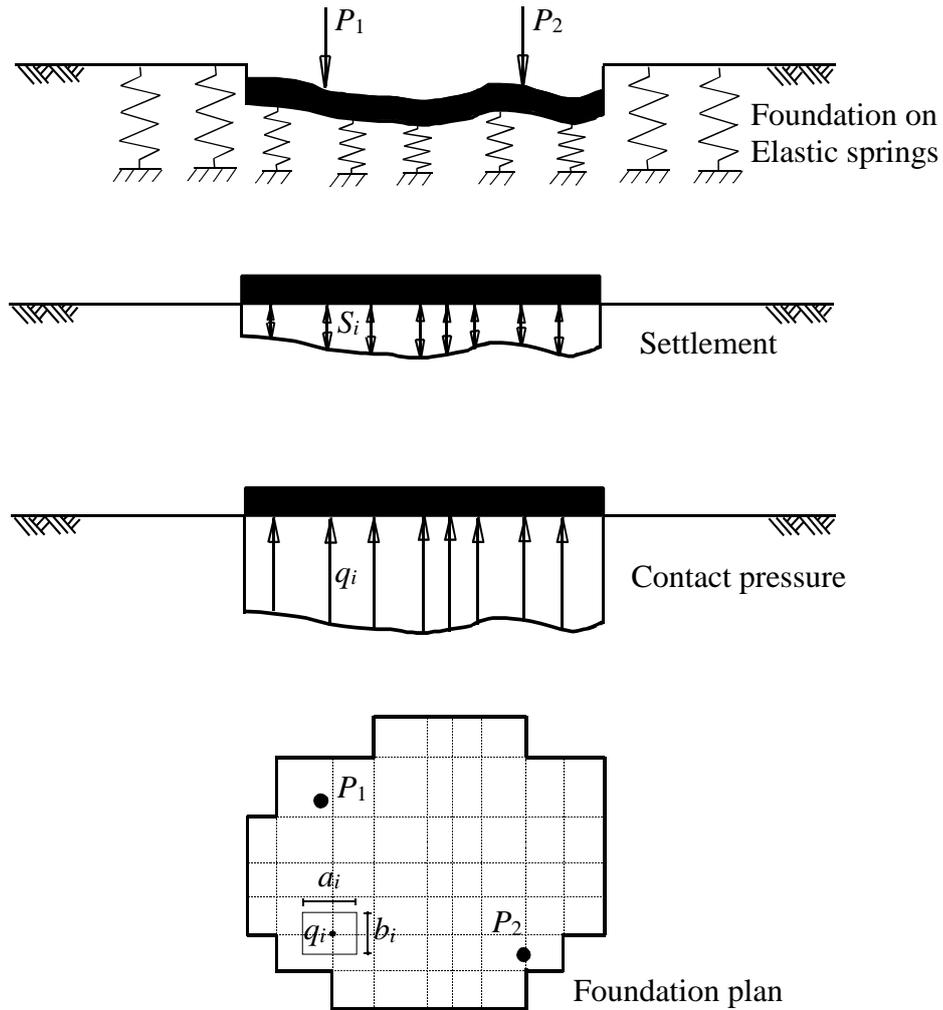
Figure 1.4   *Winkler*'s model

System of equations of Modulus of subgrade reaction

For a node i on the Finite elements-mesh, the contact force Q_i is given by

$$Q_i = a_i \, b_i \, k_{si} \, s_{i_i} \tag{1.9}$$

It should be noticed that k_{si} is the modulus of subgrade reaction at node i. It may be constant for the entire foundation (Constant modulus of subgrade reaction - method 1) or variable from a node to another (Variable modulus of subgrade reaction - method 2).

Considering the entire foundation, Equation 1.9 can be rewritten in matrix form as

$$\{Q\} = [k_s]\{s\} \tag{1.10}$$

Complete stiffness formulation of Modulus of subgrade reaction

The foundation will deflect under the action of the total external forces $\{F\}$ due to known applied loads $\{P\}$ and the unknown soil reactions $\{Q\}$, where

$$\{F\} = \{P\} - \{Q\} \tag{1.11}$$

The equilibrium of the raft-soil system is expressed by the following matrix equation

$$\left[k_p\right]\{\delta\} = \{P\} - \{Q\} \tag{1.12}$$

Considering the compatibility of deformation between the plate and the soil medium, where the soil settlement s_i equal to the plate deflection w_i, Equation 1.10 for *Winkler*'s model can be substituted into Equation 1.12 as

$$\left[\left[k_p\right] + \left[k_s\right]\right]\{\delta\} = \{P\} \tag{1.13}$$

Equation 1.13 shows that the stiffness matrix of the whole raft-soil system is the sum of the plate and the soil stiffness matrices, $[k_p] + [k_s]$.

Equation solver of Modulus of subgrade reaction

It should be noticed that the soil stiffness matrix $[k_s]$ is a purely diagonal matrix for *Winkler*'s model (methods 2 and 3). Therefore, the total stiffness matrix for the plate and the soil is a banded matrix. Then, the system of linear Equations 1.13 is solved by Banded coefficients-technique. Since the total stiffness matrix is a banded matrix, the Equation solver 1.12 takes short computation time by applying these methods 2 and 3.

The unknown variables in Equation 1.13 are the nodal displacements w_i ($w_i = s_i$) and the nodal rotations θ_{xi} and θ_{yi} about *x*- and *y*-directions. After solving the system of linear equation 1.13, substituting the obtained settlements s_i in Equation 1.10, gives the unknown contact forces Q_i.

1.3.3   Modification of modulus of subgrade reaction by iteration (method 4 - *Winkler*'s model/ Continuum model)

This method was proposed by *Ahrens/ Winselmann* (1984), which based on the soil, is represented by variable moduli of subgrade reactions similar to the Continuum model. In the method the raft and soil medium are treated separately, the results of one analysis forming the boundary conditions for the subsequent analysis as part of an iterative process. By modifying the variable moduli through the iterative process, the compatibility between the soil and raft interface is reached. The obtained results here are similar to those by Continuum model. The method is not only used for analysis of the foundations by Continuum model but also by modulus of subgrade reaction with variable moduli. The first iterative cycle gives an analysis for modulus of subgrade reaction with variable moduli. The results at any intermediate iteration cycle may be considered as acceptable results, which in fact lie between *Winkler*'s model with

variable moduli and Continuum model.
The iteration process of this method can be described as follows:

i)   First, uniform distribution of contact pressure $q^{(o)}$ on the bottom of the foundation is assumed as

$$q^{(o)} = \frac{N}{A_f} \tag{1.14}$$

ii)   For a set of grid points of Finite elements-mesh, the soil settlement s_i at point i due to contact forces in manner described later for Continuum model is obtained from

$$s_i^{(j)} = \sum_{i=1}^{n} c_{i,k}\, Q_k \tag{1.15}$$

iii)   The spring stiffness k_i from the soil settlement s_i and contact force Q_i is computed from

$$k_i^{(j)} = \frac{Q_i^{(j)}}{s_i^{(j)}} \tag{1.16}$$

iv)   The foundation is analyzed as plate on springs, the spring coefficients are used to generate the soil stiffness matrix $[k_s]$. This matrix will be a diagonal matrix. Therefore, adding the soil stiffness matrix $[k_s]$ to the plate stiffness matrix $[k_p]$ is easy. Then, the overall matrix for raft-soil system becomes a banded matrix. The entire system equation is expressed as

$$\left[\,[k_p] + [k_s]\,\right]\{\delta\} = \{P\} \tag{1.17}$$

v)   A set of nodal displacements $\{\delta\}$ is obtained by solving the system equation 1.17 using the Banded coefficients-technique

vi)   The soil settlements s_i are compared with the corresponding plate deflections w_i, which were computed from the system equation 1.17

$$\varepsilon = \left\| s_i - w_i \right\| \tag{1.18}$$

vii)   If the accuracy does not reach to a specified tolerance ε a new set of contact forces are obtained using

$$Q_i^{(j+1)} = k_i^{(j)}\, w_i^{(j)} \tag{1.19}$$

The steps ii to vii are repeated until the accuracy reaches to a specified tolerance ε, which means that sufficient compatibility between the plate deflections w_i and the soil settlements s_i is reached in the plate-soil interface. Figure 1.5 shows the iteration cycle of the iteration process.

A good advantage of this method is, that it can easily eliminate the contact pressure if negative pressure appeared or consider nonlinear soil response. By analysis both the raft and subsoil separately, some former restrictions on maximum problem size can be avoided. Particularly, the soil flexibility matrix no longer needs to be inverted as followed by classical analysis of Continuum model. Generally, computing and storing the soil flexibility matrix is necessary only once, at the beginning of the analysis. During the second and subsequent iteration cycles, soil settlements can be determined by multiplying the flexibility matrix by the vector of modified contact forces. Consequently, the maximum permissible number of nodes is greatly increased. It needs also less computation time than that of the elimination method used in the analysis of Continuum model.

P_1 P_2

Uniform contact pressure

$q^{(o)} = N/A_f$

$S_i^{(j)}$

Soil settlement
$s_i^{(j)} = \sum c_{i,k} Q_k^{(j)}$

P_1 P_2

$k_i^{(j)}$

System with springs
$k_i^{(j)} = Q_i^{(j)}/s_i^{(j)}$

$w_i^{(j)}$

Plate deflection w
$[[k_p] + [k_s]] \{\delta\} = \{P\}$

New contact forces
$Q_i^{(j+1)} = k_i^{(j)} w_i^{(j)}$

Contact pressure

$S_i^{(j)}$ $w_i^{(j)}$

Compare s with w
$\varepsilon = | s_i - w_i |$

No

Convergence reached
$w_i^{(j)} \approx s_i^{(j)}$

J = Iterative cycle No.

i = Node No.

Yes
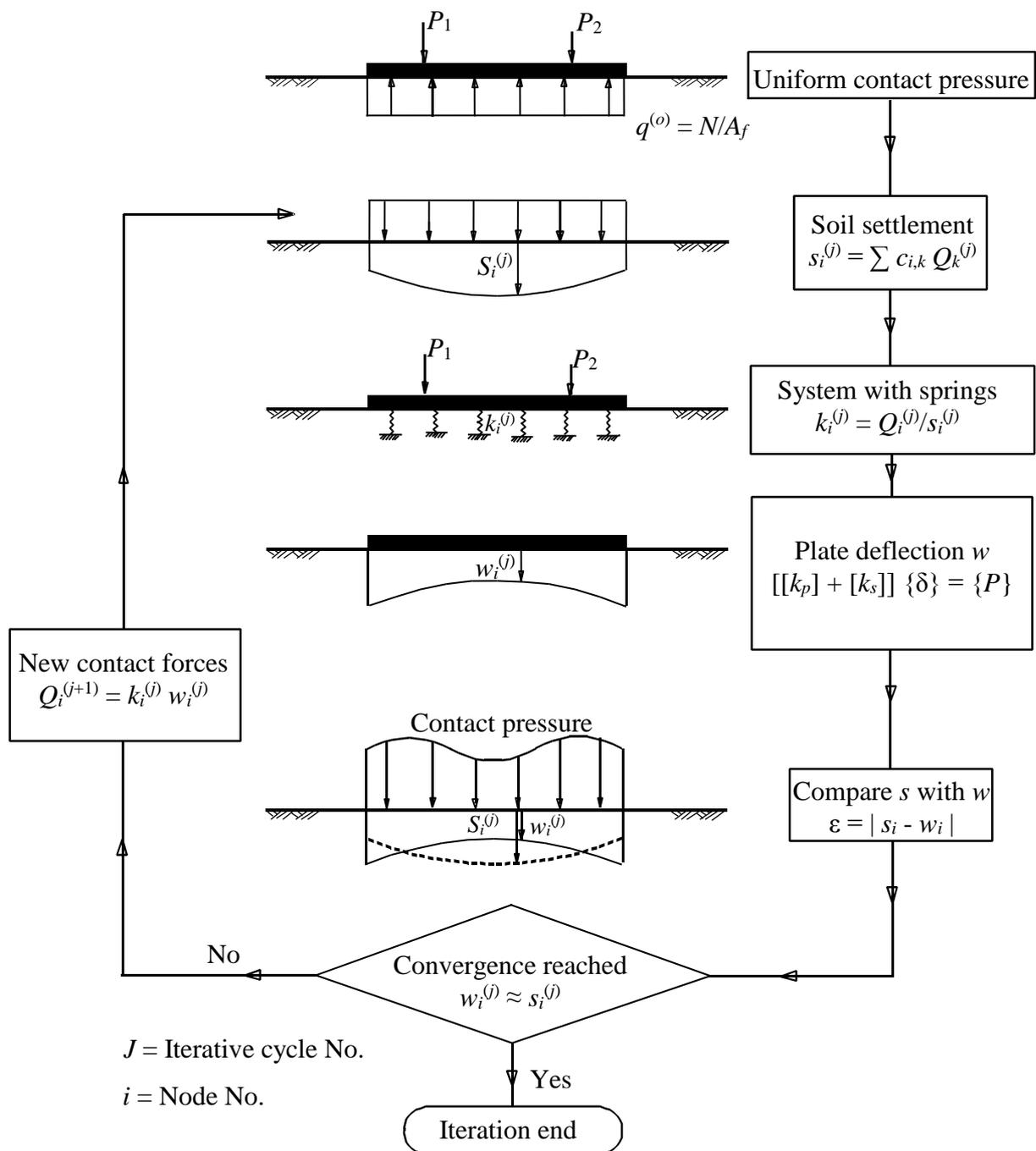
Iteration end

Figure 1.5   Iteration cycle of the iteration process

1.3.4   Modulus of compressibility method for elastic raft on half-space soil medium
(method 5 - Isotropic elastic half-space soil medium - Continuum model)

Continuum model was first proposed by *Ohde* (1942), which based on the settlement will occur not only under the loaded area but also outside (Figure 1.6). Otherwise, the settlement at any nodal point is affected by the forces at all the other nodal points.
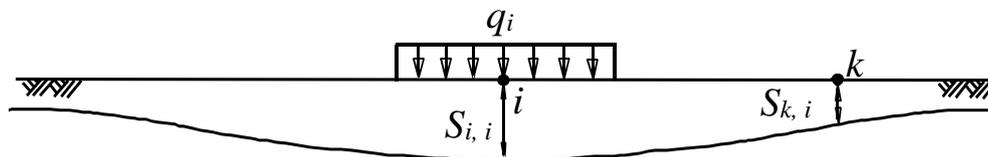
Influence line of elastic displacement

Figure 1.6   Continuum model

Continuum model assumes continuum behavior of the soil, where the soil is represented as isotropic elastic half-space medium or layered medium. Consequently, this model overcomes the assumption of *Winkler*'s model, which does not take into account the interaction between the different points of the soil medium. Representation of soil as a continuum medium is more accurate as it realizes the interaction among the different points of the continuum medium. However, it needs mathematical analysis that is more complex. The earliest application for rafts on continuum medium using Finite elements-method related to *Cheung/ Zienkiewicz* (1965). These authors considered the soil as isotropic elastic half-space medium.

The isotropic elastic half-space soil medium bases on *Boussinesq*'s solution (1885). The medium in this solution is semi-infinite homogeneous isotropic linear elastic solid subjected to a concentrated force. The force acts normal to the plane boundary at the surface. This basic solution can be used to obtain the surface settlement of isotropic elastic half-space soil medium subjected to a concentrated load acting on the ground surface.

Modulus of compressibility method for elastic raft on half-space soil medium (method 5), which is described here, considers the interaction between the raft and soil. It represents the soil as isotropic elastic half-space medium (Figure 1.7).
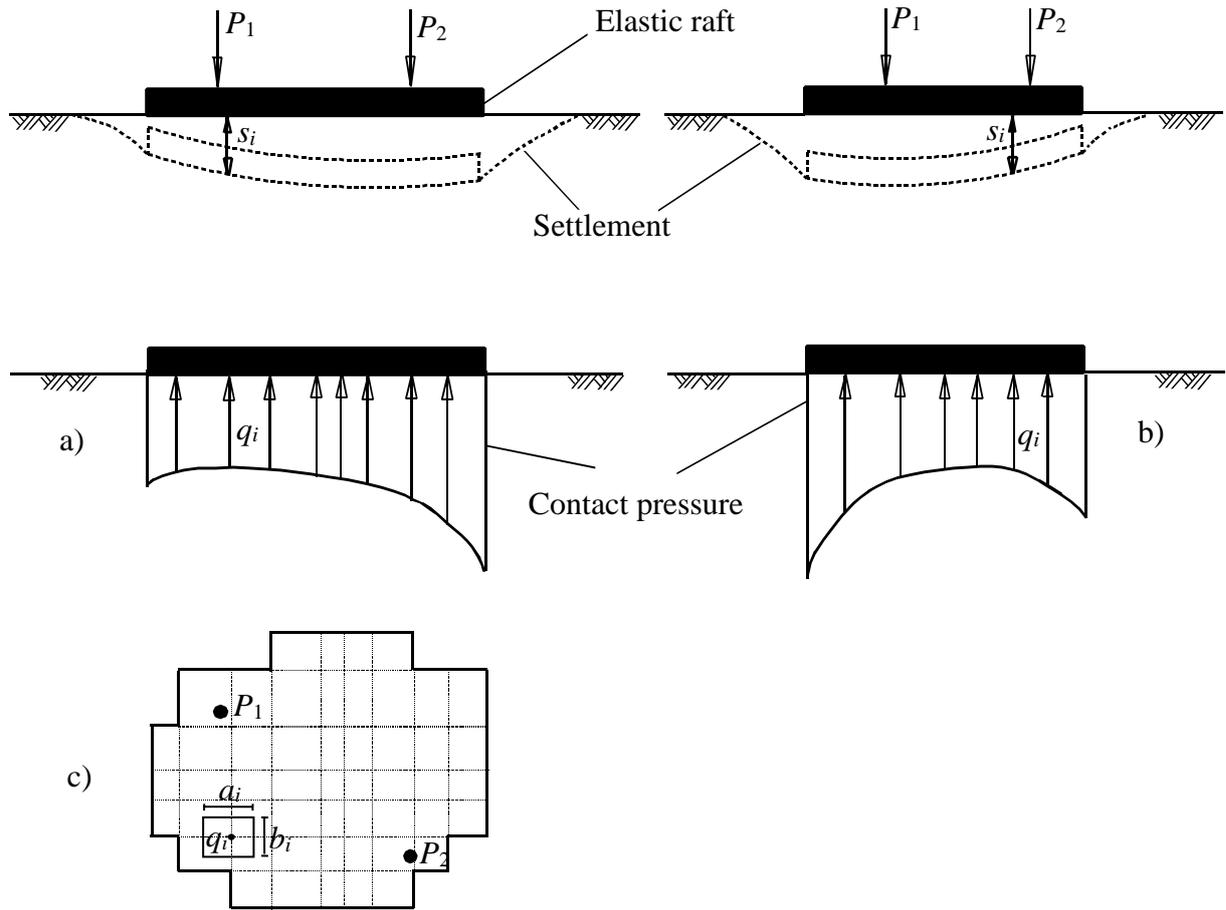
Figure 1.7   Contact pressure distribution and soil settlement
under elastic raft on Continuum medium
a) Section parallel to *x*-direction
b) Section parallel to *y*-direction
c) Foundation plan

Settlement at a depth *z* due to a concentrated load

Figure 1.8 shows a concentrated load Q acting on the surface of isotropic elastic half-space medium. The settlement $s(z)$ at a depth z due to this load can be expressed as

$$s(z) = \frac{Q}{2 \pi E_s} \left(\frac{(1+\nu_s)\, z^2}{(r^2 + z^2)^{3/2}} + \frac{2\,(1-\nu_s^2)}{(r^2 + z^2)^{1/2}} \right)$$

(1.20)
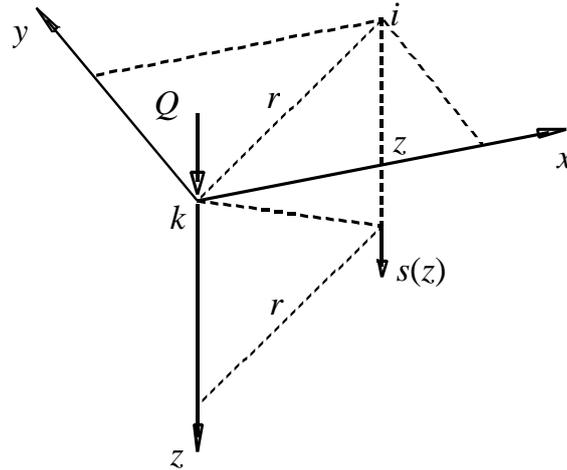
<u>Figure 1.8</u>   Settlement $s(z)$ due to a concentrated load on elastic half-space medium

Settlement at the surface due to a concentrated load

The settlement $s(0)$ at the surface outside the point of application of the concentrated load is obtained by putting $z = 0$ in Equation 1.20

$$s\,(0) = \frac{Q\,(1 - \nu_s^{\ 2})}{\pi\,E_s\,r} \tag{1.21}$$

Settlement at the surface under the concentrated load

Equation 1.21 cannot be directly applied to determine the settlement under the concentrated load. Therefore, the concentrated load is converted to an equivalent uniform load over a rectangular area $a \times b$. Then, the settlement $s(0)$ at the center of the uniformly loaded rectangular area $a \times b$ can be obtained by integrating Equation 1.21 over that area as shown in Figure 1.9 and Equation 1.22

$$s\,(0) = \frac{Q\,(1 - \nu_s^{\ 2})}{\pi\,E_s\,a\,b}\,2\,\int_{\zeta=0}^{\zeta=a/2} 2\,\int_{\eta=0}^{\eta=b/2} \frac{d\zeta\ d\eta}{\sqrt{\left(\zeta^2 + \eta^2\right)}} \tag{1.22}$$

Equation 1.22 after integration becomes

$$s\,(0) = \frac{2\,Q\,(1 - \nu_s^{\ 2})}{\pi\,E_s}\left(\frac{1}{a}\ln\left[\frac{a}{b} + \sqrt{\frac{a^2}{b^2} + 1}\right] + \frac{1}{b}\ln\left[\frac{b}{a} + \sqrt{\frac{b^2}{a^2} + 1}\right]\right) \tag{1.23}$$
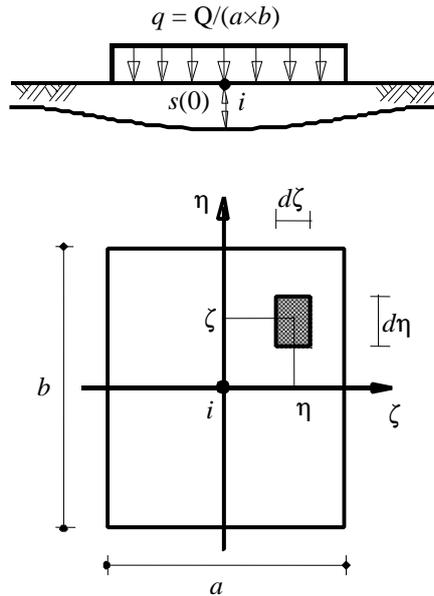
Figure 1.9   Settlement due to loaded area $a \times b$ on elastic half-space medium

Formulation of flexibility matrix of soil as elastic half-space soil medium

Determination of the settlement $s_{i,i}$

The settlement $s_{i,i}$ of node i, due to contact force Q_i on that node for isotropic elastic half-space soil medium can be expressed by

$$s\,(0) = \frac{2\,Q_i\,(1-\nu_s{}^2)}{\pi\,E_s}\left(\frac{1}{a_i}\ln\left[\frac{a_i}{b_i}+\sqrt{\frac{a_i{}^2}{b_i{}^2}+1}\right]+\frac{1}{b_i}\ln\left[\frac{b_i}{a_i}+\sqrt{\frac{b_i{}^2}{a_i{}^2}+1}\right]\right)\tag{1.24}$$

Equation 1.24 is simplified to

$$s_{i,i} = c_{i,i}\,Q_i\tag{1.25}$$

The ratio between the settlement $s_{i,i}$ of point i and the contact force Q_i at that point is termed the flexibility coefficient $c_{i,i}$ [m/kN]. It can be recognized as the settlement of a point i due to a unit load at that point.

Determination of the settlement $s_{i,k}$

The settlement $s_{i,k}$ of node i, due to contact force Q_k on node k for isotropic elastic half-space soil medium, Figure 1.10, can be expressed by

$$s_{i,k} = \frac{Q_k\,(1-\nu_s{}^2)}{\pi\,E_s\,r_{i,k}} = c_{i,k}\,Q_k\tag{1.26}$$

The ratio between the settlement $s_{i,k}$ of point i and the contact force Q_k at a point k is termed the flexibility coefficient $c_{i,i}$ [m/kN]. It can be recognized as the settlement of a point i due to a unit load at a point k.
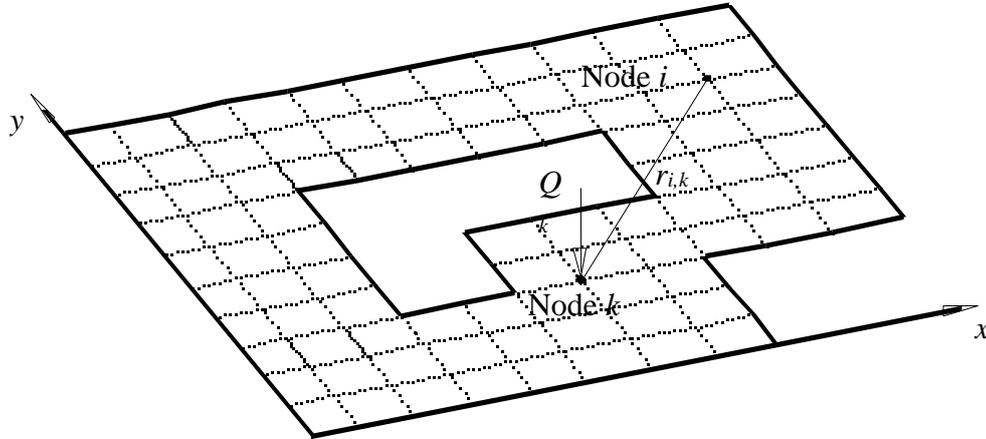
Figure 1.10   Settlement $s_{i,k}$ of node i due to contact force Q_k at node k

Assembling of the flexibility matrix for isotropic elastic half-space soil medium

To find the settlement s_i at node i, Equation 1.25 is applied for that node i, while Equation 1.26 is applied for the other remaining nodes considering contact forces over nodes. For a set of grid points of Finite elements-mesh, the settlement at point i is obtained from

$$
\begin{aligned}
s_i &= s_{i,1} + s_{i,2} + s_{i,3} + \ldots + s_{i,n} \\
&= c_{i,1}\,Q_1 + c_{i,2}\,Q_2 + c_{i,3}\,Q_3 + \ldots + c_{i,n}\,Q_n
\end{aligned}
\tag{1.27}
$$

Equation 1.27 in series form is

$$
s_i = \sum_{k=1}^{n} c_{i,k}\,Q_k
\tag{1.28}
$$

Equation 1.28 for the entire foundation in matrix form is

$$
\begin{Bmatrix} s_1 \\ s_2 \\ s_3 \\ \\ \ldots \\ s_n \end{Bmatrix}
=
\begin{bmatrix}
c_{1,1} & c_{1,2} & c_{1,3} & & \ldots & c_{1,n} \\
c_{2,1} & c_{2,2} & c_{2,3} & & \ldots & c_{2,n} \\
c_{3,1} & c_{3,2} & c_{3,3} & & \ldots & c_{3,n} \\
& & & & & \\
\ldots & \ldots & \ldots & & \ldots & \ldots \\
c_{n,1} & c_{n,2} & c_{n,3} & & \ldots & c_{n,n}
\end{bmatrix}
\begin{Bmatrix} Q_1 \\ Q_2 \\ Q_3 \\ \\ \ldots \\ Q_n \end{Bmatrix}
\tag{1.29}
$$

Equation 1.29 is simplified to

$$\{s\} = [c]\{Q\} \tag{1.30}$$

To assemble the flexibility matrix of the soil $[c]$, each node is loaded by a unit contact force and the resulting settlements in all remaining nodes and in the loaded node are calculated. Inverting the flexibility matrix $[c]$, gives the $[n \times n]$ stiffness matrix of the soil $[k_s]$ corresponding to the contact forces at the n nodal points such that

$$\{Q\} = [k_s]\{s\} \tag{1.31}$$

Complete stiffness formulation for isotropic elastic half-space soil medium

The foundation will deflect under the action of the total external forces $\{F\}$ due to known applied loads $\{P\}$ and the unknown soil reactions $\{Q\}$, where

$$\{F\} = \{P\} - \{Q\} \tag{1.32}$$

The equilibrium of the raft-soil system is expressed by the following matrix equation

$$[k_p]\{\delta\} = \{P\} - \{Q\} \tag{1.33}$$

Considering the compatibility of deformation between the plate and the soil medium, where the soil settlement s_i is equal to the platIe deflection w_i, Equation 1.30 for Continuum model can be substituted into Equation 1.32 as

$$\left[[k_p] + [k_s]\right]\{\delta\} = \{P\} \tag{1.34}$$

Equation 1.34 shows that the stiffness matrix of the whole raft-soil system is the sum of the plate and the soil stiffness matrices, $[k_p] + [k_s]$.

It should be noticed that the matrix $[k_s]$ is not compatible with the matrix $[k_p]$, because the degrees of freedom in Equation 1.31 differ from that in Equation 1.33. To overcome this problem, Equation 1.31 can be treated by extending the row and column of matrix $[k_s]$ in the same manner as the matrix $[k_p]$. Consequently, the operation of matrix equations can then be accepted.

Equation solver for isotropic elastic half-space soil medium

It should be noticed that the matrix $[k_s]$ is full symmetrical matrix for isotropic elastic half-space soil medium. Therefore, the total stiffness matrix for the raft and the soil is also full symmetrical matrix.

The system of linear equations is solved by *Gauss* elimination-technique. Since the total stiffness matrix is a full matrix, the equation solver 1.34 takes long computation time by applying this method. The unknown variables in Equation 1.34 are the nodal displacements w_i ($w_i = s_i$) and the nodal rotations θ_{xi} and θ_{yi} about the x- and y-directions. After solving the system of linear Equation 1.34, substituting the obtained settlements s_i in Equation 1.31, gives the unknown contact forces Q_i.

1.3.5 Modulus of compressibility method for elastic raft on layered soil medium (method 6 - Solving system of linear equations by iteration - Layered soil medium - Continuum model)

Introduction

Available solutions for the analysis of foundations using Continuum model either representing the soil as isotropic elastic half-space soil medium or Layered soil medium were presented by many authors. But the major difficulty for practical problems to apply this model lies in solving large set of equations, which requires large computer storage and long computation time.

Numbers of attempts have been made to overcome this problem, among these are:

Haung (1974) proposed a method for analyzing a symmetrically loaded foundation by taking into account the condition of symmetry. Consequently, the simultaneous equations can be reduced by considering only a part of the foundation rather than the whole foundation. The analysis is carried out for a quarter of the foundation if the raft and soil are symmetrical about both x- and y-axes, or for half of the foundation if the raft and soil are symmetrical about x- or y-axis. Nevertheless, most of the foundations in practice are not symmetrically loaded.

Haung (1974) proposed an iterative scheme to convert the overall stiffness matrix into a half band matrix by adding a part of the soil stiffness matrix to the plate stiffness matrix. Then, simultaneous equations can be solved by iteration method. Nevertheless, it was found that when the number of equations is large while the bandwidth is small, the displacements may not converge, and large bandwidth should be used.

Cheung (1978) proposed a method to modify the overall stiffness matrix into a banded diagonal matrix which can be solved by using Banded coefficients-technique. Modification of this matrix bases on the assumption that the deflection at a point is affected only by forces acting on surrounding points. Nevertheless, it is found that this foundation model is less accurate.

Ahrens/ Winselmann (1984) and *Stark/ Majer* (1988) proposed an iteration method for the Continuum model using variable moduli of subgrade reactions. The iteration process is repeated until compatibility between the plate deformations due to the moduli of subgrade reactions and the soil settlements due to the corresponding contact pressures is reached. *El Gendy* (1994) showed that the number of iterative cycles required for this method increase with increasing the number of elements and the iteration may not converge for grate number of elements.

Lopes/ Gusmão (1991) suggested that in many cases the foundation subjects to symmetrical vertical loading. Therefore, the effects of some of the load components, such as moments, may be ignored and only the vertical reactions may be considered. In such cases, the size of vectors and matrices are considerably reduced.

El Gendy (1994) proposed an iterative scheme to convert the overall stiffness matrix into a banded matrix by converting the soil stiffness matrix to a diagonal matrix. Then, the simultaneous equations can be solved by Banded coefficients-technique. *El Gendy* (1998) modified the same iteration scheme by converting the soil stiffness matrix into equivalent symmetrical banded matrix. A comparison of this method with other available iteration methods shows that it converges more rapidly. The iteration method of *El Gendy* (1998) is considered in the program *ELPLA* up Version 7.0, which is described in the next pages.

Description of method

To describe the proposed iteration method, consider a raft resting on a layered soil medium or isotropic elastic half-space soil medium. The contact pressure q_i at node i under the raft is replaced by equivalent contact force Q_i.

For a set of grid points of Finite elements-mesh, the soil settlement s_i at point i due to contact forces in manner described earlier for Continuum model is obtained from

$$s_i = \sum_{k=1}^{n} c_{i,k} \, Q_k \tag{1.35}$$

Considering the entire foundation, Equation 1.34 can be rewritten in matrix form as

$$\{s\} = [c]\{Q\} \tag{1.36}$$

Inverting the flexibility matrix $[c]$, gives the stiffness matrix of the soil $[k_s]$ corresponding to the contact forces at the n nodal points such that

$$\{Q\} = [k_s]\{s\} \tag{1.37}$$

Complete stiffness formulation

The foundation will deflect under the action of the total external forces $\{F\}$ due to known applied loads $\{P\}$ and the unknown soil reactions $\{Q\}$, where

$$\{F\} = \{P\} - \{Q\} \tag{1.38}$$

The equilibrium of the raft-soil system is expressed by the following matrix equation

$$\left[k_p \right] \{\delta\} = \{P\} - \{Q\}$$ (1.39)

Considering the compatibility of deformation between the plate and the soil medium, where the soil settlement s_i is equal to the plate deflection w_i, Equation 1.37 for Continuum model can be substituted into Equation 1.39 as

$$\left[\left[k_p \right] + \left[k_s \right] \right] \{\delta\} = \{P\}$$ (1.40)

It should be noticed that the plate stiffness matrix $[k_p]$ is a banded matrix and the soil stiffness matrix $[k_s]$ is a full unsymmetrical matrix for layered soil medium and a full symmetrical matrix for isotropic elastic half-space soil medium. The major difficulty for practical problems lies in solving large set of equations, which requires large computer storage and long computation time. In order to overcome this problem, it is possible to convert the soil stiffness matrix $[k_s]$ to a symmetrical banded matrix $[k']$ of half bandwidth equal to that of the plate stiffness matrix $[k_p]$. Then, it can be easily added the matrix $[k']$ to the matrix $[k_p]$. The resultant matrix will be also a banded matrix. Consequently, Equation 1.40 can be solved by using the Banded coefficients-technique.

Banded matrix formulation

To illustrate how to convert the soil stiffness matrix $[k_s]$ to a symmetrical banded matrix, consider the simple example of the foundation shown in Figure 1.11. The foundation has 9 nodes, each node has three unknown deformations w, θ_x and θ_y. There are 27 simultaneous equations. The foundation of 9 nodes yields to a plate stiffness matrix $[k_p]$ with a half bandwidth $N_w = 15$.
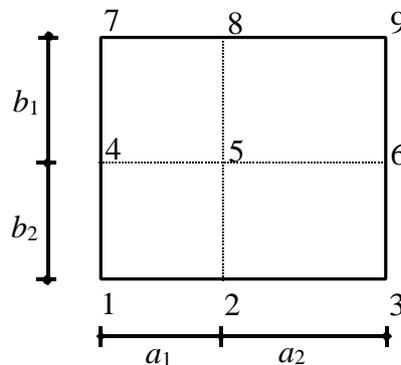
Figure 1.11   Foundation of 9 nodes

The matrix $[k_s]$ can be divided into two matrices $[k_1]$ and $[k_2]$ as follows

$$\left[k_s \right] = \left[k_1 \right] + \left[k_2 \right]$$ (1.41)

Equation 1.41 can be rewritten with matrix coefficients in details as

$$
\overset{\displaystyle \overbrace{\hphantom{k_{1,1}\ k_{1,2}\ k_{1,3}\ k_{1,4}\ k_{1,5}}}^{N_w/3}}{
\begin{bmatrix}
k_{1,1} & k_{1,2} & k_{1,3} & k_{1,4} & k_{1,5} & k_{1,6} & k_{1,7} & k_{1,8} & k_{1,9} \\
k_{2,1} & k_{2,2} & k_{2,3} & k_{2,4} & k_{2,5} & k_{2,6} & k_{2,7} & k_{2,8} & k_{2,9} \\
k_{3,1} & k_{3,2} & k_{3,3} & k_{3,4} & k_{3,5} & k_{3,6} & k_{3,7} & k_{3,8} & k_{3,9} \\
k_{4,1} & k_{4,2} & k_{4,3} & k_{4,4} & k_{4,5} & k_{4,6} & k_{4,7} & k_{4,8} & k_{4,9} \\
k_{5,1} & k_{5,2} & k_{5,3} & k_{5,4} & k_{5,5} & k_{5,6} & k_{5,7} & k_{5,8} & k_{5,9} \\
k_{6,1} & k_{6,2} & k_{6,3} & k_{6,4} & k_{6,5} & k_{6,6} & k_{6,7} & k_{6,8} & k_{6,9} \\
k_{7,1} & k_{7,2} & k_{7,3} & k_{7,4} & k_{7,5} & k_{7,6} & k_{7,7} & k_{7,8} & k_{7,9} \\
k_{8,1} & k_{8,2} & k_{8,3} & k_{8,4} & k_{8,5} & k_{8,6} & k_{8,7} & k_{8,8} & k_{8,9} \\
k_{9,1} & k_{9,2} & k_{9,3} & k_{9,4} & k_{9,5} & k_{9,6} & k_{9,7} & k_{9,8} & k_{9,9}
\end{bmatrix}} =
$$

$$
\overset{\displaystyle \overbrace{\hphantom{k_{1,1}\ k_{1,2}\ k_{1,3}\ k_{1,4}\ k_{1,5}}}^{N_w/3}}{
\begin{bmatrix}
k_{1,1} & k_{1,2} & k_{1,3} & k_{1,4} & k_{1,5} & 0 & 0 & 0 & 0 \\
 & k_{2,2} & k_{2,3} & k_{2,4} & k_{2,5} & k_{2,6} & 0 & 0 & 0 \\
 & & k_{3,3} & k_{3,4} & k_{3,5} & k_{3,6} & k_{3,7} & 0 & 0 \\
 & & & k_{4,4} & k_{4,5} & k_{4,6} & k_{4,7} & k_{4,8} & 0 \\
 & & & & k_{5,5} & k_{5,6} & k_{5,7} & k_{5,8} & k_{5,9} \\
 & & & & & k_{6,6} & k_{6,7} & k_{6,8} & k_{6,9} \\
 & & & & & & k_{7,7} & k_{7,8} & k_{7,9} \\
 & & & & & & & k_{8,8} & k_{8,9} \\
 & & & & & & & & k_{9,9}
\end{bmatrix}} + \quad (1.42)
$$

$$
\overset{\displaystyle \overbrace{\hphantom{k_{1,1}\ k_{1,2}\ k_{1,3}\ k_{1,4}\ k_{1,5}}}^{N_w/3}}{
\begin{bmatrix}
0 & 0 & 0 & 0 & 0 & k_{1,6} & k_{1,7} & k_{1,8} & k_{1,9} \\
k_{2,1}\text{-}k_{1,2} & 0 & 0 & 0 & 0 & 0 & k_{2,7} & k_{2,8} & k_{2,9} \\
k_{3,1}\text{-}k_{1,3} & k_{3,2}\text{-}k_{2,3} & 0 & 0 & 0 & 0 & 0 & k_{3,8} & k_{3,9} \\
k_{4,1}\text{-}k_{1,4} & k_{4,2}\text{-}k_{2,4} & k_{4,3}\text{-}k_{3,4} & 0 & 0 & 0 & 0 & 0 & k_{4,9} \\
k_{5,1}\text{-}k_{1,5} & k_{5,2}\text{-}k_{2,5} & k_{5,3}\text{-}k_{3,5} & k_{5,4}\text{-}k_{4,5} & 0 & 0 & 0 & 0 & 0 \\
k_{6,1} & k_{6,2}\text{-}k_{2,6} & k_{6,3}\text{-}k_{3,6} & k_{6,4}\text{-}k_{4,6} & k_{6,5}\text{-}k_{5,6} & 0 & 0 & 0 & 0 \\
k_{7,1} & k_{7,2} & k_{7,3}\text{-}k_{3,7} & k_{7,4}\text{-}k_{4,7} & k_{7,5}\text{-}k_{5,7} & k_{7,6}\text{-}k_{6,7} & 0 & 0 & 0 \\
k_{8,1} & k_{8,2} & k_{8,3} & k_{8,4}\text{-}k_{4,8} & k_{8,5}\text{-}k_{5,8} & k_{8,6}\text{-}k_{6,8} & k_{8,7}\text{-}k_{7,8} & 0 & 0 \\
k_{9,1} & k_{9,2} & k_{9,3} & k_{9,4} & k_{9,5}\text{-}k_{5,9} & k_{9,6}\text{-}k_{6,9} & k_{9,7}\text{-}k_{7,9} & k_{9,8}\text{-}k_{8,9} & 0
\end{bmatrix}}
$$

where the matrix $[k_1]$ is a symmetrical banded matrix that has the same half bandwidth of matrix $[k_p]$ and the second matrix $[k_2]$ can be converted to a diagonal matrix as described in the iteration process.

Iteration process

The iteration process of the method can be described as follows:

i)   First, uniform distribution of contact pressure $q^{(o)}$ on the bottom of the foundation is assumed as

$$q^{(o)} = \frac{N}{A_f} \tag{1.43}$$

ii)   The soil settlements s_i due to contact forces Q_i in manner described either earlier for isotropic elastic half-space soil medium or later for layered soil medium are obtained from

$$\{s\} = [c]\{Q\} \tag{1.44}$$

iii)   A set of nodal forces $\{Q_A\}$ are computed from the matrix $[k_2]$ and the soil settlements $\{s\}$ as

$$\{Q_A\} = [k_2]\{s\} \tag{1.45}$$

iv)   The matrix $[k_2]$ is converted to a equivalent diagonal matrix $[k^*_2]$. The coefficients of the diagonal matrix are obtained from

$$k_{i,i} = \frac{Q_{A_i}}{s_i} \tag{1.46}$$

v)   The equivalent symmetrical banded matrix $[k']$ for the soil stiffness matrix $[k_s]$ is

$$[k'] = [k_1] + [k^*_2] \tag{1.47}$$

vi)   Now, adding the equivalent soil stiffness matrix $[k']$ to the plate stiffness matrix $[k_p]$ is easy. Then, the overall matrix becomes a banded matrix. The entire system equation is expressed as

$$\left[[k_p] + [k']\right]\{\delta\} = \{P\} \tag{1.48}$$

vii)   A set of nodal displacements $\{\delta\}$ is obtained by solving the system equation 1.48 using the Banded coefficients-technique

viii)   The soil settlements s_i are compared with the corresponding plate deflections w_i, which were computed from the system equation 1.48

$$\varepsilon = \left\| s_i - w_i \right\|$$
(1.49)

ix)   If the accuracy does not reach to a specified tolerance ε a new set of contact forces are obtained using

$$\{Q_A\} = [k_2]\{s\}$$
(1.50)

The steps ii to viii are repeated until the accuracy reaches to a specified tolerance ε, which means that sufficient compatibility between the plate deflections w_i and the soil settlements s_i is reached in the plate-soil interface. Figure 1.12 shows the flow chart of the iteration process.

A good advantage of this iteration method is that it requires much less computer memory than the elimination method. It needs also less computation time than that of the elimination method used in the analysis of Continuum model. Much fewer cycles are needed to obtain a satisfactory accuracy, nearly two or three cycles. Consequently, the maximum permissible number of nodes is greatly increased. It can easily eliminate the contact pressure if negative pressure appeared or consider nonlinear soil response. By analysis of both the raft and subsoil separately, some former restrictions on maximum problem size can be avoided.

```
                              ( Start )
                                 │
                                 ▼
          ┌──────────────────────────────────────────┐
          │  Compute the avarage contact pressure     │
          └──────────────────────────────────────────┘
                                 │
                                 ▼
             ┌────────────────────────────────┐
             │      Find the matrices $[k_1]$   │
             │           and $[k_2]$            │
             └────────────────────────────────┘
                                 │
      ┌──────────────────────────┤
      │                          ▼
      │         ┌────────────────────────────────────┐
      │         │     Find the soil settlement $s$     │
      │         │       $\{s\} = [c]\,\{Q\}$           │
      │         └────────────────────────────────────┘
      │                          │
      │                          ▼
      │     ┌──────────────────────────────────────────┐
      │     │  Compute a set of nodal forces $\{Q_A\}$   │
      │     │       $\{Q_A\} = [k_2]\,\{s\}$             │
      │     └──────────────────────────────────────────┘
      │                          │
      │                          ▼
      │   ┌────────────────────────────────────────────────┐
      │   │ Convert the matrix $[k_2]$ to diagonal matrix    │
      │   │ $[k^{*}_2]$                                       │
      │   └────────────────────────────────────────────────┘
      │                          │
      │                          ▼
      │  ┌──────────────────────────────────────────────────┐
      │  │  Find the equivalent symmetrical banded matrix     │
      │  │        $[k'] = [k_1] + [k^{*}_2]$                   │
      │  └──────────────────────────────────────────────────┘
      │                          │
      │                          ▼
      │  ┌──────────────────────────────────────────────────┐
      │  │ Find the plate deflection $w$ from FE-plate analysis│
      │  │   $[[k_p] + [k']]\,\{\delta\} = \{P\}$              │
      │  └──────────────────────────────────────────────────┘
      │                          │
      │                          ▼
      │        ┌──────────────────────────────┐   Yes
      │        │    Convergence reached        ├──────► ( End )
      │        │    $w_i^{(j)} \approx s_i^{(j)}$│
      │        └──────────────────────────────┘
      │                          │ No
      │                          ▼
      │   ┌──────────────────────────────────────────┐
      └───┤    Find the new contact pressure           │
          │        $\{Q\} = [k_s]\,\{w\}$               │
          └──────────────────────────────────────────┘
```
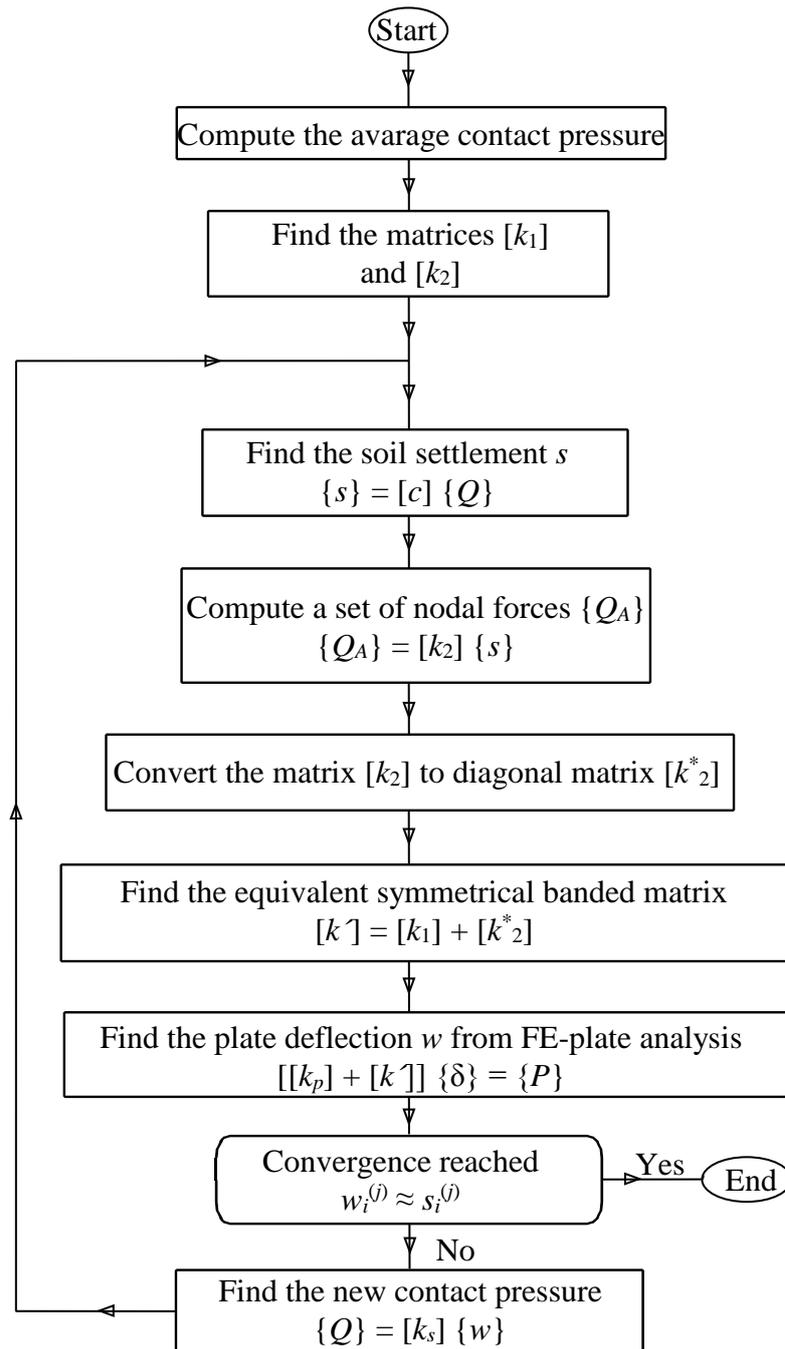
Figure 1.12   Flow chart of the iteration process

1.3.6   Modulus of compressibility method for elastic raft on layered soil medium (method 7 - Solving system of linear equations by elimination - Layered soil medium - Continuum model)

In reality, the soil profile is usually nonhomogeneous. The most likely profile is layered. In addition, foundations are almost never placed at the ground surface. Therefore, an improvement needs to be applied to half-space soil medium concerning the assumption that the load is applied at the surface of homogeneous isotropic elastic half-space medium. Representing the soil as layered continuum medium is more complicated than that as isotropic elastic half-space soil medium. *Kany* (1954) presented an extension of *Ohde*'s method (1942) to strip footing resting on nonhomogeneous and anisotropic medium. It can be applied for rafts as described in the following section.

Settlement at a depth z due to a loaded area

The settlement at the corner of a loaded area can be determined in a manner similar to that at the center of a loaded area, which was described in section 1.3.4. This is done by integrating equation 1.20 over a loaded area. Figure 1.13 shows a loaded area q of size $a \times b$ acting on the surface of isotropic elastic half-space medium.
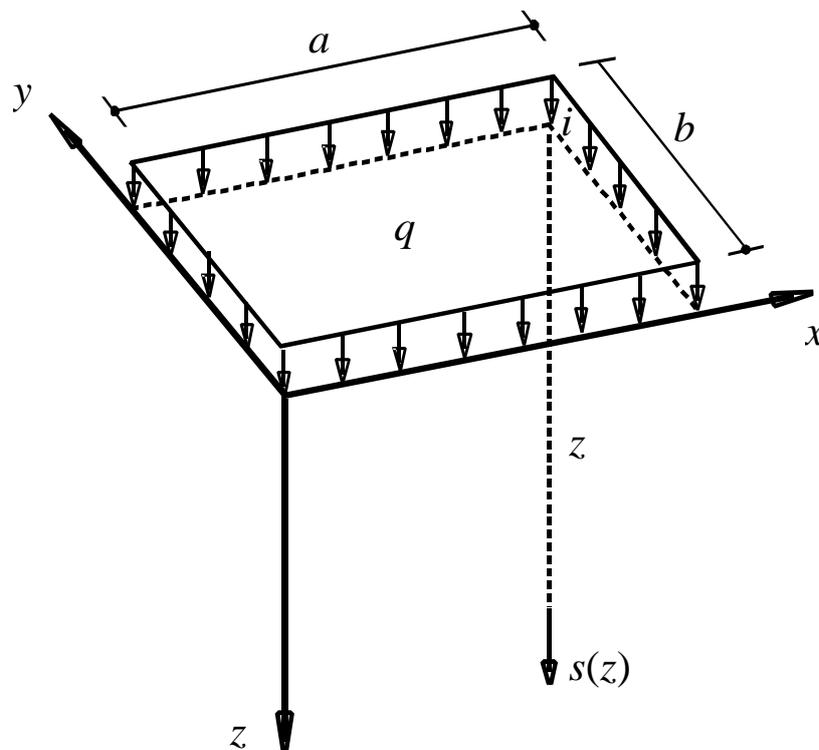
Figure 1.13   Settlement $s(z)$ under the corner of a loaded area on elastic half-space medium

According to *Steinbrenner* (1934), the settlement $s(z)$ at a depth z under the corner of the loaded area is given by

$$s(z) = \frac{q(1-v_s^2)}{2\pi E_s}\left(b\ln\frac{(c+a)}{(c-a)} + a\ln\frac{(c+b)}{(c-b)}\right)$$
$$-\frac{q(1-v_s-2v_s^2)}{2\pi E_s}\left(z\tan^{-1}\frac{ab}{zc}\right) \tag{1.51}$$

Settlement at the surface due to a loaded area

The settlement $s(0)$ of a point at the surface under the corner of a rectangular loaded area is obtained by putting $z = 0$ in Equation 1.51

$$s(0) = \frac{q(1-v_s^2)}{2\pi E_s}\left(b\ln\frac{(m+a)}{(m-a)} + a\ln\frac{(m+b)}{(m-b)}\right) \tag{1.52}$$

Where in Equations 1.50 and 1.51 is $c = \sqrt{a^2+b^2+z^2}$ and $m = \sqrt{a^2+b^2}$

Settlement of a finite layer due to a loaded area

For the settlement Equations 1.51 and 1.52 presented above, it was assumed that the soil layer extends to an infinite depth. However, if a rigid base at a depth $z = h$ underlies the soil layer, the settlement s_h of the layer can be approximately calculated as (Figure 1.14)

$$s_h = s(0) - s(z) \tag{1.53}$$

Subtracting Equation 1.51 from Equation 1.52 yields

$$s_h = \frac{q(1-v_s^2)}{2\pi E_s}\left(b\ln\frac{(c-a)(m+a)}{(c+a)(m-a)} + a\ln\frac{(c-b)(m+b)}{(c+b)(m-b)}\right)$$
$$-\frac{q(1-v_s-2v_s^2)}{2\pi E_s}\left(z\tan^{-1}\frac{ab}{zc}\right) \tag{1.54}$$

Equation 1.54 can be simplified to

$$s_h = \frac{q}{E_s}f \tag{1.55}$$
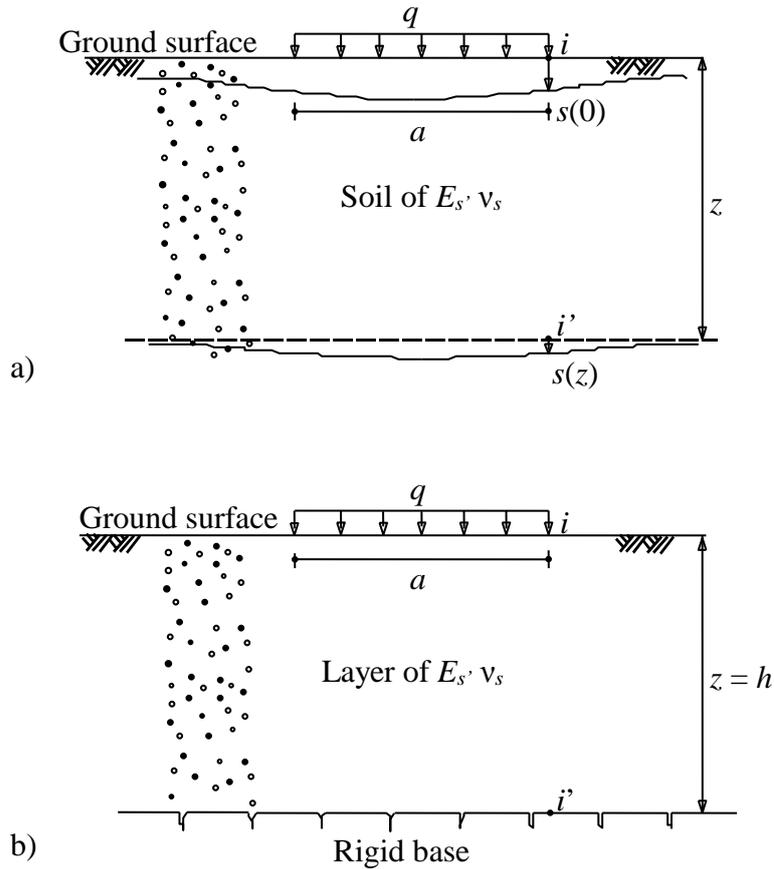
Figure 1.14   a) Isotropic elastic half-space soil medium
               b) Elastic layer on rigid base

Settlement of multi-layers due to a loaded area

Obviously, it can generalize this approach to consider multi-layers of soil. Each has different elastic material and thickness as shown in Figure 1.15. The vertical settlement of a layer l in an n layered system is given by

$$s_l = q\left(\frac{f^{(l)} - f^{(l-1)}}{E_s^{(l)}}\right) = q\left(\frac{\Delta f^{(l)}}{E_s^{(l)}}\right) \tag{1.56}$$

The total settlement for n layered system is

$$s = q\left(\frac{f^{(1)}}{E_s^{(1)}} + \sum_{l=2}^{n}\frac{\Delta f^{(l)}}{E_s^{(l)}}\right) \tag{1.57}$$

Considering *Poisson*'s ratio v_s for all soil layers is constant as its value for most soil types ranges between 0.3 and 0.5.
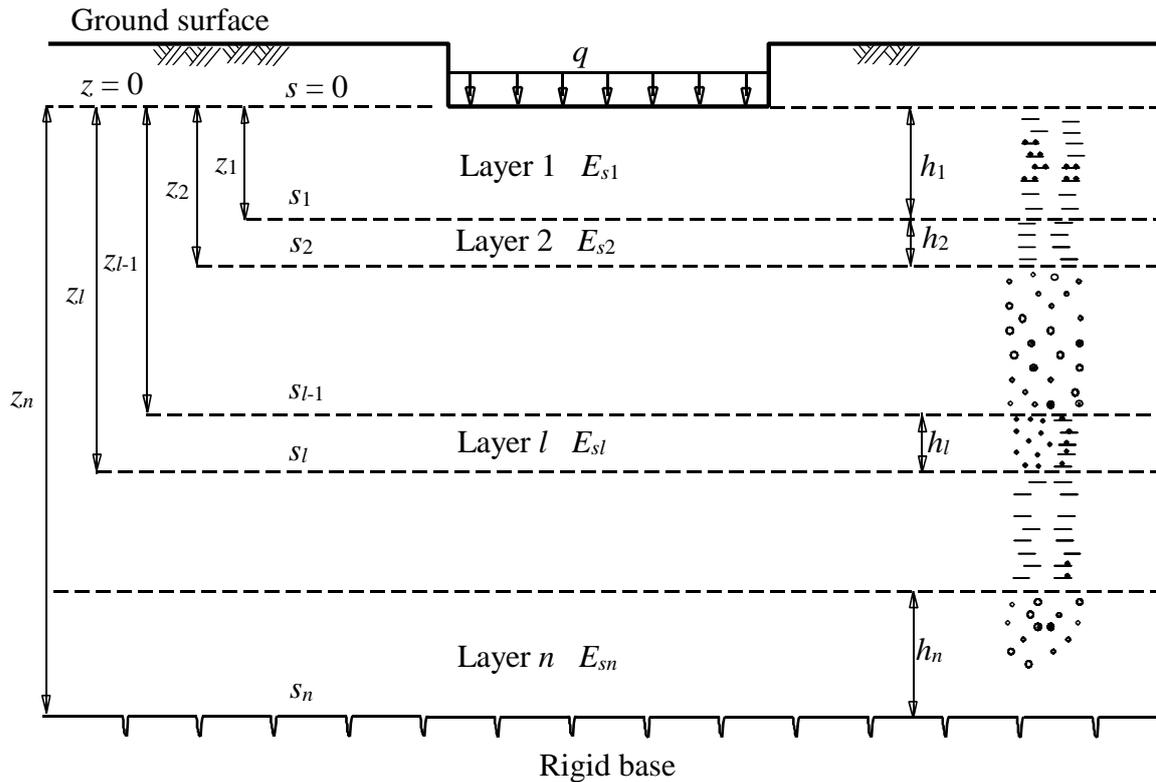
Figure 1.15   Layered system

Settlement at an interior point of loaded area

So far it has been considered the settlement beneath a corner of a loaded area. To find the settlement at any other point the principle of superposition can be used. The settlement at an interior point of the rectangular loaded area is given by the sum of the settlements at the corners of four sub-loaded areas. To determine the settlement coefficient $f^{(l)}$ for a layer l at an interior point i of the rectangular loaded area shown in Figure 1.16, the Formula of *Kany* (1974) can be applied as

$$f^{(l)} = f^{(l)}_1 + f^{(l)}_2 + f^{(l)}_3 + f^{(l)}_4$$

$$= \frac{1}{2\pi} \sum_{n=1}^{4} \left[(1-v_s^2) \left\{ b_n \ln \frac{(c_n - a_n)(M + a_n)}{(c_n + a_n)(M - a_n)} \right. \right. \tag{1.58}$$

$$\left. \left. + a_n \ln \frac{(c_n - b_n)(M + b_n)}{(c_n + b_n)(M - b_n)} \right\} + (1 - v_s - 2v_s^2) z_l \tan^{-1} \frac{a_n b_n}{z_l c_n} \right]$$

Where in Equation 1.58 is $c_n = \sqrt{a_n^2 + b_n^2 + z_l^2}$ und $M = \sqrt{a_n^2 + b_n^2}$

The value z_l means the level of the lower side of the layer l from the foundation level.
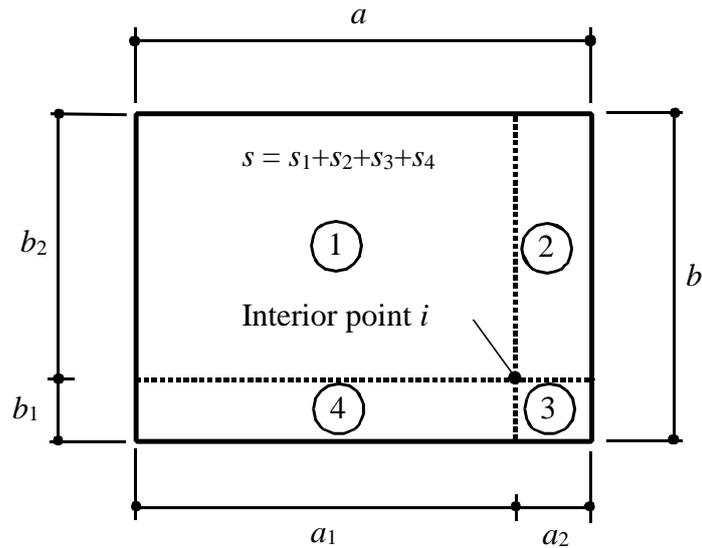
Figure 1.16   Superposition of four loaded areas to find the settlement at an interior point i

Settlement at a point outside the loaded area

Adding and subtracting corner settlements for four loaded areas can obtain the settlement of any point outside the loaded area as shown in Figure 1.17. First, the settlement s_1 as if the entire region defined by load q is determined. Then, the settlements due to the two edge loaded areas s_2 and s_3 are subtracted. Finally, the settlement s_4 is added since it has been subtracted twice in s_2 and s_3. Using the same process, the settlement coefficient $f^{(l)}$ for a layer l at an exterior point i of the rectangular loaded area shown in Figure 1.17 is given by

$$f^{(l)} = f^{(l)}_1 - f^{(l)}_2 - f^{(l)}_3 - f^{(l)}_4 \tag{1.59}$$
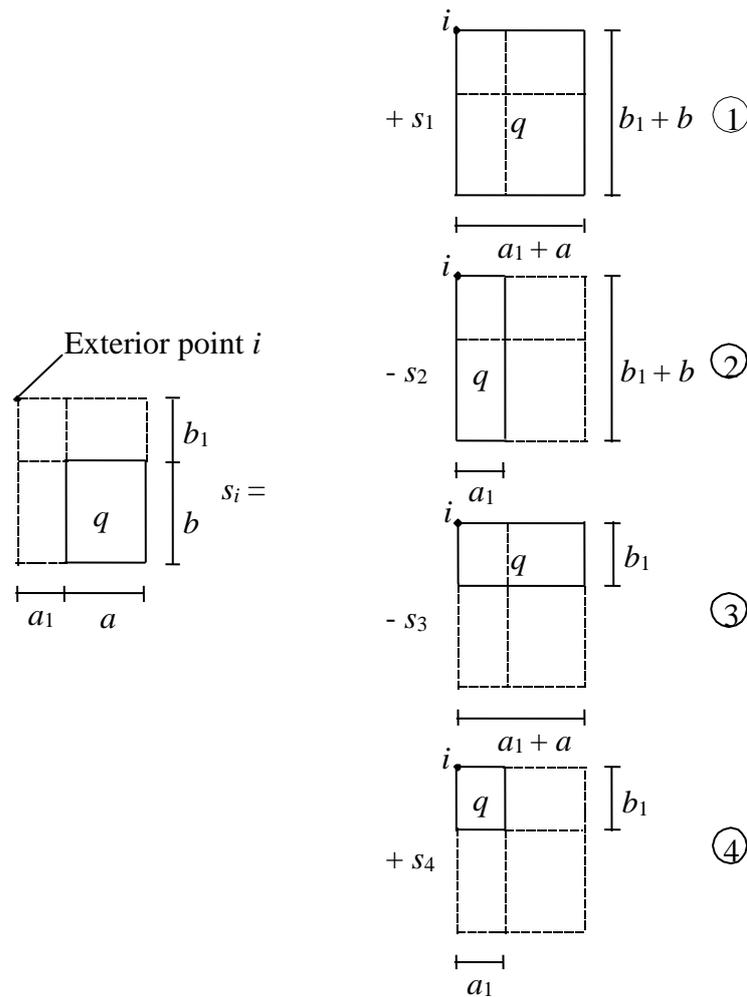
Figure 1.17   Superposition of four loaded areas to find the settlement at an exterior point i

For any point i of coordinates (ζ, η) inside or outside the loaded area $a \times b$ (Figure 1.18) the settlement coefficient $f^{(l)}$ can be obtained according to *Poulos/ Davis* (1974) using the principle of superposition by the following general Equation 1.60

$$f^{(l)} = f(\zeta, \eta) - f(\zeta - a, \eta) - f(\zeta, \eta - b) + f(\zeta - a, \eta - b) \tag{1.60}$$

a) Point i lies inside the loaded area

b) Point i lies outside the loaded area

c) Point i lies outside the loaded area
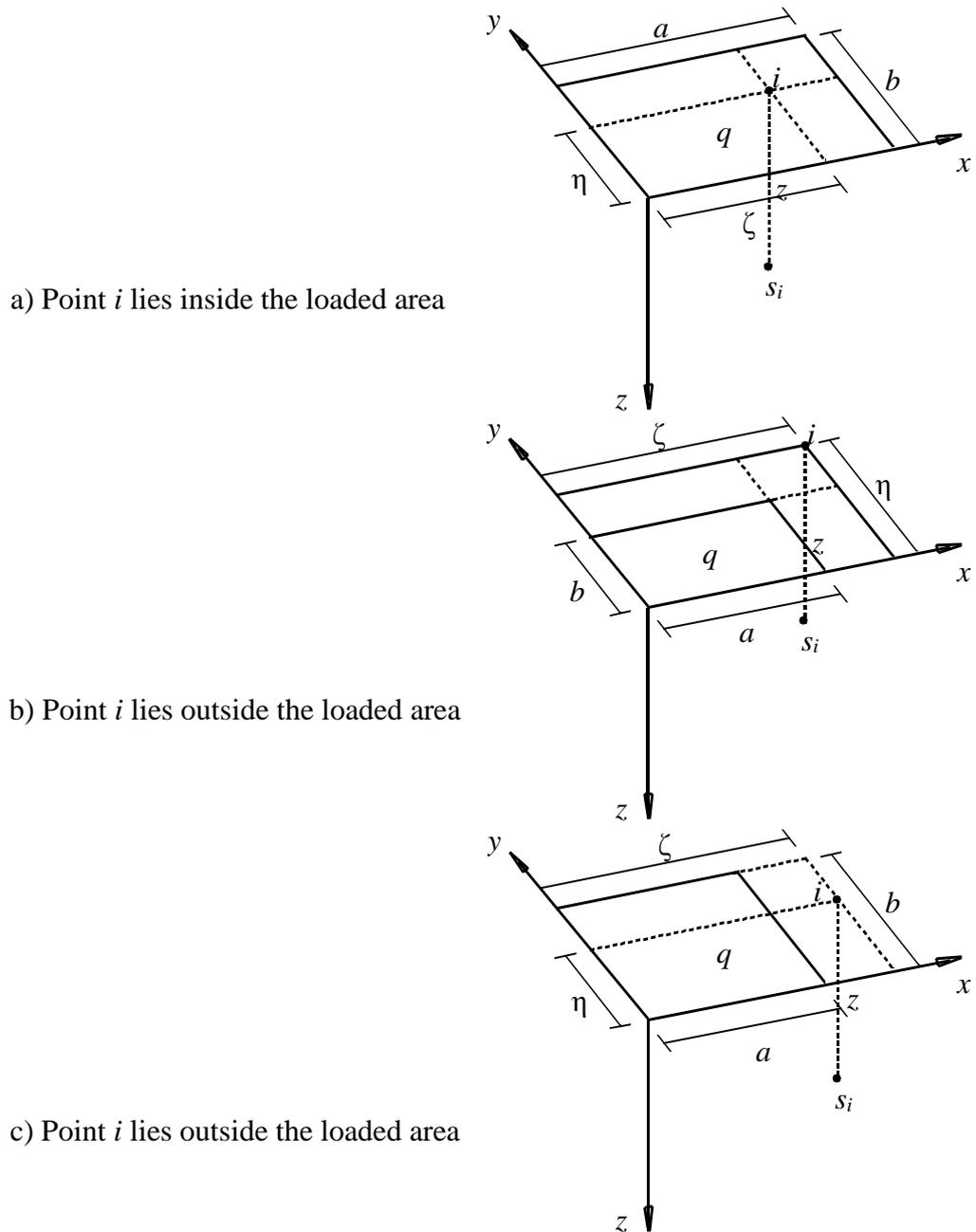
Figure 1.18   Superposition of four loaded areas to find the settlement at any point i

Formulation of the flexibility matrix for layered soil medium
Determination of the settlement $s_{i,i}$

Because the formula of *Steinbrenner* (1934) is valid for surface loadings, where the plate element is supposed to be rigid with respect to the subsoil, compatibility between plate displacement and surface settlement is required. *Graßhoff* (1955) defined the Characteristic point to be that point of a surface area loaded by a uniformly distributed pressure, where the settlement due to that pressure is identical with the displacement of a rigid foundation of similar dimensions and loading. For a rectangular element $a \times b$, the characteristic point takes the coordinates $a_c = 0.87a$ and $b_c = 0.87b$ as shown in Figure 1.19.
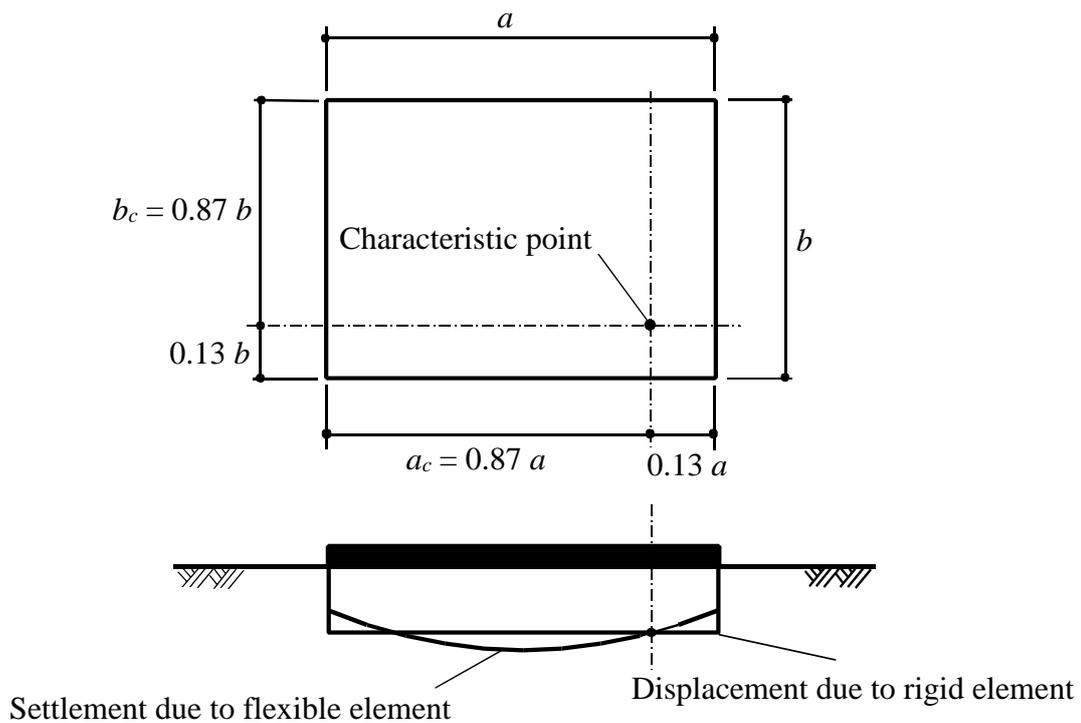
Figure 1.19   Characteristic point of the settlement

Considering the settlement under the characteristic point for the loaded area $a_i * b_i$ around a node i, the settlement $s_{i,i}$ of a node i, due to contact force Q_i on that node for layered soil medium can be expressed as

$$s_{i,i} = \frac{Q_i}{a_i\, b_i}\left(\frac{f^{(1)}}{E_s^{(1)}} + \sum_{l=2}^{n} \frac{\Delta f^{(l)}}{E_s^{(l)}} \right) = c_{i,i}\, Q_i \tag{1.61}$$

The ratio between the settlement $s_{i,i}$ of a point i and the contact force Q_i at that point is termed the flexibility coefficient $c_{i,i}$ [m/kN]. It can be recognized as the settlement of a point i due to a unit load at that point.

Determination of the settlement $s_{i,k}$

For a loaded area $a_k \times b_k$ around node k, Figure 1.20, the settlement $s_{i,k}$ of a node i, due to contact force Q_k on node k for layered soil medium can be expressed as

$$s_{i,k} = \frac{Q_k}{a_k\, b_k}\left(\frac{f^{(1)}}{E_s^{(1)}} + \sum_{l=2}^{n} \frac{\Delta f^{(l)}}{E_s^{(l)}} \right) = c_{i,k}\, Q_k \tag{1.62}$$

The ratio between the settlement $s_{i,k}$ of a point i and the contact force Q_k at a point k is termed the flexibility coefficient $c_{i,i}$ [m/kN]. It can be recognized as the settlement of a point i due to a unit load at a point k.
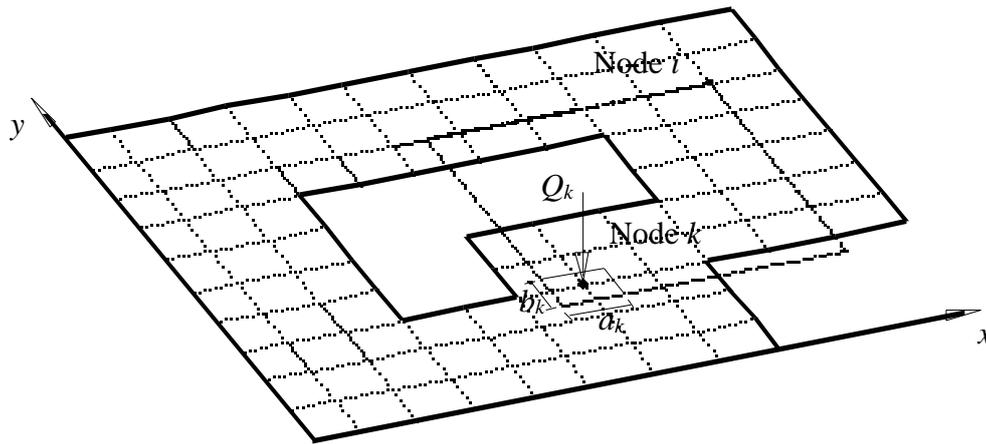
Figure 1.20   Settlement $s_{i,k}$ of a node i due to contact force $Q_k = q_k\, a_k\, b_k$ at node k

It can be noticed that the flexibility coefficients for isotropic elastic half-space medium may be obtained by applying the layered soil medium. In this case, the soil layer must extend to a depth that can be considered as an infinite depth (for example $z \approx 10^{10}$ [m]). In the program *ELPLA*, layered soil medium is available in methods 4, 6, 7, 8 and 9 while isotropic elastic half-space medium is available only in method 5.

Assembling of the flexibility matrix for layered soil medium

To find the settlement s_i at a node i, Equation 1.61 is applied for that node i, while Equation 1.62 is applied for the other remaining nodes considering contact forces over nodes. For a set of grid points of Finite elements-mesh, the settlement at a point i is obtained from

$$s_i = s_{i,1} + s_{i,2} + s_{i,3} + \dots + s_{i,n}$$
$$= c_{i,1}\, Q_1 + c_{i,2}\, Q_2 + c_{i,3}\, Q_3 + \dots + c_{i,n}\, Q_n \tag{1.63}$$

Equation 1.63 in series form is

$$s_i = \sum_{k=1}^{n} c_{i,k} \, Q_k \qquad (1.64)$$

Equation 1.64 for the entire foundation in matrix form is

$$
\begin{Bmatrix} s_1 \\ s_2 \\ s_3 \\ \\ \ldots \\ s_n \end{Bmatrix}
=
\begin{bmatrix}
c_{1,1} & c_{1,2} & c_{1,3} & & \ldots & c_{1,n} \\
c_{2,1} & c_{2,2} & c_{2,3} & & \ldots & c_{2,n} \\
c_{3,1} & c_{3,2} & c_{3,3} & & \ldots & c_{3,n} \\
& & & & & \\
\ldots & \ldots & \ldots & & \ldots & \ldots \\
c_{n,1} & c_{n,2} & c_{n,3} & & \ldots & c_{n,n}
\end{bmatrix}
\begin{Bmatrix} Q_1 \\ Q_2 \\ Q_3 \\ \\ \ldots \\ Q_n \end{Bmatrix}
\qquad (1.65)
$$

Equation 1.65 is simplified to

$$\{s\} = [c]\{Q\} \qquad (1.66)$$

To assemble the flexibility matrix of the soil $[c]$, each node is loaded by a unit contact force and the resulting settlements in all remaining nodes and in the loaded node are calculated. Inverting the flexibility matrix $[c]$, gives the $[n \times n]$ stiffness matrix of the soil $[k_s]$ corresponding to the contact forces at the n nodal points such that

$$\{Q\} = [k_s]\{s\} \qquad (1.67)$$

Complete stiffness formulation for layered soil medium

The foundation will deflect under the action of the total external forces $\{F\}$ due to known applied loads $\{P\}$ and the unknown soil reactions $\{Q\}$, where

$$\{F\} = \{P\} - \{Q\} \qquad (1.68)$$

The following matrix equation expresses the equilibrium of the raft-soil system

$$[k_p]\{\delta\} = \{P\} - \{Q\} \qquad (1.69)$$

Considering the compatibility of deformation between the plate and the soil medium, where the soil settlement s_i is equal to the plate deflection w_i, Equation 1.67 for Continuum model can be substituted into Equation 1.69 as

$$\big[[k_p] + [k_s]\big]\{\delta\} = \{P\} \qquad (1.70)$$

Equation 1.70 shows that the stiffness matrix of the whole raft-soil system is the sum of the plate and the soil stiffness matrices, $[k_p] + [k_s]$.

It should be noticed that the matrix $[k_s]$ is not compatible with the matrix $[k_p]$, because the degrees of freedom in Equation 1.67 differ from that in Equation 1.69. To overcome this problem, Equation 1.67 can be treated by extending the row and column of matrix $[k_s]$ in the same manner as the matrix $[k_p]$. Consequently, the operation of matrix equations can then be accepted.

Equation solver for layered soil medium

It should be noticed that the matrix $[k_s]$ is full unsymmetrical matrix for layered soil medium. Therefore, the total stiffness matrix for the raft and the soil is also full unsymmetrical matrix.

The system of linear equations is solved by *Gauss* elimination-technique. Since the total stiffness matrix is a full matrix, the equation solver 1.70 takes long computation time by applying this method. The unknown variables in Equation 1.70 are the nodal displacements w_i ($w_i = s_i$) and the nodal rotations θ_{xi} and θ_{yi} about the *x*- and *y*-directions. After solving the system of linear equation 1.70, substituting the obtained settlements s_i in Equation 1.67, gives the unknown contact forces Q_i.

1.3.7 Modulus of compressibility method for rigid raft on layered soil medium (method 8 - Layered soil medium - Continuum model)

In many practice cases, treating the raft as completely rigid raft is convenient. Here, two conclusions can be drawn concerning raft settlement:

- For a raft without moments or without eccentricity about both axes, the settlement will be uniform under the raft

- For a raft with moments, the raft will rotate as a rigid body and there will be differential vertical movement between points on the raft, but all points will remain in the same plane

Therefore, the displacements are considered linearly distributed on the bottom of the raft.

The method developed here considers the interaction between the raft and soil. It represents the soil as layered medium or isotropic elastic half-space medium.

In the general case of a foundation with an arbitrary unsymmetrical shape and loading, according to *Kany* (1972) the unknowns of the interaction problem, Figure 1.21, are:

- n contact pressures q_i
- Rigid body translation of the raft w_o at the centroid
- Rigid body rotation θ_x of the raft about the *x*-axis of the geometry centroid
- Rigid body rotation θ_y of the raft about the *y*-axis of the geometry centroid

To determine these $n + 3$ unknowns, n compatibility equations of rigid raft displacements with the soil settlements at the n nodal points are considered. In addition, the three equations of overall equilibrium of the raft are also considered.

**Formulation of the rigid raft on layered soil medium**
Soil settlements

To describe the method, consider a general raft resting on a layered soil medium (isotropic elastic half-space soil medium may be also applied), Figure 1.21. The contact pressure q_i at a node i under the raft is replaced by equivalent contact force Q_i. For a set of grid points of elements-mesh, the settlement at a point i is obtained from

$$s_i = \sum_{k=1}^{n} c_{i,k}\, Q_k \tag{1.71}$$

Considering the entire foundation, Equation 1.71 can be rewritten in matrix form as

$$\{s\} = [c]\{Q\} \tag{1.72}$$

Inverting the flexibility matrix $[c]$, gives the stiffness matrix of the soil $[k_s]$ corresponding to the contact forces at the n nodal points such that

$$\{Q\} = [k_s]\{s\} \tag{1.73}$$
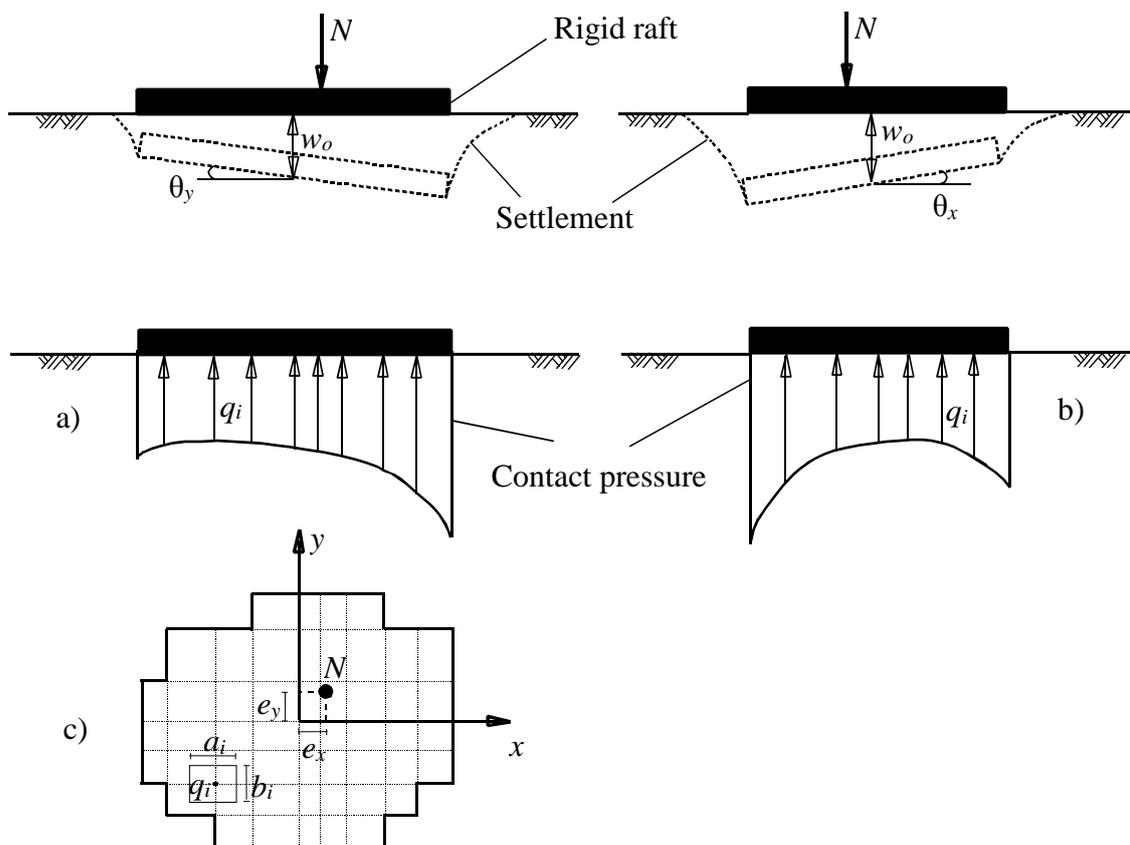
Figure 1.21   Contact pressure distribution and soil settlement under a rigid raft
              a) Section parallel to x-direction
              b) Section parallel to y-direction
              c) Foundation plan

Rigid body translation w_o and rotations θ_{xo} and θ_{yo}

Due to the raft rigidity, the following linear relation (plane translation) expresses the settlement s_i at a node i that has coordinates (x_i, y_i) from the geometry centroid

$$s_i = w_o + x_i \tan\theta_y + y_i \tan\theta_x \tag{1.74}$$

Equation 1.74 is rewritten in matrix form for the entire foundation as

$$\begin{Bmatrix} s_1 \\ s_2 \\ s_3 \\ \\ ... \\ s_n \end{Bmatrix} = \begin{bmatrix} 1 & x_1 & y_1 \\ 1 & x_2 & y_2 \\ 1 & x_3 & y_3 \\ \\ ... & ... & ... \\ 1 & x_n & y_n \end{bmatrix} \begin{Bmatrix} w_o \\ \tan\theta_y \\ \tan\theta_x \end{Bmatrix} \tag{1.75}$$

Equation 1.75 is simplified to

$$\{s\} = [X]^T \{\Delta\} \tag{1.76}$$

Equilibrium of the vertical forces

The resultant N due to external vertical forces acting on the raft must be equal to the sum of contact forces

$$N = Q_1 + Q_2 + Q_3 + ... + Q_n \tag{1.77}$$

Equilibrium of the moments

The moment due to resultant N about the y-axis must be equal to the sum of moments due to contact forces about that axis

$$N\,e_x = Q_1\,x_1 + Q_2\,x_2 + Q_3\,x_3 + ... + Q_n\,x_n \tag{1.78}$$

Similarly, the equilibrium equation for moments about the x-axis is

$$N\,e_y = Q_1\,y_1 + Q_2\,y_2 + Q_3\,y_3 + ... + Q_n\,y_n \tag{1.79}$$

Equations 1.77, 1.78 and 1.79 are rewritten for the entire foundation in matrix form as

$$\begin{Bmatrix} N \\ N\,e_x \\ N\,e_y \end{Bmatrix} = \begin{bmatrix} 1 & 1 & 1 & & \dots & 1 \\ x_1 & x_2 & x_3 & & \dots & x_n \\ y_1 & y_2 & y_3 & & \dots & y_n \end{bmatrix} \begin{Bmatrix} Q_1 \\ Q_2 \\ Q_3 \\ \\ \dots \\ Q_n \end{Bmatrix}$$ (1.80)

Equation 1.80 is simplified to

$$\{N\} = [X]\{Q\}$$ (1.81)

Substituting Equation 1.73 and 1.76 in Equation 1.81 gives the following linear system of equations

$$\{N\} = [X]\{k_s\}[X]^T \{\Delta\}$$ (1.82)

Solving this system of linear equations 1.82, gives w_o, $\tan\theta_x$ and $\tan\theta_y$.

Substituting these values in Equation 1.76, then in Equation 1.73 gives the following matrix equation to find the n unknown contact forces

$$\{Q\} = \{k_s\}[X]^T \{\Delta\}$$ (1.83)

Substituting also the values w_o, $\tan\theta_x$ and $\tan\theta_y$ in Equation 1.72, gives the n settlements.

Case of uniform settlement

For a raft without moments or without eccentricity about both axes, the settlement will be uniform ($s_i = w_o$) and the raft will not rotate ($\theta_{xo} = \theta_{yo} = 0$). Therefore, the unknowns of the problem reduce to n contact pressures q_i and rigid body translation w_o.

Derivation of uniform settlement w_o

The derivation of the uniform settlement for the rigid raft can be carried out by equating the settlement s_i by uniform settlement w_o for all nodes in Equation 1.73. In this case, the contact forces can be rewritten as a function in the terms $k_{i,j}$ of the soil stiffness matrix as follows

$$\left.\begin{aligned} Q_1 &= k_{1,1}\,w_o + k_{1,2}\,w_o + k_{1,3}\,w_o + \dots + k_{1,n}\,w_o \\ Q_2 &= k_{2,1}\,w_o + k_{2,2}\,w_o + k_{2,3}\,w_o + \dots + k_{2,n}\,w_o \\ Q_3 &= k_{3,1}\,w_o + k_{3,2}\,w_o + k_{3,3}\,w_o + \dots + k_{3,n}\,w_o \\ \\ \\ Q_n &= k_{n,1}\,w_o + k_{n,2}\,w_o + k_{n,3}\,w_o + \dots + k_{n,n}\,w_o \end{aligned}\right\}$$ (1.84)

Carrying out the summation of the all contact forces

$$\sum_{i=1}^{n} Q_i = w_o \sum_{i=1}^{n} \sum_{j=1}^{n} k_{i,j} \qquad (1.85)$$

The rigid body translation w_o, which equals to the settlement s_i at all nodes, is obtained from

$$w_o = \frac{\displaystyle\sum_{i=1}^{n} Q_i}{\displaystyle\sum_{i=1}^{n} \sum_{j=1}^{n} k_{i,j}} = \frac{N}{\displaystyle\sum_{i=1}^{n} \sum_{j=1}^{n} k_{i,j}} \qquad (1.86)$$

Substituting this value of w_o in Equation 1.73 gives the n unknown contact forces Q_i.

It should be noticed that Equation 1.85 is analogous to the Equation 1.8 for *Winkler*'s model. Therefore, the summation of terms $k_{i,j}$ (= N/w_o) may be used to determine the modulus of subgrade reaction k_s.

1.3.8   Modulus of compressibility method for flexible foundation on layered soil medium (method 9 - Layered soil medium - Continuum model)

If the foundation is perfectly flexible (such as an embankment), then the contact stress will be equal to the gravity stress exerted by the foundation on the underlying soil.

For the set of grid points of the foundation, the soil settlements are

$$\{s\} = [c]\{Q\} \qquad (1.87)$$

If the foundation carries concentrated loads, Equation 1.87 may not be able to determine the vertical stress at a point below the concentrated load. In this case, the system equation of the elastic solution can be used to simulate the flexible foundation by assuming a very small raft rigidity D tends to zero, Equation 1.88

$$D = \frac{E_b \, d^3}{12 \, (1 - v_b^2)} \cong 0 \qquad (1.88)$$

In Equation 1.88, the value of D is nearly equal to zero when for an example $E_b = 1 \times 10^{-8}$ [kN/m^2].

1.4   Symmetrical system

In many practical problems, both the raft and loading are symmetric. *Deninger* (1964) by using the Finite differences and *Haung* (1974) by using the Finite elements analyzed a symmetrically loaded raft by taking into account the condition of symmetry. In this case, the raft system equations can be solved by considering only a part of it rather than the entire raft. A quarter of the raft will be analyzed if the problem is symmetrical about both *x*- and *y*-axes, a half of the raft if the problem is symmetrical about *x*- or *y*-axis. Therefore, the computational time and computer storage can be considerably reduced.

Derivation of flexibility coefficients for symmetrical system

The nodal numbering of the set of grid nodes from 1 to *n* is replaced by another coordinate numbering from (1, 1) to (*N*, *M*) as shown in Figure 1.22.
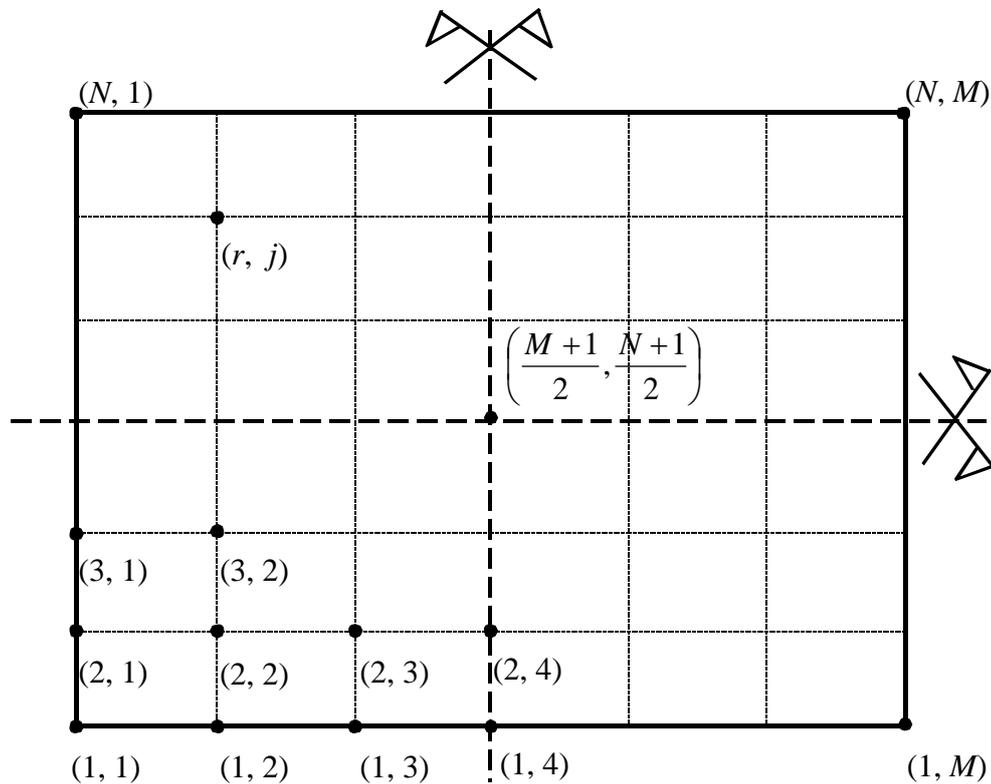
Figure 1.22   Numbering of nodes by symmetrical cases

The settlement equation at a node *i* can be rewritten as

$$s_i = \sum_{k=1}^{n} c_{i,k} \, Q_k = s_{(r,\,j)} = \sum_{(l,m)=(1,1)}^{(N,M)} c_{(r,\,j),(l,m)} \, Q_{(l,m)} \qquad (1.89)$$

where:

$c_{(r,j),(l,m)}$ Flexibility coefficient [m/kN] for a point of coordinate (r, j) due to a unit contact
force $Q_{(l,m)}$ [kN] at a node of coordinate (l, m)

l and r Grid numbers in x-direction
m and j Grid numbers in y-direction

Case of symmetry about the x-axis

Due to symmetry about the x-axis the following conditions are drawn

$$
\begin{aligned}
Q_{(1,1)} &= Q_{(N,1)} & Q_{(2,1)} &= Q_{(N-1,1)} & \cdots \\
Q_{(1,2)} &= Q_{(N,2)} & Q_{(2,2)} &= Q_{(N-1,2)} & \cdots \\
Q_{(1,3)} &= Q_{(N,3)} & Q_{(2,3)} &= Q_{(N-1,3)} & \cdots \\
& & & & \\
Q_{(1,M)} &= Q_{(N,M)} & Q_{(2,M)} &= Q_{(N-1,M)} & \cdots
\end{aligned}
\tag{1.90}
$$

Then, the flexibility coefficients can be rewritten in a form of composite coefficients such as

$$
\begin{aligned}
s_{(r,j)} = & \left[c_{(r,j),(1,1)} + c_{(r,j),(N,1)} \right] Q_{(1,1)} + \left[c_{(r,j),(1,2)} + c_{(r,j),(N,2)} \right] Q_{(1,2)} + \\
& \ldots + \left[c_{(r,j),(\frac{N+1}{2},M)} + c_{(r,j),(\frac{N+1}{2},M)} \right] Q_{(\frac{N+1}{2},M)}
\end{aligned}
\tag{1.91}
$$

Equation 1.91 is simplified to

$$
\begin{aligned}
s_{(r,j)} = & \, c'_{(r,j),(1,1)} \, Q_{(1,1)} + c'_{(r,j),(1,2)} \, Q_{(1,2)} + \\
& \ldots + c'_{(r,j),(\frac{N+1}{2},M)} \, Q_{(\frac{N+1}{2},M)}
\end{aligned}
\tag{1.92}
$$

In general form, the settlement equation in case of symmetry about the x-axis will be

$$
s_{(r,j)} = \sum_{(l,m)=(1,1)}^{(\frac{N+1}{2},M)} c'_{(r,j),(l,m)} \, Q_{(l,m)}
\tag{1.93}
$$

where:

$C'_{(r,j),(l,m)}$ Coefficient of flexibility in case of symmetry about the x-axis

The unknowns in Equation 1.93 are the contact forces $Q_{(1,1)}$ to $Q_{([N+1]/2,M)}$, as total $M \times (N+1)/2$
values.

Case of symmetry about the *y*-axis

Due to symmetry about the *y*-axis the following conditions are drawn

$$
\begin{aligned}
Q_{(1,1)} &= Q_{(1,M)} & Q_{(1,2)} &= Q_{(1,M-1)} & \cdots \\
Q_{(2,1)} &= Q_{(2,M)} & Q_{(2,2)} &= Q_{(2,M-1)} & \cdots \\
Q_{(3,M)} &= Q_{(3,M)} & Q_{(3,2)} &= Q_{(3,M-1)} & \cdots \\
& & & & \\
Q_{(N,1)} &= Q_{(N,M)} & Q_{(N,2)} &= Q_{(N,M-1)} & \cdots
\end{aligned}
\tag{1.94}
$$

Then, the flexibility coefficients can be rewritten in a form of composite coefficients such as

$$
s_{(r,j)} = \left[c_{(r,j),(1,1)} + c_{(r,j),(1,M)} \right] Q_{(1,1)} + \left[c_{(r,j),(1,2)} + c_{(r,j),(1,M-1)} \right] Q_{(1,2)} +
$$
$$
\ldots + \left[c_{(r,j),(N,\frac{M+1}{2})} + c_{(r,j),(N,\frac{M+1}{2})} \right] Q_{(N,\frac{M+1}{2})}
\tag{1.95}
$$

Equation 1.95 is simplified to

$$
s_{(r,j)} = c'_{(r,j),(1,1)} \, Q_{(1,1)} + c'_{(r,j),(1,2)} \, Q_{(1,2)} +
$$
$$
\ldots + c'_{(r,j),(N,\frac{M+1}{2})} \, Q_{(N,\frac{M+1}{2})}
\tag{1.96}
$$

In general form, the settlement equation in case of symmetry about the *y*-axis will be

$$
s_{(r,j)} = \sum_{(l,m)=(1,1)}^{(N,\frac{M+1}{2})} c'_{(r,j),(l,m)} \, Q_{(l,m)}
\tag{1.97}
$$

where:
$C'(r, j), (l, m)$ Coefficient of flexibility in case of symmetry about the *y*-axis

The unknowns in the Equation 1.97 are the contact forces $Q_{(1,\ 1)}$ to $Q_{(N,\ [M+1]/2)}$, as total $N \times (M+1)/2$ values.

Case of symmetry about *x*-and *y*-axes

Due to symmetry about both *x*- and *y*-axes the following conditions are drawn

$$
\left.
\begin{aligned}
Q_{(1,1)} &= Q_{(1,M)} = Q_{(N,1)} = Q_{(N,M)} \\
Q_{(1,2)} &= Q_{(1,M-1)} = Q_{(N,2)} = Q_{(N,M-1)} \\
Q_{(1,3)} &= Q_{(1,M-2)} = Q_{(N,3)} = Q_{(N,M-2)} \\
&\quad\quad ... \\
&\quad\quad ... \\
&\quad\quad ...
\end{aligned}
\right\}
\tag{1.98}
$$

Then, the flexibility coefficients can be rewritten in a form of composite coefficients such as

$$
s_{(r,j)} = \left[c_{(r,j),(1,1)} + c_{(r,j),(1,M)} + c_{(r,j),(N,1)} + c_{(r,j),(N,M)} \right] Q_{(1,1)}
$$

$$
+ \left[c_{(r,j),(1,2)} + c_{(r,j),(1,M-1)} + c_{(r,j),(N,2)} + c_{(r,j),(N,M-1)} \right] Q_{(1,2)}
\tag{1.99}
$$

$$
+ ... + \left[4\, c_{(r,j),(\frac{N+1}{2},\frac{M+1}{2})} \right] Q_{(\frac{N+1}{2},\frac{M+1}{2})}
$$

Equation 1.99 is simplified to

$$
s_{(r,j)} = c'_{(r,j),(1,1)}\, Q_{(1,1)} + c'_{(r,j),(1,2)}\, Q_{(1,2)} +
$$
$$
... + c'_{(r,j),(\frac{N+1}{2},\frac{M+1}{2})}\, Q_{(\frac{N+1}{2},\frac{M+1}{2})}
\tag{1.100}
$$

In general form, the settlement equation in case of symmetry about both *x*-and *y*-axes will be

$$
s_{(r,j)} = \sum_{(l,m)=(1,1)}^{(\frac{N+1}{2},\frac{M+1}{2})} c'_{(r,j),(l,m)}\, Q_{(l,m)}
\tag{1.101}
$$

where:
$C'_{(r,j),(l,m)}$ Coefficient of flexibility in case of symmetry about both *x*-and *y*-axes

The unknowns in the Equation 1.101 are the contact forces $Q_{(1,\,1)}$ to $Q_{([N+1]/2,\,[M+1]/2)}$, as total $(N+1)\times(M+1)/4$ values.

The settlement equations of the antimetrical cases can be derived in a similar manner to that of symmetrical case.

1.5   Antimetrical system

If the raft is symmetric in shape and unsymmetric in loading, it will be possible to divide this general case of loading into two cases of symmetrical and antimetrical loading as shown in Figure 1.23. Then, the analysis can be carried out for half the raft twice.

Figure 1.23   General case of loading by symmetrical and antimetrical loading

It should be noticed that by using the advantage of symmetry, the original flexibility matrix $[c]$, which has dimension of $[N \times M]^2$ will be reduced to dimension of $[(N+1/2) \times M]^2$, $[N \times (M+1)/2]^2$ and $[(N+1)/2 \times (M+1)/2]^2$ in the cases of symmetry about x-axis, y-axis and double symmetry about both x- and y-axes, respectively.

1.6   Boundary conditions by symmetrical and antimetrical cases

General boundary conditions for analysis of the raft in bending are zero deflections w and rotations θ_x and θ_y along the fixed edge. Zero rotations about the x-axis ($\theta_x = 0$) or the y-axis ($\theta_y = 0$) along the simply supported edge whenever is applicable in direction x or y.

For symmetrical and antimetrical cases of loading some corresponding appropriate boundary conditions must be applied to all nodes on the axis of symmetry as follows:

-       Symmetry about x-axis makes the rotations θ_x for all the nodes along the x-axis to be zero, Figure 1.24a

-       Symmetry about y-axis makes the rotations θ_y for all the nodes along the y-axis to be zero, Figure 1.24b

-       Antisymmetry about the x-axis makes the deflections w for all the nodes along the x-axis to be zero, Figure 1.24c

-       Antisymmetry about the y-axis makes the deflections w for all the nodes along the y-axis

to be zero, Figure 1.24d
This can be easily handled by setting the element values of the corresponding column and row in the entire stiffness matrix zero.


a) Symmtrical case about *x*-axis

b) Symmtrical case about *y*-axis

c) Antiymmtrical case about *x*-axis

d) Antiymmtrical case about *y*-axis
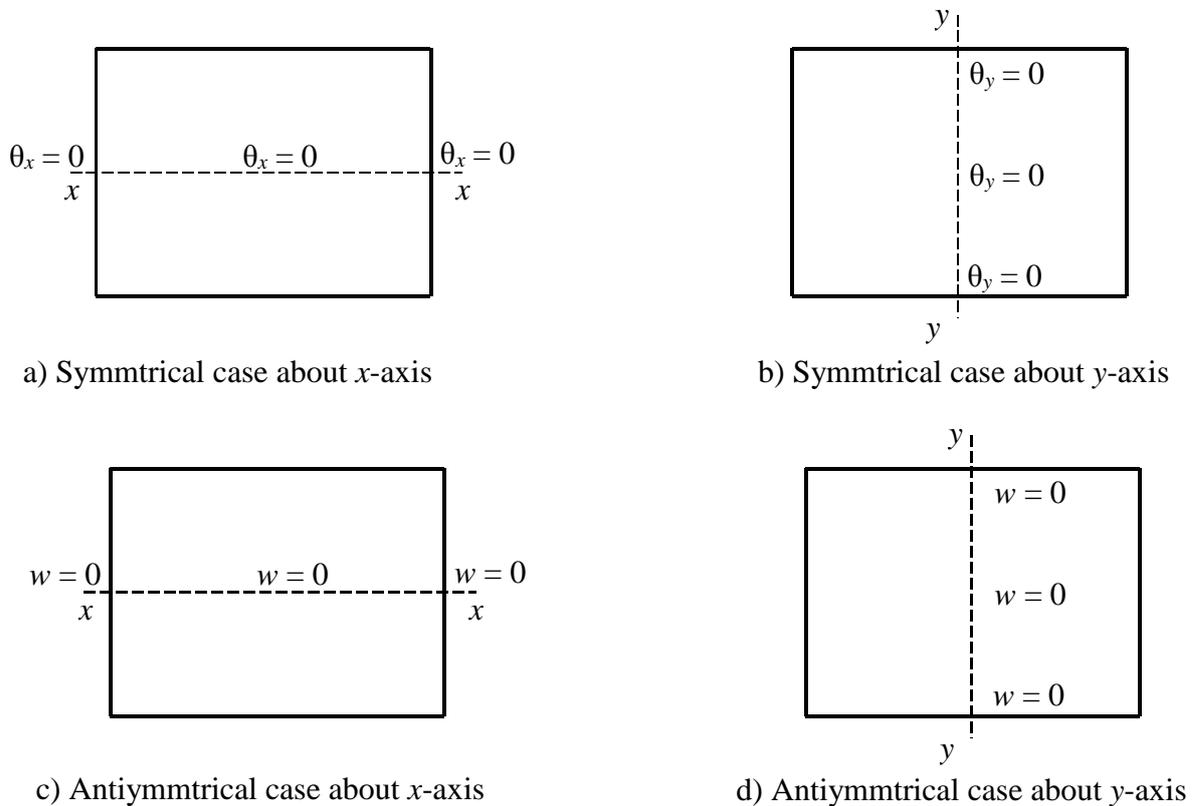
Figure 1.24   Boundary condition for symmetrical and antisymmetrical cases

1.7   Bilinear soil behavior

A simplified way was supposed to improve the deformation behavior of the soil by dividing the stress settlement curve into two regions, Figure 1.25. In the first region the ground will settle until reaching an overburden load q_v according to the modulus of compressibility W_s. In the second region after reaching the load q_v the ground will settle more under load q according to the modulus of compressibility E_s until reaching the total load q_o.
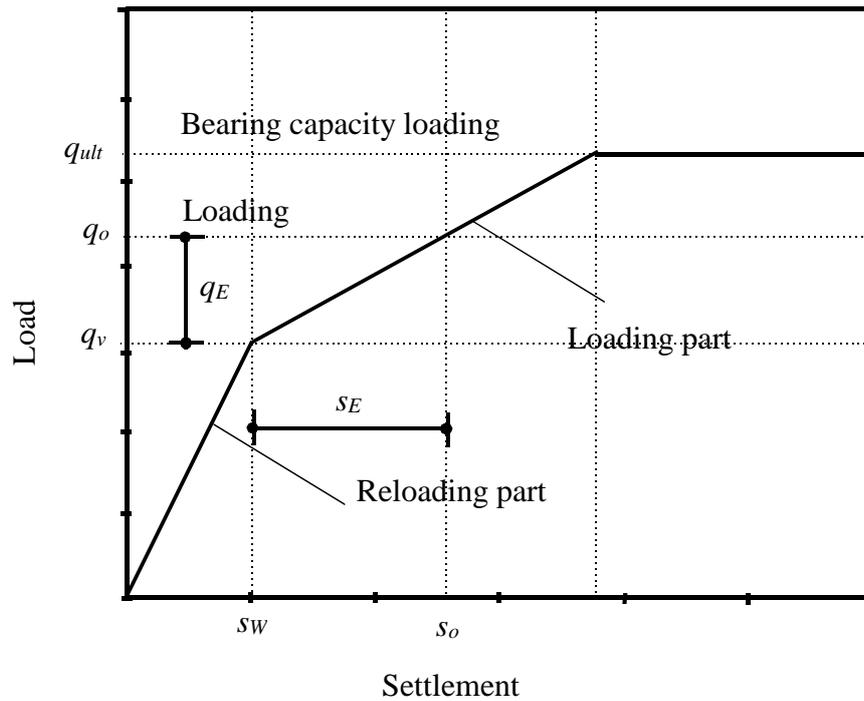
Figure 1.25   Load settlement diagram (bilinear relation)

Therefore, the settlement s_i of the foundation can be derived from two variations such that

$$s_i = s_{Wi} + s_{Ei} \tag{1.102}$$

Equation 1.102 for the entire foundation in matrix form is

$$\{s\} = \{s_W\} + \{s_E\} \tag{1.103}$$

It can be generally said that the total contact pressure on the foundation is given by

$$q_{oi} = q_{vi} + q_{Ei} \tag{1.104}$$

The bilinear relation of the soil deformation may be taken into consideration as follows.

At first it should be carried out a primary calculation by one of the following two cases:

Case 1: $q_{vi} < q_o$ **at all nodes i on the grid of the raft mesh**

The settlement equation will be

$$\{s\} = [c_W]\{Q_v\} + [c_E]\{Q_E\}$$
$$[k_{sE}]\{s\} = [k_{sE}][c_W]\{Q_v\} + \{Q_E\}$$

$$(1.105)$$

Then, the raft equation due to bilinear soil behavior in a matrix form is given by

$$\left[[k_p] + [k_{sW}]\right]\{\delta\} = \{P\} + \left[[k_{sE}][c_W] - [I]\right]\{Q_v\}$$

$$(1.106)$$

Case 2: $q_{vi} > q_o$ **at all nodes i on the grid of the raft mesh**

The settlement equation will be

$$\{s\} = [c_W]\{Q_o\}$$
$$[k_{sW}]\{s\} = \{Q_o\}$$

$$(1.107)$$

Then, the raft equation due to bilinear soil behavior in a matrix form is given by

$$\left[[k_p] + [k_{sW}]\right]\{\delta\} = \{P\}$$

$$(1.108)$$

If one of the above two cases is not existent, an iterative solution for the settlement equation will be necessary.

1.8   Variable foundation levels
1.8.1   Variable foundation levels by neighboring rafts

Sometimes, by determination the influence of the neighboring rafts or the interaction among system of rafts, the foundation levels of the rafts are variable as shown in Figure 1.26. In this case, the foundation levels of the rafts must be related to a specified datum H_m.

The z-value of flexibility coefficient for any soil layer under the raft can be expressed by

$$z_{ikl} = (z_{il} - t_{fi}) - H_{mi} + H_{mk}$$

$$(1.109)$$

It should be noticed that the foundation level H_m under the specified datum is negative.
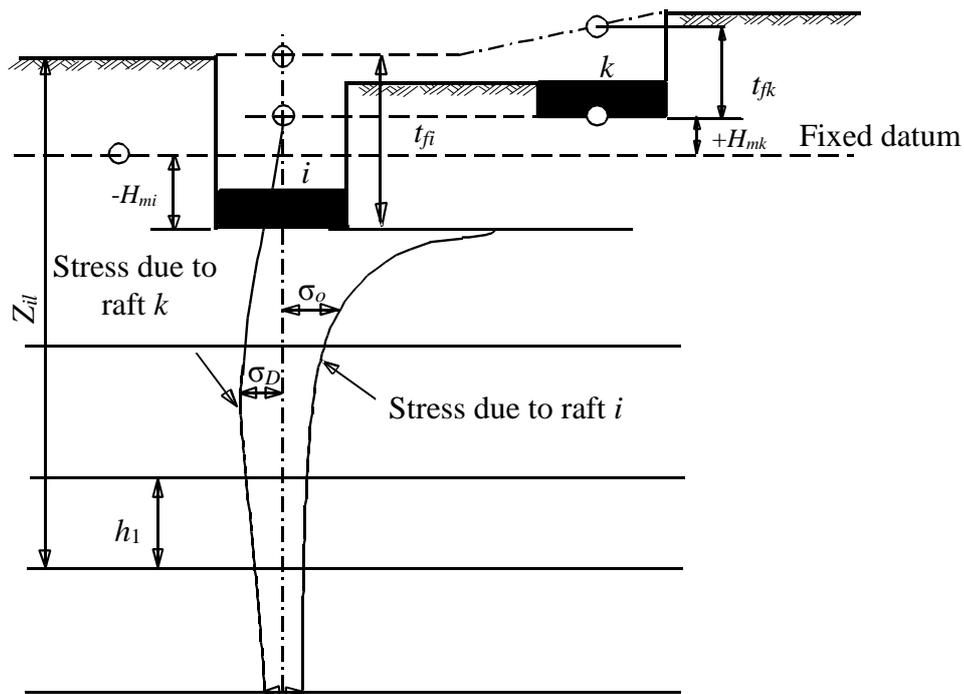
Figure 1.26   Settlement influence of raft k on the raft i

1.8.2   Variable foundation levels with variable raft thickness

By analysis of rafts, there are three possibilities to define the raft thickness:

a)   The raft thickness for the entire raft is constant.
        In this case, there is only one foundation level tf (Figure 1.27a)

b)   Variable raft thickness with constant foundation level.
        In this case, the foundation level tf is also constant (Figure 1.27b)

c)   Variable raft thickness with variable foundation level. In this case, the foundation level is
        variable (Figure 1.27c). The z-value of flexibility coefficient for any soil layer under the
        raft can be expressed by

$$z_{ikl} = (z_{il} - t_{fk}) \tag{1.110}$$
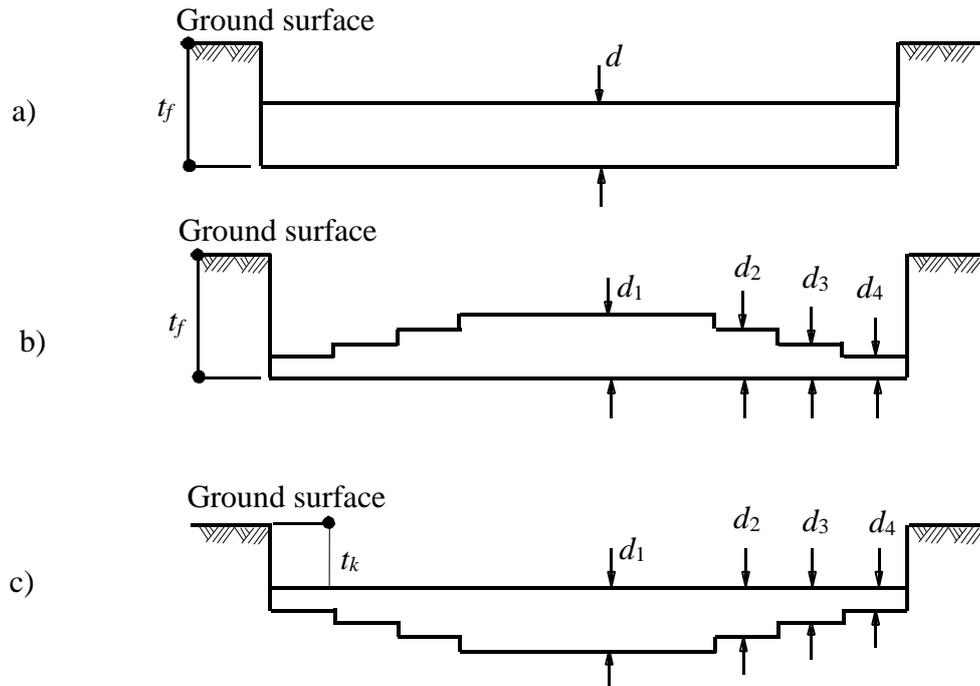
Figure 1.27   Three possibilities concerning raft thickness

1.9   Effect of groundwater pressure

If the water table is located above the foundation, the foundation will be exposed to an additional negative pressure q_w due to the effect of groundwater. In this case, the system equation will be

$$\left[\left[k_p \right] + \left[k_{sW} \right] \right] \{\delta\} = \{P\} - \{Q_w\} \tag{1.111}$$

1.10   Effect of temperature difference

Sometimes, a temperature difference ΔT occurs between the upper and lower surface of the raft. An example for this case is when a fire oven is constructed directly on the raft in an industry structure.

The deformation in the raft due to temperature difference can be evaluated as follows:

The nodal displacement $\{\delta\}_i$ at a node i of the raft must be replaced by $\{\delta\} - \{\Delta\}$, in which

$$\Delta_i = \begin{Bmatrix} t_i \\ 0 \\ 0 \end{Bmatrix}_i \tag{1.112}$$

By assuming the warped surface as part of a sphere, it can be proven from geometry, Figure 1.28, that

$$t_i = \frac{\alpha_T \, \Delta T \, r_i^2}{2d} \quad [m] \tag{1.113}$$

where:

t_i Amount of curvature [m] at a node i

α_T Coefficient of thermal expansion of concrete [1/°C]

r_i Distance [m] from a node i to the center of the raft where curling is zero

d Thickness of the raft [m]

ΔT Temperature difference between the upper and lower surface of the raft in which
        $\Delta T = T_o - T_u$ [°C]

T_o Temperature at the upper surface of the raft [°C]

T_u Temperature at the lower surface of the raft [°C]

Positive deflection when the raft warps down with a temperature at the top bigger than that at the bottom. Due to temperature difference, the total settlement on the foundation can be expressed as

$$\{s\} = \{s_o\} + \{s_T\} \tag{1.114}$$

where:

$\{s_o\}$ Vector of the settlement due to the loads acting on the foundation

$\{s_T\}$ Vector of the additional displacement due to the temperature difference

Then, the raft equation due to influence of temperature difference in matrix form is

$$\left[[k_p] + [k_s] \right] \{\delta\} = \{P\} + [k_s]\{s_T\} \tag{1.115}$$

$$R_s = \frac{d}{\alpha_T \, \Delta T}$$
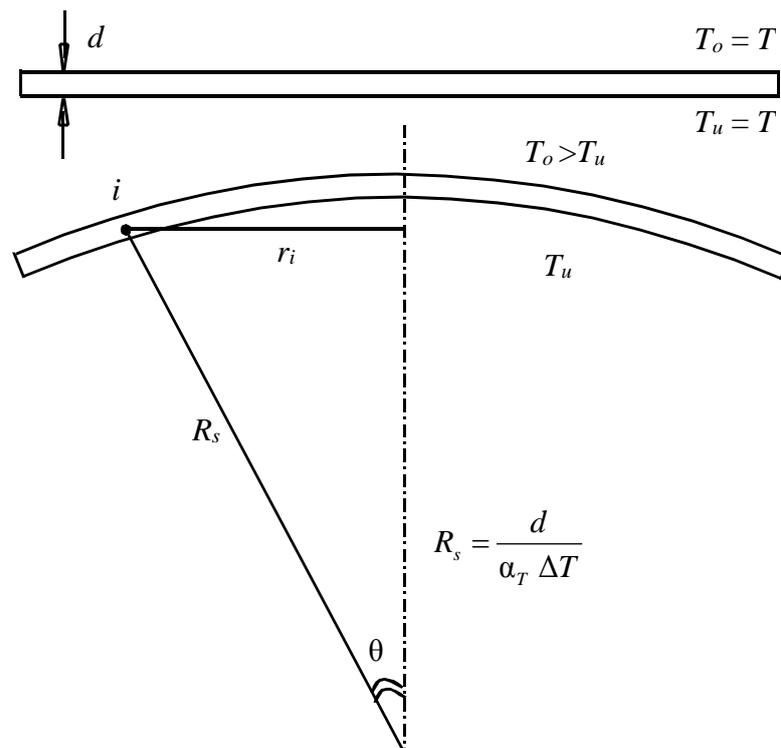
Figure 1.28   Temperature effect on the raft foundation

1.11   Analysis of ribbed raft

The traditional structural analysis of the foundation using Finite elements-method requires two main types of elements. The first type is grid element used to analyze strip foundations or grid foundations. The second type of finite elements is the plate element used to analyze footings or rafts. The conventional methods for analysis of foundations consider only one type of elements.

The combined problems of foundations with others stiffeners were treated by many authors. *Deninger* (1964) presented a method for analysis of rectangular rafts that was stiffened through rigid walls by Finite differences-method. *Zienkiewicz/ Cheung* (1970) introduced a solution for floor slab with edge beams. *Lee/ Brown* (1972) analyzed plane frame on two dimensional foundations by using beam elements for the frame and plate bending elements for the foundation. *Mikhaiel* (1978) considered the effect of shear walls and floor rigidity by using a combination between plate bending and plain stress elements. *Bazaraa/ Shaheen/ Sabry/ Krem* (1991) studied the effect of tie beams on the behavior of the footings. The footings were represented by the plate bending elements, while the tie beams were represented by grid elements. *Bazaraa/ Ghabrial/ Henedy* (1997) studied the effect of boundary retaining walls on the raft behavior by using a mesh of plate bending-plain stress element combinations.

Ribbed raft may be used for many structures with heavy loads or large spans, if a flat level for the first floor is not required. Consequently the volume of concrete is reduced. Such structures are silos and elevated tanks. Although this type of foundation has many disadvantages if used in normal buildings, it is still used by many designers. Such disadvantages are the raft that needs deep foundation level under the ground surface, fill material on the foundation to make a flat level and an additional slab on the fill material to construct the first floor. The use of ribbed raft relates to the simplicity of analysis by hand calculations.

ELPLA was developed to analyze ribbed raft using a combination of two finite element types. The raft is represented by plate bending elements according to the two-dimensional nature of foundation. Grid elements are considered to represent the girder action along the raft. The whole stiffness matrix of the raft with girders is the sum of the two stiffness matrices of the raft and girders.

Ribbed raft can be analyzed using plate elements together with grid elements placed in the region close to plate element boundaries as shown in Figure 1.29. To consider the compatibility of deformation between the plate and grid elements, a grid element that has the same degree of freedom of plate element at each intersection node must be chosen.
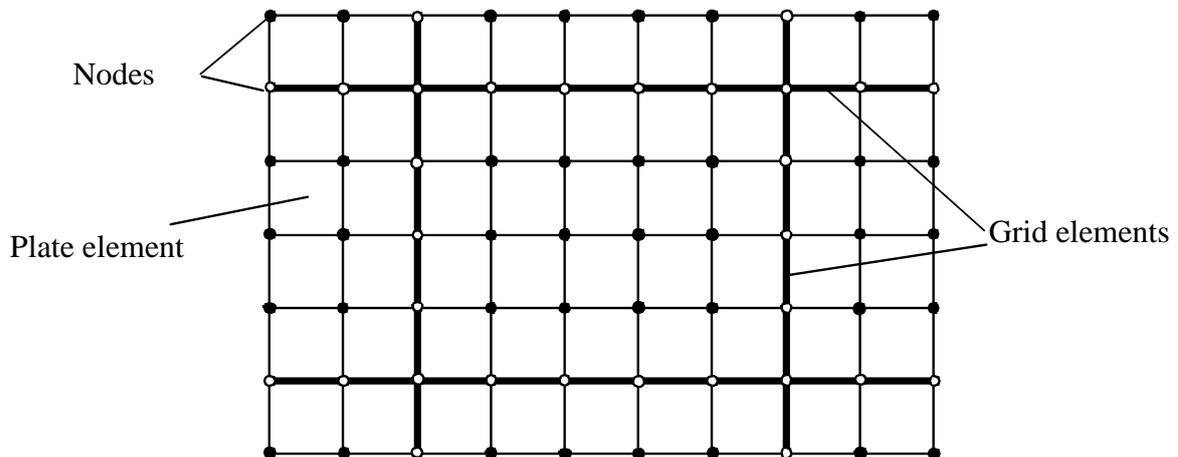
Figure 1.29   Finite elements-net of ribbed raft

The equilibrium of the foundation for simple assumption model is expressed by

$$\left[\left[k_p\right]+\left[k_g\right]\right]\{\delta\}=\{P\}-\{Q\}$$
(1.116)

while for *Winkler*'s and Continuum models is expressed by

$$\left[\left[k_p\right]+\left[k_g\right]+\left[k_s\right]\right]\{\delta\}=\{P\}$$
(1.117)

Chapter 2

Foundations on Irregular Subsoil

Contents

2.1   Introduction

Most of the available solutions used to determine the flexibility coefficient, or the modulus of subgrade reaction, assume that the subsoil consists of a homogeneous layer. In reality, the soil consists of different material features in vertical and horizontal directions. In practice, a number of vertical soil profiles define the soil under the foundation. Each one has multi-layers with different soil materials. Therefore, three-dimensional coefficient of flexibility, or variable modulus of subgrade reaction, must be taken into consideration. *Kany* (1972) determined the two-dimensional flexibility coefficient for beam foundation by determining flexibility coefficients for the existing boring logs first. Then, by interpolation you can obtain the other coefficients outside the boring logs. The following paragraph describes the methods that are available in program *ELPLA* to determine the three-dimensional coefficient of flexibility or variable modulus of subgrade reaction.

2.2   Subareas method

El Gendy (1994) proposed a simplified method to obtain the three-dimensional coefficient of flexibility or variable modulus of subgrade reaction by dividing the whole foundation area into subareas. Each subarea corresponds to one of the soil boring logs as shown in Figure 2.1. The method may be used if there is no great difference in the soil layers of the boring logs.
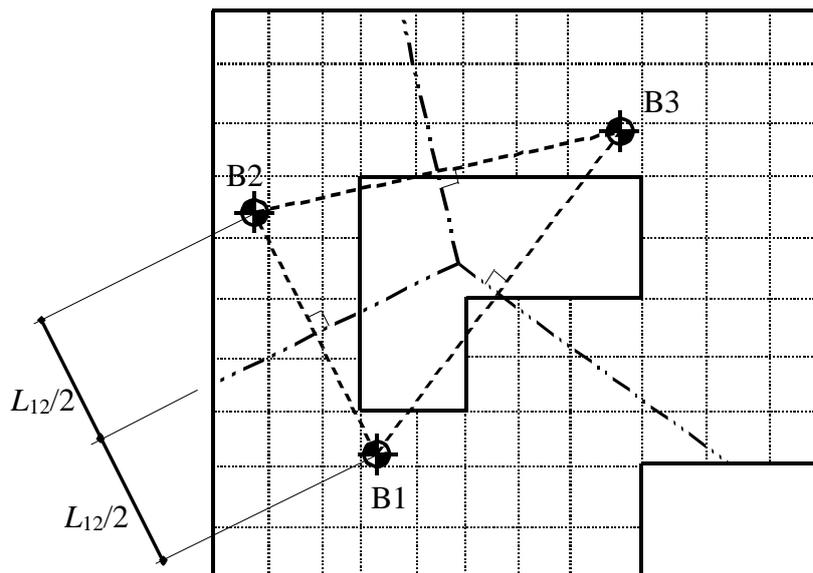
Figure 2.1   Boring locations and subareas

2.3   Interpolation method

Kany/ El Gendy (1995) proposed an accurate method to determine the three-dimensional flexibility coefficient or variable modulus of subgrade reaction for irregular foundation by interpolation, as described below.

2.3.1   Determination of variable modulus of subgrade reaction k_s

Initially, a number of main moduli k_{sm} equal to the number of boring logs should be determined. Each modulus corresponds to one of the soil boring logs and is calculated from the elastic material of that boring.

The following steps and Figure 2.2 describe the determination of the main modulus k_{sm}:

i)   First, assume average or linear distribution of contact pressure q_i on the bottom of the foundation

ii)   Find the soil settlements s_i due to assumed contact pressures. According to *Ohde* (1942), the settlement is given by

$$s_i = \sum_{j=1}^{n} c_{i,j}\, q_j \tag{2.1}$$

where:
$c_{i,j}$ flexibility coefficient of a node i due to a unit load at field j

iii)   Find the nodal modulus k_i at each node on the bottom of the foundation due to the above soil settlements and pressures. According to *Winkler* (1867), the modulus k_i at node i is given by

$$k_i = \frac{q_i}{s_i} \tag{2.2}$$

iv)   Find the mean modulus k_{sm} for the whole foundation area of nodes n

$$k_{sm} = \frac{1}{n} \sum_{i=1}^{n} k_i \tag{2.3}$$

The steps ii to iv are repeated for each boring.

Linear soil pressure

Settlement due to linear soil pressure

Nodal modulus of subgrade reaction
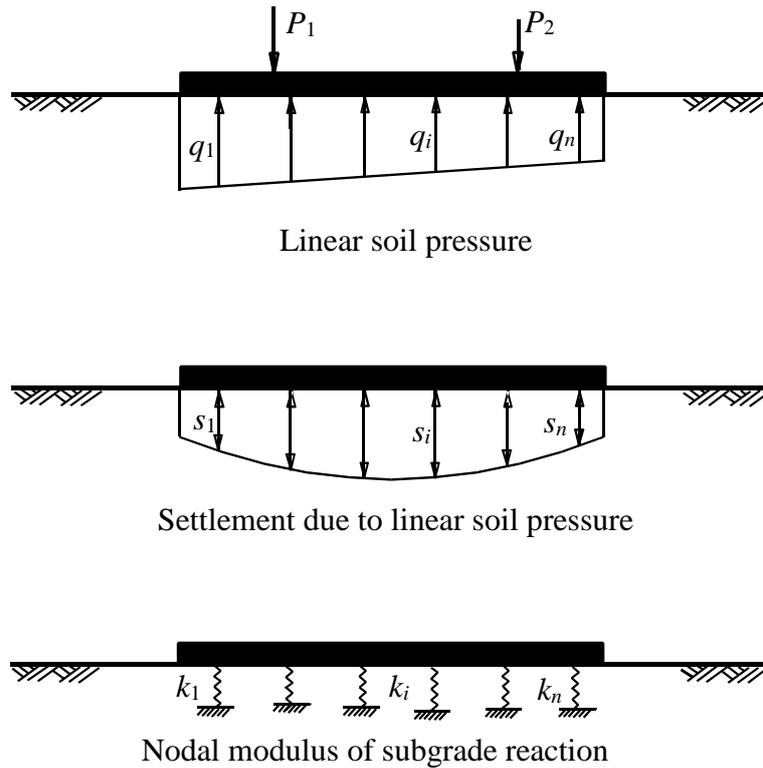
Figure 2.2   Determination of main modulus k_{sm}

Once the mean moduli k_{sm} have been calculated, the variable modulus of subgrade reaction k_s can be determined for all nodes on the bottom of the slab as follows:

It is assumed that the foundation area is divided into three region types as shown in Figure 2.3.

Type I
This region is a triangular region. Three boring logs confine such a region. To determine the modulus k_s for a node lying at a point (x, y) in a triangular region, assumes a plane function passed through the three boring logs to represent the modulus k_s such that

$$k_s = a + bx + cy \qquad (2.4)$$

Such a function will involve three undetermined coefficients: a, b and c. These coefficients can be determined using a system of three linear equations consisting of the known mean moduli k_{sm} and coordinates (x, y) for the three boring logs. Figure 2.3 illustrates an example of region type I through the dark shaded area, which is confined by boring logs B1, B3 and B4.

Type II

One or more sides of the foundation and two boring logs confine this region. Using a linear interpolation between the mean moduli k_{sm} for the two boring logs can obtain the modulus k_s for a node lying in this region. Equation 2.5 and Figure 2.3 indicate an example for region type II through the area confined by boring logs B1, B4 and foundation sides.

$$k_s = k^1{}_{sm} + \frac{\eta}{l}\left(k^2{}_{sm} - k^1{}_{sm}\right)$$

(2.5)

where:

$k^1{}_{sm}$ and $k^2{}_{sm}$	Mean moduli of boring logs B1 and B2, respectively
l	Distance between boring B1 and B2
η	Distance between the node and boring B1

Type III

One or more sides of the foundation and one boring confine this region. The modulus k_s for a node lying in this region is equal to the mean modulus k_{sm} of that boring. Figure 2.3 indicates an example for region type III through the area confined by boring B3 and foundation sides.
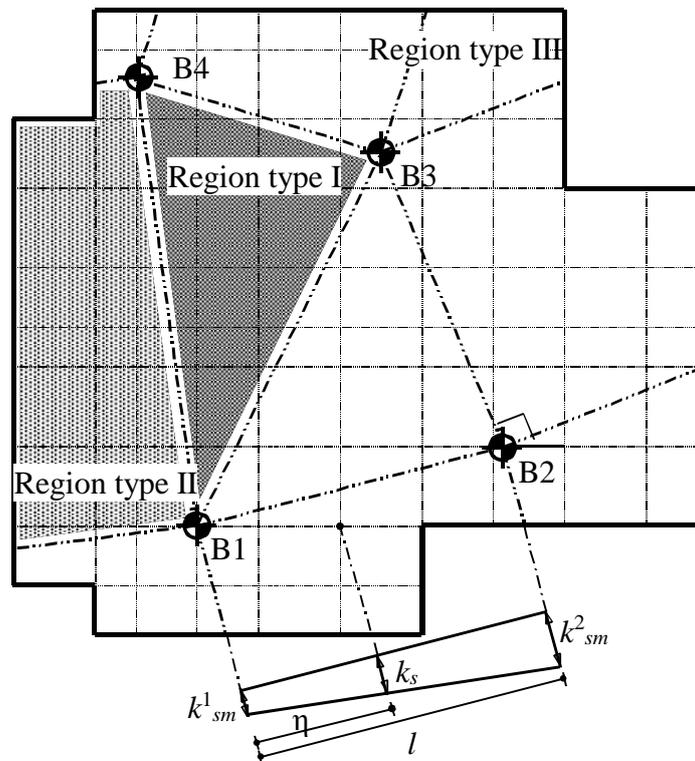
Figure 2.3   Boring locations and region types

2.3.2   Determination of three-dimensional coefficient of flexibility $c_{i,j}$

In a similar way to the previous analysis for *Winkler*'s model, the foundation area is divided into the same three region types. Equation 2.4 for region type I can be rewritten as

$$c_{i,j} = a + bx + cy \qquad\qquad (2.6)$$

As by determination of the main moduli k_{sm} for *Winkler*'s model, the main flexibility coefficients $c_{m\,i,j}$ are determined for boring logs. Then, the undetermined coefficients a, b and c in this case, are obtained from the mean flexibility coefficients $c_{m\,i,j}$ of the three boring logs and their coordinates (x, y). Equation 2.5 for region type II can be rewritten as

$$c_{i,j} = c^1_{m\,i,j} + \frac{\eta}{l}\left(c^2_{m\,i,j} - c^1_{m\,i,j}\right) \qquad\qquad (2.7)$$

where:
$c^1_{m\,i,j}$ and $c^2_{n\,i,j}$ Mean flexibility coefficients of boring logs B1 and B2, respectively

Region type III is the simplest one. The flexibility coefficient $c_{i,j}$ of this region is determined from the material of its corresponding boring.

It is important to note that:

-        If only two boring logs define the subsoil under the foundation or the boring logs lie in the same line, region type I will be eliminated

-        However the above analysis of three dimensional subsoil is derived for isolated foundation, but it is also possible to use this analysis for system of footings or foundations as shown in Figure 2.4
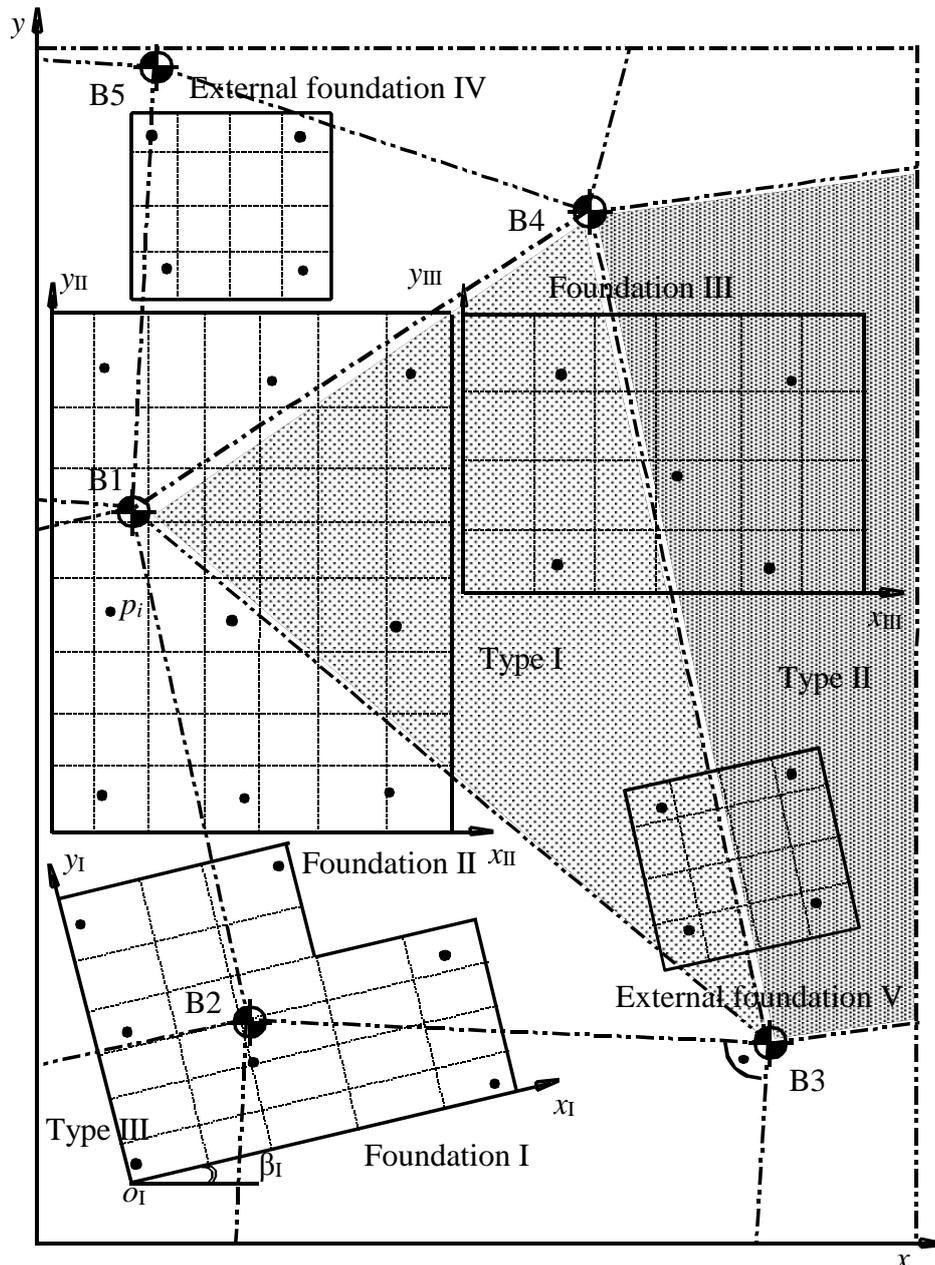
Figure 2.4   System of three foundations I, II and III with two additional
                       external foundations IV and V on irregular subsoil

2.3.3   Numbering of boring logs

The arrangement of subareas or triangle regions leads to different results of modulus of subgrade reactions or flexibility coefficients. Therefore, a role may be used here to set the subareas for the subareas method or triangle regions for the interpolation method automatically. According to the role, defining a boring as pole for the other boring logs is necessary. This boring must be numbered by No. 1. Figure 2.5 shows different arrangements of triangle regions when five boring logs define the subsoil.
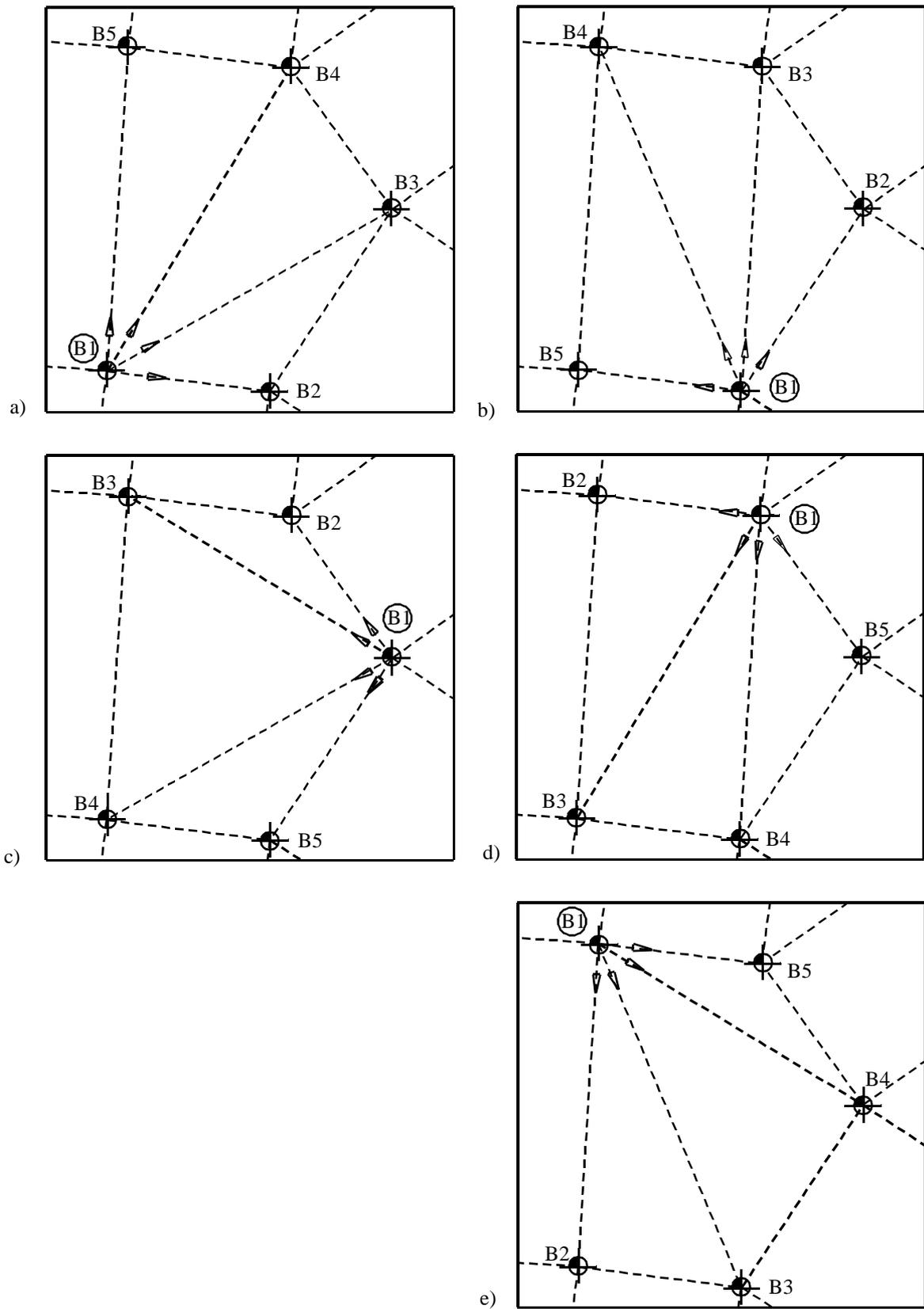
Figure 2.5   Different arrangements of triangle regions a) to e)

2.3.4   Determination of limit depth for irregular subsoil

The assumption of isotropic elastic half-space soil medium requires an infinite soil layer having the same compressibility under the foundation. Practically, the soil consists of many layers with different soil materials. For layered soil medium the number of layers in a boring to be considered when determining the flexibility coefficient $c_{i,k}$ depends on the level of the rigid surface or on the limit depth z_g where no settlement occurs. The limit depth z_g in a system of foundations is the level of which the stress σ_U reaches a standard ratio ξ of the initial vertical stress σ_V as indicated in Figure 2.6 and Equation 2.8

$$\sigma_U = \zeta \ \sigma_V \tag{2.8}$$

where:

$\sigma_U = \sigma_E + \sigma_D$ Stress due to the foundation load and the external foundation loads [kN/m²]
σ_E Stress due to the foundation load [kN/m²]
σ_D Stress due to the external foundation loads [kN/m²]
$\sigma_V = \Sigma \gamma z$ Stress due to the self-weight of the soil layers [kN/m²]
γ Unit weight of the soil layer [kN/m³]
z Depth of the soil layer [m]

An examination from *Amman/ Breth* (1972) showed that the values ξ may be taken as $\xi = 0.8$, especially for reloading soil. The standard value of ξ according to DIN 4019 is $\xi = 0.2$.
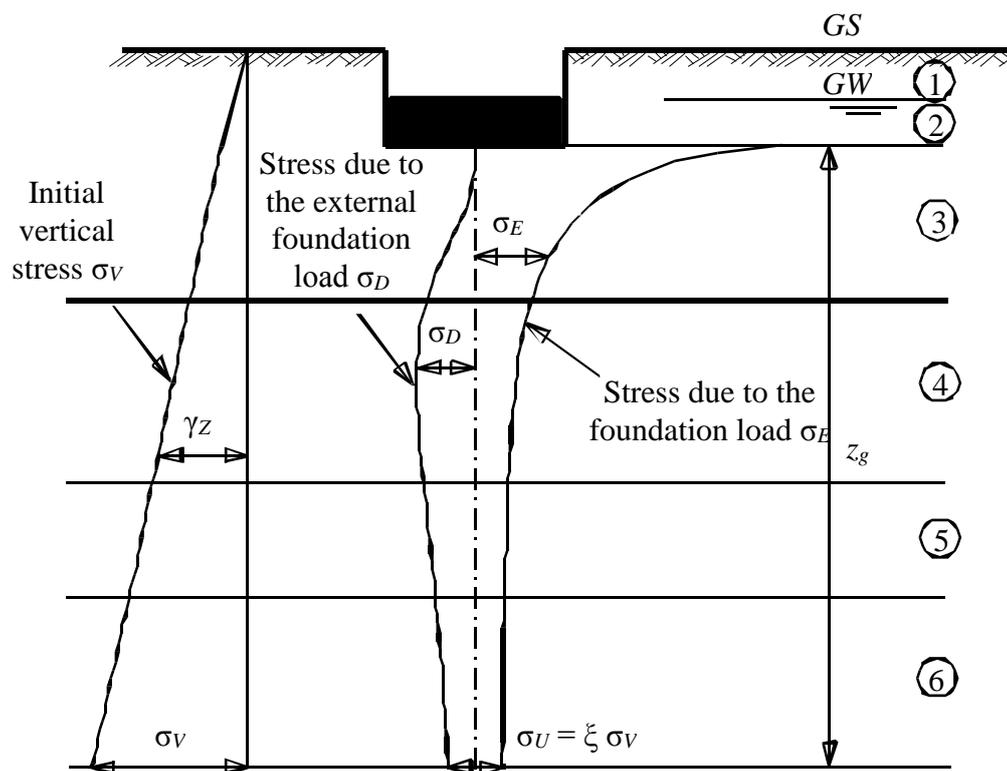

Figure 2.6   Limit depth z_g under a foundation

The problem of the three-dimensional subsoil model is that many boring logs characterize the soil under the system of foundations. *Kany/ El Gendy* (1997) solved this problem for the three-dimensional subsoil model. In which main limit depths for each foundation should be determined. Each limit depth corresponds to one of the soil boring logs and that foundation. It is determined from the material of that boring and the stress under that foundation. The soil pressures under foundations are assumed to be known and distributed uniformly on the bottom of the foundations.

To take into account the irregularity of the subsoil material in *x*- and *y*-directions considering the effective soil layers, the flexibility coefficient $c_{i,k}$ must be determined using the limit depths.

Example 2.1   Analysis of a square raft on irregular subsoil

1   Description of the problem

This example is carried out to show the influence of irregular subsoil on the values of settlements, contact pressures and moments.

The analysis of the square raft is carried out by the two familiar types of soil models: *Winkler*'s and Continuum models for elastic foundations, besides the analysis of rigid raft on Continuum model, using the following three calculation methods:

Method 3   Variable modulus of subgrade reaction method
Method 7   Modulus of compressibility method
Method 8   Rigid raft on compressible subsoil

A square raft of 10 [m] side is subdivided into 144 square elements as shown in Figure 2.7. The raft thickness is $d = 0.4$ [m].

2   Soil properties

3 boring logs characterize the subsoil under the raft. Each boring has a soil layer of thickness 10 [m], resting on a rigid base as shown in Figure 2.7. The modulus of compressibility E_s represents the irregularity of the soil material in x- and y-directions, which in this example is chosen to be variable. The moduli of compressibility of the three borings are:

E_{s1} =   6666.67   [kN/m^2]
E_{s2} = $1.5 \times E_{s1}$ [kN/m^2]
E_{s3} = $2.0 \times E_{s1}$ [kN/m^2]
with average value of $E_s = 10000$ [kN/m^2]

The moduli of compressibility lead to the following mean moduli of subgrade reactions for the three borings:

k_{sm1} =   1448   [kN/m^3]
k_{sm2} = $1.5 \times k_{sm1}$ [kN/m^3]
k_{sm3} = $2.0 \times k_{sm1}$ [kN/m^3]
with average value of $k_{sm} = 1563$ [kN/m^3]

Possion's ratio is $v_s = 0.3$ for the soil material of the borings.

3   Loads

The external loads are chosen to be symmetrical about the raft center. The loads are four symmetrically loads, each of $P = 500$ [kN] as shown in Figure 2.7. The self weight of the raft is ignored.
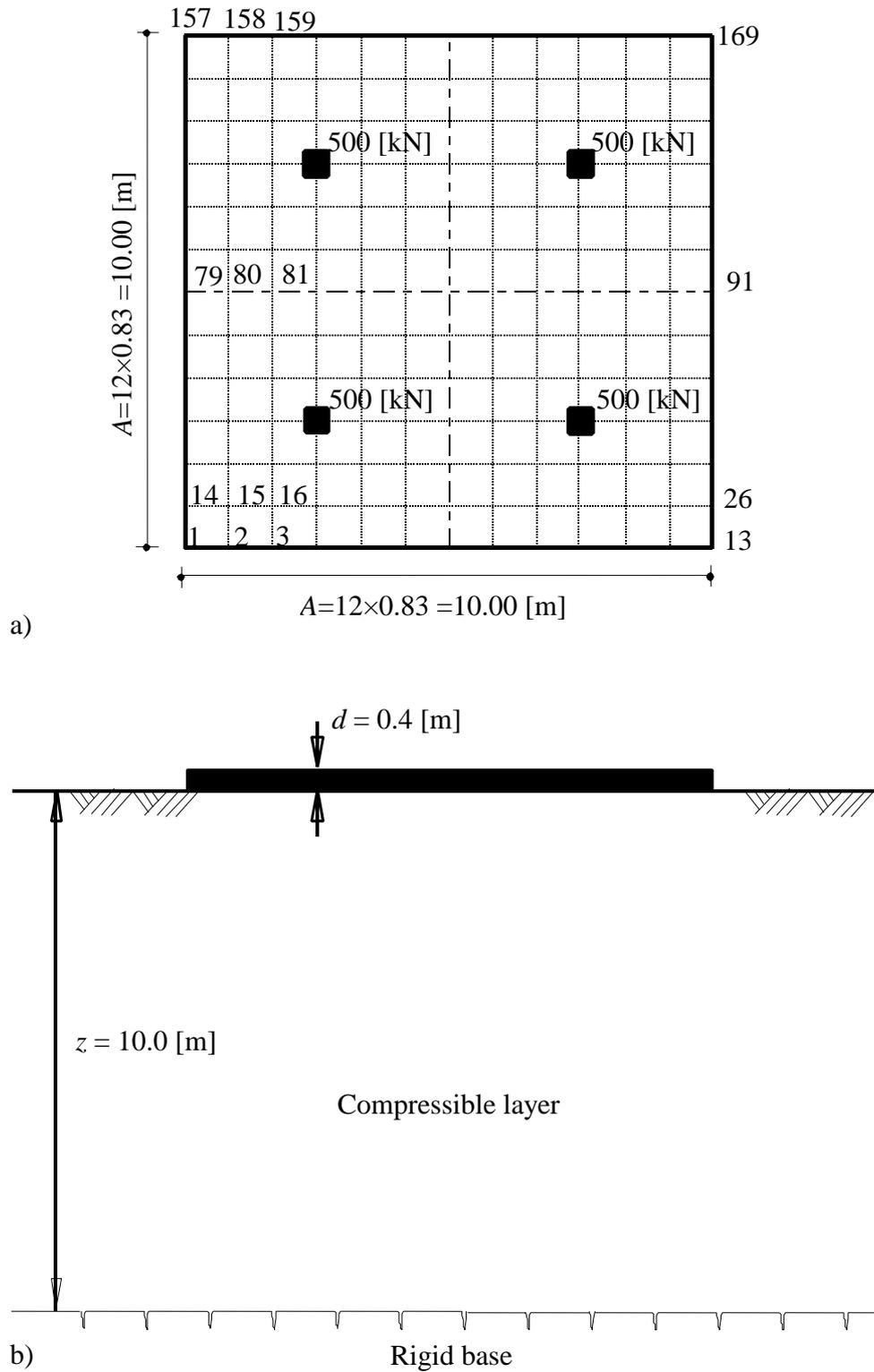
Figure 2.7   a) Raft numbering, loading and dimensions
   b) Soil cross-section
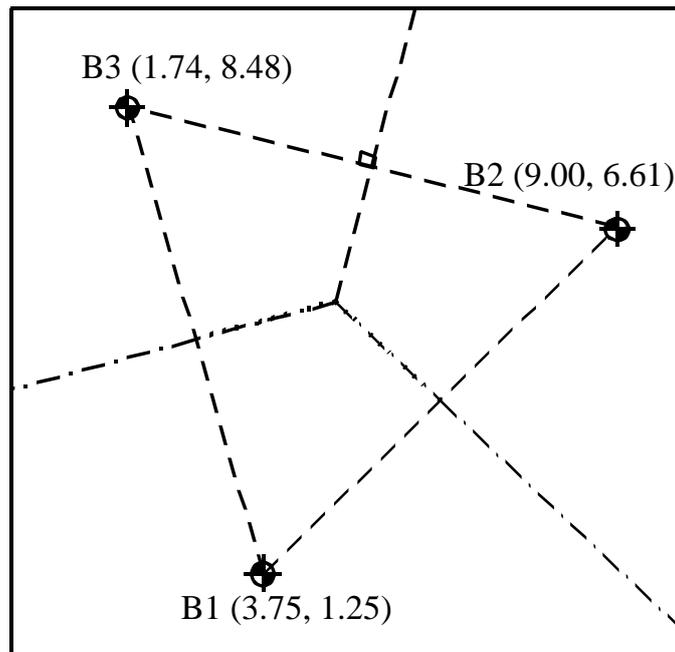
Figure 2.8   Boring locations and subareas (Subareas method)
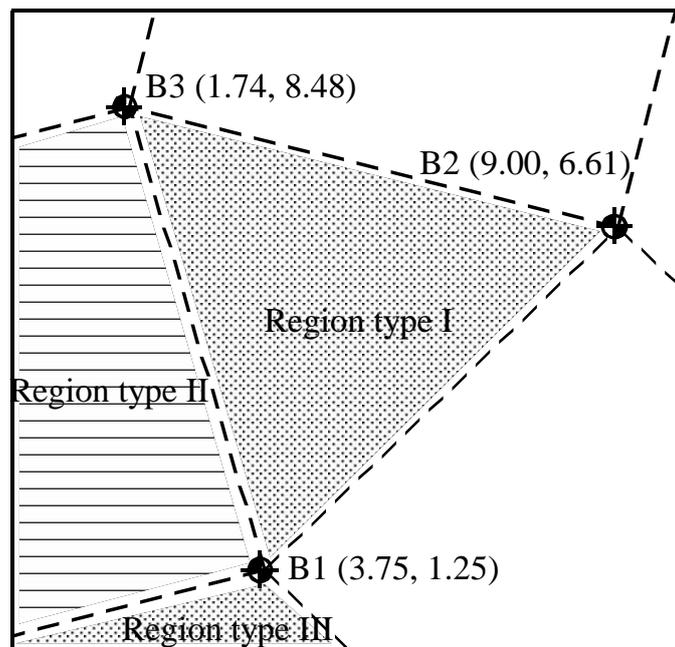
Figure 2.9   Boring locations and region types (Interpolation method)

4   Raft material

The raft material is supposed to have the following parameters:

Young's modulus	E_b	$= 2 \times 107$	[kN/m^2]
Poisson's ratio	ν_b	$= 0.25$	[-]
Unit weight of raft material	γ_b	$= 0.0$	[kN/m^3]

Unit weight of raft material is chosen $\gamma_b = 0.0$ to neglect the own weight of the raft.

5   Analysis of the raft

For comparison, the flexibility coefficient and the modulus of subgrade reaction are determined by the following two methods:

-        Subareas method, Figure 2.8
-        Interpolation method, Figure 2.9

6   Results and evaluation

Figures 2.10 and 2.11 show the contour lines of settlements for each of the two types of soil models (*Winkler*'s model 3 and Continuum model 7), while Figure 2.12 shows contour lines of settlements for the rigid raft on the Continuum model 8. The flexibility coefficients for the three calculation methods are obtained using the interpolation method. As expected, the settlement form is unsymmetric about the raft center when the irregularity of the subsoil is considered, although the raft is symmetric in shape and carries symmetrical loads. The Figures 2.10 to 2.12 show that the boring which has minimum value of E_s (boring B1) leads to higher settlements at nodes close to that boring.

Figure 2.13 shows the contour lines of settlements when the soil is a regular layer having a constant value of $E_s = 10000$ [kN/m^2]. A comparison between Figure 2.12 and Figure 2.13 shows a great variation of settlement shape when using variable E_s values. This means that the detailed variation of soil properties with vertical and horizontal directions must be taken into account.

Figures 2.14 to 2.17 present a comparison between the results computed by the interpolation method and that of the subareas method. Figures 2.14 and 2.15 show the contact pressures at the edge of the raft (node 157 to 169) for the two types of soil models (*Winkler*'s model 3 and Continuum model 7), while Figure 2.16 shows the contact pressures at the edge of the raft for the rigid raft on Continuum model 8. Figure 2.17 shows the bending moments at the middle of the raft, section I-I, for Continuum model 7. From the above comparison, it can be concluded that the continuity requirement of the soil material between the adjacent borings is not met when using the subareas method. Therefore, it is expected that the results of the subareas method will not be as accurate as those of the interpolation method, especially if the borings have great differences in the soil material. This is explained in Figures 2.14 to 2.17 where the subareas method leads to a sudden change in the contact pressures and moments between two adjacent

subareas.
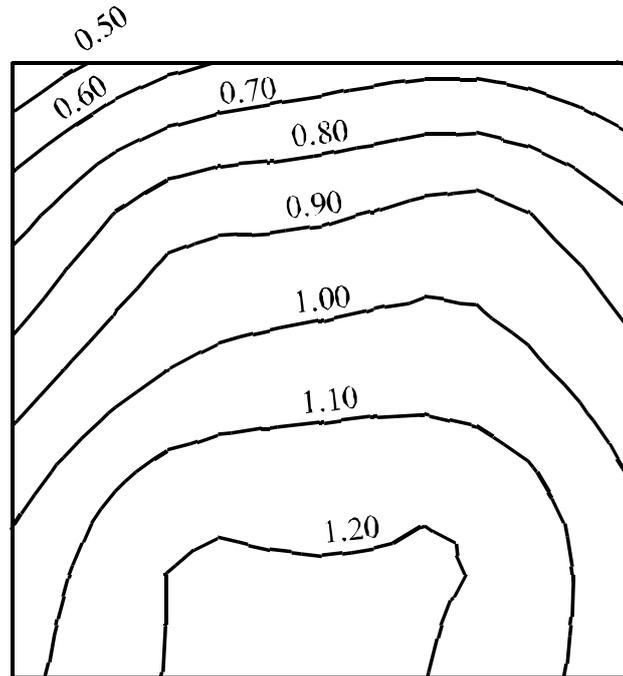
Figure 2.10   Contour lines of settlements [cm] for *Winkler*'s model 3
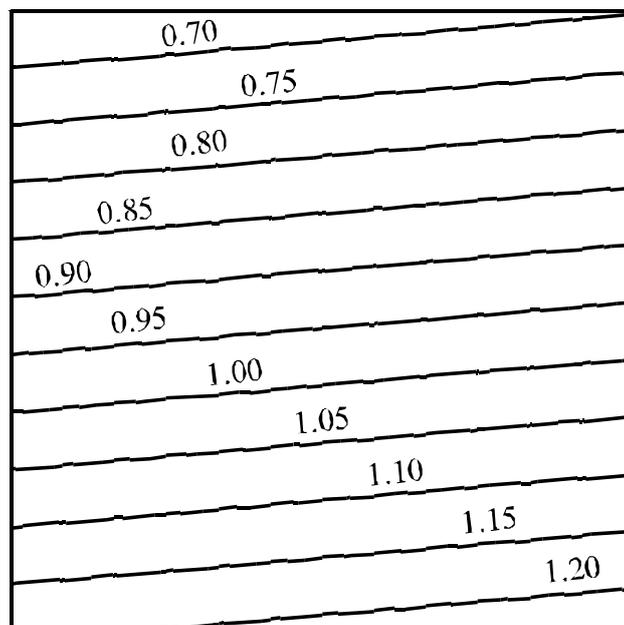
Figure 2.11   Contour lines of settlements [cm] for rigid raft on Continuum model 8
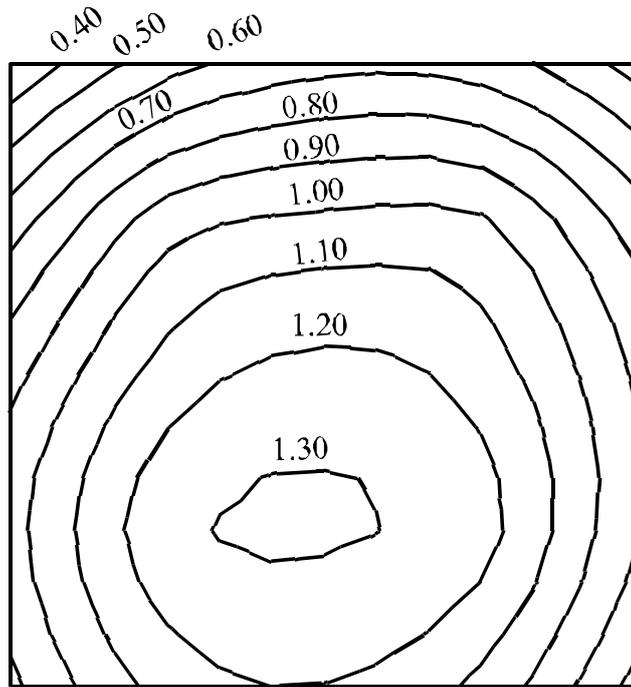
Figure 2.12   Contour lines of settlements [cm] for Continuum model 7
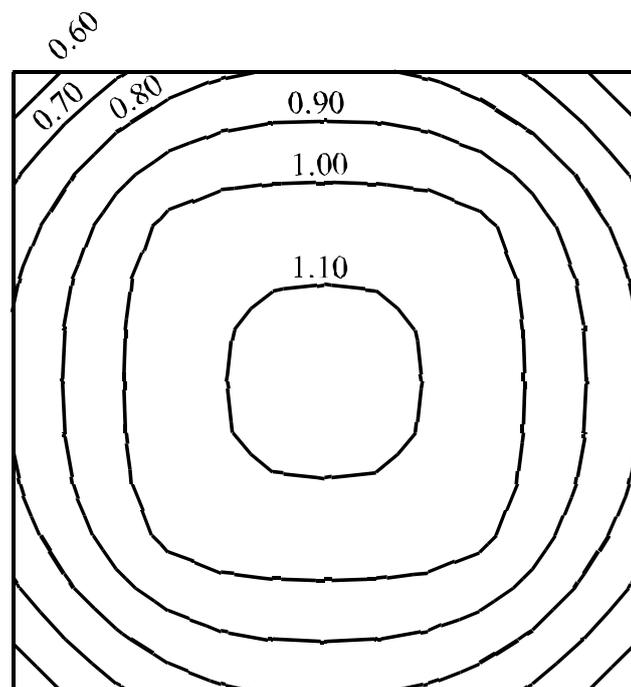
Figure 2.13   Contour lines of settlements [cm] for Continuum model 7, constant E_s

Node No.
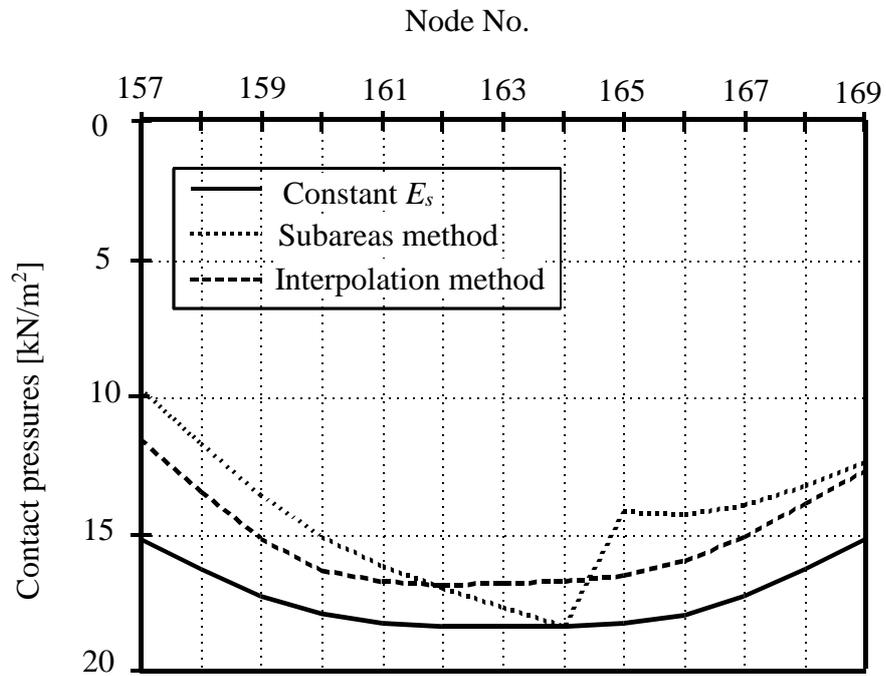
Figure 2.14   Contact pressures at the raft edge for *Winkler*'s model 3

Node No.
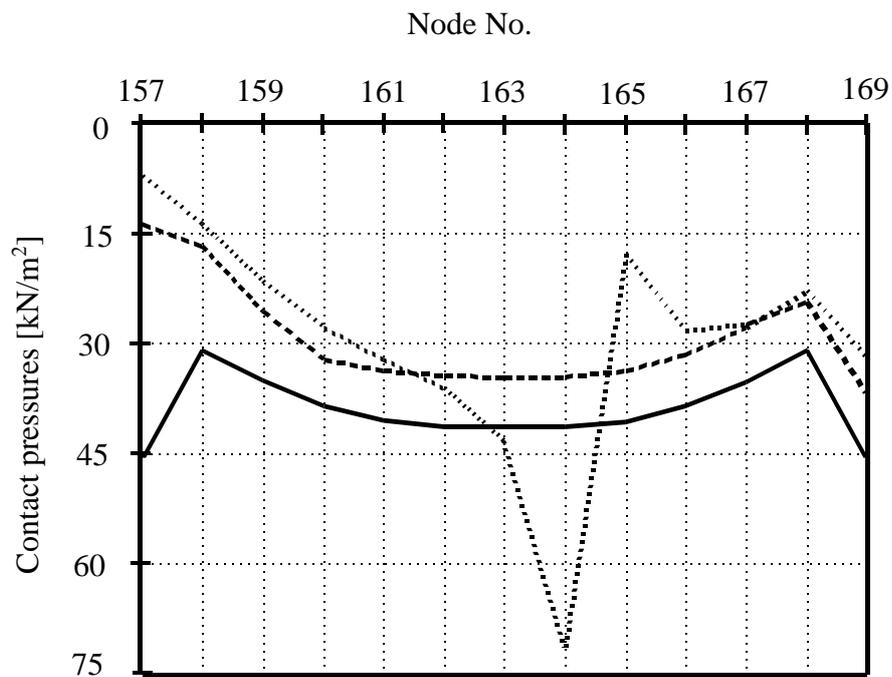
Figure 2.15   Contact pressures at the raft edge for Continuum model 7

Node No.
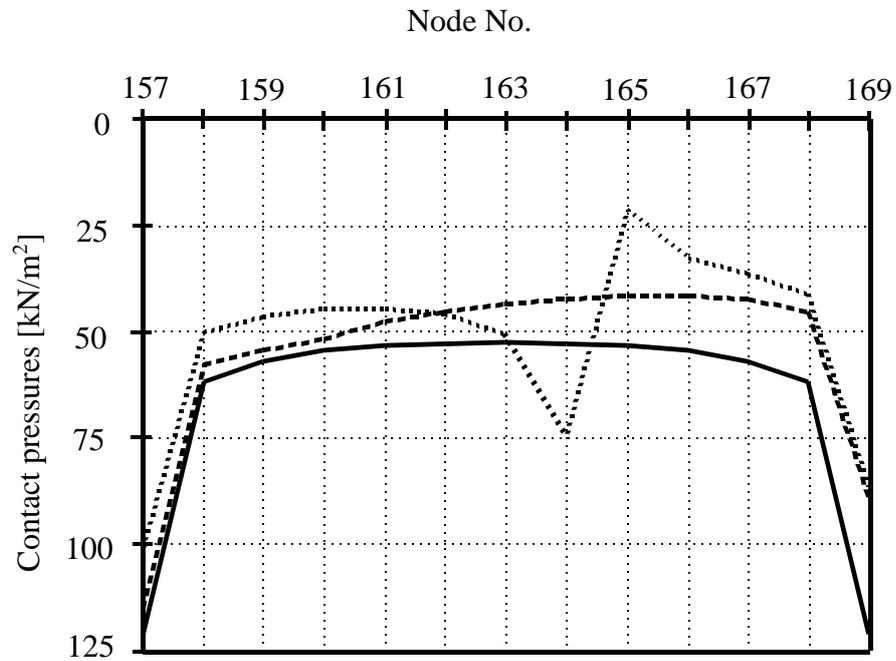
Figure 2.16   Contact pressures at the raft edge for rigid raft on Continuum model 8

Node No.
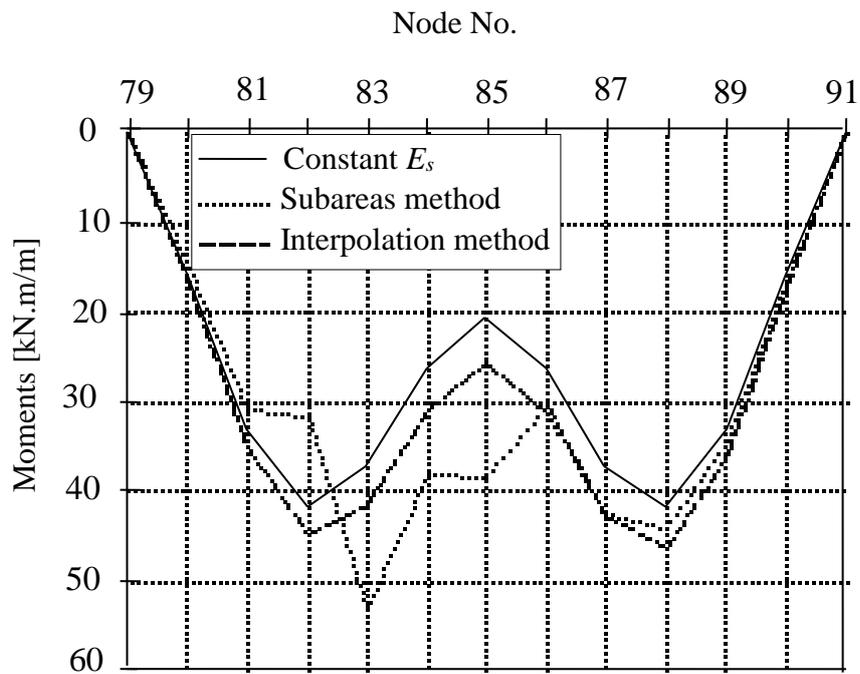
Figure 2.17   Moments at the raft middle for Continuum model 7

Example 2.2   Analysis of an irregular raft on irregular subsoil

1   Description of the problem

A general example is carried out to show the applicability of the different mathematical models for analysis of irregular rafts on irregular subsoil.

In one case the raft carries many types of external loads: concentrated loads [kN], uniform load [kN/m^2], line load [kN/m] and moments [kN.m] in both x- and y-directions as shown in Figure 2.18.
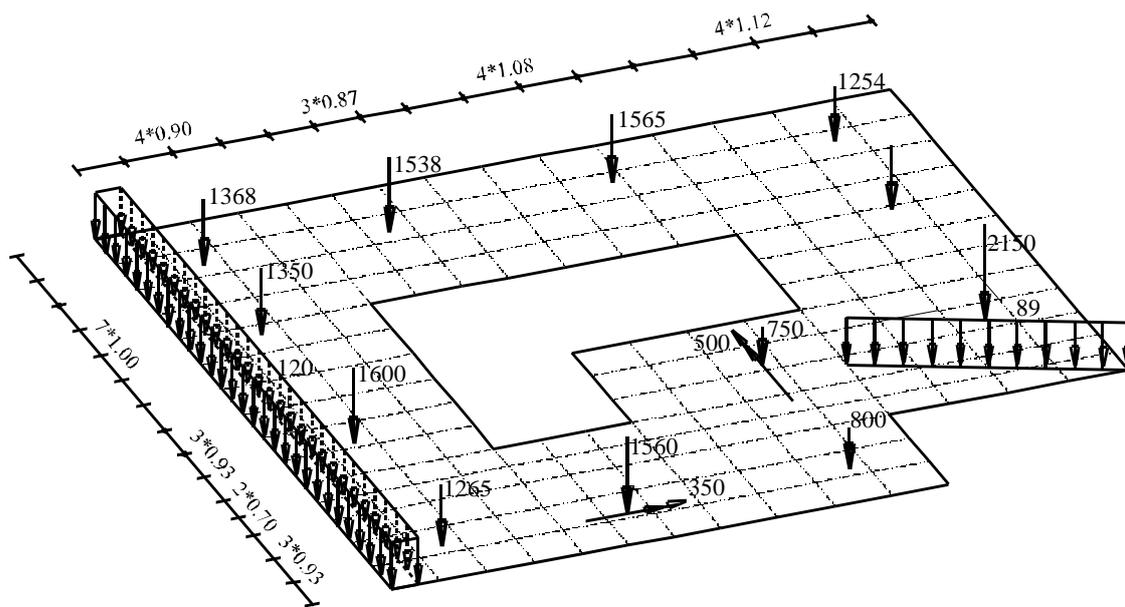

Figure 2.18   Raft dimensions [m] and loads

2   Soil properties

Three boring logs characterize the subsoil under the raft. Each boring has three layers with different soil materials. The moduli of compressibility of the three layers for loading are E_{s1} = 9500 [kN/m^2], E_{s2} = 22000 [kN/m^2] and E_{s3} = 120000 [kN/m^2] while for reloading are W_{s1} = 26000 [kN/m^2], W_{s2} = 52000 [kN/m^2] and W_{s3} = 220000 [kN/m^2]. *Poisson*'s ratio is 0.0 [-] for all soil layers. The level of foundation is d_f = 2.7 [m] while the level of ground water is GW = 1.5 [m]. Unit weight of the soil above the ground water is γ_s = 19 [kN/m^3] while under the ground water is γ'_s = 9 [kN/m^3]. The effect of reloading and water pressure is taken into account. Figure 2.19 shows boring logs and locations.

a)

0.00

GW=1.5

3.8

8.20

10.0

14.1

12.7

18.2

20.0   20.0   20.0

Sil
$E_s = 9500$ [kN/m^2]
$W_s = 26000$ [kN/m^2]
$\gamma_s = 19$ [kN/m^3]

Fine sand
$E_s = 22000$ [kN/m^2]
$W_s = 52000$ [kN/m^2]

Gravel
$E_s = 120000$ [kN/m^2]
$W_s = 220000$ [kN/m^2]

b)

B2   B1   B3

B2 (1.00, 9.00)   B3 (10.00, 11.00)   B1 (4.00, 3.00)

Figure 2.19   a) Boring locations and interpolation regions
                b) Boring logs B1 to B3

3   Raft material and thickness

The raft material is supposed to have the following parameters:

Young's modulus	E_b	$= 2 \times 107$	[kN/m^2]
Poisson's ratio	ν_b	$= 0.25$	[-]
Unit weight of raft material	γ_b	$= 0.0$	[kN/m^3]
Raft thickness	d	$= 0.5$	[m]

Unit weight of raft material is chosen to be $\gamma_b = 0.0$ to neglect the own weight of the raft in the analysis.

4   Analysis of the raft

The analysis of the raft is carried out by the eight mathematical calculation methods in Table 2.1. The methods are represented by the three subsoil models: Simple assumption, *Winkler*'s and Continuum models.

Table 2.1   Calculation methods

Method No.	Method
1	Linear contact pressure
2	Constant modulus of subgrade reaction
3	Variable modulus of subgrade reaction
4	Modification of modulus of subgrade reaction by iteration
5	Modulus of compressibility method for elastic raft on half-space soil medium
6	Modulus of compressibility method for elastic raft on layered soil medium (iter.)
7	Modulus of compressibility method for elastic raft on layered soil medium (eli.)
8	Modulus of compressibility method for rigid raft on layered soil medium

To carry out a comparison for the different calculation methods and mathematical models, the example is analyzed first by the modulus of compressibility method 7 for layered soil medium. Then, the same example with the same loads is analyzed again by the other seven different numerical calculation methods. The elastic parameters are assumed to represent the same type of soil, which is considered in the first analysis. By weighing the elastic parameters of each layer in a multilayered system according to its influence on settlement an "equivalent" modulus of compressibility for the entire subsoil mass for isotropic elastic half-space model 5 and an "equivalent" constant modulus of subgrade reaction for *Winkler*'s model 2 are determined. Main moduli of subgrade reactions for the three boring logs can be also determined for *Winkler*'s model 3. The equivalent elastic parameters can then be used to obtain the settlements, contact pressures, moments and shear forces in the raft by the different calculation methods.

The equivalent elastic parameters are:

For isotropic elastic half space model 5
E_{sm} =   9500   [kN/m^2]

For constant modulus of subgrade reaction model 2
k_{sm} =   3517   [kN/m^3]

For variable modulus of subgrade reaction model 3
k_{sm1} =   5254   [kN/m^3]   for Boring B1
k_{sm2} =   2982   [kN/m^3]   for Boring B2
k_{sm3} =   2315   [kN/m^3]   for Boring B3

5   Results and discussion

The extreme values of the results are given in Table 2.2. Figures 2.20 to 2.28 show the settlements and contact pressures on the raft for the eight calculation methods.

Table 2.2   Maximum and Minimum values of settlements s and contact pressures q for the different calculation methods

Method	No.	$s_{max.}$ [cm]	$s_{min.}$ [cm]	$q_{max.}$ [kN/m^2]	$q_{min.}$ [kN/m^2]
Linear contact pressure	1	-	-	127	65
Constant modulus of subgrade reactions	2	5.38	0.46	189	16
Variable modulus of subgrade reactions	3	6.52	0.47	194	18
Modification of modulus of subgrade	4	4.42	1.15	586	19
Isotropic elastic half space	5	11.28	8.51	572	16
Modulus of compressibility - elastic raft	6 and 7	4.42	1.15	586	19
Modulus of compressibility - rigid raft	8	4.24	1.51	560	48
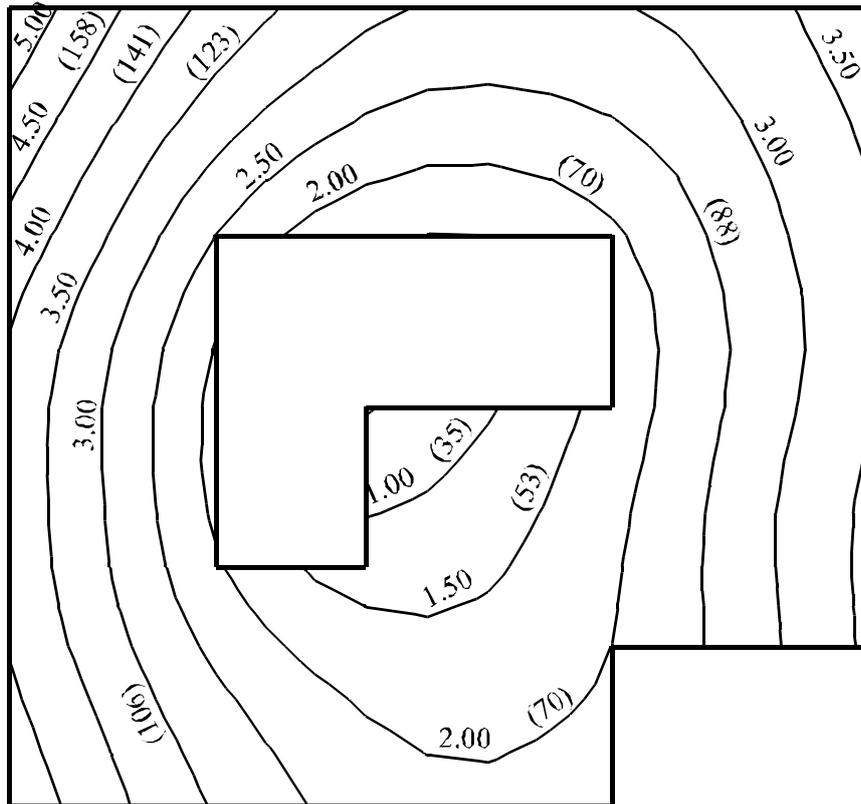
Figure 2.20   Contour lines of settlements [cm] and contact pressures [kN/m²]
   (in brackets for constant modulus of subgrade reaction method 2)
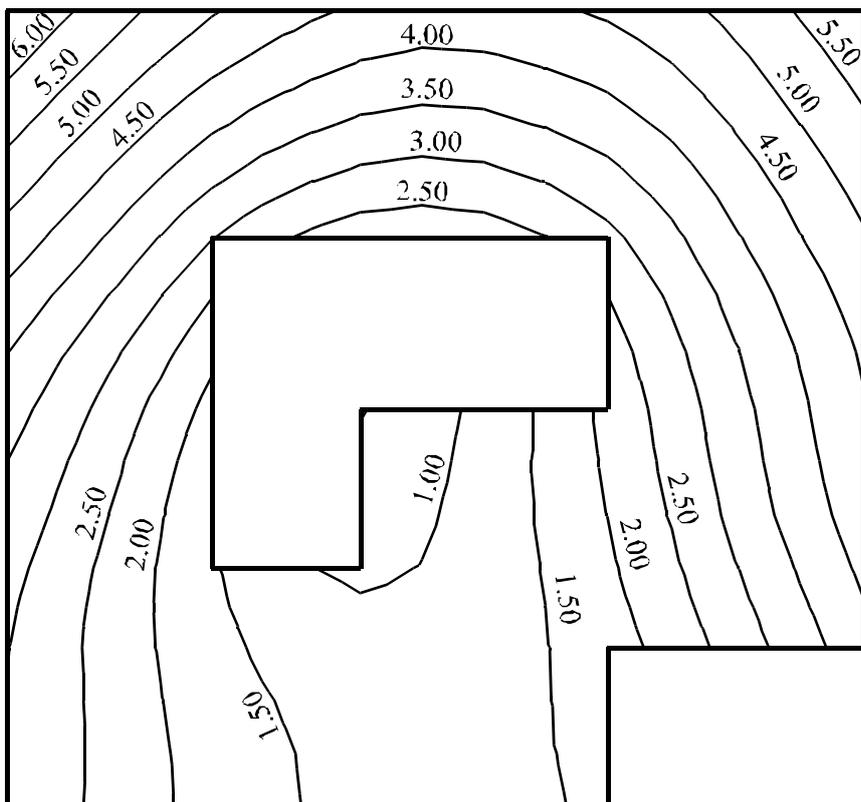
Figure 2.21   Contour lines of settlements [cm] for variable modulus of subgrade reactions 3

Figure 2.22   Contour lines of settlements [cm] for isotropic elastic half-space model 5


Figure 2.23   Contour lines of settlements [cm] for methods 4, 6 and 7
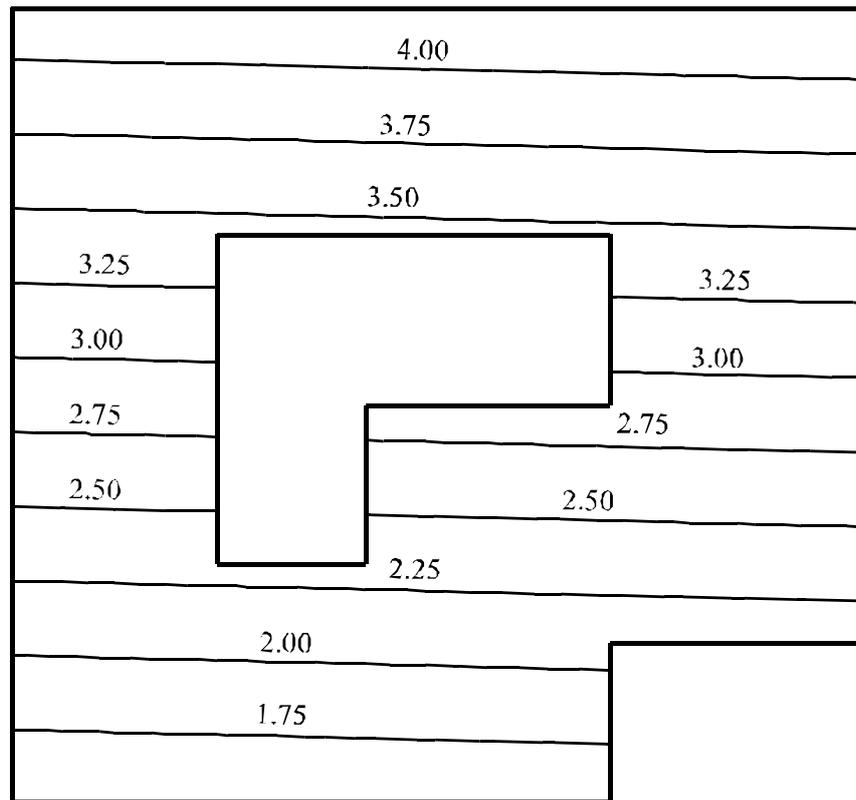
Figure 2.24   Contour lines of settlements [cm] under rigid raft 8
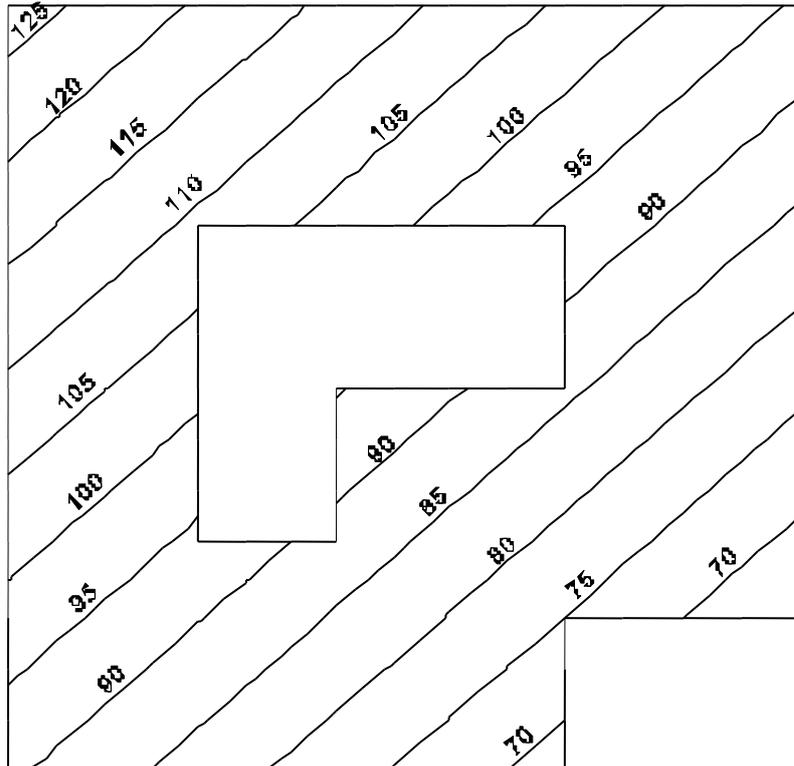
Figure 2.25   Contour lines of contact pressures [kN/m^2] by method 1
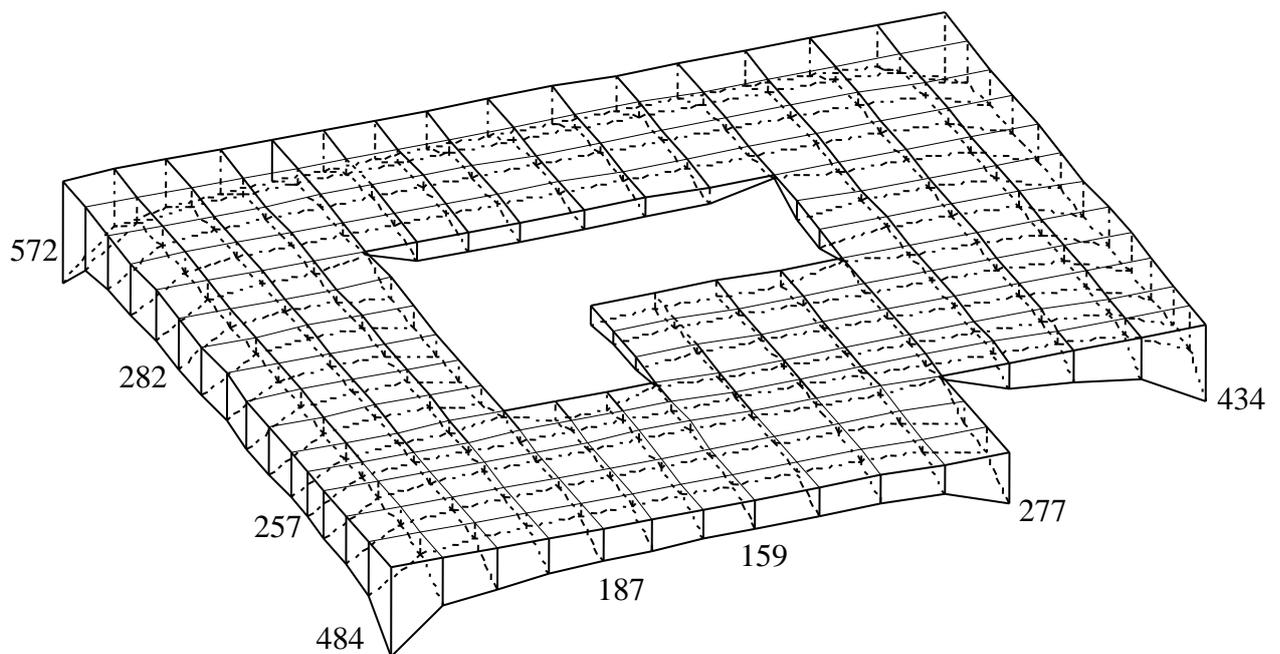
Figure 2.26   Contact pressures [kN/m^2] for isotropic elastic half-space model 5
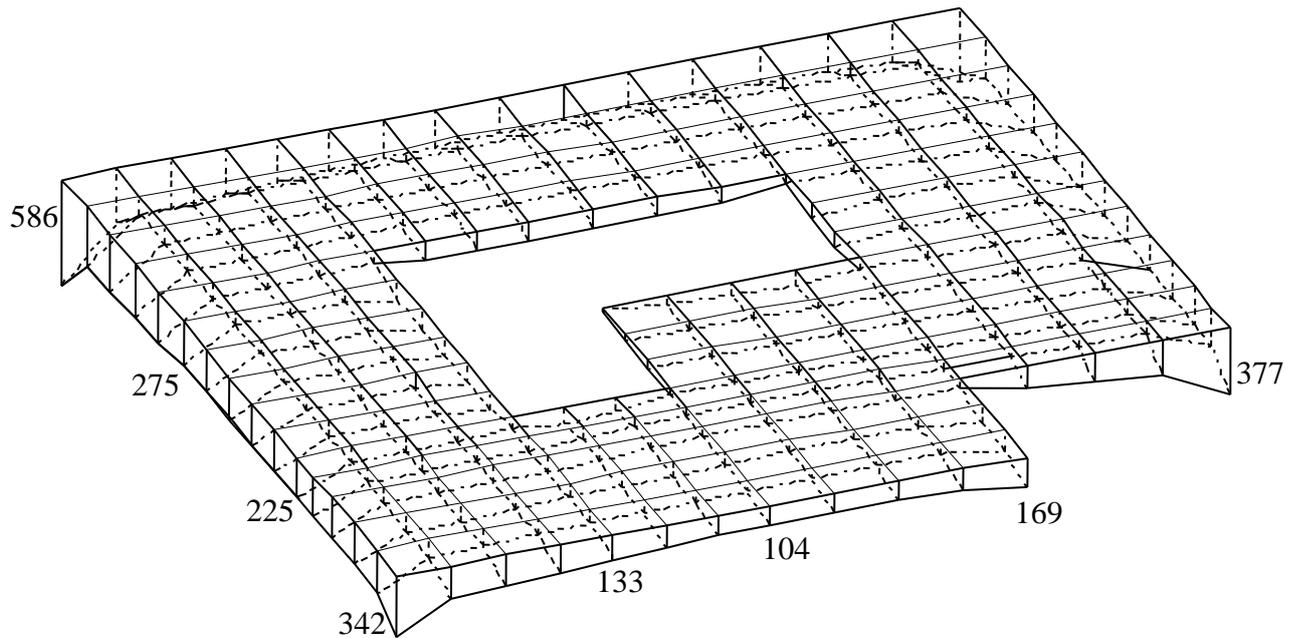
Figure 2.27   Contact pressures [kN/m^2] for methods 4, 6 and 7
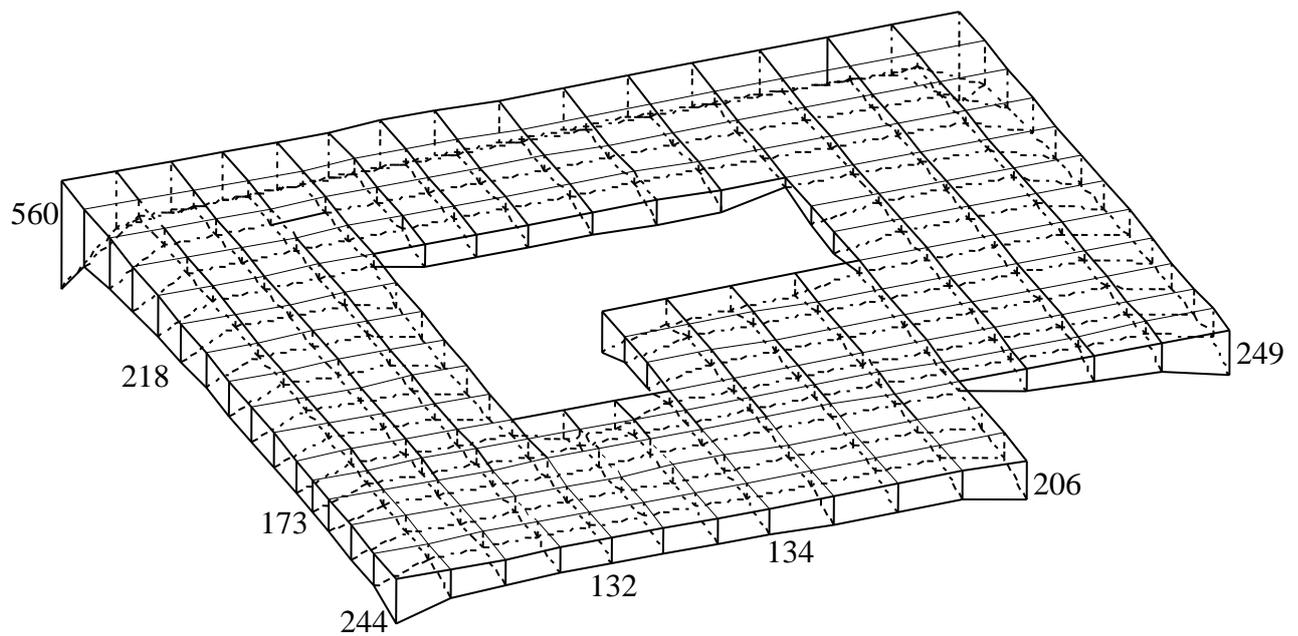

Figure 2.28   Contact pressures [kN/m^2] under the rigid raft 8

Through Table 2.2 and Figures 2.20 to 2.28 the following conclusions can be drawn:

-        It is important to say that the linear contact pressure method 1 does not depend on the behavior of the subsoil mass below the foundation and there is no compatibility between raft deformation and soil settlement in this method

-        The elastic parameters for isotropic elastic half-space 5 and constant modulus of subgrade reaction 2 are valid for the whole subsoil mass but for the variable modulus of subgrade reaction 3 are variable from a node to another

-        For the two iteration methods 4 and 6 and rigid raft 8, the elastic parameters are the same as those of the first analysis method 7 and can be taken without any change

-        The influence of surrounding structures and external loads can be taken into consideration only for the Continuum model (methods 4, 5, 6, 7 and 8)

-        The influences of temperature change cannot be taken into consideration for the Linear contact pressure (method 1)

-        Furthermore, the influence of reloading can be taken into consideration only for the methods 4, 6, 7 and 8

-        The results of calculation of the rigid raft (method 8) do not change from the raft thickness $d = d_{\mathrm{rigid}}$ to $d = \infty$

-        As from the assumption of the isotropic elastic half-space model 5, the soil under the foundation extends to an infinitely thick layer. The settlement will be similar in shape but greater in value to that of the layered model 7, Figures 2.21 and 2.23

-        The Continuum model (methods 4, 5, 6, 7 and 8) shows that the contact pressure is minimum on the middle of the raft and maximum at its edges, Figures 2.26, 2.27 and 2.28

-        Figure 2.25 shows that the contact pressure for the Linear contact pressure (method 1) takes linear form under the raft

-        As from the assumption of *Winkler*'s model (method 2) the soil pressure q_i at any point i will be equal to the settlement s_i at that point multiplied by the modulus of subgrade reaction k_s. The contour lines of contact pressures will be similar to that of settlements, only the values of s_i should be multiplied by k_s. Therefore, the contour lines of both contact pressures and settlements are plotted in a figure for the *Winkler*'s model 2 as shown in Figure 2.20

-        It can be seen from Table 2.2 that the maximum and minimum values of contact pressures for the Linear contact pressure, constant modulus of subgrade reaction and variable modulus of subgrade reaction are nearly the same. In addition, the maximum and minimum values of settlements for constant and variable modulus of subgrade reaction methods (methods 2 and 3) are nearly the same

Example 2.3   Analysis of system of footings on irregular subsoil

1   Description of the problem

The influence of irregularity of the subsoil material on the behavior of foundations is illustrated through the study of the differential settlements for a system of 9 footings. Consider the group of footings shown in Figure 2.29 and Table 2.3. Thickness of footings is $d = 0.5$ [m]. Unit weight of the footing is $\gamma_f = 25$ [kN/m^3]. Arrangement of footings and footing loads are shown in Figure 2.29a.

2   Soil properties

The group of footings is resting on a three-dimensional subsoil model. Four boring logs characterize the subsoil under the footings. Each boring has three layers as shown in Figure 2.29 and Table 2.4. *Poisson*'s ratio is $\nu_s = 0.3$ [-] for all soil layers. The level of ground water is $GW = 1.3$ [m], while the level of foundation for all footings is $t_f = 2.2$ [m] under the ground surface. The effects of reloading and water ground are taken into account. Boring locations and section through B1-B2 are shown in Figure 2.29.

Table 2.3   Loads, dimensions and origin coordinates of the footings

| Footing No.	Load P [kN]	Dimensions		Origin coordinates		
		Length [m]	Width [m]	x [m]	y [m]	β [°]
1	2500	2.0	2.0	1.00	1.00	0
2	900	1.5	1.5	6.25	1.25	0
3	800	1.5	1.5	11.25	1.25	0
4	2500	2.0	2.0	1.50	6.00	0
5	5400	3.0	3.0	5.00	6.00	0
6	950	1.5	1.5	11.25	6.25	0
7	5400	4.5	2.0	2.12	8.7	45
8	3000	2.5	2.0	5.75	11.00	0
9	2000	2.0	1.5	10.00	10.25	0
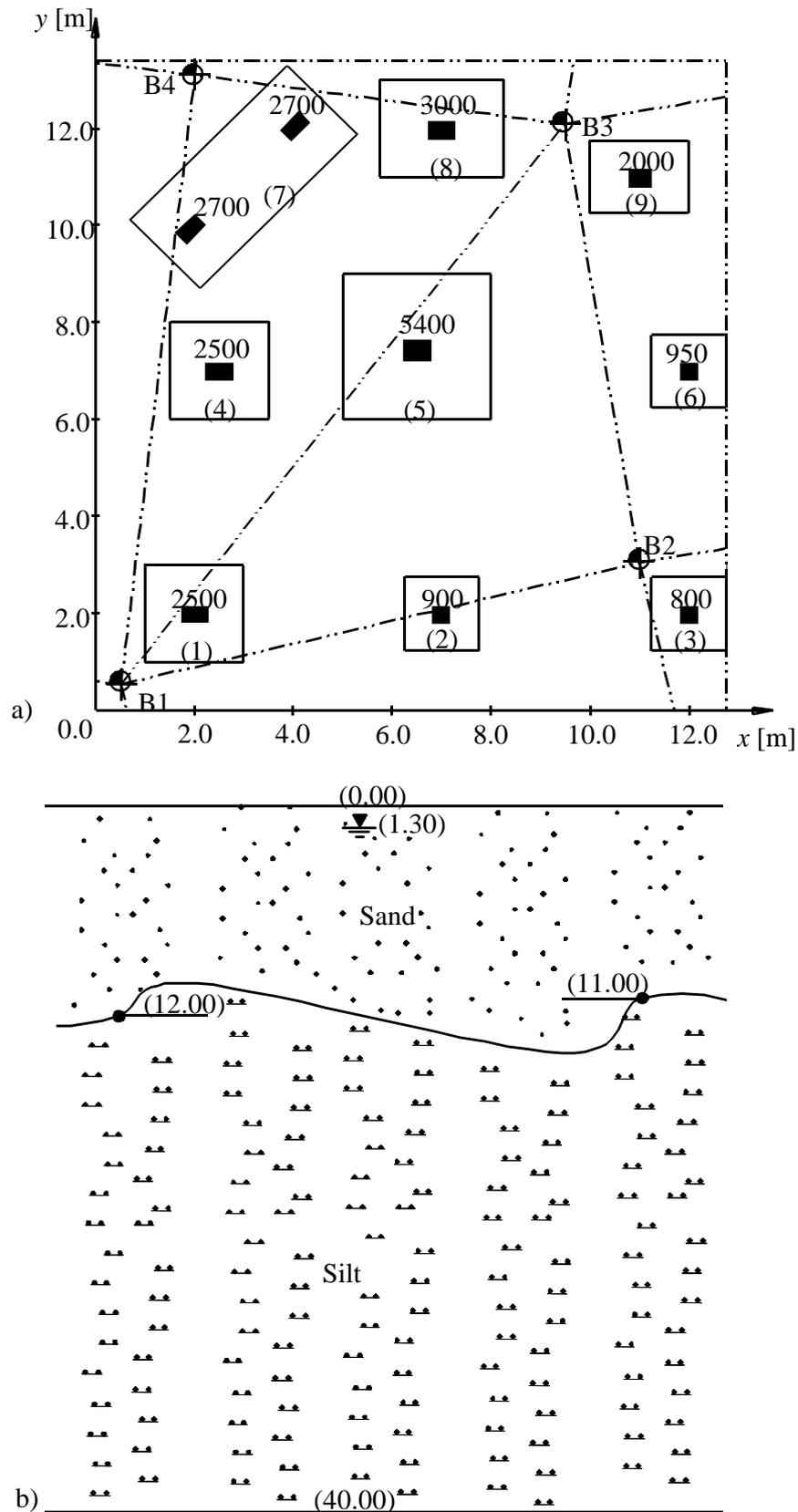
Figure 2.29   a) Arrangement of footings, footing loads [kN] and boring locations
                b) Section through B1-B2

Table 2.4   Soil material and layer levels for the four borings

Layer No.	Type of soil	Layer level under the ground surface z [m]	Modulus of elasticity for		Unit weight of the soil
			loading E_s [kN/m^2]	reloading W_s [kN/m^2]	γ_s [kN/m^3]
1	Sand	1.3	98 000	135 000	19
2	Sand	12/11/14/10	98 000	135 000	11.2
3	Silt	40	9 500	12 000	12

3   Analysis and results

Because the footing dimensions are relatively small, the footings may be treated as rigid footings resting on compressible subsoil. In this case, it is enough to determine the soil settlement at the footing centers. For a good judgment on the proposed analysis, the group of footings has been treated four times according to the following cases:

i)   The limit depths for all boring logs are obtained due to the maximum loaded footing (footing 5)

ii)   The limit depths for all boring logs are obtained due to the minimum loaded footing (footing 3)

iii)   Without limit depths: the last layer for each boring extends to a depth of 40 [m] below the ground surface

iv)   The limit depth is obtained through interpolation

The limit depths are determined at the level of which the stress σ_U due to footings reaches the ratio ζ = 0.2 of the initial vertical stress σ_V. The limit depths of boring B1 to B4 due to footing 3 are shown in Figure 2.30 while those due to footing 5 are shown in Figure 2.31. The limit depths for the maximum loaded footing (footing 5) are ranged from 16.90 [m] to 17.00 [m] while those for the minimum loaded footing (footing 3) are ranged from 11.31 [m] to 11.39 [m]. Table 2.5 shows the central settlements of the footings for the four cases. As expected, the numerical results show that the limit depths have a significant influence on the settlement of the footings. It can be seen from Table 2.5 that there is a great difference in the settlement values by applying the four cases. Case i) gives high values of settlement where that of case ii) is small and that of case iii) is very high. This proves that the interpolation analysis is a suitable procedure to study the interaction of a group of footings. Table 2.5 shows also that cases i) and ii) give only the accurate settlements under footings 5 and 3, respectively. Where the settlement under footing 5 is $s_5 = 3.70$ [cm] while that under footing 3 is $s_3 = 0.48$ [cm].
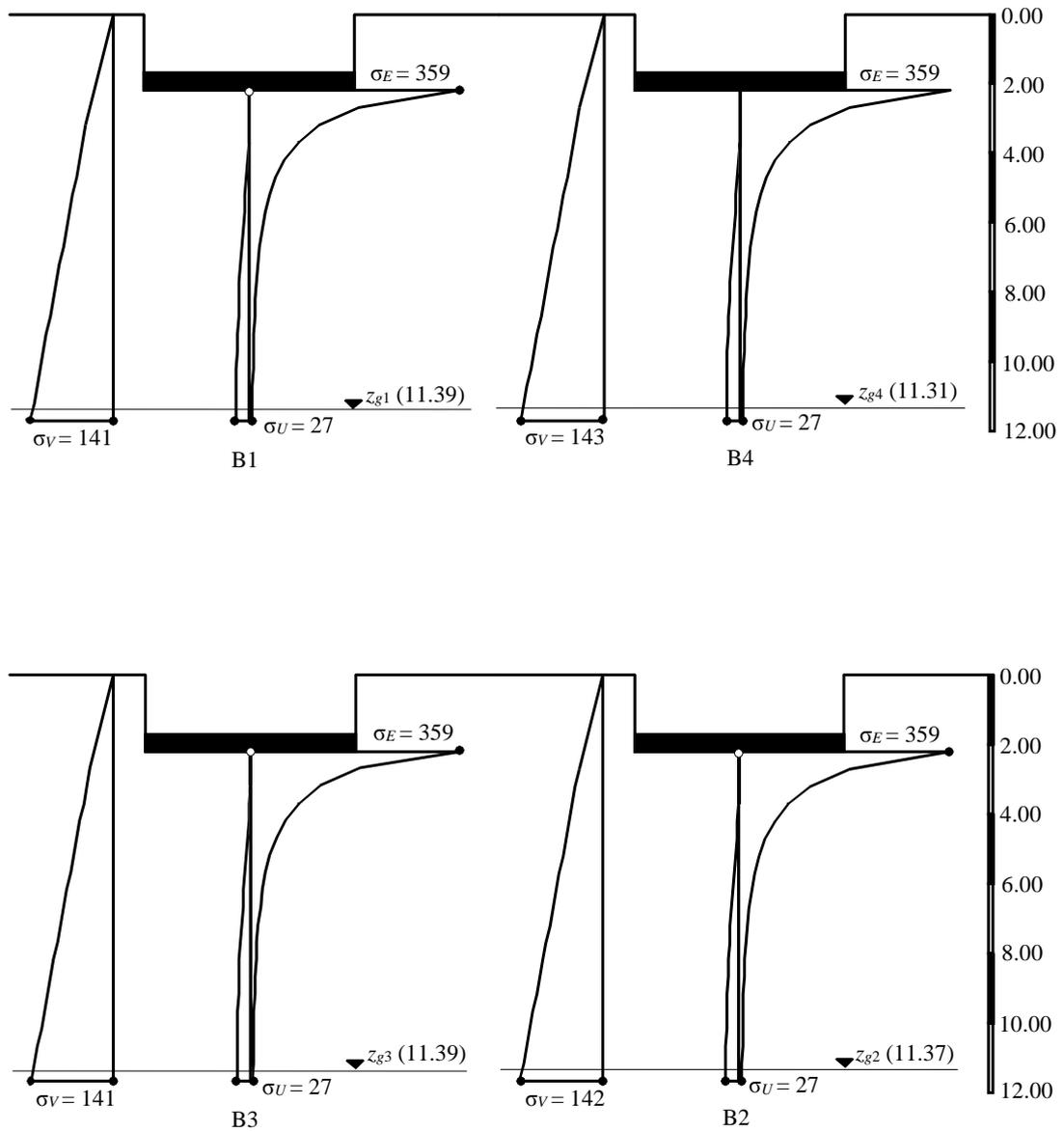
Figure 2.30   Limit depths of boring logs B1 to B4 due to footing 3
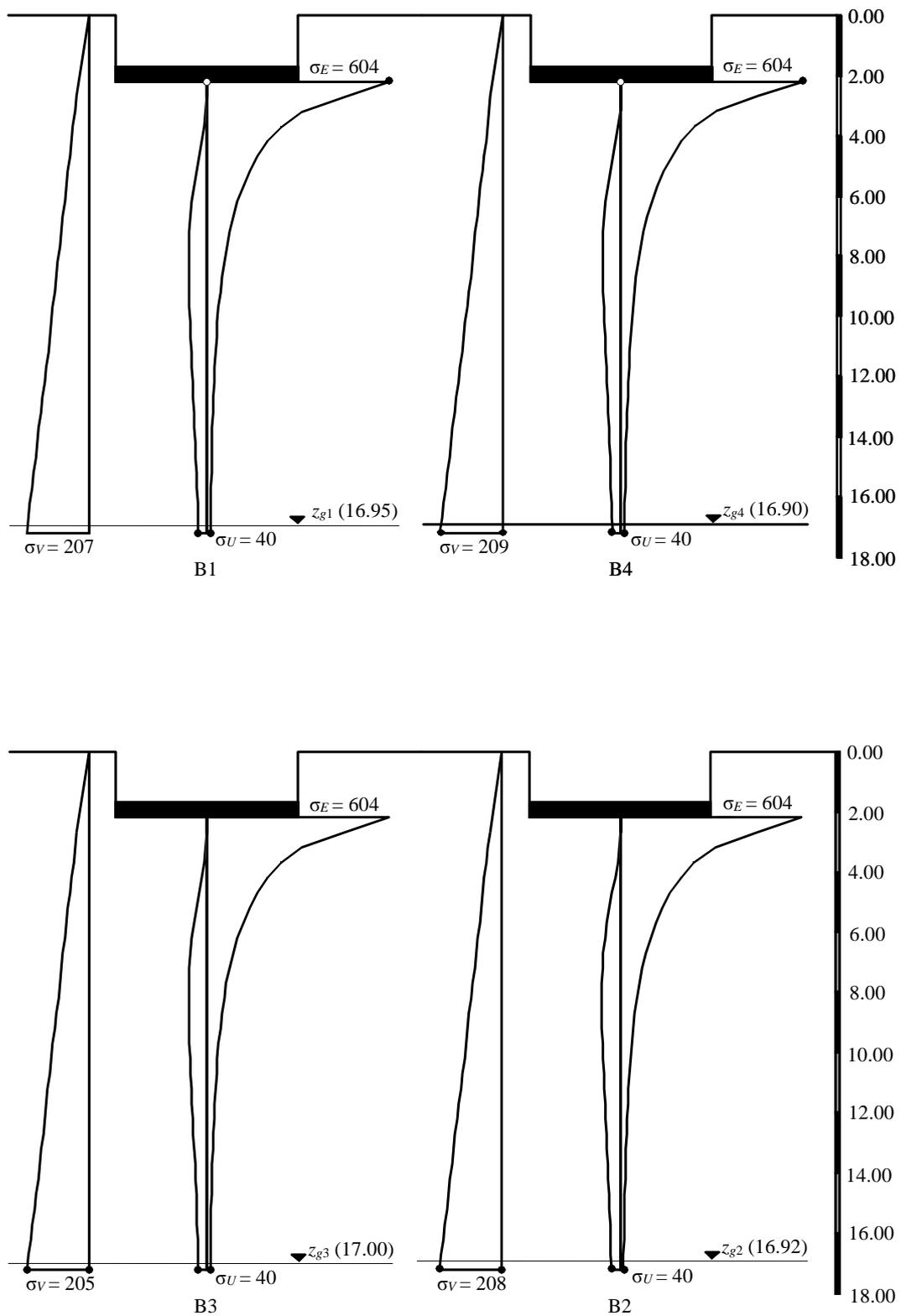
Figure 2.31   Limit depths of boring logs B1 to B4 due to footing 5

Table 2.5   Central settlements of the footings

Footing No.	Calculation of central settlement [cm] based on			
	Limit depths related to footing 5	Limit depths related to footing 3	Without limit depths $z = 40$ [m]	Limit depths related to its corresponding footing
1	2.58	0.91	6.07	1.74
2	2.55	0.63	6.19	1.80
3	1.81	0.48	4.86	0.48
4	4.15	1.55	8.35	3.99
5	3.70	1.45	8.05	3.70
6	2.30	0.66	5.91	1.55
7	4.56	1.94	8.67	4.34
8	3.48	1.50	7.59	3.26
9	2.33	0.96	6.05	1.72

Chapter 3

Influence of Neighboring Foundations
and Buried Structures

Contents

3.1   Introduction

In many situations, it becomes important to assess the behavior of a foundation due to its interaction with another neighboring foundation or external load.

First, it must be distinguished between two types of problems concerning neighboring foundations:

-       The first problem occurs when a new building is constructed beside an existing one.
        In this case, the new building will cause an additional settlement under the existing structure due to the increase of stress in soil

-       The second problem occurs when structures are constructed simultaneously.
        In this case, there will be interaction of foundations due to the overlapping of stresses through the soil medium, although the structures are not statically connected. The interaction of foundations will cause additional settlements under all foundations

The study of interaction between a foundation and another neighboring foundation or an external load has been considered by several authors. *Mikhaiel* (1978) presented an application on the use of the elastic half-space model in the determination of the effect of neighboring loads on the existing building. *Selvadurai* (1983) examined the interaction between a rigid circular foundation and an external load.

The additional settlement due to neighboring foundations, external loads and buried structures can be considered as indicated in the next paragraphs.

3.2   Influence of neighboring foundations

Figure 3.1 shows a neighboring foundation B. This foundation causes an additional settlement on the examined foundation A. The additional settlement due to a neighboring foundation can be considered as follows:
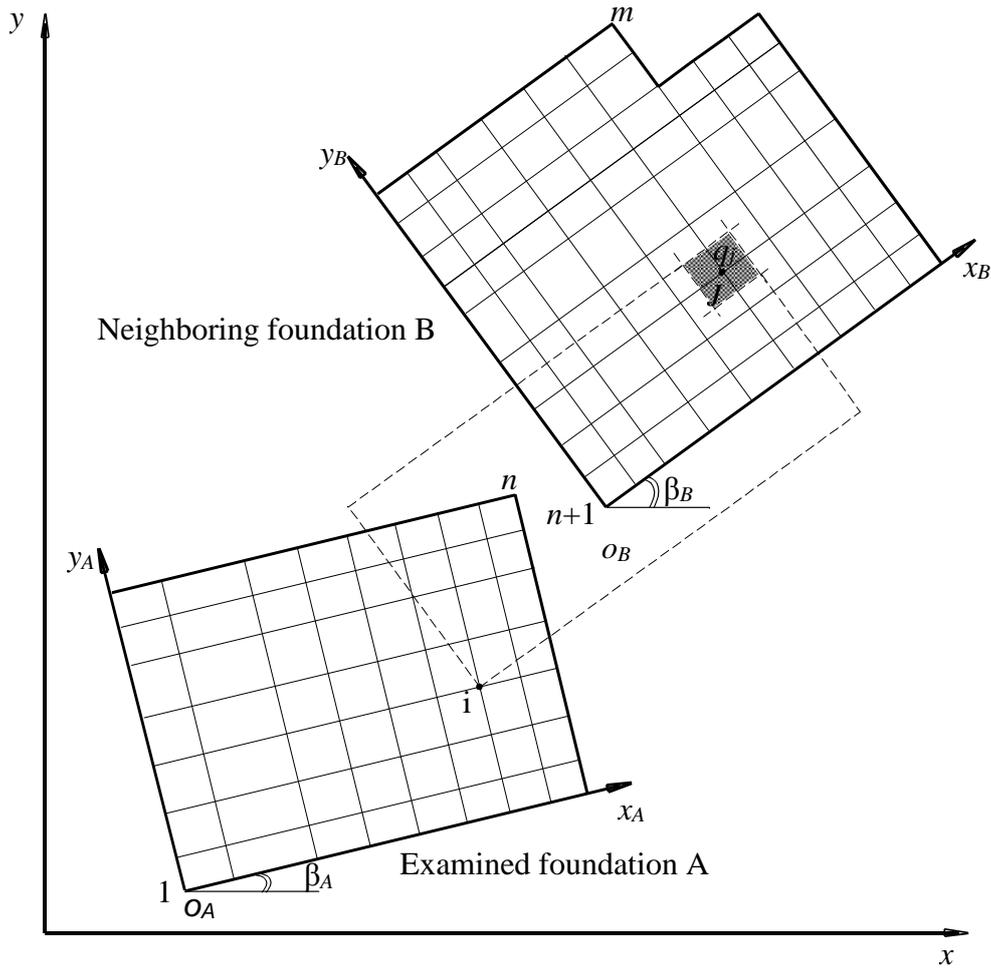
<u>Figure 3.1</u>   Examined foundation A with a neighboring foundation B

The presence of neighboring loads will cause additional settlements $s_{i.D}$ at nodal points of the existing foundation. The additional settlement $s_{i.D}$ at the nodal point i is given by

$$s_{i.D} = \sum_{r=n+1}^{r=m} c_{i,\,n+1}\, Q_{n+r} \tag{2.1}$$

where:

$c_{i,\,n+r}$ Flexibility coefficient of the node i due to a unit load at node $n + r$ [m/kN]

Q_{n+r} Contact force at node $n + r$ [kN]

r Node No. in the neighboring foundation B

Due to the neighboring foundation, the total settlement on the foundation A can be expressed in matrix form as

$$\{s\} = \{s_o\} + \{s_D\} \tag{2.2}$$

or

$$\{s\} = [c]\{Q\} + [c_D]\{Q_D\} \tag{2.3}$$

where:
{s}   Vector of the total settlement of the examined foundation A
{s_o}   Vector of the settlement due to stress of the examined foundation A
{s_D}   Vector of the additional settlement due to stress of neighboring foundation B
{Q_D}   Vector of contact forces for the examined foundation A
[c]   Flexibility matrix of the soil for the examined foundation A
[c_D]   Flexibility matrix of the soil due to the neighboring foundation B
{Q_D}   Vector of contact forces due to the neighboring foundation B

Through inversion of the matrix [c], the following equation will be given

$$\{Q\} = [k_s]\{s\} + [k_s]\{s_D\} \tag{2.4}$$

or

$$\{Q\} = [k_s]\{s\} + [k_s][c_D]\{Q_D\} \tag{2.5}$$

Then, the system equation of the examined foundation A due to influence of neighboring foundation B in matrix form is

$$\left[[k_p] + [k_s]\right]\{\delta\} = \{P\} + [k_s][c_D]\{Q_D\} \tag{2.6}$$

where:
[k_P]   Plate stiffness matrix of the examined foundation A
[k_s]   Soil stiffness matrix for the examined foundation A
{δ}   Vector of nodal displacements of the examined foundation A
{P}   Vector of applied loads on the examined foundation A

3.3   Influence of buried structures

Buried structures such as tunnels and culverts cause lowering of the ground. If a foundation exists above such structures, it will be affected by an additional settlement $s_{i.V}$ at the node i due to vertical displacement through the influence of buried structures.

Then, the total additional settlement $s_{i.A}$ at the node i of the foundation due to external influences is

$$s_{i.A} = s_{i.V} + s_{i.D} \tag{2.7}$$

Example 3.1   Settlement outside the foundation

1   Description of the problem

Besides the possibility of studying the influence of neighboring structures on the foundation by the program *ELPLA*, the described algorithm of *ELPLA* can be used also for the calculation of settlements outside the foundation. This can be carried out through one of the following two ways:

i)   Using a net for the foundation and the unloaded areas outside the foundation. Then, the rigidity of the unloaded areas can be eliminated by assuming very small thickness

ii)   Using two independent nets, one for the foundation and the other for the unloaded areas outside the foundation as considered in this example

Figure 3.2 shows an irregular raft that has the contact area I with opening inside it. It is required to determine the settlements at the area II around the raft and at the opening of area III.

2   Soil properties

The raft of contact area I and the outside areas II and III are on regular subsoil. The soil is supposed to have the following parameters:

Modulus of compressibility E_s = 9500 [kN/m^2]
Poisson's ratio ν_s = 0.0   [-]

The displacement of the soil is considered only in the vertical direction. Therefore, *Poisson*'s ratio for the soil is assumed to be zero.

3   Raft material and thickness

The raft material and thickness are supposed to have the following parameters:

Young's modulus E_b = 2×10^7 [kN/m^2]
Poisson's ratio ν_b = 0.25   [-]
Unit weight γ_b = 0   [kN/m^3]
Raft thickness d = 0.7   [m]

Unit weight of the raft material is assumed zero to neglect its own weight in the analysis.

4   Loads

The raft carries 12 concentrated loads as shown in Figure 3.2.

5   Mathematical model

The influence of surrounding structures and external loads can be taken into consideration only for the Continuum model (methods 4, 5, 6, 7 and 8). The Continuum model bases on the settlement at any node is affected by the contact forces at all the other nodes. In this example, the Isotropic elastic half-space soil medium (method 5) is chosen to analyze the raft I and outside areas II and III.

6   Analysis

To carry out the analysis, the raft I and the outside areas II and III are subdivided into two independent element nets as shown in Figure 3.2b. Two independent names are chosen to define the data of the raft and the outside areas. The origin coordinates of the raft are $(x_o, y_o) = (8.0, 8.0)$, while for the outside areas are $(0.0, 0.0)$.

The analysis of the raft I is carried out to obtain the contact pressures under it first. Due to these contact pressures, settlements will occur not only under the raft I but also outside under areas II and III. Then, the settlements of the outside areas II and III are determined.

7   Results

Figure 3.3 shows the contact pressures under the raft I that cause the settlements under it and also at the outside areas II and III. Figure 3.4 shows the contour lines of the settlements under the raft.

Figure 3.5a shows the settlement at the middle section *s-s* of the outside areas II and III, while Figure 3.5b shows the contour lines of the settlements. As it is expected, the greatest values of settlements are near the raft.
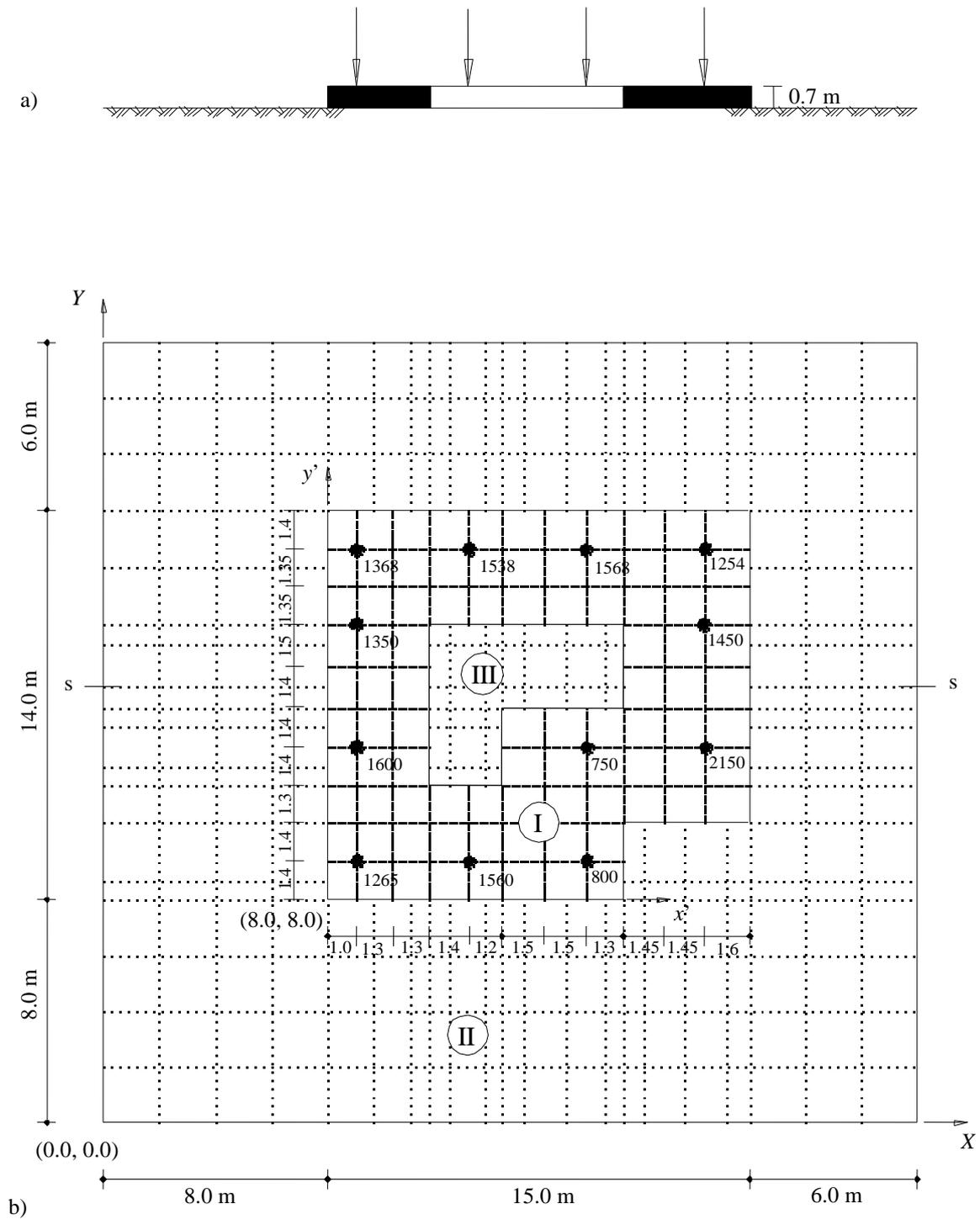
Figure 3.2   a) Section s-s through the raft
               b) Raft (area I) with loads [kN] and neighboring areas II and III
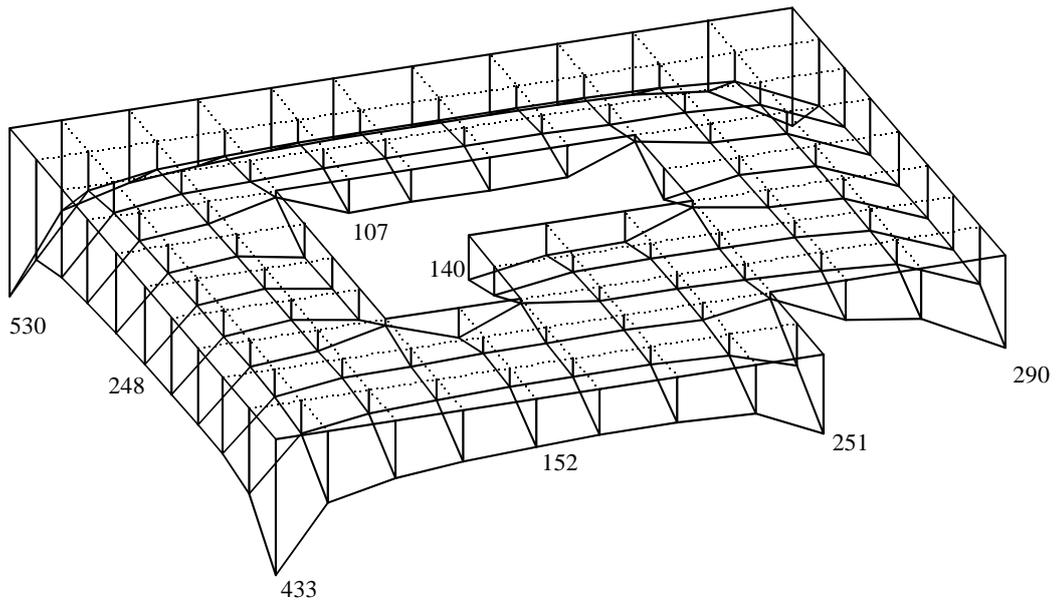
Figure 3.3   Contact pressures [kN/m^2] under the raft
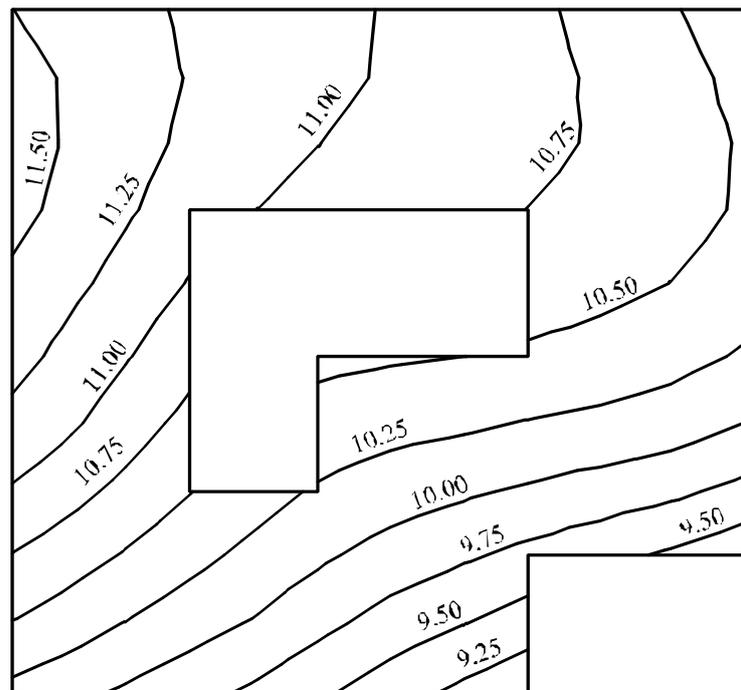

Figure 3.4   Contour lines of settlements [cm] under the raft
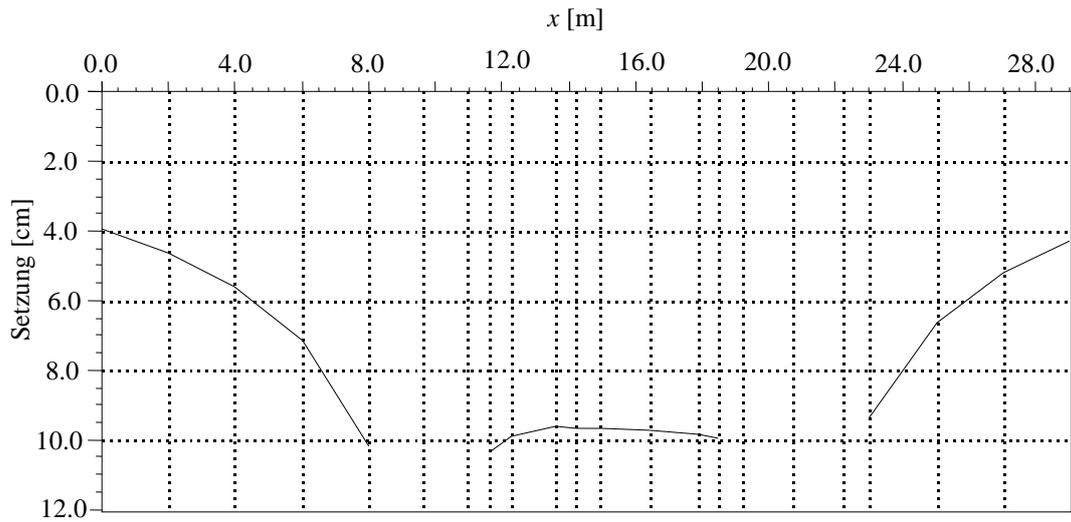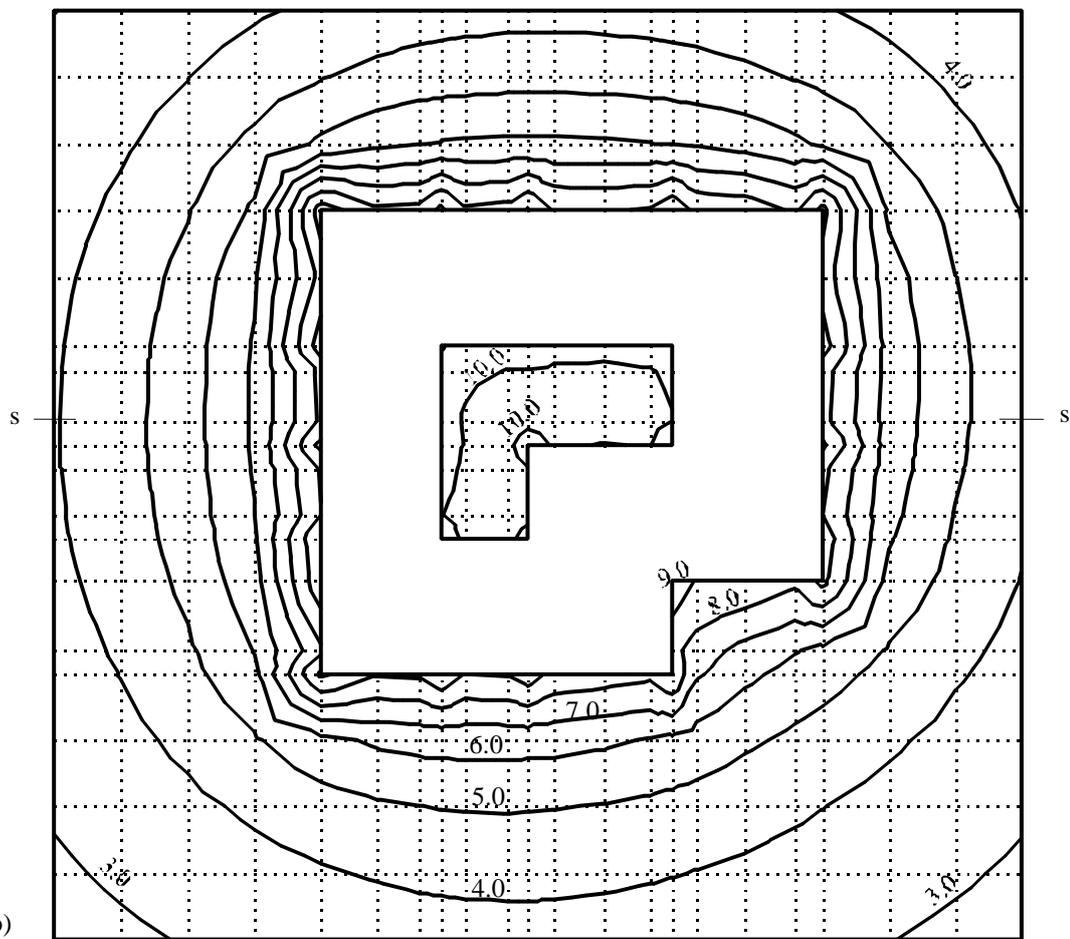
Figure 3.5   a) Settlements of neighboring areas II and III at section s-s
               b) Contour lines of settlements [cm] of neighboring areas II and III

Example 3.2   Influence of a new neighboring building II on an old one I

1   Description of the problem

For the explanation of the influence of a neighboring building, the influence of a new building on an existing old one is examined in this example.

Figure 3.6 shows plan and section of a new building II beside a similar old one I. The building I was constructed since long time, while the building II will be constructed close to the first one. The two buildings have the same construction geometry and loads. Also, every building is symmetrical about both x- and y-axes.

2   Soil properties

The subsoil under the buildings consists of a layer of stiff plastic clay 5.70 [m] thick, overlying a rigid base (Figure 3.6a). The soil is supposed to have the following parameters:

Modulus of compressibility for loading	E_s	= 5 000	[kN/m^2]
Modulus of compressibility for reloading	W_s	= 15 000	[kN/m^2]
Unit weight	γ_s	= 18	[kN/m^3]
Poisson's ratio	ν_s	= 0.0	[-]

The displacement of the soil is considered only in the vertical direction. Therefore, *Poisson*'s ratio for the clay is assumed to be zero.

3   Foundation material and thickness

Foundation material and thickness are supposed to have the following parameters:

Young's modulus	E_b	= 2×10^7	[kN/m^2]
Poisson's ratio	ν_b	= 0.25	[-]
Unit weight	γ_b	= 0.0	[kN/m^3]
Foundation thickness	d	= 1.0	[m]

Unit weight of the foundation material is assumed zero to neglect its own weight in the analysis.

4   Mathematical model

The influence of surrounding structures and external loads can be taken into consideration only for the Continuum model (methods 4 to 9). The Continuum model bases on the settlement at any node is affected by the forces at all the other nodes. In this example, the Modulus of compressibility method (method 7) is chosen to analyze both of the two buildings.

5   Analysis

To analyze the foundations, each foundation is subdivided into elements with 189 nodes as shown in Figure 3.6b. Two independent names are chosen to define the data of the two buildings. The data are quite similar for the two buildings except the origin coordinates, which are chosen to be (x_o, y_o) = (10.28, 0.0) and (0.0, 0.0) for buildings I and II, respectively. In spite of the two buildings are closed to each other, a small distance of 20 [cm] is assumed between them to avoid overlapping their nodes.

The analysis of the new building II is carried out first to obtain the contact pressures under it. Due to these contact pressures, settlements will occur not only under the building II but also outside under the building I. Then, under the assumption that left beside the old building a new building will be constructed, the contact pressures, settlements and internal forces of the old building are determined.

6   Results and evaluation

Figure 3.7a shows the contact pressure distribution that was originally available under the old building. As it is expected, the contact pressures are distributed symmetrically, because the building was analyzed under the assumption that the loads are symmetrically applied.

Figure 3.7b on the right shows the changes in contact pressures under the old building, while the opposite figure on the left shows the contact pressures under the new building. Through comparison it is to recognize that considerable differences occur in the contact pressure distribution under the old building. The contact pressures became smaller at the edge between new building and old building due to the additional settlements from the influence of the neighboring building. From equilibrium of the vertical forces, the contact pressures became larger in the middle of the old building. Of course, the change in contact pressure distribution under the building will cause also changing and shifting the stress of the old building. Accordingly, the moments of the old building will be affected.

Figure 3.8a shows the settlements as contour lines under the old building I without the influence of the neighboring building. Because there is a centric resultant load, the settlements are symmetrical.

Figure 3.8b on the right shows the settlements of the old building I and on the left the settlements of the new building II. As it is expected, the old building settled additionally at the edge to the new building. Consequently, the settlements are regressive on the right side of the old building. This means a tilt of the old building occurs.

Figure 3.9 shows the settlements s, contact pressures q and moments m_x at the middle of the foundations for both buildings I and II.

From the results it is recognized furthermore, that the settlements at the edge nodes of the old building near to the new building increase strongly (Figure 3.9a). Therefore, the settlement increased from 4.79 [cm] to 7.31 [cm] at the middle of the foundation.

The influence of the neighboring building is very clearly noticeable in curves of Figure 3.9c. Due to the greatest positive moment (column moment with load $P = 2000$ [kN]), which increased from 787 [kNm/m] (only new building) to 654 [kNm/m], the sign of the field moment is changed. The field moment (only new building) reaches 20 [kNm/m], while with the influence of a neighboring building at the same node the field moment reaches -200 [kNm/m].

By these results you can now estimate the addition stress on the old building due to the influence of the new building and consequently prevent damages of the old building.

$E_b = 2 \times 10^7$ [kN/m^2]
$\nu_b = 0.15$ [-]
$\gamma_b = 0.0$ [kN/ m^3]

(0.00)

(1.50)

$d = 1.0$ m

Clay, stiff plastic

$E_s = 5000$ [kN/m^2]
$W_s = 15000$ [kN/m^2]
$\gamma_s = 18$ [kN/ m^3]

(7.20)

Rock

a) Section a-a

$P_1 = 500$ [kN]
$P_2 = 1000$ [kN]
$P_3 = 2000$ [kN]

New building II   Old building I

$14 \times 0.72 = 10.08$ m

$14 \times 0.72 = 10.08$ m $14 \times 0.72 = 10.08$ m

b) Plan
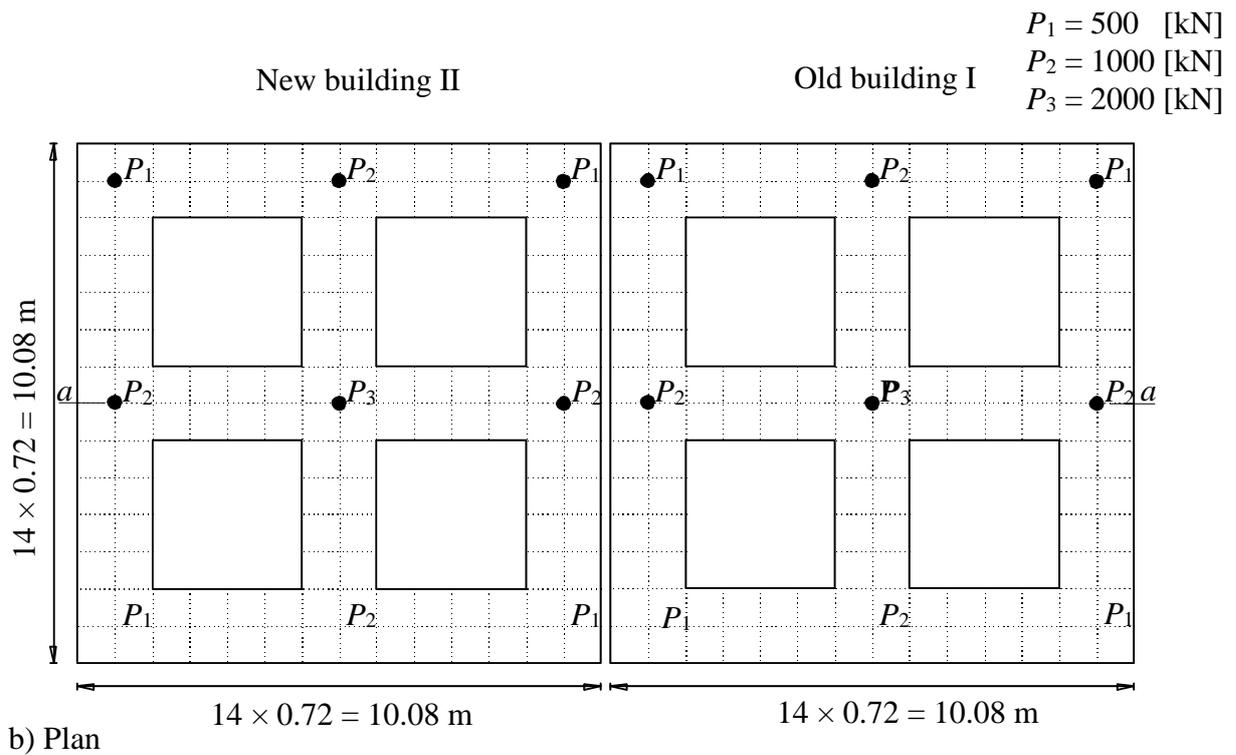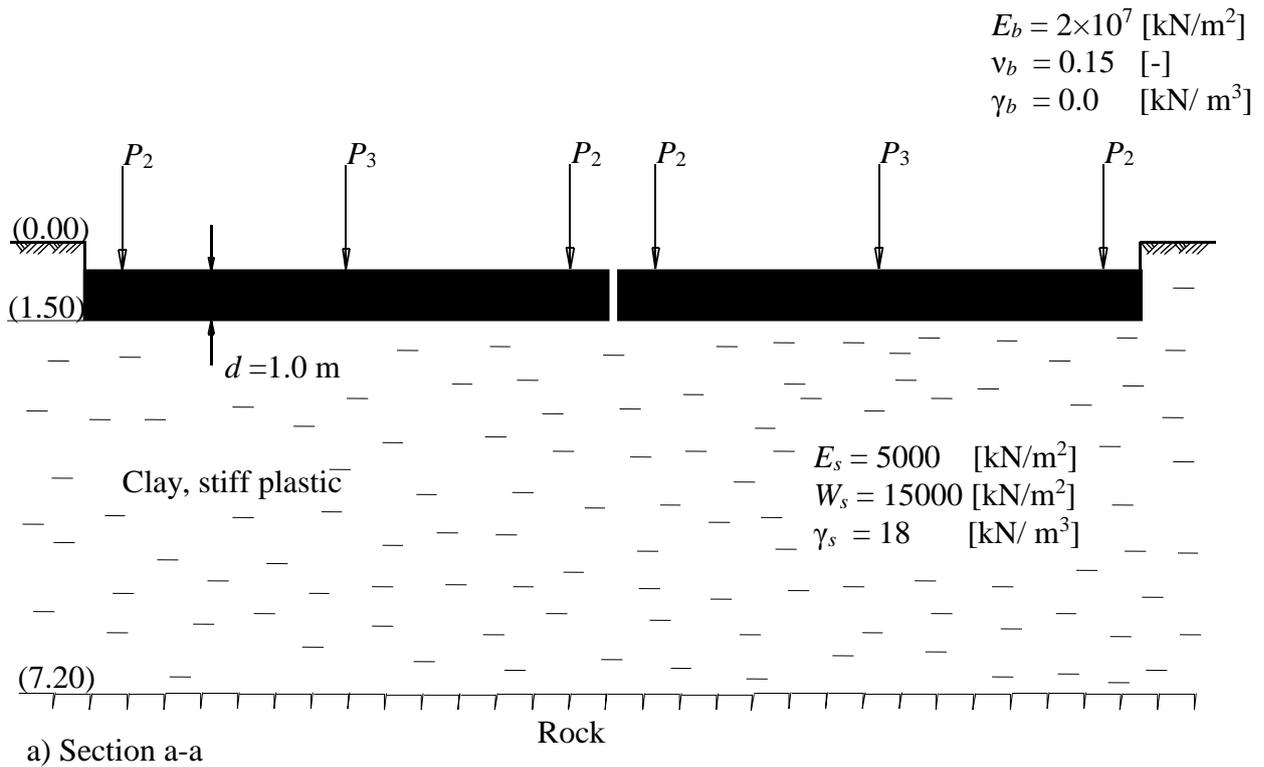
Figure 3.6   Action of new building II on the old building I

Old building

a) Only old building

New building   Old building

b) New building + old building
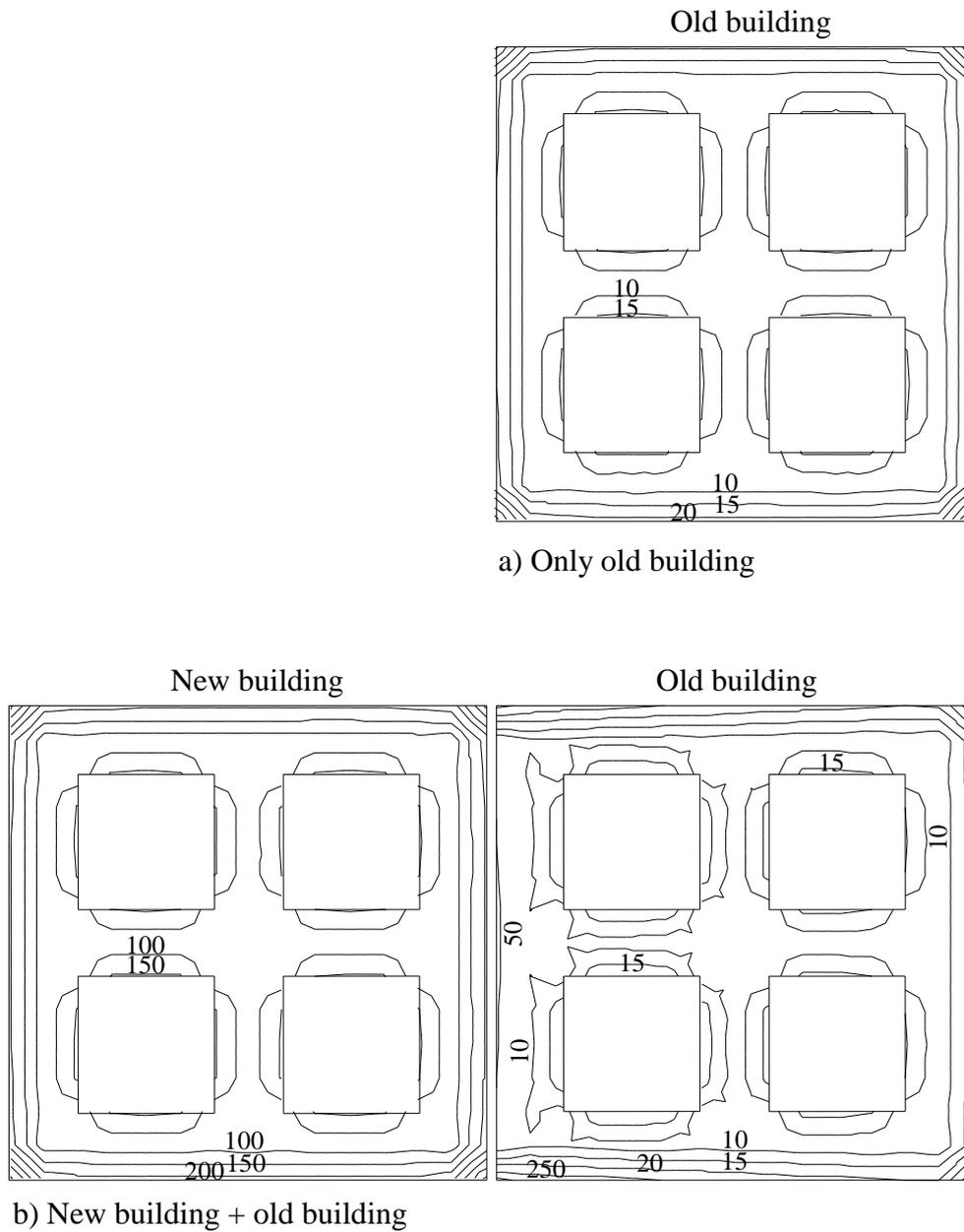
Figure 3.7   Contour lines of contact pressures [kN/m^2] under the new and old buildings

Old building

a) Only old building

New building   Old building

b) New building + old building
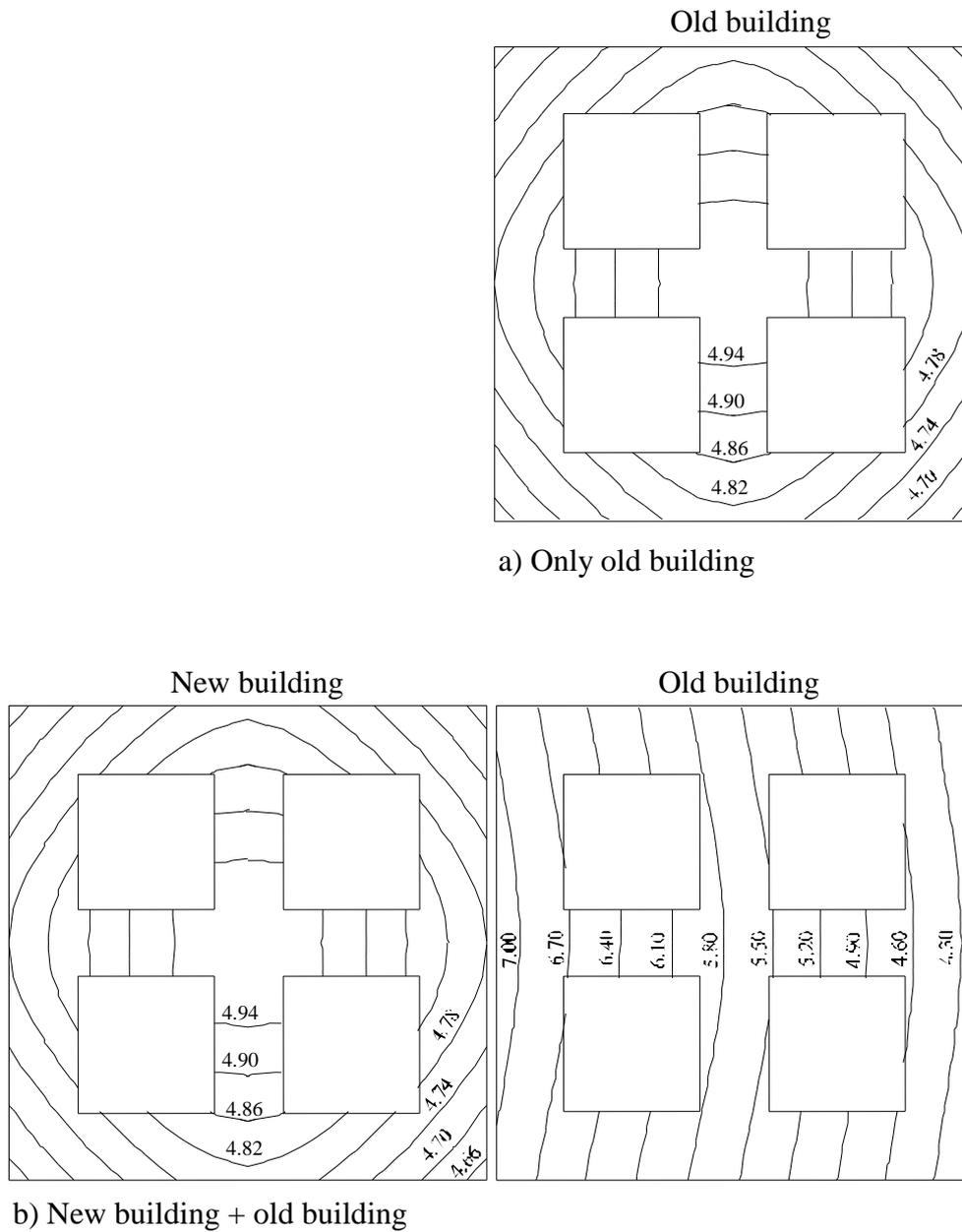
Figure 3.8   Contour lines of settlements [cm] under the new and old buildings
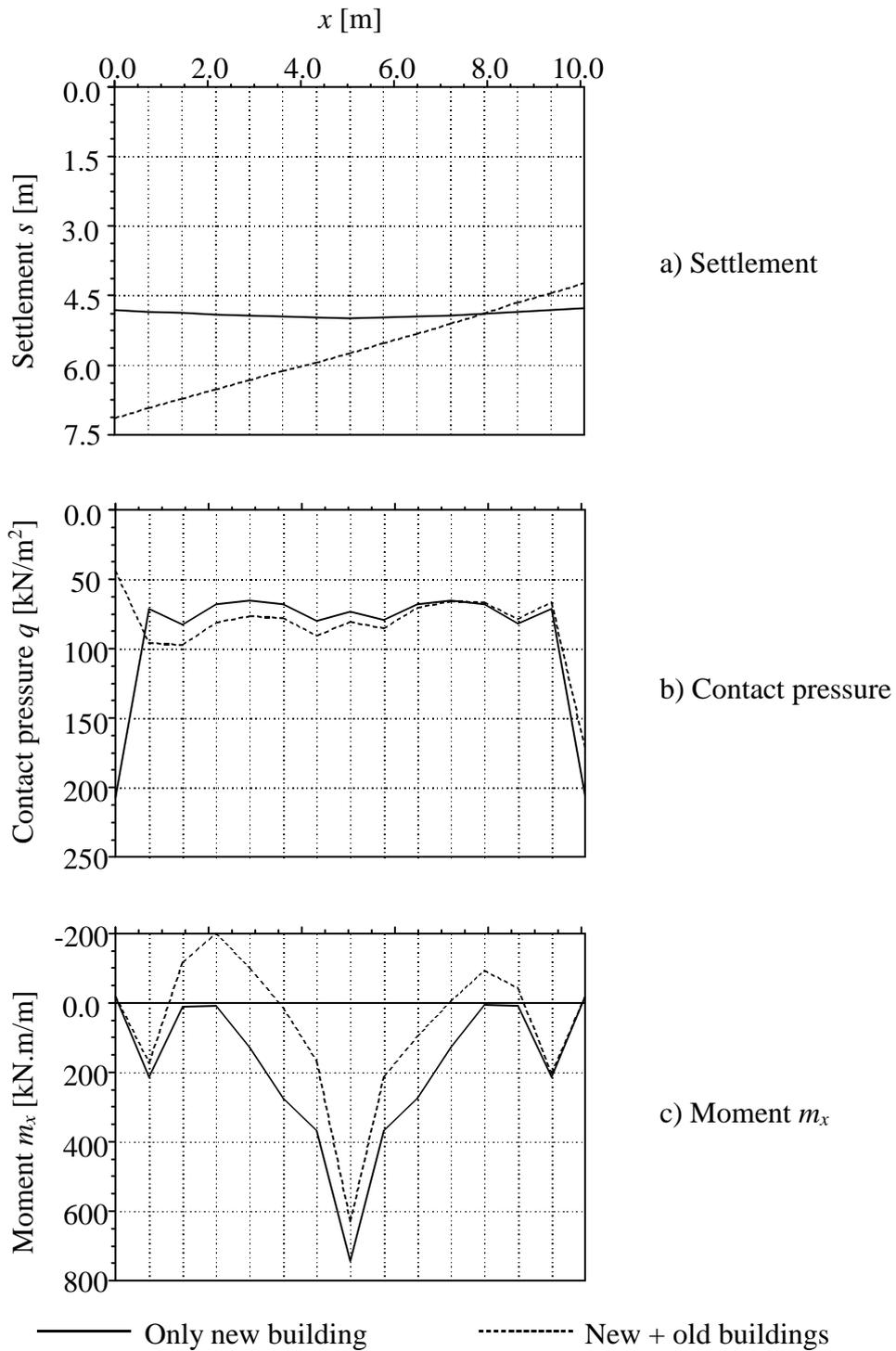
Figure 3.9   Settlements, contact pressures and moments at the middle of the foundation

Example 3.3 Influence of ground lowering on a building due to a tunnel

1   Description of the problem

Figure 3.10 shows a raft of a building that consists of two rectangular parts, which are completely connected. The raft is 50 [cm] thick and has a foundation depth of 2.50 [m] under the ground surface. It is planned to construct a tunnel diagonally to the building axis. A primary estimation expects that the tunnel will cause a settlement trough of about 9 [m] width with a maximum lowering of 3 [cm] for the building ground. The settlement trough is plotted in Figure 3.10 as contour lines, running symmetrically to the tunnel axis. The influence of the settlement trough due to construction of the tunnel is considered in the analysis of the raft. The raft carries two equal column loads, each of $P = 18000$ [kN] and line loads of $p = 300$ [kN/m] from edge walls. The edge walls have 0.30 [m] breadth and 3 [m] height.

2   Soil properties

The subsoil under the raft is defined by 3 boring logs B1 to B3 up to 14 [m] under the ground surface. The subsoil consists of two soil layers of clay and sandstone, which are not horizontally stratified as shown in Figure 3.10 and Table 3.1. *Poisson*'s ratio for the soil is $\nu_s = 0.3$ [-].

Tabelle 3.1   Soil properties

Layer No.	Type of soil	Depth of layer underground surface z [m]	Modulus of compressibility of the soil for		Unit weight of the soil γ_s [kN/m³]
			Loading E_s [kN/m²]	Reloading W_s [kN/m²]	
1	Clay	5.5/ 6.3/ 7.0	10000	30000	18
2	Sandstone	14	160000	400000	21

3   Raft material and properties

The raft material is reinforced concrete and has the following properties:

Young's modulus E_b $= 3 \times 10^7$ [kN/m²]
Shear modulus G_b $= 1.25 \times 10^7$ [kN/m²]
Poisson's ratio ν_b $= 0.2$ [-]
Unit weight γ_b $= 25$ [kN/m³]

The rigidity of the edge walls (0.30 [m] breadth and 3 [m] height) is simulated through beam elements along the raft edge with the following data:

Moment of inertia I $= 0.675$ [m⁴]
Torsional inertia J $= 0.0253$ [m⁴]

4   Analysis of the raft

The raft is subdivided into 112 square finite elements. Each element has a side of 1.5 [m] as shown in Figure 3.10. The analysis of the raft is carried out by the modulus of compressibility method (method 7). To consider the irregularity of subsoil under the raft, the flexibility coefficients are determined through bilinear interpolation. To examine the influence of the tunnel on the raft, the analysis of the raft is carried out first without consideration of the tunnel, then with consideration of the estimated settlements due to presence of the tunnel.

5   Results and discussion

The results of the settlements, contact pressures and moments are presented in Figures 3.11 to 3.13. It can be concluded from the figures that:

-        The contact pressure under the columns become higher, while that at the field between columns become smaller

-        Due to the effect of the tunnel, the settlement under the raft at area above the tunnel will increase while the contact pressure will decrease. The change in the moment at this area is also remarkable

-        Moments become higher under the column, while that in the fields between columns become smaller. However, overall the change in the moments in this example is not great

a)

b)
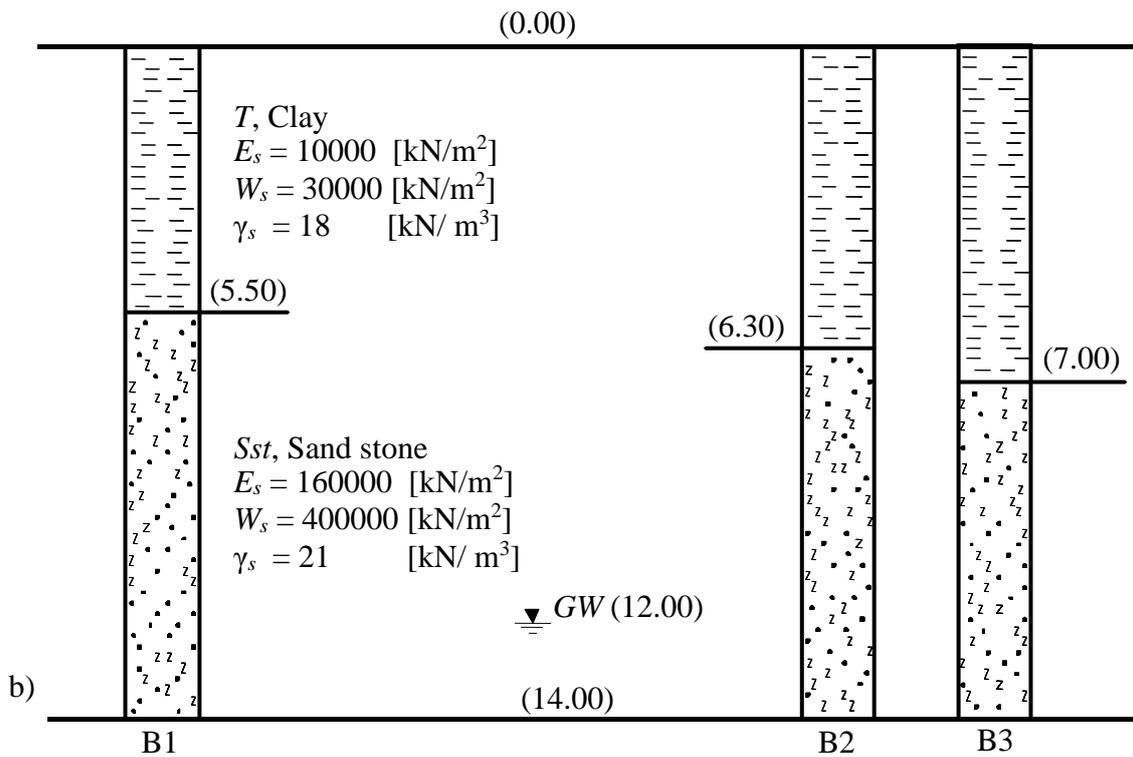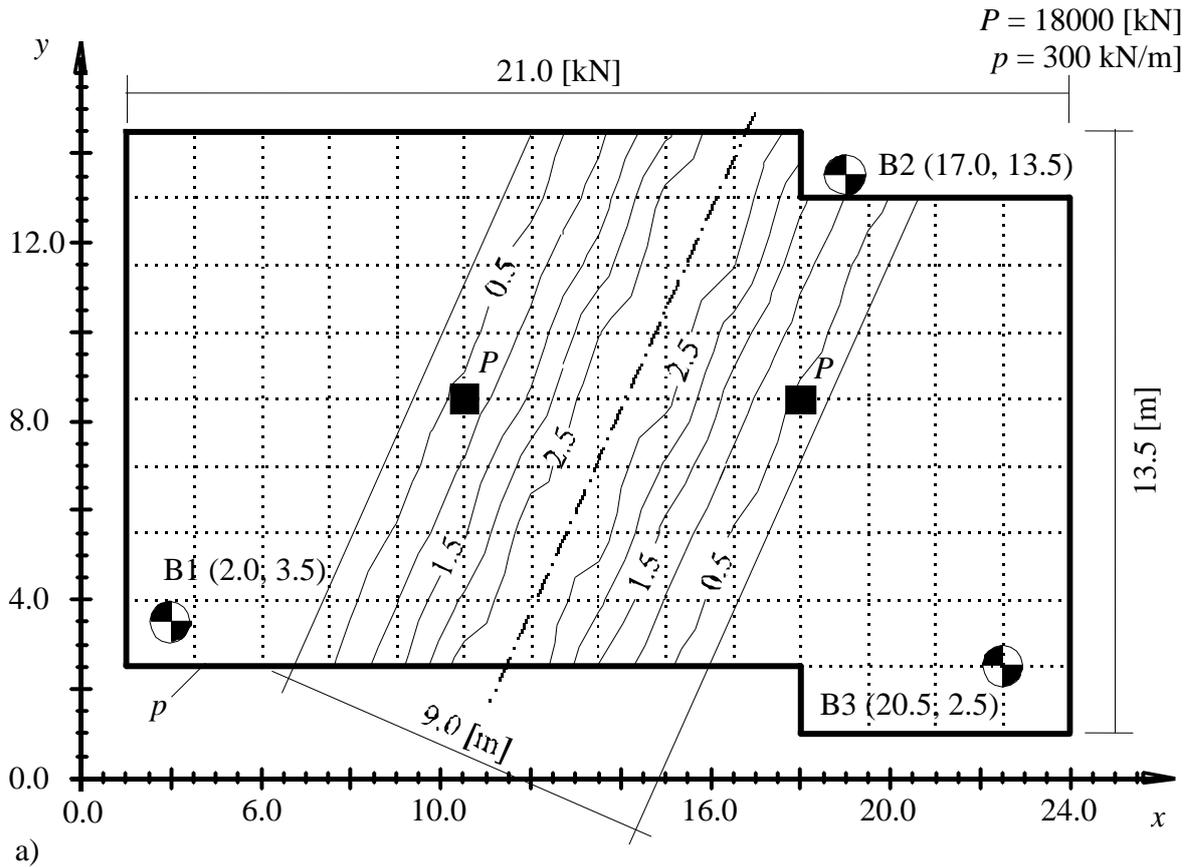
Figure 3.10   a) Raft plan, settlement trough due to tunnel as contour lines and loads
                b) Boring logs B1 to B3

a)

b)
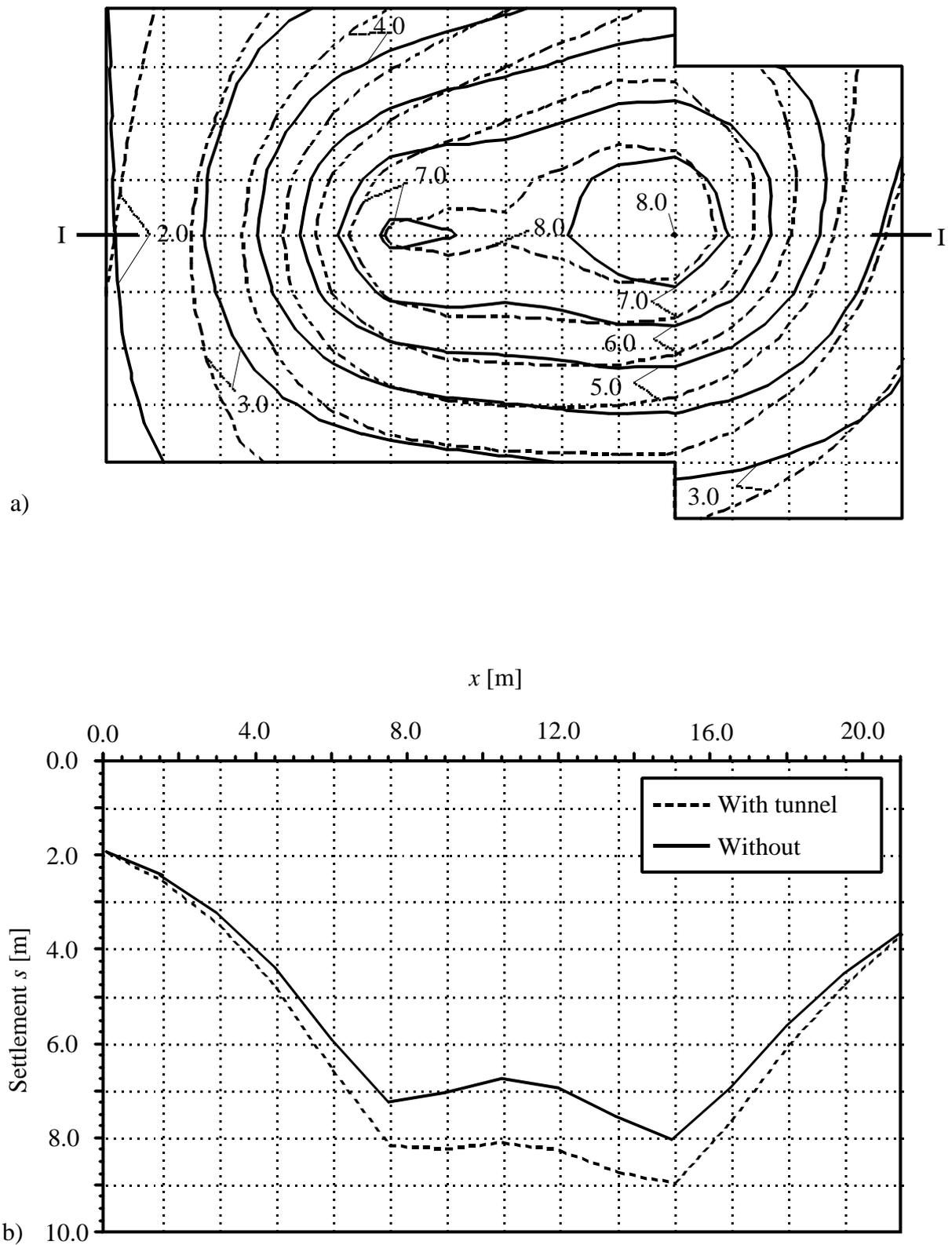
Figure 3.11   Settlements s [cm] without and with consideration of the tunneling
                a) Contour lines
                b) Section I-I

a)

x [m]

b)
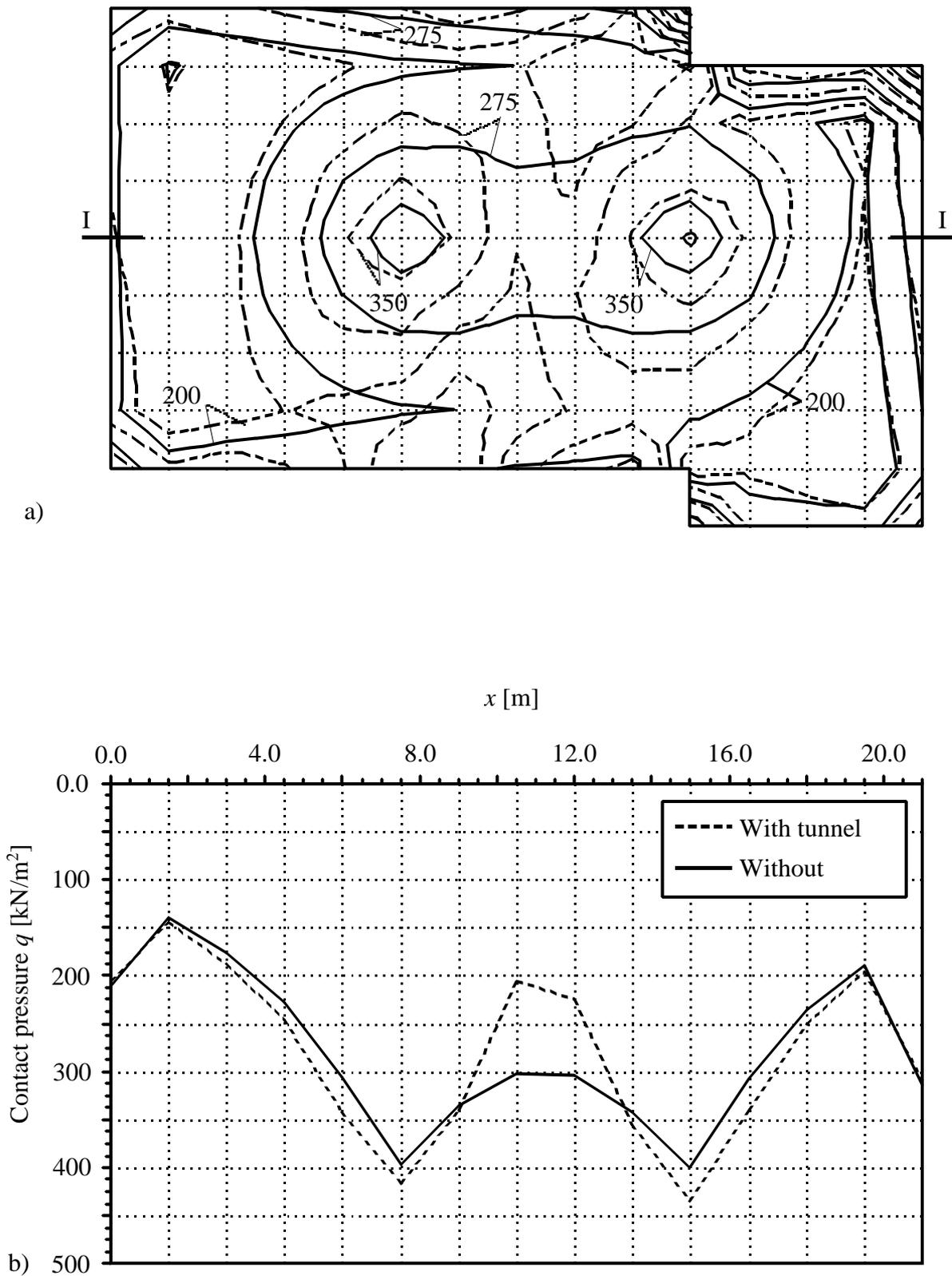
Figure 3.12   Contact pressures q [kN/m²] without and with consideration of the tunneling
a) Contour lines
b) Section I-I

a)

x [m]

Moment m_x [kN.m/m]

- - - With tunnel

—— Without

b)
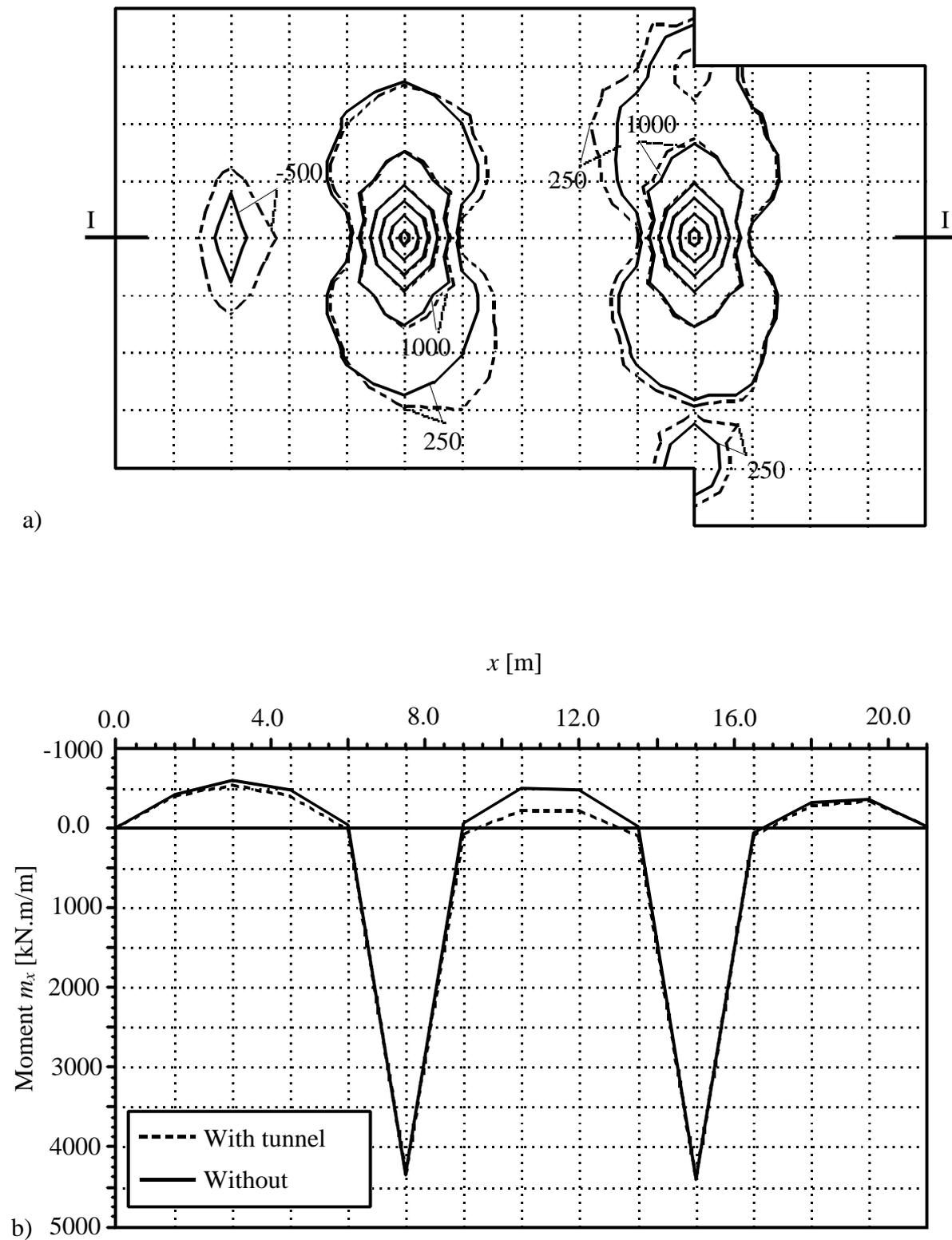
Figure 3.13   Moments m_x [kN.m/m] without and with consideration of the tunneling
a) Contour lines
b) Section I-I

Chapter 4

System of many Foundations

Contents

4.1   Introduction

In many practical cases, it becomes important to study the interaction of elastic or rigid foundations, which are constructed simultaneously. In this case, there will be interaction of foundations due to the overlapping of stresses through the soil medium however the structures are not statically connected. The interaction of foundations will cause additional settlements under all foundations.

The conventional solution of this problem assumes that the contact pressure of the foundation is known and distributed linearly on the bottom of it. Accordingly, the soil settlements due to the system of foundations can be easily determined.

This assumption may be correct for small foundations, but for big foundations, it is preferred to analyze the foundation as a plate resting on either elastic springs (*Winkler*'s model) or continuum model. In spite of the simplicity of the first model in application, one cannot consider the effect of neighboring foundations or the influence of additional exterior loads. Thus, because *Winkler*'s model is based on the contact pressure at any point on the bottom of the foundation is proportional to the deflection at that point, independent of the deflections at the other points. Representation of soil as Continuum model (methodes 4, 5, 6, 7 and 8) enables one to consider the effect of external loads.

The study of interaction between a foundation and another neighboring foundation or an external load has been considered by several authors. *Stark* (1990) presented an example for the interaction between two rafts. *Kany* (1972) presented an analysis of a system of rigid foundations. In addition, he presented a solution of system of foundations considering the rigidity of the superstructure using a direct method (*Kany* 1977). Recently, *Kany/ El Gendy* (1997) and (1999) presented an analysis of system of elastic or rigid foundations on irregular subsoil model using an iterative procedure.

This section presents a general solution for the analysis of system of foundations, elastic or rigid, using the iterative procedure of *Kany/ El Gendy* (1997) and (1999).

4.2   Definition of system of foundations

To describe the analysis of system of slab foundations, consider the example system of slabs shown in Figure 4.1. The system consists of three different slabs I, II and III. It is supposed to be constructed separately simultaneously. The three slabs are divided into square elements having $r = r_I + r_{II} + r_{III}$ nodes. The node numbering and loads are defined in the global system of coordinate x-y as shown in Figure 4.1. The contact pressure q_i at a node i is replaced by equivalent contact force Q_i. Additional two external foundations IV and V are constructed after the system of the three slabs is carried out. Those two external foundations will provide an additional settlement $s_{i,A}$ at a node i.
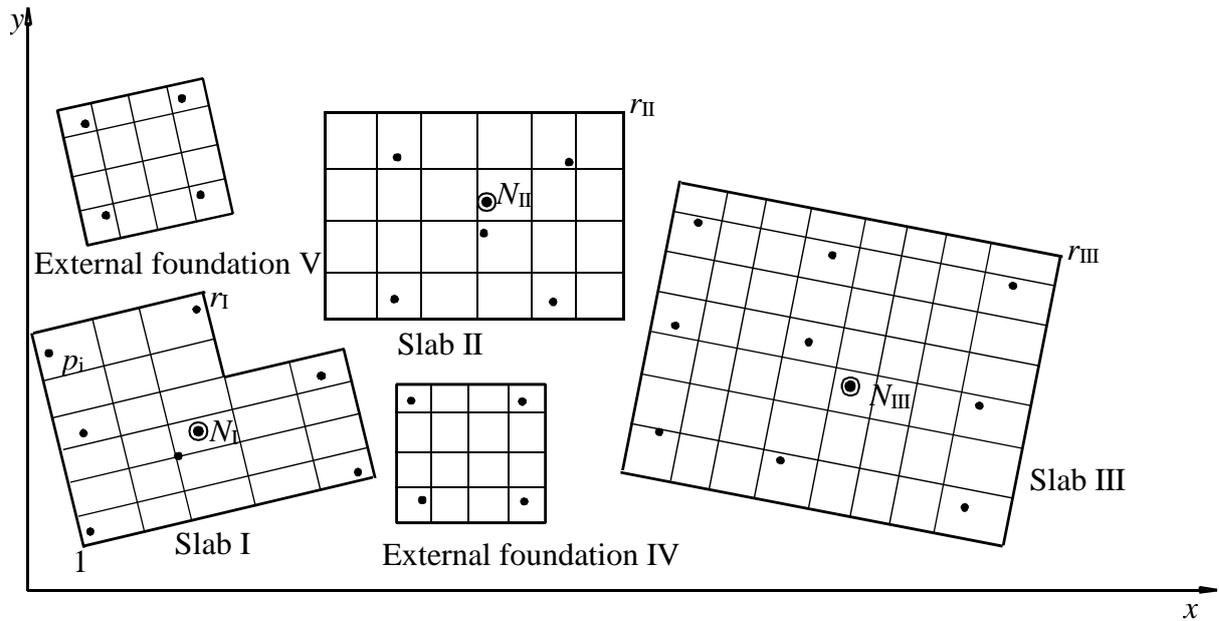
Figure 4.1   Plan of a system of three slabs (I to III) and two external foundations IV and V

4.3   Summation equation of settlement

For the set of grid points of the three slabs, the settlement s_i at a point i is defined by series of unknown contact pressures Q_k as shown in Equation 4.1

$$s_i = \sum_{k=1}^{k=r} (c_{i,k}\, Q_k) + s_{i.A} \tag{4.1}$$

where:
$c_{i,k}$ Flexibility coefficient of node i due to a unit load at node k
$s_{i.A}$ Additional settlement at that node due to external influences (foundations IV and V)

4.4   Assembling the flexibility matrix

The analysis of an isolated foundation on three-dimensional subsoil model, which was presented by *Kany/ El Gendy* (1995), may be used also here for the analysis of system of foundations.

Assembling the total flexibility matrix for the system of slabs in Figure 4.1, which has total number of $r = 145$ nodes, requires to do $r^2 = 21025$ settlement calculations through Equation 4.1 (without external foundations IV and V).

Equation 4.1 can be rewritten in matrix form as

$$\begin{Bmatrix} \{s\}_I \\ \{s\}_{II} \\ \{s\}_{III} \end{Bmatrix} = \begin{bmatrix} [c]_{I,I} & [c]_{I,II} & [c]_{I,III} \\ [c]_{II,I} & [c]_{II,II} & [c]_{II,III} \\ [c]_{III,I} & [c]_{III,II} & [c]_{III,III} \end{bmatrix} \begin{Bmatrix} \{Q\}_I \\ \{Q\}_{II} \\ \{Q\}_{III} \end{Bmatrix} + \begin{Bmatrix} \{s_A\}_I \\ \{s_A\}_{II} \\ \{s_A\}_{III} \end{Bmatrix} \tag{4.2}$$

where:

$\{s\}_I$ Settlement vector of the slab I

$[c]_{I,J}$ Flexibility matrix of the slab I due to contact pressure of slab J

$\{Q\}_I$ Contact force vector of the slab I

$\{s_A\}_I$ Additional settlement vector of the slab I due to external influences
        (foundations IV and V)

Inverting the total flexibility matrix gives the total soil stiffness matrix as

$$\begin{Bmatrix} \{Q\}_I \\ \{Q\}_{II} \\ \{Q\}_{III} \end{Bmatrix} = \begin{bmatrix} [c]_{I,I} & [c]_{I,II} & [c]_{I,III} \\ [c]_{II,I} & [c]_{II,II} & [c]_{II,III} \\ [c]_{III,I} & [c]_{III,II} & [c]_{III,III} \end{bmatrix}^{-1} \left(\begin{Bmatrix} \{s\}_I \\ \{s\}_{II} \\ \{s\}_{III} \end{Bmatrix} - \begin{Bmatrix} \{s_A\}_I \\ \{s_A\}_{II} \\ \{s_A\}_{III} \end{Bmatrix} \right) \tag{4.3}$$

4.5   Analysis of system of elastic foundations
4.5.1   Assembling the system of linear equations

For big foundations, the foundation is treated as a plate on elastic medium. From the finite element analysis of the plate, the equilibrium of foundation I is expressed by the following matrix equation

$$[k_p]_I \{\delta\}_I = \{P\}_I - \{Q\}_I \tag{4.4}$$

In the same manner for foundation II

$$[k_p]_{II} \{\delta\}_{II} = \{P\}_{II} - \{Q\}_{II} \tag{4.5}$$

and for foundation III

$$[k_p]_{III} \{\delta\}_{III} = \{P\}_{III} - \{Q\}_{III} \tag{4.6}$$

where:

$\{p\}_I, \{p\}_{II}$ und $\{p\}_{III}$ External force vectors of slabs I, II and III

$\{\delta\}_I, \{\delta\}_{II}$ und $\{\delta\}_{III}$ Deformation vectors of slabs I, II and II

$[k_p]_I, [k_p]_{II}$ und $[k_p]_{III}$ Plate stiffness matrix of slabs I, II and III

Equations 4.4, 4.5 and 4.6 are rewritten in matrix form as

$$\begin{bmatrix} \begin{bmatrix} K_p \end{bmatrix}_I & \begin{bmatrix} 0 \end{bmatrix} & \begin{bmatrix} 0 \end{bmatrix} \\ \begin{bmatrix} 0 \end{bmatrix} & \begin{bmatrix} K_p \end{bmatrix}_{II} & \begin{bmatrix} 0 \end{bmatrix} \\ \begin{bmatrix} 0 \end{bmatrix} & \begin{bmatrix} 0 \end{bmatrix} & \begin{bmatrix} K_p \end{bmatrix}_{III} \end{bmatrix} \begin{Bmatrix} \{\delta\}_I \\ \{\delta\}_{II} \\ \{\delta\}_{III} \end{Bmatrix} = \begin{Bmatrix} \{P\}_I \\ \{P\}_{II} \\ \{P\}_{III} \end{Bmatrix} - \begin{Bmatrix} \{Q\}_I \\ \{Q\}_{II} \\ \{Q\}_{III} \end{Bmatrix} \qquad (4.7)$$

Substituting Equation 4.3 into Equation 4.7 gives the following linear system equations in matrix form as

$$\begin{bmatrix} \begin{bmatrix} K_p \end{bmatrix}_I & \begin{bmatrix} 0 \end{bmatrix} & \begin{bmatrix} 0 \end{bmatrix} \\ \begin{bmatrix} 0 \end{bmatrix} & \begin{bmatrix} K_p \end{bmatrix}_{II} & \begin{bmatrix} 0 \end{bmatrix} \\ \begin{bmatrix} 0 \end{bmatrix} & \begin{bmatrix} 0 \end{bmatrix} & \begin{bmatrix} K_p \end{bmatrix}_{III} \end{bmatrix} \begin{Bmatrix} \{\delta\}_I \\ \{\delta\}_{II} \\ \{\delta\}_{III} \end{Bmatrix} = \begin{Bmatrix} \{P\}_I \\ \{P\}_{II} \\ \{P\}_{III} \end{Bmatrix} -$$

$$\begin{bmatrix} [c]_{I,I} & [c]_{I,II} & [c]_{I,III} \\ [c]_{II,I} & [c]_{II,II} & [c]_{II,III} \\ [c]_{III,I} & [c]_{III,II} & [c]_{III,III} \end{bmatrix}^{-1} \left(\begin{Bmatrix} \{s\}_I \\ \{s\}_{II} \\ \{s\}_{III} \end{Bmatrix} - \begin{Bmatrix} \{s_A\}_I \\ \{s_A\}_{II} \\ \{s_A\}_{III} \end{Bmatrix} \right) \qquad (4.8)$$

Considering the compatibility of deformations between the slab and the soil medium, where the soil settlement s is equal to the slab deflection w, Equation 4.8 becomes

$$\begin{bmatrix} \begin{bmatrix} \begin{bmatrix} K_p \end{bmatrix}_I & \begin{bmatrix} 0 \end{bmatrix} & \begin{bmatrix} 0 \end{bmatrix} \\ \begin{bmatrix} 0 \end{bmatrix} & \begin{bmatrix} K_p \end{bmatrix}_{II} & \begin{bmatrix} 0 \end{bmatrix} \\ \begin{bmatrix} 0 \end{bmatrix} & \begin{bmatrix} 0 \end{bmatrix} & \begin{bmatrix} K_p \end{bmatrix}_{III} \end{bmatrix} \begin{bmatrix} [c]_{I,I} & [c]_{I,II} & [c]_{I,III} \\ [c]_{II,I} & [c]_{II,II} & [c]_{II,III} \\ [c]_{III,I} & [c]_{III,II} & [c]_{III,III} \end{bmatrix}^{-1} \end{bmatrix} \begin{Bmatrix} \{\delta\}_I \\ \{\delta\}_{II} \\ \{\delta\}_{III} \end{Bmatrix} = \begin{Bmatrix} \{P\}_I \\ \{P\}_{II} \\ \{P\}_{III} \end{Bmatrix} +$$

$$\begin{bmatrix} [c]_{I,I} & [c]_{I,II} & [c]_{I,III} \\ [c]_{II,I} & [c]_{II,II} & [c]_{II,III} \\ [c]_{III,I} & [c]_{III,II} & [c]_{III,III} \end{bmatrix}^{-1} \begin{Bmatrix} \{s_A\}_I \\ \{s_A\}_{II} \\ \{s_A\}_{III} \end{Bmatrix} \qquad (4.9)$$

The above system of linear equations can be solved by *Gauss* elimination method or by iterative procedure according to *Kany/ El Gendy* (1997).

4.6   Analysis of system of rigid foundations
4.6.1   Assembling the system of linear equations

The settlement s_i of the slab I at a node i due to slab rigidity is expressed by the following linear relation (plane translation)

$$s_i = w_{o.I} + x_i \tan\theta_{y.I} + y_i \tan\theta_{x.I} \qquad (4.10)$$

where:

$w_{o.I}$ Rigid body translation of slab I at the slab centroid
$\theta_{x.I}$ Rigid body rotation of slab I about the x-axis
$\theta_{y.I}$ Rigid body rotation of slab I about the y-axis

Equation 4.10 for slab I can be rewritten in matrix form

$$\{s\}_{\mathrm{I}} = [X]^{T}{}_{\mathrm{I}} \{\Delta\}_{\mathrm{I}} \tag{4.11}$$

where:
$\{\Delta\}_{\mathrm{I}}$ Vector of translation $w_{o.\mathrm{I}}$ and rotations $\tan \theta_{y.\mathrm{I}}$ and $\tan \theta_{x.\mathrm{I}}$ of slab I
$[X]^{T}{}_{\mathrm{I}}$ Vector of coordinates x and y of slab I, $[X]^{T}{}_{\mathrm{I}} = [1, x, y]$

In the same manner for foundation II

$$\{s\}_{\mathrm{II}} = [X]^{T}{}_{\mathrm{II}} \{\Delta\}_{\mathrm{II}} \tag{4.12}$$

and for foundation III

$$\{s\}_{\mathrm{III}} = [X]^{T}{}_{\mathrm{III}} \{\Delta\}_{\mathrm{III}} \tag{4.13}$$

Equations 4.11, 4.12 and 4.13 are rewritten in matrix form

$$\begin{Bmatrix} \{s\}_{\mathrm{I}} \\ \{s\}_{\mathrm{II}} \\ \{s\}_{\mathrm{III}} \end{Bmatrix} = \begin{bmatrix} [X]^{T}{}_{\mathrm{I}} & [0] & [0] \\ [0] & [X]^{T}{}_{\mathrm{II}} & [0] \\ [0] & [0] & [X]^{T}{}_{\mathrm{III}} \end{bmatrix} \begin{Bmatrix} \{\Delta\}_{\mathrm{I}} \\ \{\Delta\}_{\mathrm{II}} \\ \{\Delta\}_{\mathrm{III}} \end{Bmatrix} \tag{4.14}$$

4.6.1.1   Equilibrium of the vertical forces

For each of the three slabs, the resultant N_i due to external vertical forces acting on the slabs must be equal to the sum of contact forces, where

$$\left.\begin{aligned} N_{\mathrm{I}} &= Q_1 + Q_2 + Q_3 + ... + Q_{r_{\mathrm{I}}} \\ N_{\mathrm{II}} &= Q_{r_{\mathrm{I}+1}} + Q_{r_{\mathrm{I}+2}} + Q_{r_{\mathrm{I}+3}} + ... + Q_{r_{\mathrm{II}}} \\ N_{\mathrm{III}} &= Q_{r_{\mathrm{II}+1}} + Q_{r_{\mathrm{II}+2}} + Q_{r_{\mathrm{II}+3}} + ... + Q_{r_{\mathrm{III}}} \end{aligned}\right\} \tag{4.15}$$

4.6.1.2   Equilibrium of the moments

For each of the three slabs, the moment due to resultant N_i about the y-axis must be equal to the sum of moments due to contact pressure forces about that axis, where

$$\left.\begin{aligned} N_{\mathrm{I}} \, x_{N_{\mathrm{I}}} &= Q_1 \, x_1 + Q_2 \, x_2 + Q_3 \, x_3 + ... + Q_{r_{\mathrm{I}}} \, x_{r_{\mathrm{I}}} \\ N_{\mathrm{II}} \, x_{N_{\mathrm{II}}} &= Q_{r_{\mathrm{I}+1}} \, x_{r_{\mathrm{I}+1}} + Q_{r_{\mathrm{I}+2}} \, x_{r_{\mathrm{I}+2}} + Q_{r_{\mathrm{I}+3}} \, x_{r_{\mathrm{I}+3}} + ... + Q_{r_{\mathrm{II}}} \, x_{r_{\mathrm{II}}} \\ N_{\mathrm{III}} \, x_{N_{\mathrm{III}}} &= Q_{r_{\mathrm{II}+1}} \, x_{r_{\mathrm{II}+1}} + Q_{r_{\mathrm{II}+2}} \, x_{r_{\mathrm{II}+2}} + Q_{r_{\mathrm{II}+3}} \, x_{r_{\mathrm{II}+3}} + ... + Q_{r_{\mathrm{III}}} \, x_{r_{\mathrm{III}}} \end{aligned}\right\} \tag{4.16}$$

The equilibrium equations for moments about the *x*-axis are given by

$$
\left.
\begin{array}{llllllll}
N_{I}\, y_{N_{I}} & = & Q_{1}\, y_{1} & + & Q_{2}\, y_{2} & + & Q_{3}\, y_{3} & + & \ldots & + & Q_{r_{I}}\, y_{r_{I}} \\
N_{II}\, y_{N_{II}} & = & Q_{r_{I+1}}\, y_{r_{I+1}} & + & Q_{r_{I+2}}\, y_{r_{I+2}} & + & Q_{r_{I+3}}\, y_{r_{I+3}} & + & \ldots & + & Q_{r_{II}}\, y_{r_{II}} \\
N_{III}\, y_{N_{III}} & = & Q_{r_{II+1}}\, y_{r_{II+1}} & + & Q_{r_{II+2}}\, y_{r_{II+2}} & + & Q_{r_{II+3}}\, y_{r_{II+3}} & + & \ldots & + & Q_{r_{III}}\, y_{r_{III}}
\end{array}
\right\}
\qquad (4.17)
$$

Equations 4.15, 4.16 and 4.17 are rewritten in matrix form as

$$
\begin{Bmatrix} \{N\}_{I} \\ \{N\}_{II} \\ \{N\}_{III} \end{Bmatrix} =
\begin{bmatrix} [X]_{I} & [0] & [0] \\ [0] & [X]_{II} & [0] \\ [0] & [0] & [X]_{III} \end{bmatrix}
\begin{Bmatrix} \{Q\}_{I} \\ \{Q\}_{II} \\ \{Q\}_{III} \end{Bmatrix}
\qquad (4.18)
$$

Substituting Equation 4.18 and 4.14 into Equation 4.3, gives the following linear system of equations in matrix form

$$
\begin{Bmatrix} \{N\}_{I} \\ \{N\}_{II} \\ \{N\}_{III} \end{Bmatrix} =
$$

$$
\begin{bmatrix} [X]_{I} & [0] & [0] \\ [0] & [X]_{II} & [0] \\ [0] & [0] & [X]_{III} \end{bmatrix}
\begin{bmatrix} [c]_{I,I} & [c]_{I,II} & [c]_{I,III} \\ [c]_{II,I} & [c]_{II,II} & [c]_{II,III} \\ [c]_{III,I} & [c]_{III,II} & [c]_{III,III} \end{bmatrix}^{-1}
\begin{bmatrix} [X]^{T}_{I} & [0] & [0] \\ [0] & [X]^{T}_{II} & [0] \\ [0] & [0] & [X]^{T}_{III} \end{bmatrix}
\begin{Bmatrix} \{\Delta\}_{I} \\ \{\Delta\}_{II} \\ \{\Delta\}_{III} \end{Bmatrix}
\quad (4.19)
$$

$$
- \begin{bmatrix} [X]_{I} & [0] & [0] \\ [0] & [X]_{II} & [0] \\ [0] & [0] & [X]_{III} \end{bmatrix}
\begin{bmatrix} [c]_{I,I} & [c]_{I,II} & [c]_{I,III} \\ [c]_{II,I} & [c]_{II,II} & [c]_{II,III} \\ [c]_{III,I} & [c]_{III,II} & [c]_{III,III} \end{bmatrix}^{-1}
\begin{Bmatrix} \{s_{A}\}_{I} \\ \{s_{A}\}_{II} \\ \{s_{A}\}_{III} \end{Bmatrix}
$$

The above system of linear equations 4.19 can be solved by *Gauss* elimination method or by iterative procedure according to *Kany/ El Gendy* (1999).

Through solving the system of linear equations 4.19, get $w_{o.I}$, $\tan \theta_{x.I}$, $\tan \theta_{y.I}$, $w_{o.II}$, $\tan \theta_{x.II}$, $\tan \theta_{y.II}$, $w_{o.III}$, $\tan \theta_{x.III}$ and $\tan \theta_{y.III}$. Substituting these values in Equation 4.14, then substituting Equation 4.14 in 4.3, get the following matrix equation to find the n unknown contact pressure forces Q_1 to Q_r

$$
\begin{Bmatrix} \{Q\}_{I} \\ \{Q\}_{II} \\ \{Q\}_{III} \end{Bmatrix} =
\begin{bmatrix} [c]_{I,I} & [c]_{I,II} & [c]_{I,III} \\ [c]_{II,I} & [c]_{II,II} & [c]_{II,III} \\ [c]_{III,I} & [c]_{III,II} & [c]_{III,III} \end{bmatrix}^{-1}
\begin{bmatrix} [X]^{T}_{I} & [0] & [0] \\ [0] & [X]^{T}_{II} & [0] \\ [0] & [0] & [X]^{T}_{III} \end{bmatrix}
\begin{Bmatrix} \{\Delta\}_{I} \\ \{\Delta\}_{II} \\ \{\Delta\}_{III} \end{Bmatrix}
$$

$$
- \begin{bmatrix} [c]_{I,I} & [c]_{I,II} & [c]_{I,III} \\ [c]_{II,I} & [c]_{II,II} & [c]_{II,III} \\ [c]_{III,I} & [c]_{III,II} & [c]_{III,III} \end{bmatrix}^{-1}
\begin{Bmatrix} \{s_{A}\}_{I} \\ \{s_{A}\}_{II} \\ \{s_{A}\}_{III} \end{Bmatrix}
\qquad (4.20)
$$

Substituting also the values w_o, tan θ_x and tan θ_y in Equation 4.14, one can get the n settlements s_1 to s_r.

4.7   Iterative procedure

For practical problems the major difficulty to study a system of foundations lies in solving large set of equations, which requires large computer storage and long computation time.

There are many iteration methods for the analysis of an isolated foundation in case of elastic foundation presented by *Haung* (1974), *Ahrens/ Winselmann* (1984), *Stark* (1990) and *El Gendy* (1994). These methods may be used here.

In the program *ELPLA*, an iteration method is developed to solve the system of linear equations for system of both elastic and rigid foundations.

The main idea of this method is that each foundation set of equations is solved alone and the soil stiffness matrix will be converted to equivalent symmetrical banded matrix in case of elastic foundations. This matrix is then simply added to that of the plate. As the plate stiffness matrix is also a banded matrix, the overall matrix can be solved by using the banded coefficients technique.

A good advantage of this iteration method is that it requires much less computer memory than the elimination method or iteration methods, which treat the total system equations of the foundations as one unit.

Start

Compute the average contact pressure

I = slab No.
N = No. of slab

$I=1$

Find the soil settlement s_o
$\{ s_o \}_I = [c]_{I, I} \{Q\}_I$

Find the additional s_r due to neighboring
foundations or any other influences

$$\{s_r\}_I = \sum_{J=1}^{N} [c]_{I,J} \{Q\}_J + \{s_A\}_I \ , \qquad J \neq I$$

Find the total soil settlement s
$\{s\}_I = \{s_o\}_I + \{s_r\}_I$

$I=I+1$

Rigid foundation — Yes →

Find the vector $\{\Delta\}$ of the rigid body
translation and rotations
about x- and y-axes
$\{N\}_I = [x]_I [k_s]_I [x]^T_I \{\Delta\}_I - [x]_I [k_s]_I \{s_r\}_I$

No

Convert the soil stiffness matrix $[k_s]$ to
equivalent symmetrical banded matrix $[k']$

Find the slab deformation w for
the rigid slab
$\{w\}_I = [x]^T_I \{\Delta\}_I$

Find the vector $\{\delta\}$ from FE-plate analysis
$[[k_p]_I + [k']]\{\delta\}_I = [P]_I + [k_s]_I \{s_r\}_I$

No ← $I = N$

Yes

Convergence reached $w \approx s$ — Yes → End

No

$I = 1$

Find the new contact pressure
$\{Q\}_I = [k_s]_I \{\{w\}_I - \{s_r\}_I\}$

$I=I+1$

Yes ← $I = N$ → No

Figure 4.2   Iteration cycle and flow chart of the iteration process

Example 4.1   Interaction of two circular rafts

1   Description of the problem

To illustrate the application of the iterative procedure of *Kany/ El Gendy* (1997) for the interactive system of foundations, consider the system of two equal large circular rafts shown in Figure 4.3. The rafts rest on a soil layer of 5 [m] thickness. Each raft has a diameter of 22 [m] and 0.65 [m] thickness. Loading on each raft consists of 24 column loads in which 16 columns loads have $P_1 = 1250$ [kN] and 8 column loads have $P_2 = 1000$ [kN]. The *Young*'s modulus of the raft material is $E_b = 2.6 \times 107$ [kN/m^2] and *Poisson*'s ratio is $\nu_b = 0.15$ [-], while the soil values are $E_s = 9500$ [kN/m^2] and $\nu_s = 0.0$ [-].

$\bullet$ $P_1 = 1250$ [kN]
$\bullet$ $P_2 = 1000$ [kN]
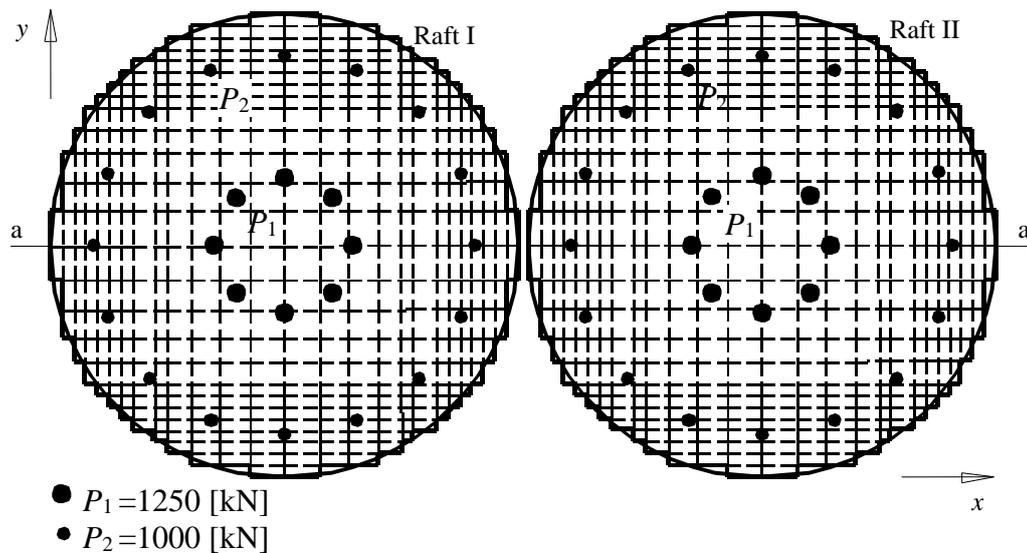
Figure 4.3   System of two circular rafts

2   Analysis

The analysis of the two rafts is carried out for two cases:

i)   without interaction between rafts

ii)   with interaction where the two rafts are constructed simultaneously

Each raft is divided into 404 elements yielding 914 and 457 nodal points, for the calculations based on system of two rafts and the isolated raft, respectively. This generates 2742 and 1371 simultaneous equations for the two calculation cases, respectively.

To analyze the rafts as system of foundations, data of the two rafts are put in two separate files (Files ha1 and ha2). Besides, a third file contains information about the system of foundations (File h12). Data of the two rafts are quite similar except the origin coordinates, which are chosen $(x_o, y_o) = (0.0, 0.0)$ and $(22.5, 0.0)$ for rafts I and II respectively.

The maximum difference between the soil settlement s [cm] and the raft deflection w [cm] is considered as an accuracy number. In this example, the accuracy is chosen 0.01 [cm]. The results are obtained by using the iterative procedure of *Kany/ El Gendy* (1997) after only four cycles for both cases with and without interaction (only isolated raft).

To show the speed of convergence of the iterative procedure of *Kany/ El Gendy* (1997), a comparison of it with modification of subgrade reaction by iteration method (*Ahrens/ Winselmann* (1984)) and that of *El Gendy* (1994) is carried out. The accuracy of computation is plotted against the iterative cycle number in Figure 4.4, for the three iteration methods where the analysis is carried out for an isolated raft. Figure 4.4 shows that the iterative procedure of *Kany/ El Gendy* (1997) converges more rapidly.
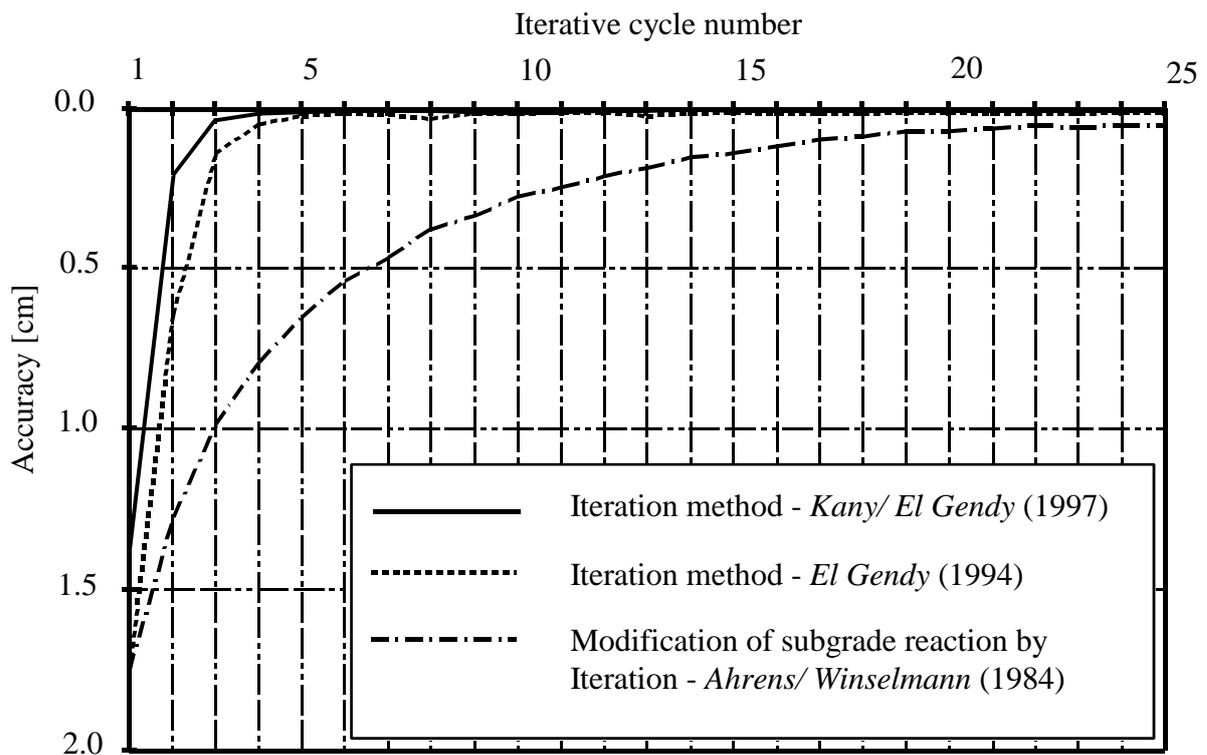
Figure 4.4   Accuracy against the iterative cycle number for the three iteration methods

3   Results and evaluation

Figure 4.5 on the left shows the contour lines of settlements under the raft I without interaction of two rafts. As it is expected, the settlements are distributed symmetrically, because the raft was analyzed under the assumption that the loads are symmetrically applied. Figure 4.5 on the right shows the contour lines of settlements under the raft II considering the interaction of two rafts. It is recognized through comparison that considerable differences occurred in settlements under the raft II. The settlements of the raft II became greater at the edge between two rafts.

Figure 4.6 shows the settlements s, contact pressures q and moments m_x at the middle of raft II for both two cases with and without interaction.

From the results, it is recognized furthermore, that the settlements of the edge nodes of the raft II near raft I increase strongly (Figure 4.6a). Therefore, the settlement increased from 5.12 [cm] to 7.75 [cm] at the middle of the raft.

Figure (4.6b) shows that the contact pressure at the edge of the raft II near the raft I decreased from 70 [kN/m^2] to 240 [kN/m^2]. The contact pressures became smaller at the edge between two rafts due to the additional settlements from the interaction of them. From equilibrium of the vertical forces, the contact pressures became larger at the middle of the raft. Naturally, the change in contact pressure distribution under the raft will cause also changing and shifting in the stress of the raft. Accordingly, the moments of the raft will be affected.

The interaction of the two rafts is clearly noticeable in moments m_x (Figure 4.6c). The field moment m_x near the raft I decreased from 87 [kN.m/m] to 7 [kN.m/m] while the field moment at the center of the raft decreased from 437 [kN.m/m] to 370 [kN.m/m].
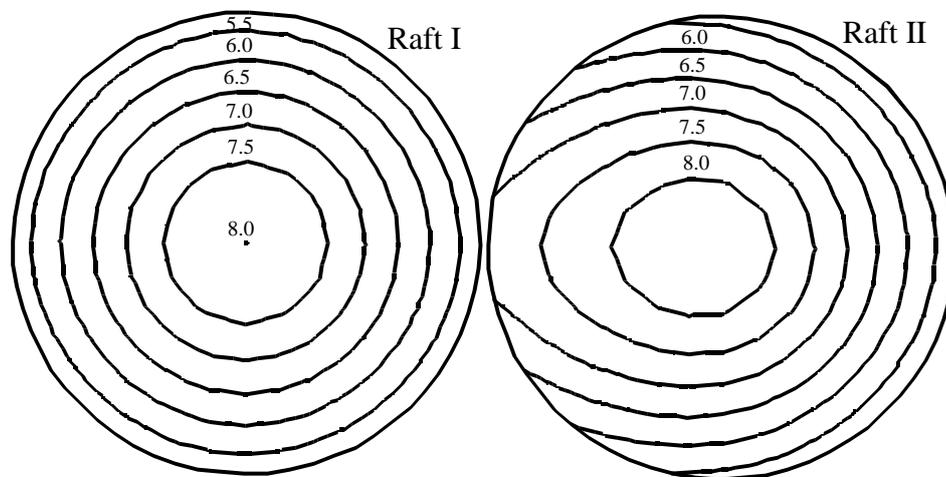

Figure 4.5   Contour lines of settlements s [cm] under raft I without interaction
   and under raft II without interaction of two rafts
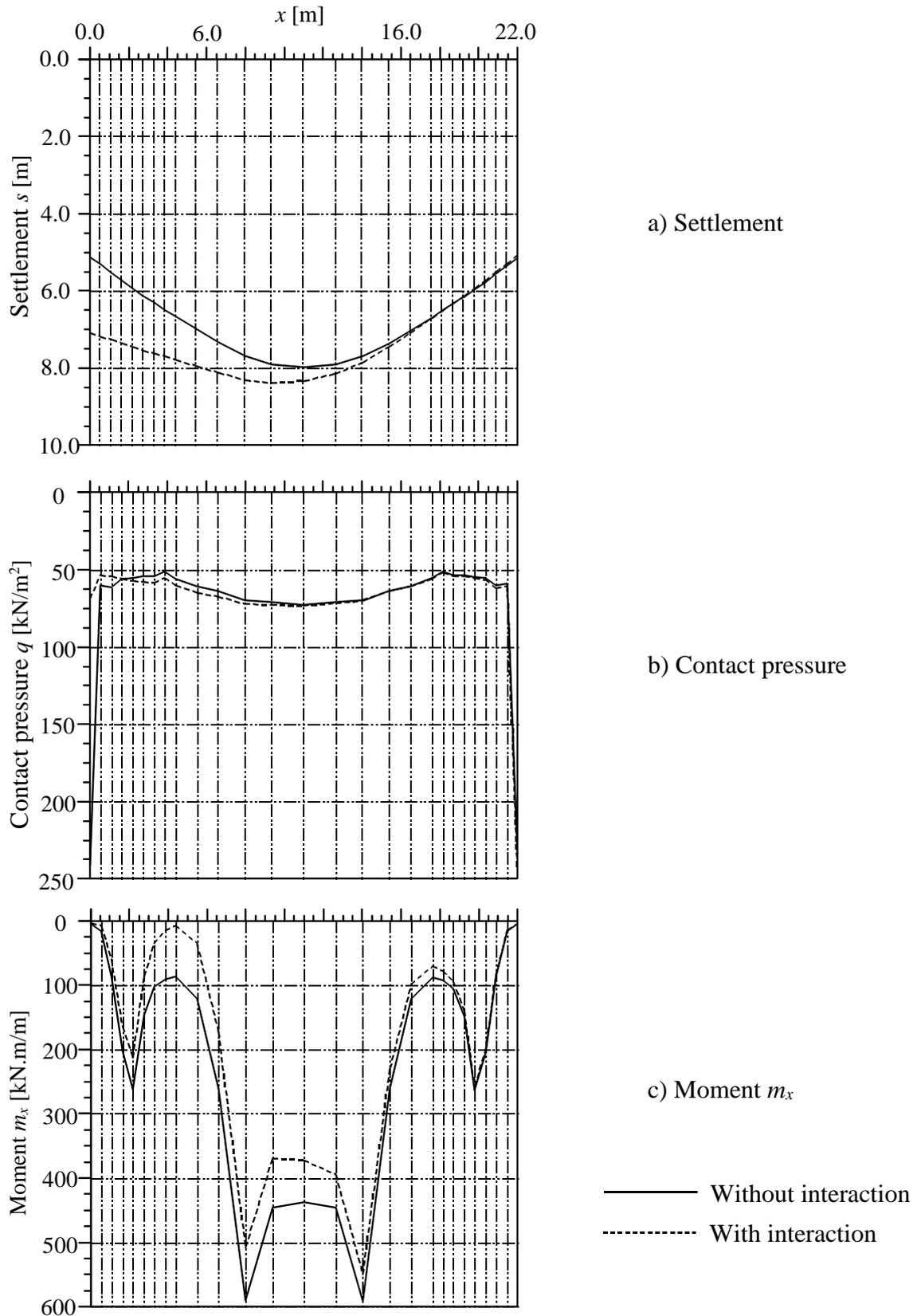
Figure 4.6   Settlements, contact pressures and moments at the middle of raft II

Example 4.2   Settlement behavior of four containers

1   Description of the problem

To verify the iterative procedure of *Kany/ El Gendy* (1997) and evaluate its accuracy for interactive large system of rigid rafts, consider the example 2 in the User's Guide of program *STAPLA* (*Kany* (1976)). The computed settlements obtained from the iterative procedure are compared with those of program *STAPLA* (*Kany* (1976)).

For a sewerage station, two isolated containers A and B were constructed simultaneously. Then, lately to extend the station another two isolated containers C and D would be constructed at the same area. Those two external C and D containers would provide an additional settlement on containers A and B.

It is required to assess the tilting of each container and the settlement considering the interaction between the containers through the subsoil at the end of construction. The tilting and settlement of the containers are main factors for designing the pipe connections.
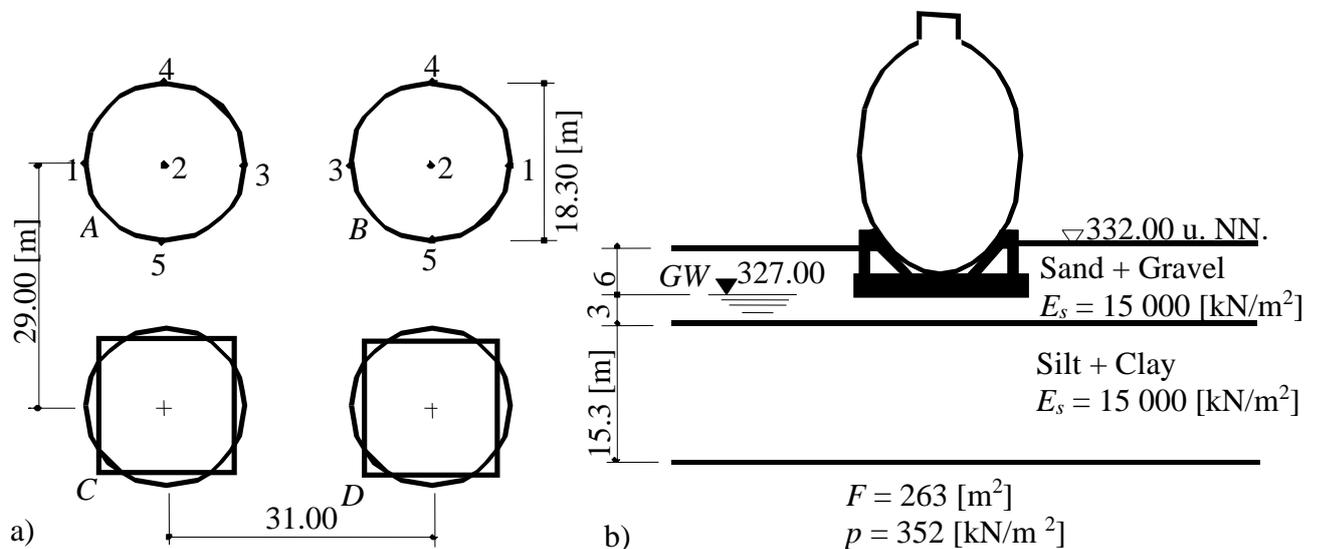
Figure 4.7   a) Location of containers to each other
                       b) Soil properties under the containers (*STAPLA, Kany* (1976))
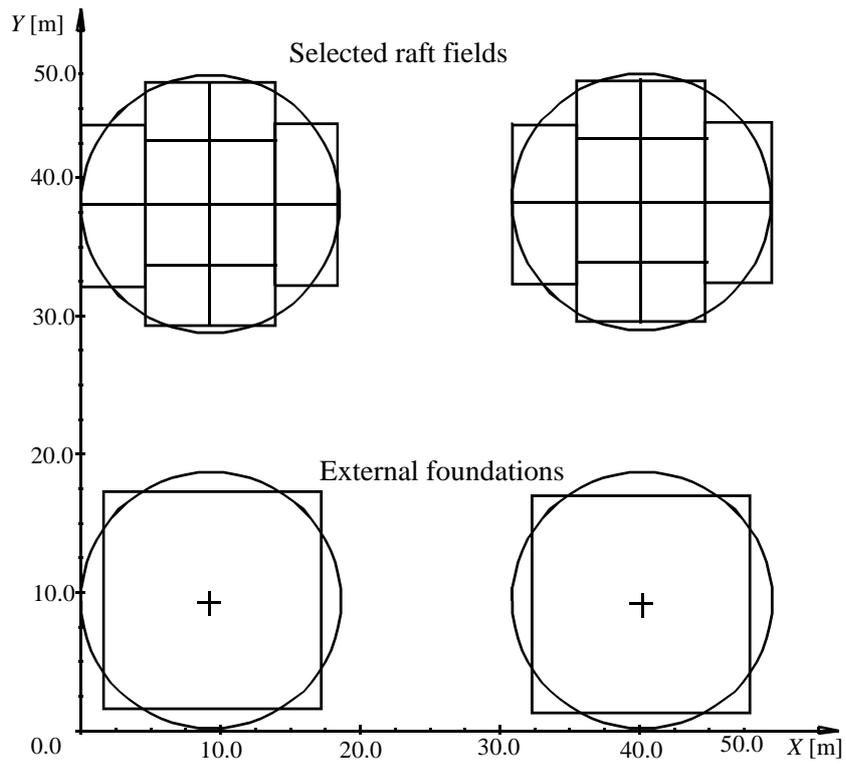
Figure 4.8   Division of the four circular rafts together into 26 fields (*STAPLA*)
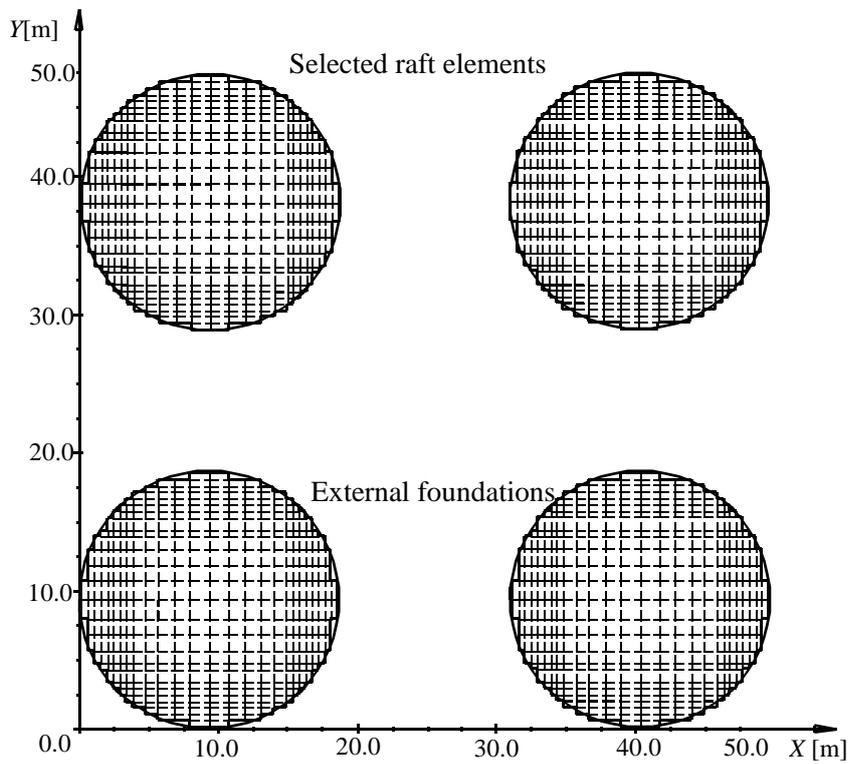
Figure 4.9   Division of the four circular rafts together into 1828 nodes (*ELPLA*)

2   Analysis

Due to the big rigidity of the concrete containers, the containers may be treated as full rigid bodies. Therefore, the foundations are assumed rigid circular rafts. To assess the tilting of the circular rafts by the Program *STAPLA* (*Kany* (1976)), the circular rafts were subdivided into a coarse mesh of rectangular fields. The total number of the fields of the four circular rafts is 26 fields as shown in Figure 4.8. The analysis is carried out to represent the final stage of construction (four containers). To reduce the computation time by the program *STAPLA* (*Kany* (1976)), the advantage of symmetry of the system of rafts about the *y-y* axis was considered in the analysis. In addition, equivalent square rafts were chosen instead of the two external circular rafts that would be constructed lately (containers C and D in Figure 4.7).

By the iterative procedure of *Kany*/ *El Gendy* (1999), dividing the same system of rafts into many elements is possible. In the example, the circular rafts were subdivided into a finer mesh of rectangular elements. The total number of nodes was 1828 nodes for the four rafts as shown in Figure 4.9.

3   Results and evaluation

To evaluate the iterative procedure, the results of settlements at five selected points as shown in Figure 4.7 were compared in Table 4.1 with those obtained from the program *STAPLA* (*Kany* (1976)). The results were considered for the final stage of construction (four containers).

It can be noticed from the comparison that there is relative difference between the results obtained by the iterative procedure and those obtained by the program *STAPLA* (*Kany* (1976)) for the five selected points. Through this comparison, it can be recognized that the settlements at a coarse fine subdivision of the raft exceed those at a fine subdivision of the raft by 4.1 [%] to 6.4 [%]. On the other hand, subdividing the circular raft into many square elements could bitterly represent its dimension. The analysis of system of rigid rafts shown in Figure 4.7 was carried out by a personal computer (300 MHZ, 4.5 GB capacity, Win 95). The iteration process needed fewer than 2 Min. at accuracy 0.0012 cm after three cycles.

Table 4.1   Comparison between settlements *s* [cm] obtained by *STAPLA* (*Kany* (1976)) and that by *ELPLA*

Point	Settlement *s* [cm]		Relative difference [%]
	STAPLA	New calculation	
1	14.51	13.74	5.6
2	14.91	14.17	5.2
3	15.31	14.61	4.8
4	14.44	13.57	6.4
5	15.38	14.78	4.1

Example 4.3   Interaction of two rafts considering two additional footings

1   Description of the problem

Besides, the possibility of analysis of large foundation system with many elements by the procedure of *Kany/ El Gendy* (1997), the mesh of the rigid foundation can be generated in analog mode to the finite element mesh of the elastic foundation in one program. Comparing results from analysis of system of rigid rafts with those of elastic or flexible rafts with the same input data is possible. Subsequently the results of the three analyses are compared in an example.

In this example, the settlements of structures due to interactive analysis of system of rigid, elastic and flexible rafts are studied. This example is chosen from *Graßhoff/ Kany* (1997). Two large rafts and additional two external footings are constructed near each other. The dimensions are shown in Figures 4.10 to 1.12 and Table 4.3.

2   Soil properties

The soil has two layers with different materials as shown in Figure 4.10 and Table 4.2. *Poisson*'s ratio is constant for both of the two soil layers and is taken $\nu_s = 0$. The foundation level for the system of rafts is 1.3 [m].

Table 4.2   Soil properties

Layer No.	Type of soil	Depth of layer underground surface z [m]	Modulus of elasticity of the soil for		Unit weight of the soil under *GW* γ_s [kN/m³]
			Loading E_s [kN/m²]	Reloading W_s [kN/m²]	
1	Silt	4.7	9000	27000	20
2	Sand	15	100000	300000	-

3   Raft material and thickness

Raft material (concrete) and thickness were supposed to have the following properties:

Young's modulus	E_b	$= 2 \times 10^7$	[kN/m²]
Poisson's ratio	ν_b	$= 0.25$	[-]
Raft thickness	d	$= 0.5$	[m]
Unit weight	γ_b	$= 0.0$	[kN/m³]

Young's modulus E_b, *Poisson*'s ratio ν_b and thickness d of rafts don't play any role for the analysis of system of rigid rafts. The self weight of the raft is ignored. Therefore, unit weight of raft material is chosen $\gamma_b = 0.0$ to neglect the own weight of the raft.
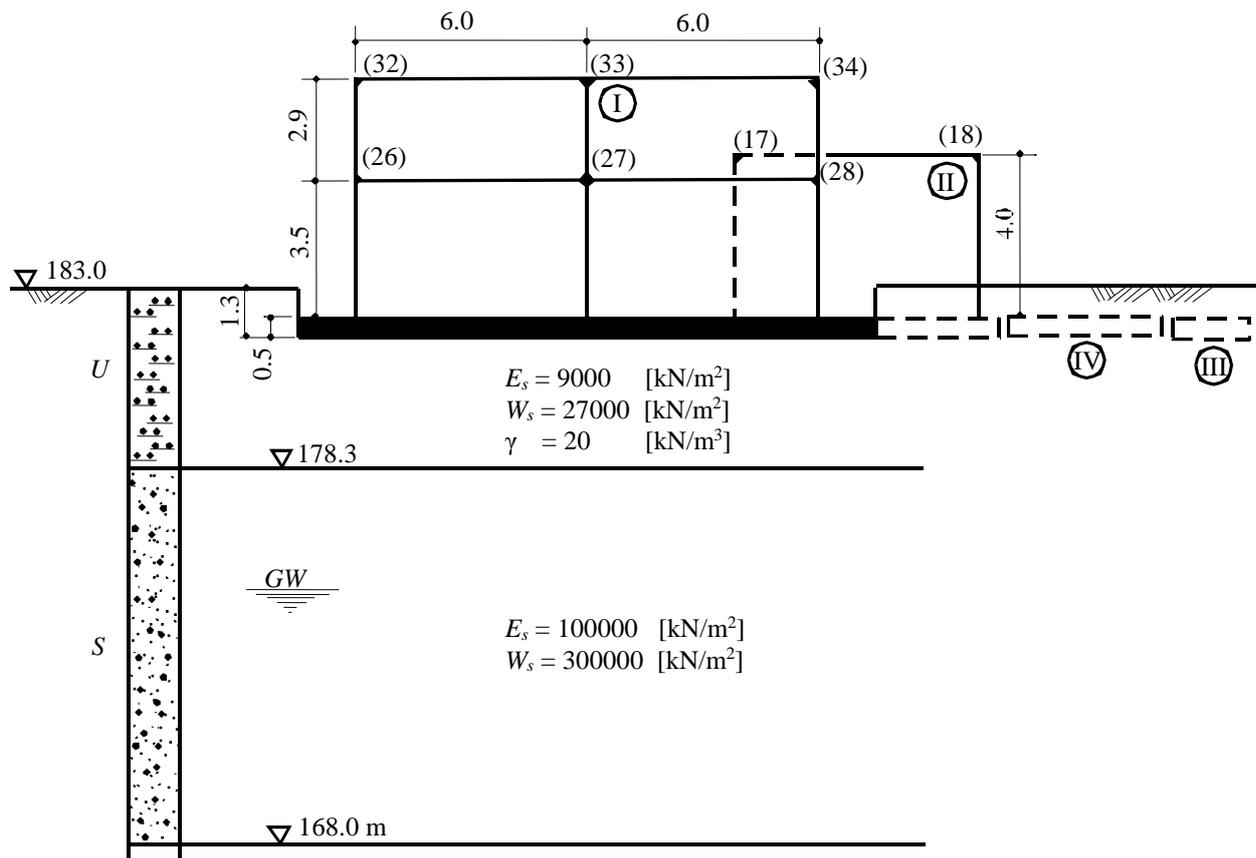
Figure 4.10   Section 1-5 with layer profile, soil properties and node numbers
              of superstructure *Graßhoff/ Kany* (1997)

Table 4.3   Dimensions of rafts I and II and footings III and IV

Foundation	Length A [m]	width B [m]	Origin coordinates	
			x [m]	y [m]
Raft I	15	8	-1.5	-0.5
Raft II	8	12	9.0	7.6
Footing III	2	2	21.0	11.0
Footing IV	4	3	17.0	1.5
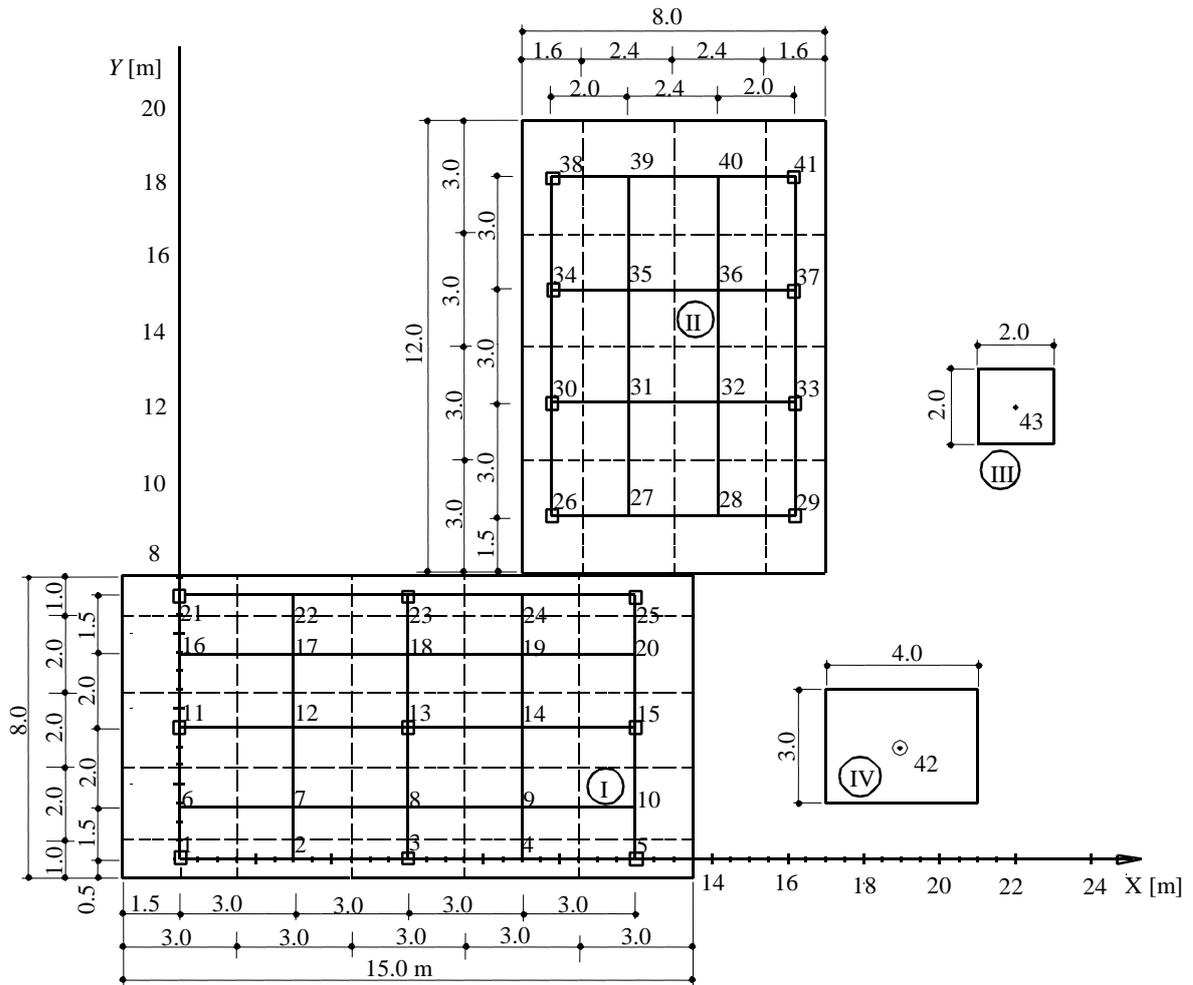
Figure 4.11   Plan view for system of rafts I and II as well as the footings III and IV
              Subdivision of the rafts: 43 fields (*Graßhoff/ Kany* (1997))
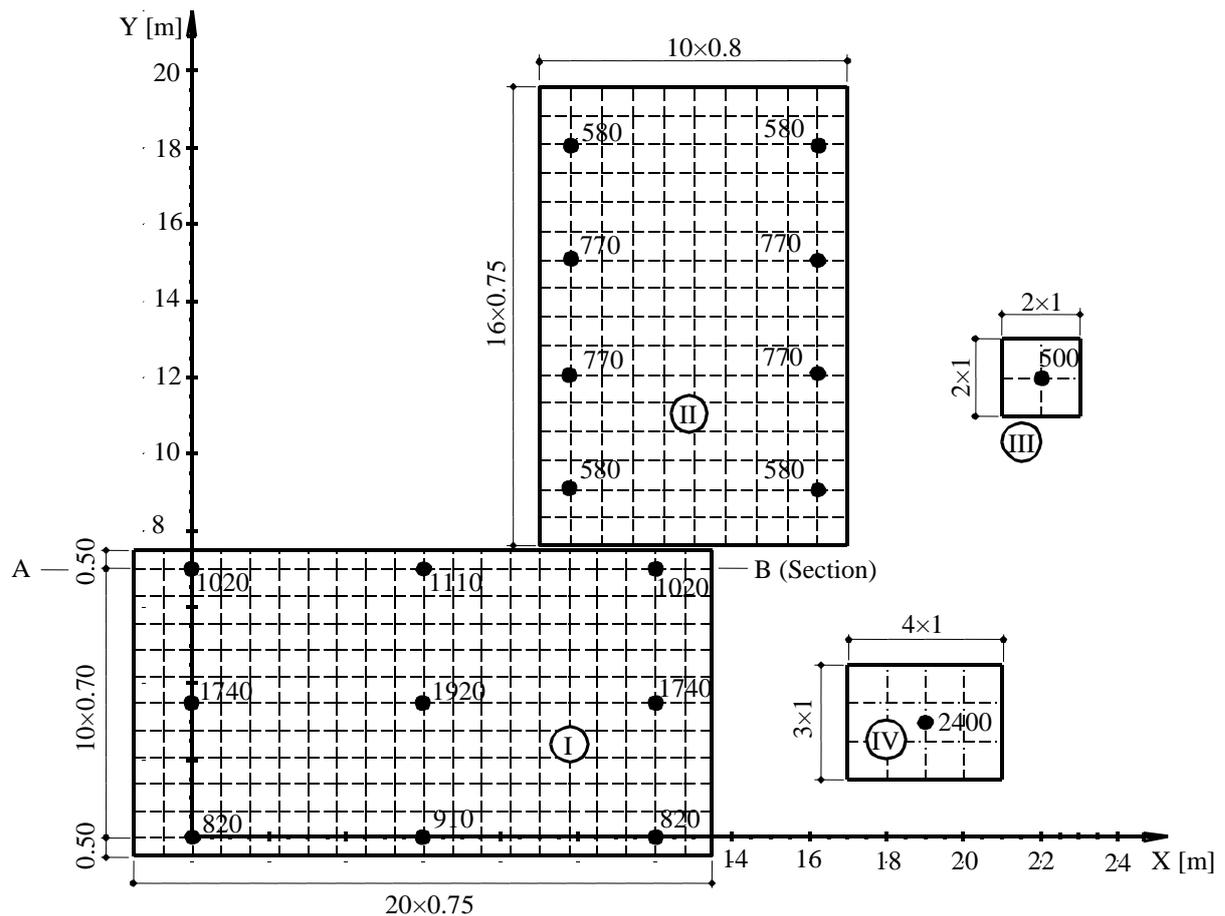
Figure 4.12   Plan view for loads [kN] on the rafts I and II as well as the footings III and IV
               Subdivision of the rafts: 489 nodes (Calculation by *ELPLA*)

4   Analysis

For the space structure system shown in Figure 4.11, the settlements at all nodes on the rafts are determined. The analysis of the two rafts I and II with external footings III and IV was carried out at three different rigidities:

1.   System of flexible rafts
2.   System of elastic rafts
3.   System of rigid rafts

With the same input data, the three analyses are carried out to allow a comparison. To represent the flexible foundations, the raft thickness is chosen $d = 20$ cm, while for elastic foundations the raft thickness is 50 [cm]. For rigid foundations, defining the raft properties is not necessary because the analysis treats the rafts as rigid bodies.

5   Results and evaluation

Figures 4.13 to 4.15 show the settlements for the system of flexible, elastic and rigid rafts, while Figure 4.16 shows in one diagram, to good comparison, the settlements of the three analyses at section A-B. Through the comparison between the results of the analysis obtained by the program *ELPLA* and those obtained by *Graßhoff/ Kany* (1997), it can be recognized that the deformation and contact pressure considering superstructure rigidity are nearly similar to those obtained by the analysis of rigid rafts.

From Tables 4.4 and 4.5 it can be seen that the superstructure rigidity has great influence on the rafts.

The analysis of the system of rafts without interaction of foundations gives symmetrical deformation for all rafts at three different rigidities, because the loads are applied symmetrical on each raft.

It can be recognized from the results that the settlements at the edge of structure I close to the neighboring structure II increase strongly. Therefore, the settlement of field 25 increases from 3.25 [cm] to 3.39 [cm] in case 1 (flexible raft), from 2.59 [cm] to 2.77 [cm] in case 2 (elastic raft) and from 2.46 [cm] to 2.65 [cm] in case 3 (rigid raft). This means that design of the rafts must consider the effect of neighboring foundations.
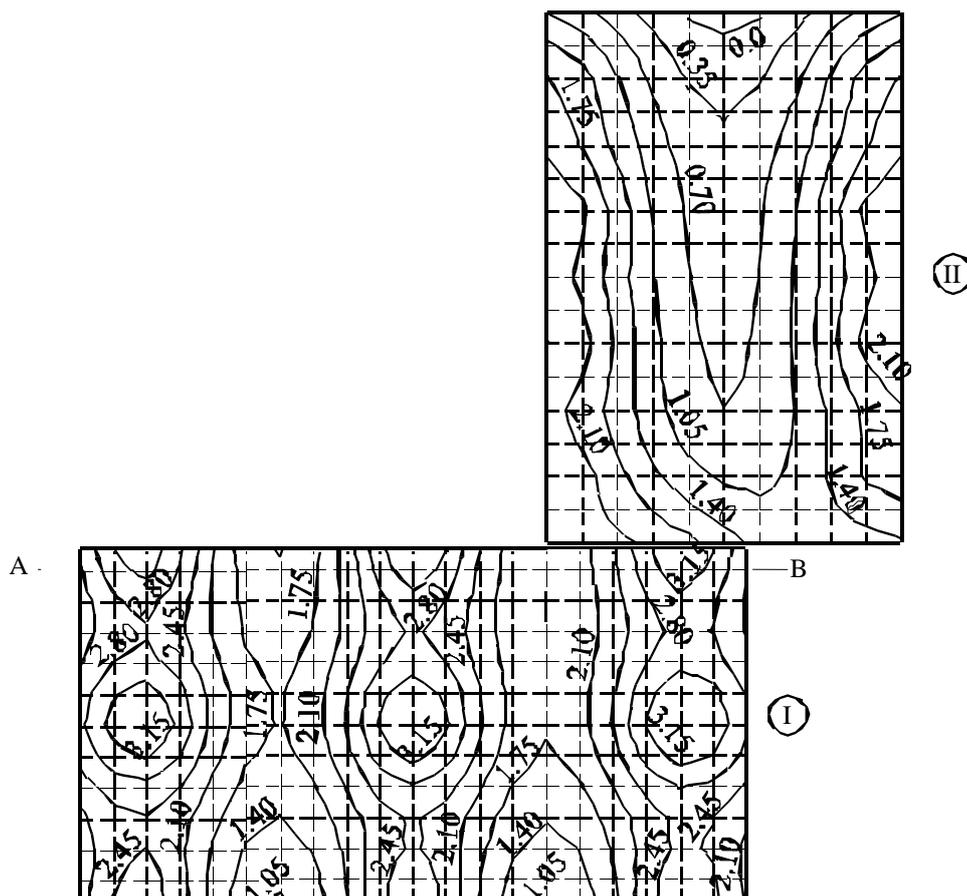

Figure 4.13   Contour lines of settlements *s* [cm] by analyzing as system of flexible rafts
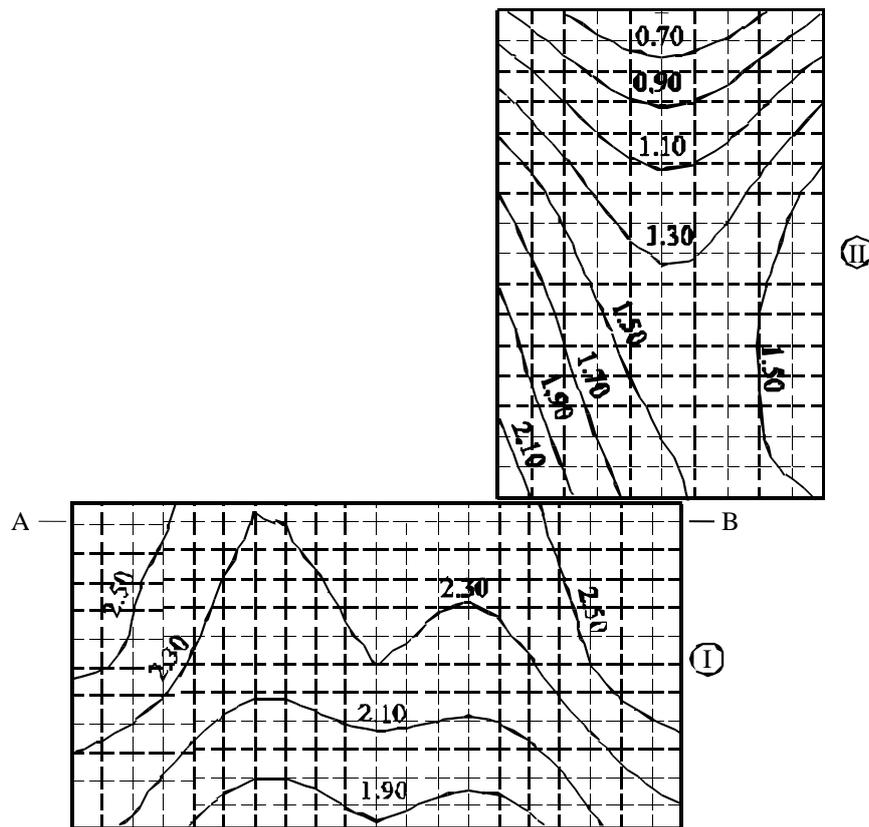
Figure 4.14   Contour lines of settlements *s* [cm] by analyzing as system of elastic rafts
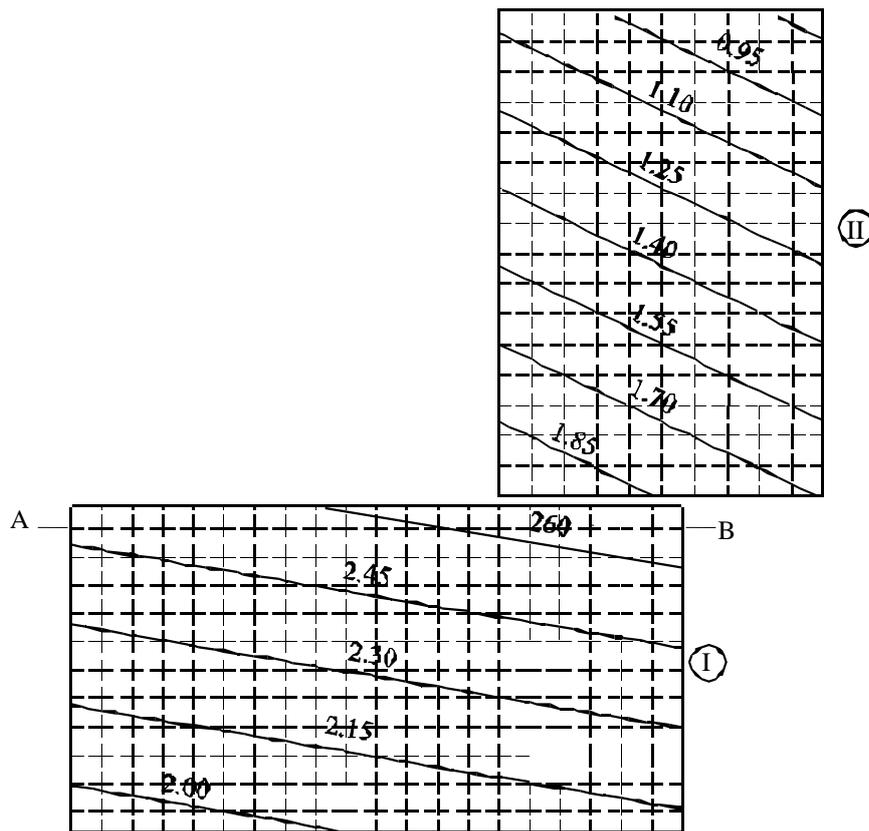
Figure 4.15   Contour lines of settlements *s* [cm] by analyzing as system of rigid rafts
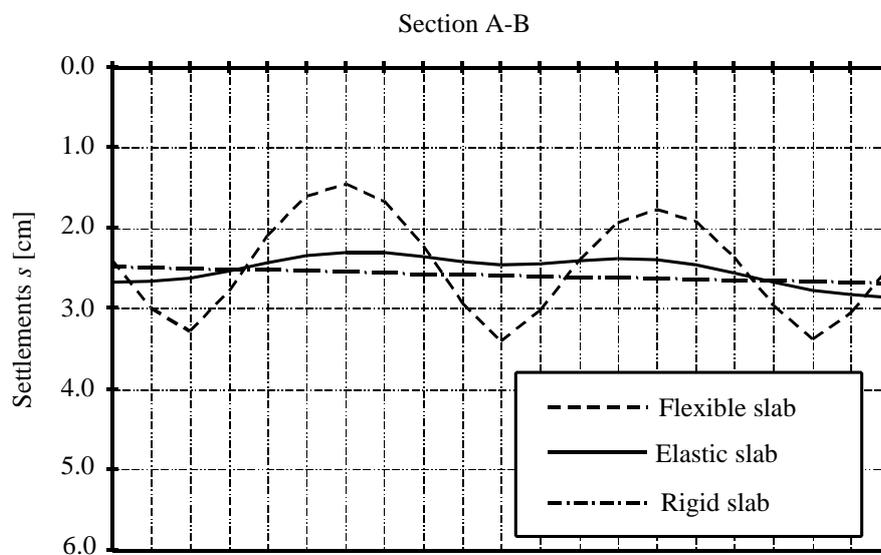
Section A-B

Figure 4.16   Settlements *s* [cm] at section A-B under raft I
                (with neighboring influence of building II and the two footings III and IV)

Table 4.4   Comparison between the analysis by *Graßhoff/ Kany* (1997) and *ELPLA*
for settlements *s* [cm] under raft I (without neighboring influence)

Type of analysis	*Graßhoff/ Kany* (1997)		New analysis	
	Point 21	Point 25	Point 21	Point 25
System of flexible rafts	3.65	3.65	3.25	3.25
System of elastic rafts	3.04	3.04	2.59	2.59
System of rigid rafts	2.78*	2.78*	2.46	2.46

* Calculated as elastic raft with the superstructure

Table 4.5   Comparison between the analysis by *Graßhoff/ Kany* (1997) and *ELPLA*
for settlements *s* [cm] under raft I
(with neighboring influence of building II and the two footings III and IV)

Type of analysis	*Graßhoff/ Kany* (1997)		New analysis	
	Point 21	Point 25	Point 21	Point 25
System of flexible rafts	3.66	4.00	3.27	3.39
system of elastic rafts	3.03	3.51	2.62	2.77
System of rigid rafts	2.79*	3.16*	2.50	2.65

* Calculated as elastic raft with the superstructure

Figure 4.13 shows that the analysis of flexible rafts leads to concentration of settlements on the nodes close to the applied loads. In the other extreme analysis case of rigid rafts, Figure 4.15 shows a linear shape of contour lines for settlements due to the neighboring influence.

The neighboring influence for the analysis of elastic rafts is also obvious in Figure 4.14. It can be concluded also from Figures 4.13 to 4.15 that although all rafts are supposed to symmetrical loading, the settlements are unsymmetrical. Unsymmetrical results are expected also for contact pressures and internal forces due to the neighboring influence.

Example 4.4 Interaction of two square rafts constructed side by side

1   Description of the problem

Settlement joints are usually used in the foundation when the intensity of loads on it differs considerably from area to another. In such case, the foundation may be divided corresponding to its load intensity to avoid cracks. A settlement joint is constructed by making a complete separated joint in the foundation or a hinged joint. If the foundation has a separated joint, each part will settle independently but it will be interaction between parts of the foundation through the subsoil. In the other case of hinged joint, there will be transmission of shearing forces between connection parts.

This example is carried out to examine the interaction of two rafts considering settlement joint. Consider two equal square rafts I and II which will be constructed side by side. Each raft has a side of 12 [m] and 0.5 [m] thickness. Raft I is subjected to a uniform load of 400 [kN/m^2], while raft II carries a uniform load of 200 [kN/m^2].

2   Soil properties

The rafts rest on a soil layer of thickness 10 [m], overlying a rigid base. The soil has the following parameters:

Modulus of compressibility for loading	E_s	= 10 000	[kN/m^2]
Modulus of compressibility for reloading	W_s	= 30 000	[kN/m^2]
Unit weight	γ_s	= 18	[kN/m^3]
Poisson's ratio	ν_s	= 0.3	[-]

3   Raft material

The raft material has the following parameters:

Young's modulus	E_b	= 2 × 10^7	[kN/m^2]
Unit weight	γ_b	= 25	[kN/m^3]
Poisson's ratio	ν_b	= 0.25	[-]

Four cases concerning the influence of neighboring structures are considered as follows:

Case 1:   Rafts I and II are constructed side by side at the same time. This case is examined for different distances c between the two rafts (Figure 4.17), where $c = 0.0$ [m], 0.01 [m], 0.1 [m], 1.0 [m] and 10 [m]

Case 2:   Raft I is constructed at first, then later the raft II. This case is examined for different distances c between the two rafts (Figure 4.17), where $c = 0.0$ [m], 0.01 [cm], 0.1 [m], 1.0 [m] and 10 [m]

Case 3:   Rather than rafts I and II, only one raft is constructed (Figure 4.18)

Case 4:   Rafts I and II are connected by a hinged joint (Figure 4.19)

4   Analysis

The rafts are subdivided into square finite elements, each element has a side of 1.5 [m] as shown in Figures 4.17 to 4.19.

The analysis of rafts in case 1 can be carried out through one of the following two ways:

-        Iteration by using two independent nets, one for raft I and the other for the second raft II

-        Without iteration by using a net for the two rafts. The free distances between the   rafts are carried out by inserting appropriate two elements between rafts. Then the boundary nodes of these elements are eliminated as considered in this example

To carry out the analysis of rafts in case 2, two independent file names define the data of the two rafts are chosen. The data are quite similar for the two rafts except the loads and the origin coordinates. The origin coordinates are chosen $(x_o, y_o) = (0.0, 0.0)$ for raft I and $(x_o, y_o) = (12.0+c, 0.0)$ for raft II. Raft II is analyzed first to obtain the contact pressures and then raft I to consider the influence of neighboring raft II.

To simulate a hinged joint between rafts in case 4 two very small elements are inserted between the rafts. Each element has 1 [cm] width and 5 [cm] thickness. The very small widths of the elements keep the distance between the rafts nearly zero, while the small thickness of the elements makes the raft rigidity at the joint very small. These boundary conditions allow interacting only the vertical forces between rafts. Moments at hinged connection will be eliminated due to the very small rigidity of connection elements.
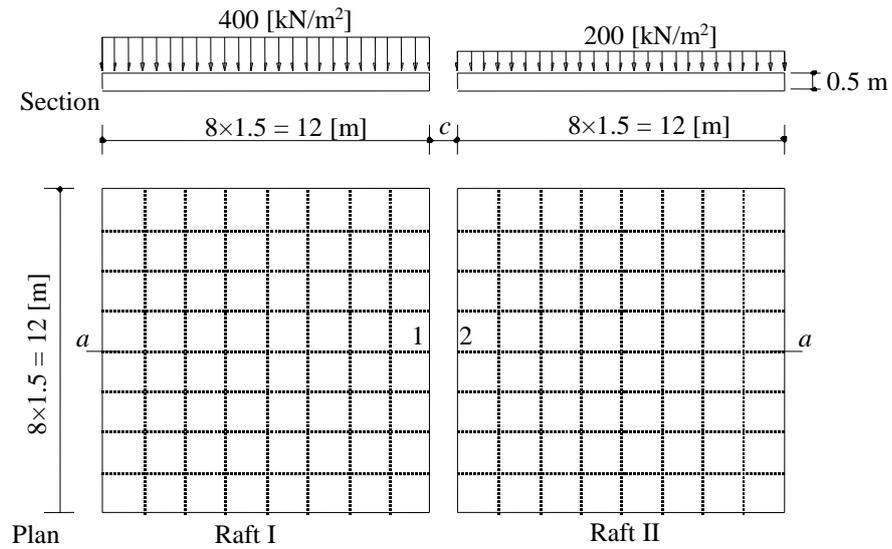
Figure 4.17   Rafts I and II are constructed side by side (cases 1 and 2)
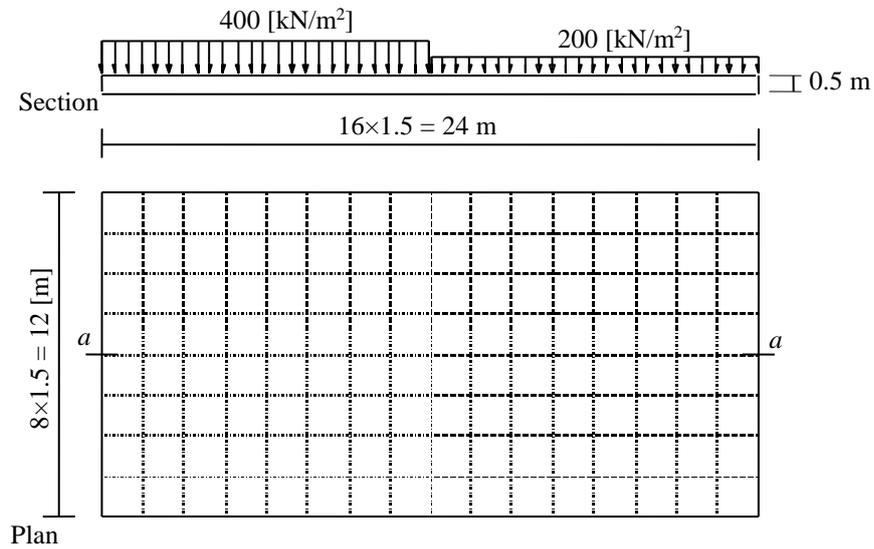
Figure 4.18   Only one raft is constructed (case 3)

Detail A   Detail B

$2 \times 1 = 2$ [cm]

5 [cm] raft thickness
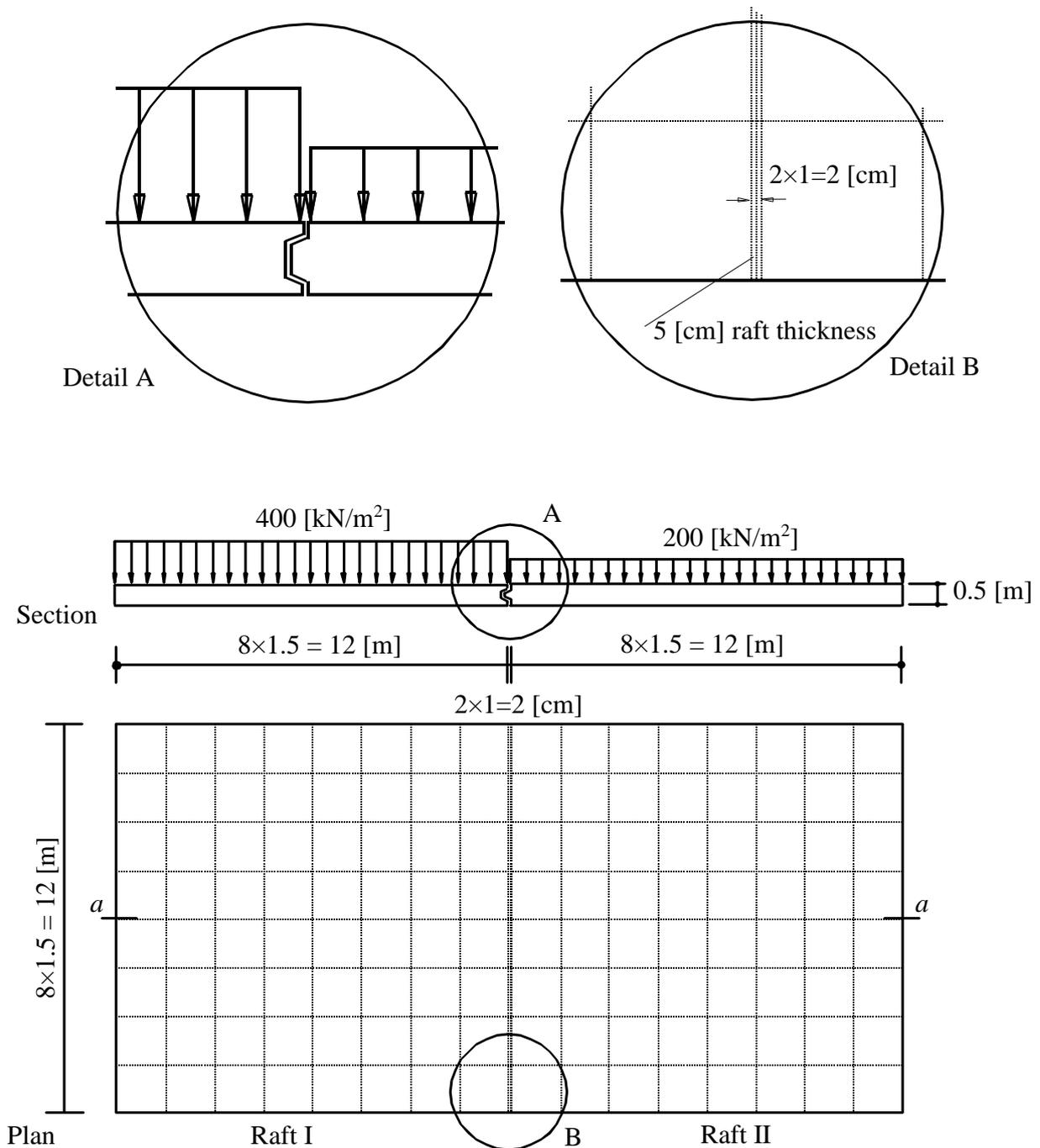
Figure 4.19   Rafts I and II are connected by a hinged joint (case 4)

5   Results and discussion

Figures 4.20 to 4.31 show the distribution of settlement, contact pressure, moment and shearing force at middle section a-a for the four cases of analyses. Tables 4.6 and 4.7 show the joint width c between the two rafts, settlements (s_1, s_2), contact pressures (q_1, q_2) at edges of the rafts (points 1 and 2) and the differences (Δs, Δq) for cases 1 and 2.

Table 4.6   Settlements s_1 and s_2 at edges of rafts I and II and differences Δs

Joint width c [m]	Rafts I and II are constructed side by side at the same time (case 1)			Raft I is constructed at first, then later raft II (case 2)		
	s_1 [cm]	s_2 [cm]	$\Delta s=s_1-s_2$ [cm]	s_1 [cm]	s_2 [cm]	$\Delta s=s_1-s_2$ [cm]
0.00	15.05	14.71	0.34	17.87	6.35	11.52
0.01	15.12	14.54	0.58	17.08	6.35	10.73
0.10	15.30	13.70	1.60	17.24	6.35	10.89
1.00	14.73	10.29	4.44	15.29	6.35	8.94
10.0	13.00	6.16	6.84	12.99	6.35	6.64
∞	13.10	6.35	6.75	13.10	6.35	6.75

Table 4.7   Contact pressures q_1 and q_2 at edges of rafts I and II and differences Δq

Joint width c [m]	Rafts I and II are constructed side by side at the same time (case 1)			Raft I is constructed at first, then later the raft II (case 2)		
	q_1 [kN/m^2]	q_2 [kN/m^2]	$\Delta q=q_1-q_2$ [kN/m^2]	q_1 [kN/m^2]	q_2 [kN/m^2]	$\Delta q=q_1-q_2$ [kN/m^2]
0.00	669	-133	802	444	368	76
0.01	664	-119	783	529	368	161
0.10	644	-53	697	495	368	127
1.00	653	160	493	616	368	248
10.0	733	367	366	733	368	365
∞	733	365	368	733	368	365

In general, it can be noticed from those figures that:

Timeout of the construction process

-        Considerable differences will be expected in the results, if the analysis is carried out for system of rafts (case 1) or for construction of a new raft II beside an existing old one I (case 2)

-        If the two rafts are constructed side by side at the same time, both rafts will lean toward each other (Figure 4.21)

-        If raft I is constructed first and then raft II, there will be an additional pressure under raft I will cause an inclination of raft I in the direction of raft II (Figure 4.25)

Settlement differences at the joint

-        For system of rafts (case 1), the settlement difference between rafts is relatively small at the joint for joint width $c = 0.0$ [cm]. The more settlement difference is for farther distance between rafts. In contrast, for the raft I with neighboring raft II (case 2) because of the pressure overlap from the neighboring raft II, the greater settlement difference is for the smaller joint width c (Figures 4.21, 4.25 and Table 4.6). This phenomenon occurs because the behavior of contact pressures of raft II has great influence on the settlement distribution of the raft I. Figures 4.20 and 4.24 show the contact pressure distribution for cases 1 and 2. The contact pressure of raft II for case 1 decrease by decreasing the width joint c, while for case 2 is independence from joint width c

-        Settlements at the edge of the raft I due to influence of neighboring raft II (case 2) are greater than those due to system of rafts (case 1)

-        Settlements from case 1 for joint width $c = 0.0$ [cm] and from cases 3 and 4 are quite similar (Figures 4.21 and 4.29)

-        If hinged joint between rafts is used (case 4), there will be continuation of settlement under the rafts (Figure 4.29)

Contact pressures

-        For system of rafts (case 1) the contact pressure distribution under the raft I is almost independent of the joint width due to the heavy load of the raft I. On the other hand, for the raft II strong dependence on the joint width is to be found because the strong edge contact pressure of the raft I, which affects on the raft II (Figure 4.23 and Table 4.7)

-        Contact pressures at the edge of the raft I, if the raft I is constructed first and then the raft II (case 2), decreases by decreasing the width joint c (Figure 4.25)

-        Contact pressures from case 3 (rafts as one unit) and 4 (rafts with hinged joint) are nearly similar (Figure 4.28)

Moments

-        For system of rafts (case 1) the maximum moments for the raft I decrease by decreasing the joint width c, while for the raft II the sign of moment is changed from positive to negative in some places. The greater negative moment for raft II is for the smaller joint width c (Figure 4.22)

-        For case 2, if the raft I is constructed first and then the raft II, the maximum moments of raft I decrease by decreasing the joint width c. The positions of maximum moments are also shifted to the opposite direction of raft II (Figure 4.26)

-        It is clear from Figure 4.30 for rafts connected with hinged joint (case 4) that, the moment at the hinged joint for the two rafts is zero. Figure 4.30 shows for case 3 that a positive moment is to be found at the connection position. Raft II for both cases 3 and 4 has a negative moment beside a positive moment

Shearing forces

-        The change in shearing forces for the raft I in case 1 is less than that in case 2 (Figures 4.23 and 4.27), while for the raft II in case 1 the singe of shearing force is changed from negative to positive at the edge of the raft. The greater positive shearing force for raft II is for the smaller joint width c (Figure 4.23)

-        For both cases 3 and 4 a positive shearing force at the connection is to be found (Figur 4.31). Maximum shearing force is for hinged connection
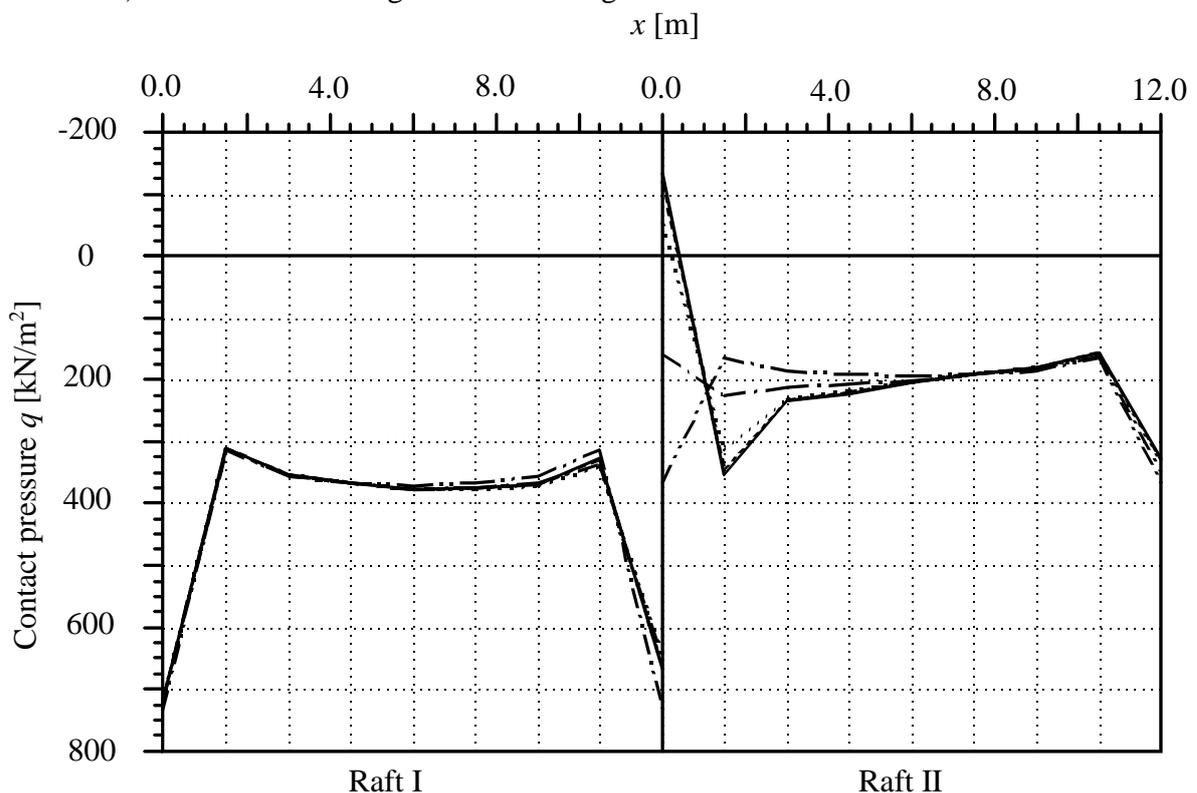

Figure 4.20   Contact pressures q at the middle section of rafts I and II
                       (constructed at the same time)
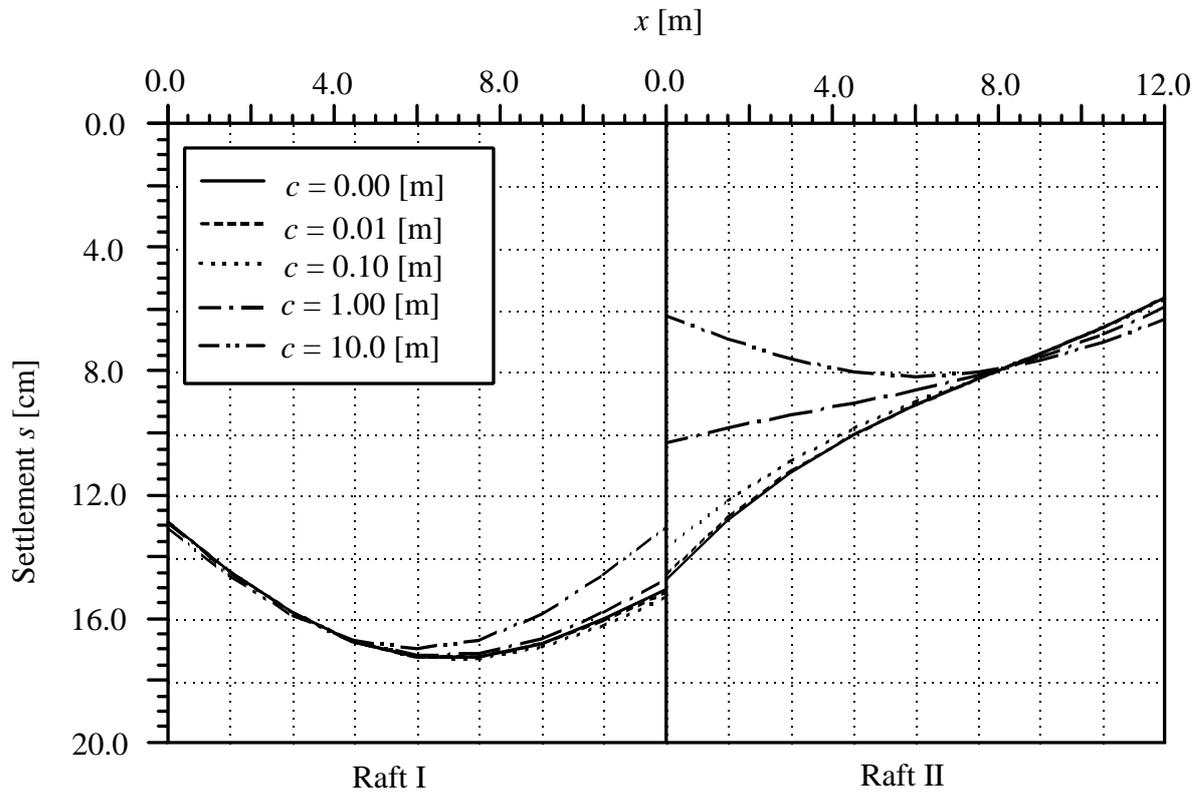
Figure 4.21   Settlements s at the middle section of rafts I and II
                (constructed at the same time)
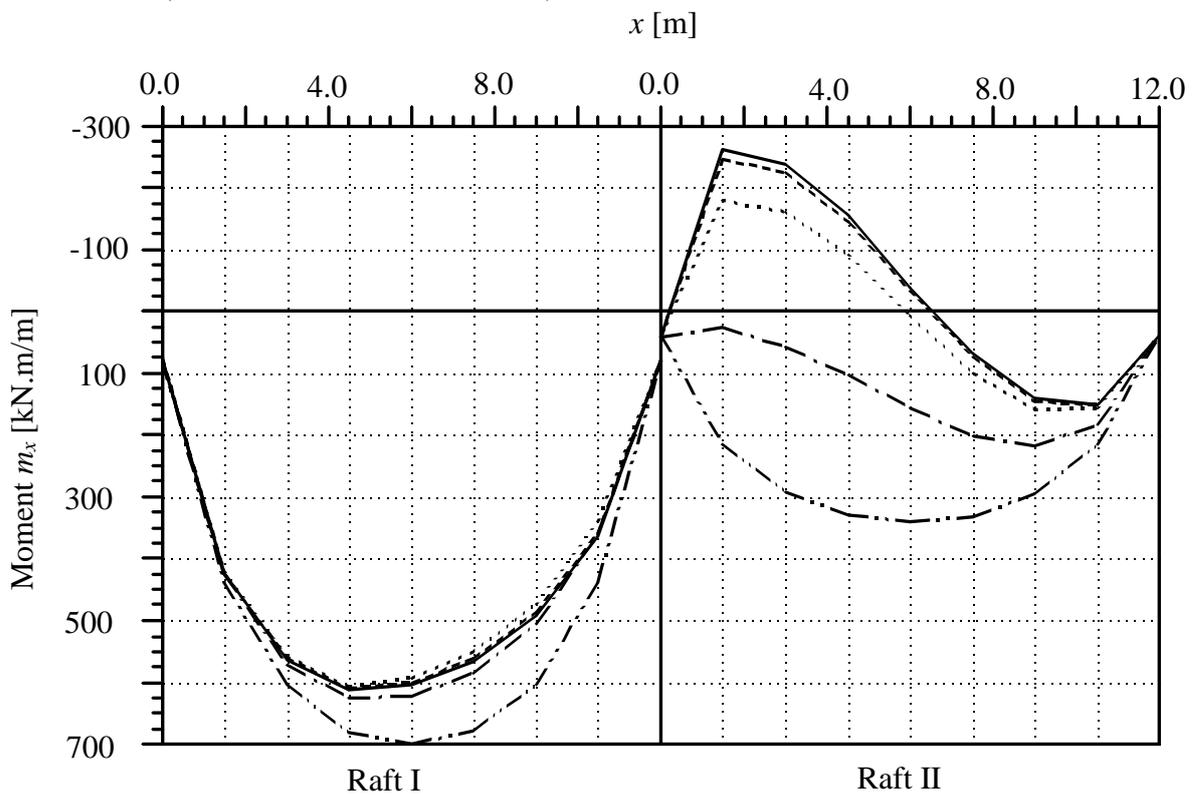

Figure 4.22   Moment m_x at the middle section of rafts I and II
   (constructed at the same time)
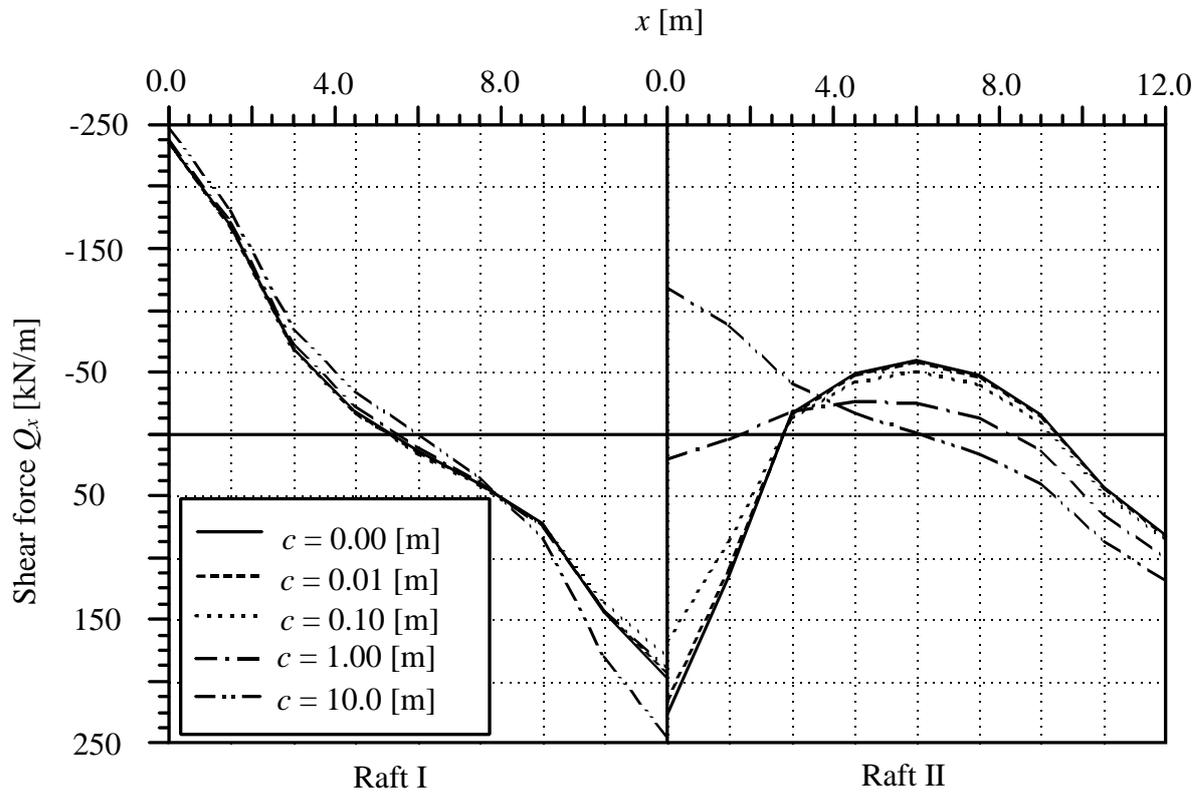
Figure 4.23   Shear forces Q_x at the middle section of rafts I and II
(constructed at the same time)
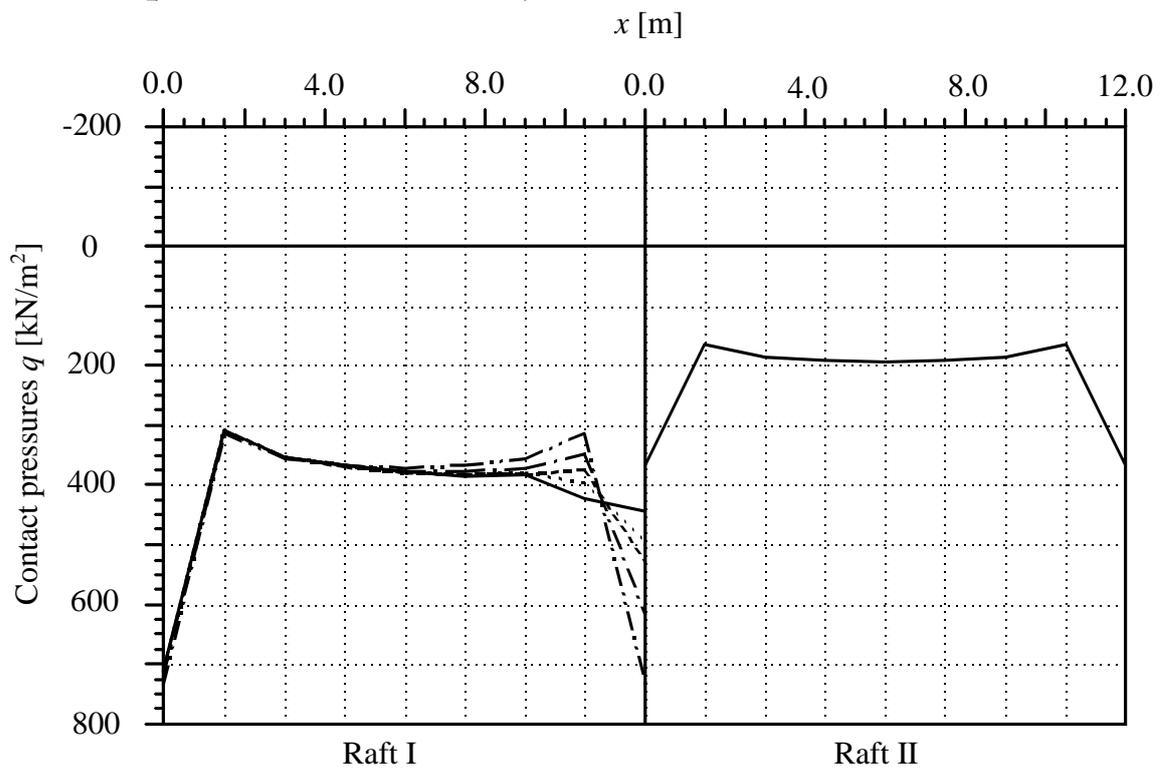
Figure 4.24   Contact pressures q at the middle section of rafts I and II
(raft I is constructed first, then later raft II)
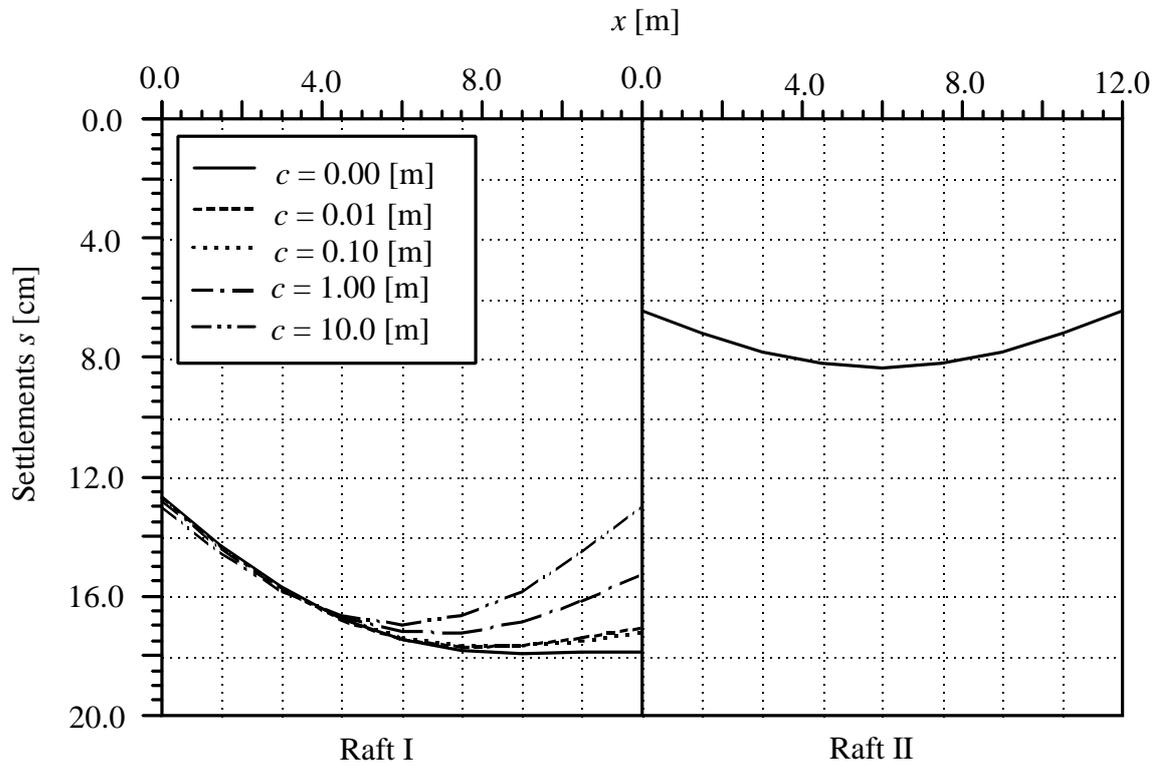
Figure 4.25   Settlements s at the middle section of rafts I and II
   (raft I is constructed first, then later raft II)
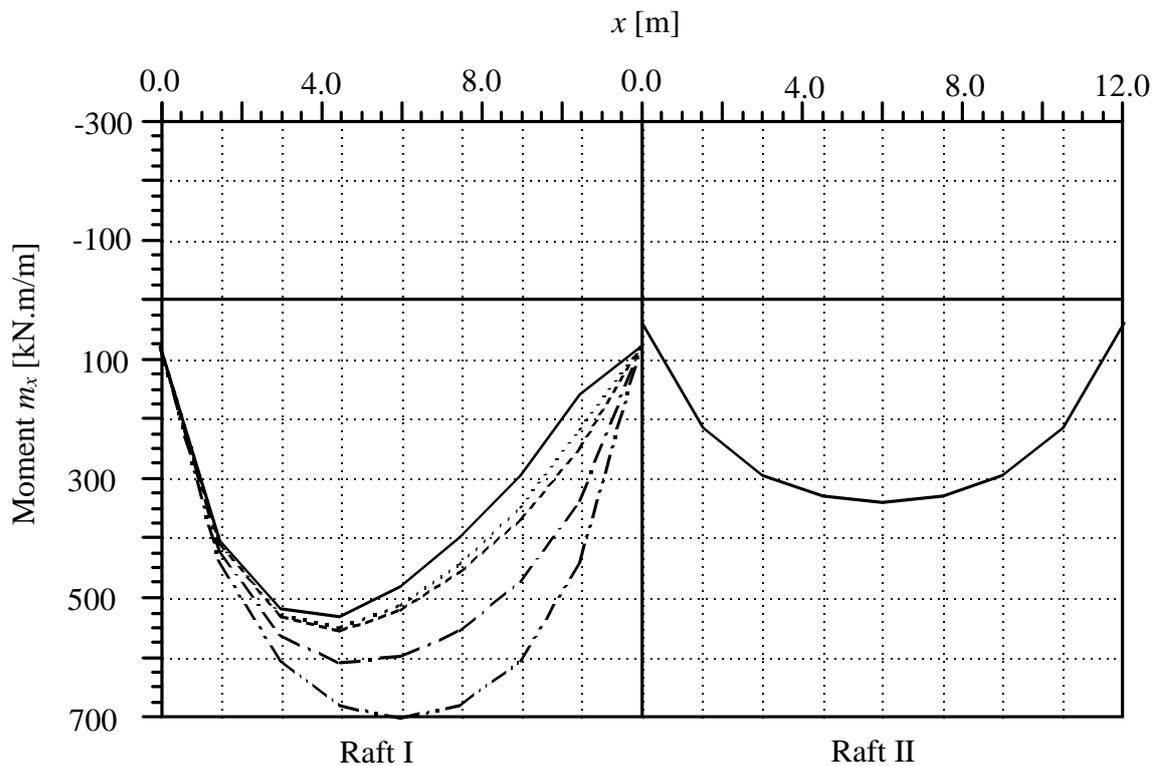
Figure 4.26   Moment m_x at the middle section of rafts I and II
              (raft I is constructed first, then later raft II)

x [m]
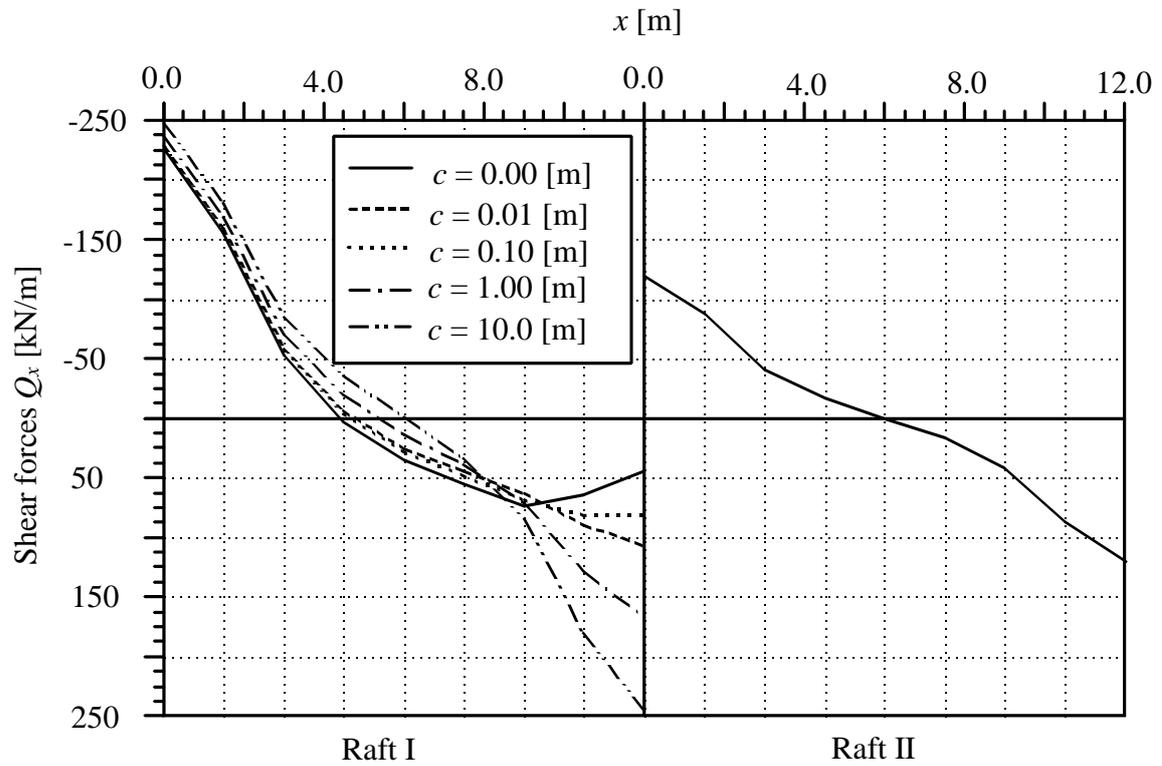
Figure 4.27   Shear forces Q_x at the middle section of rafts I and II
              (raft I is constructed at first, then later raft II)

x [m]
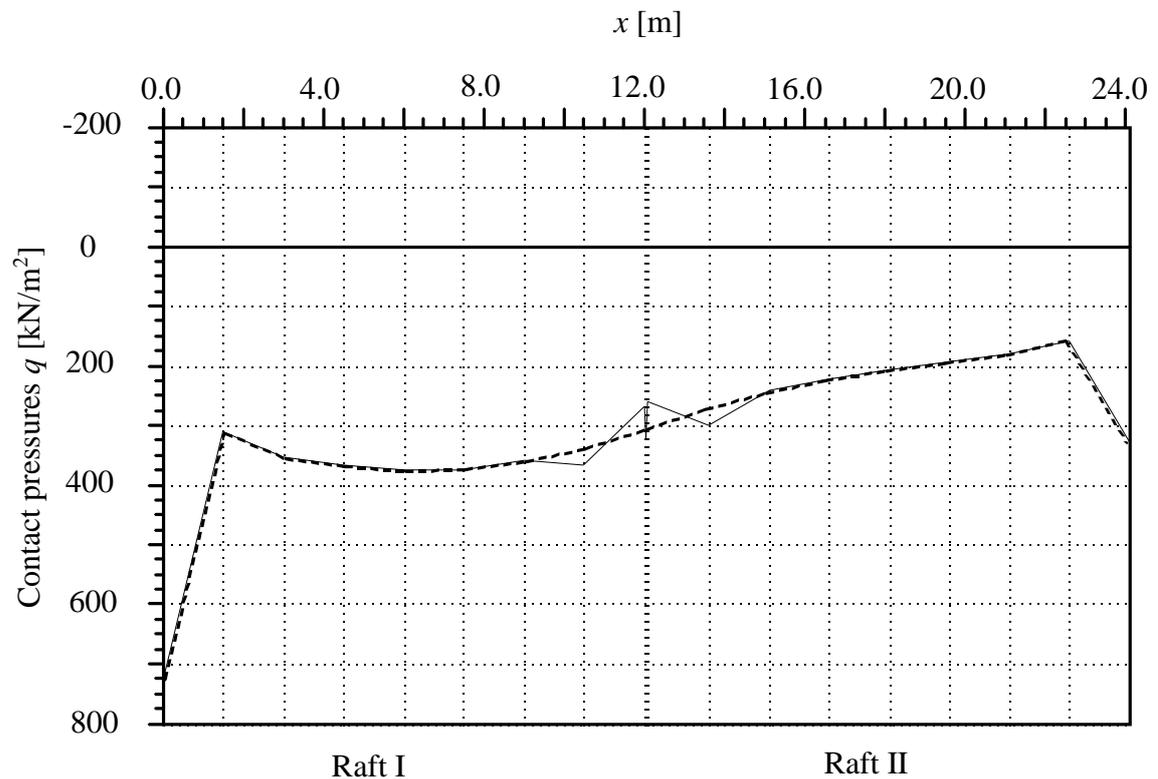
Figure 4.28   Contact pressures q at the middle section of the rafts I and II (case 3 and 4)
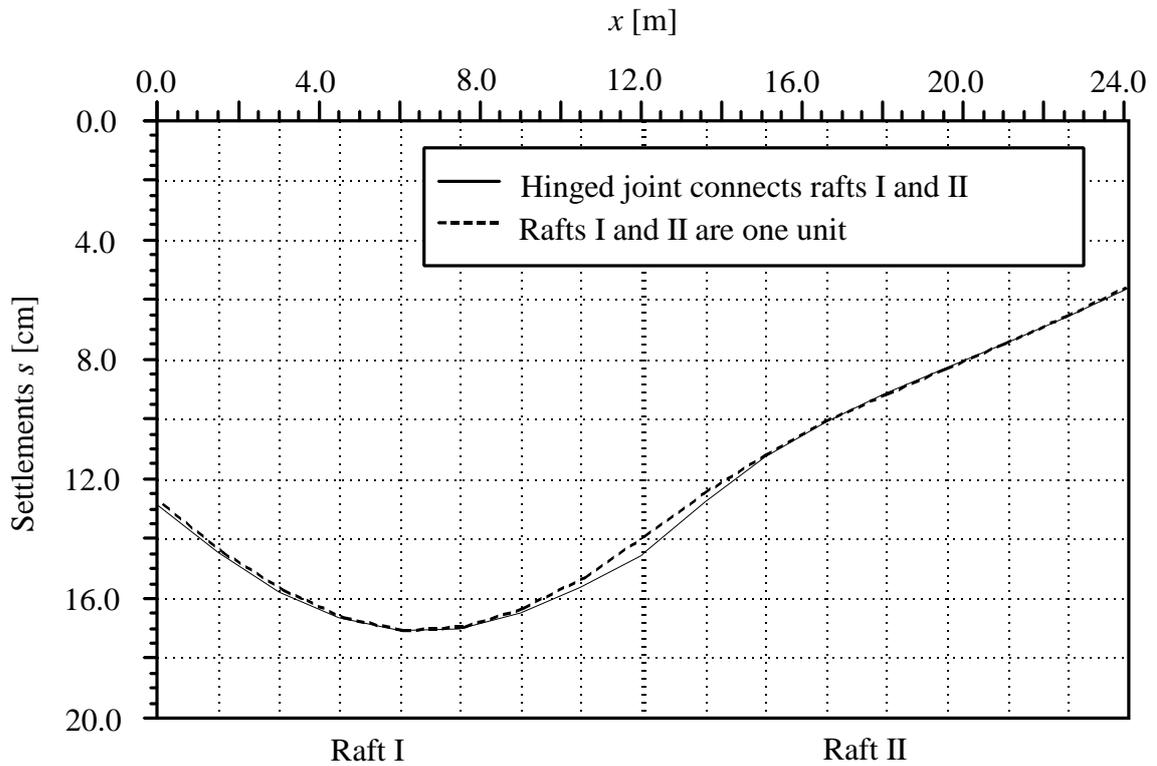
Figure 4.29   Settlements s at the middle section of the rafts I and II (case 3 and 4)
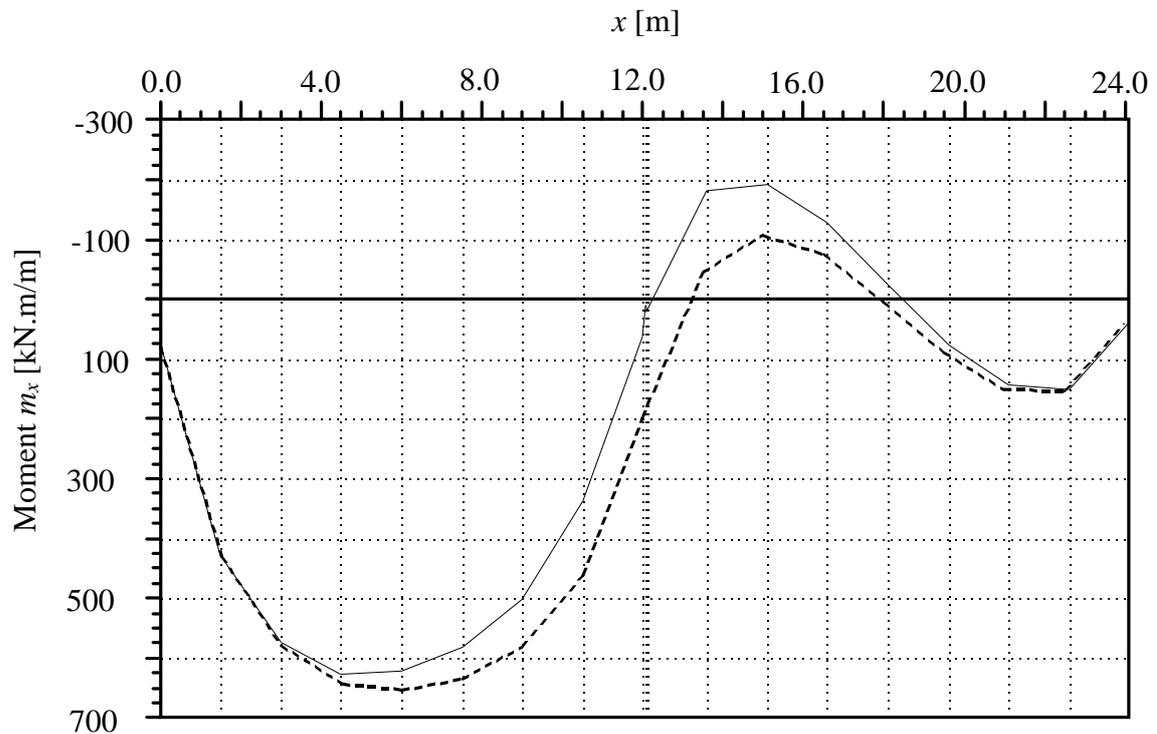

Figure 4.30   Moments m_x at the middle section of the rafts I and II (case 3 and 4)
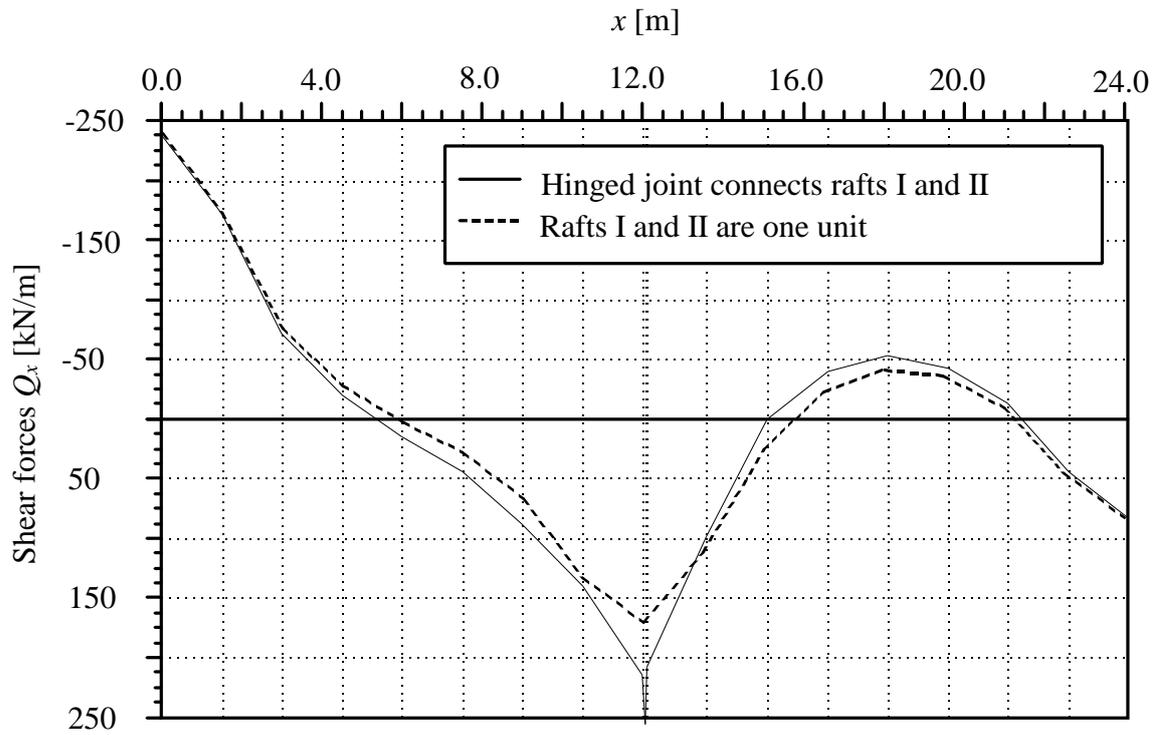
Figure 4.31   Shear forces Q_x at the middle section of the rafts I and II (case 3 and 4)

Example 4.5   Analysis of a swimming pool

1   Description of the problem

A swimming pool is supposed to be constructed at a river. The existing ground around the pool has to be increased up to a meter. The pool has dimensions of 25 [m] × 10 [m] and maximum water depth of 1.20 [m] as shown in Figure 4.32. The foundation level is 1.45 [m] under the ground surface. Slab and walls are reinforced concrete of concrete grade B 25 with thickness of 25 [cm] for slab and 20 [cm] for walls. It is divided into two independent parts through a joint at the pool middle.

The filling material around the pool is non-cohesive soil (Figures 4.33 and 4.34). The filling is supposed to be carried out after finishing the pool.

In this example, it is required to study the following:

i)   Influence of the joint on the settlements, contact pressures and internal forces of the pool slab and the pool walls in case of the pool is completely filled by water

ii)   Influence of the ground rising by additional filling soil material at the southern part of the pool on the settlement

2   Soil properties

The subsoil under the swimming pool is defined by five boring logs B1 to B5 up to 15 [m] under the ground surface. The subsoil consists of four soil layers of fill, silt with organic admixture, silt clayey and gravel, which are not horizontally stratified as shown in Figure 4.33 and Table 4.8. *Poisson*'s ratio for the soil is $v_s = 0.3$ [-]. Ground water level is 3.80 [m] under the ground surface.
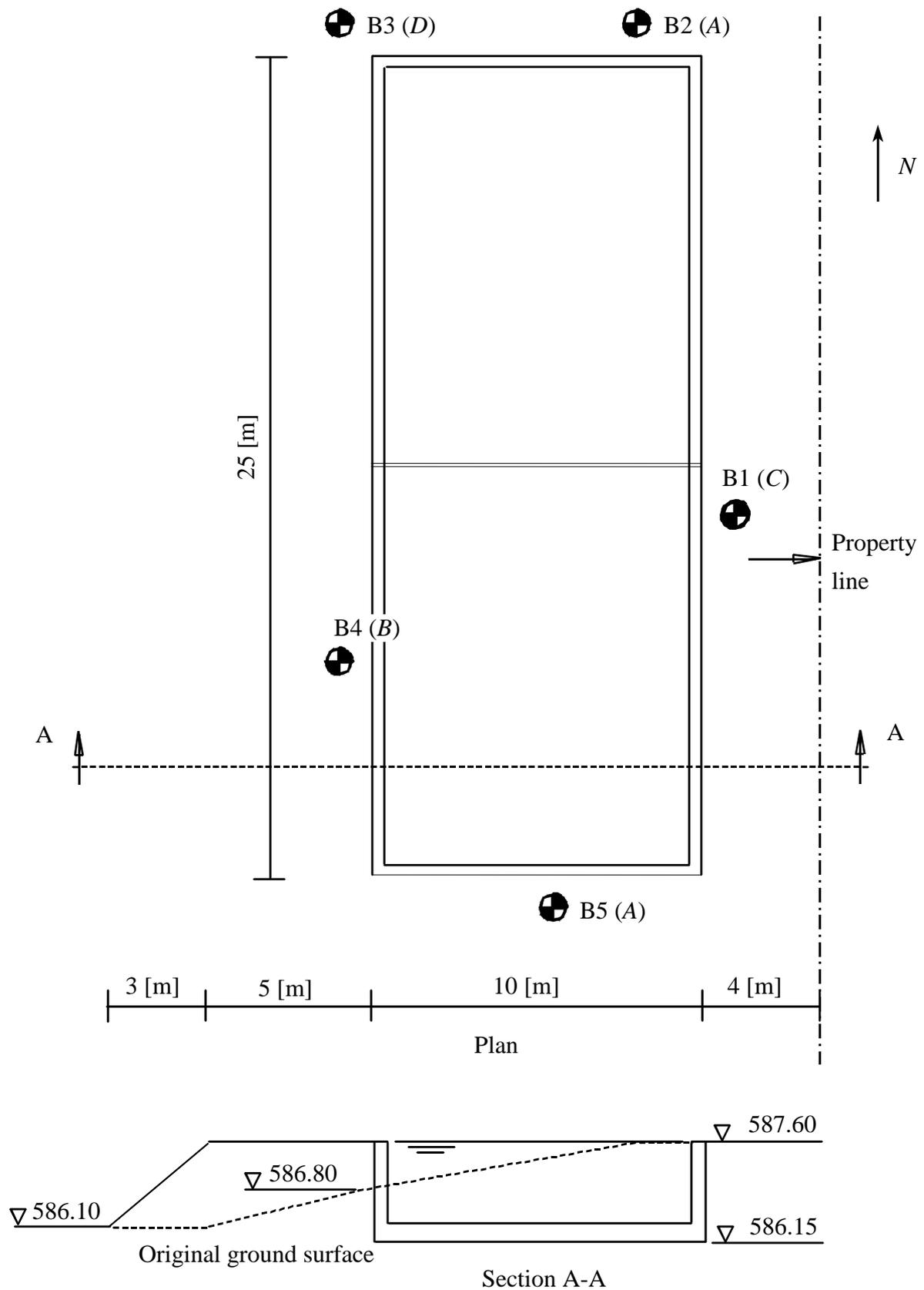
Figure 4.32   Details of the swimming pool

Legend

Fill
$E_s = 70000$ [kN/m²]
$W_s = 150000$ [kN/m²]
$\gamma_s = 19$ [kN/m³]
$\gamma'_s = 10$ [kN/m³]

Silt, organic admixture
$E_s = 4000$ [kN/m²]
$W_s = 10000$ [kN/m²]
$\gamma_s = 17.5$ [kN/m³]
$\gamma'_s = 7.5$ [kN/m³]

Silt, clayey, soft
$E_s = 450$ [kN/m²]
$W_s = 1000$ [kN/m²]
$\gamma_s = 16$ [kN/m³]
$\gamma'_s = 6$ [kN/m³]

Gravel
$E_s = 100000$ [kN/m²]
$W_s = 200000$ [kN/m²]
$\gamma_s = 20$ [kN/m³]
$\gamma'_s = 11$ [kN/m³]

▽ 587.60 m NN

(3.24)
(4.60)
(6.60)

(15.00)

B1 (*C*)

▽ 587.60 m NN

(3.24)
(3.90)
(4.90)

(3.80) ▼

(15.00)

B2 and B5 (*A*)

0.0
2.0
4.0
6.0
8.0
10.0
12.0
14.0
16.0

▽ 587.60 m NN

(3.24)
(3.60)
(4.60)

(15.00)

B3 (*D*)

▽ 587.60 m NN

(3.24)
(4.60)
(6.10)

(3.80) ▼

(15.00)

B4 (*B*)

0.0
2.0
4.0
6.0
8.0
10.0
12.0
14.0
16.0

Figure 4.33   Boring logs B1 to B5 with soil properties

Table 4.8   Soil properties

Layer No.	Type of soil	Modulus of compressibility of the soil for		Unit weight of the soil	
		Loading E_s	Reloading W_s	above GW γ_s	under GW γ'_s
1	Fill	70000	150000	19	10
2	Silt, organic admixture	4000	10000	17.5	7.5
3	Silt, clayey, soft	450	1000	16	6
4	Gravel	100000	200000	20	11

3   Raft material and properties

The material of the raft and walls is reinforced concrete of grade B 25. It has the following properties:

Young's modulus E_b $= 3 \times 10^7$ [kN/m²]
Shear modulus G_b $= 1.3 \times 10^7$ [kN/m²]
Unit weight γ_b $= 25$ [kN/m³]
Poisson's ratio ν_b $= 0.25$ [-]

4   Stiffness of edge walls

The rigidity of the edge walls (thickness $B = 0.2$ [m], height $H = 1.2$ [m]) is simulated through beam elements along the raft edge with the following data:

Moment of inertia I $= B \times \dfrac{H^3}{12}$

$$= 0.2 \times \frac{1.2^3}{12} = 0.0288 \qquad [\text{m}^4]$$

Torsional inertia J $= H \times B^3 \times \left(\dfrac{1}{3} - 0.21\right) \dfrac{B}{H} \left\{1 - \dfrac{B^4}{12 \times H^4}\right\}$

$$= 1.2 \times 0.2^3 \times \left(\frac{1}{3} - 0.21\right) \frac{0.2}{1.2} \left\{1 - \frac{0.2^4}{12 \times 1.2^4}\right\}$$

$$= 0.0286 \qquad [\text{m}^4]$$

5   Determination of settlements, contact pressures and internal forces
5.1   Studying the influence of the joint

Four cases concerning the influence of the joint are considered as follows:

Case 1   Analysis without interaction (Figure 4.34)
                The two rafts are constructed side by side separately without interaction between
                them through the soil

Case 2   Analysis with interaction but without shearing forces (Figures 4.34)
                The two rafts are constructed side by side separately with interaction only through
                the soil. The zero distance between the two rafts is represented by concrete
                elements of 1 [cm] wide and 0 [cm] thickness

Case 3   Analysis with interaction and with shearing forces (Figure 4.36)
   The two rafts are connected through hinged joint. The hinged joint is represented
                by elements of 1 [cm] wide and 2 [cm] thickness

Case 4   Analysis without joint (Figure 4.35)
                Rather than two rafts, one raft is constructed

5.2   Studying the influence of surrounding loading

To study the influence of the surrounding loading on the swimming pool due to the filling soil
material, the weight of the filling is represented by four loaded areas according to its weight
intensity as shown in Figure 4.38 and Table 4.9. The loaded areas are subdivided into four
independent nets. The analysis of these loaded areas is carried out firstly to obtain the contact
pressures under them. Due to these computed contact pressures, the settlement will occur under
the swimming pool.

Table 4.9   Properties of the loaded area

Loaded area No.	Dimensions [m]			Load	Foundation level	Origin coordinate	
	L	B	h	$p = \gamma\, h$ [kN/m²]	t_f [m]	x [m]	y [m]
1	3	35	0.75	$19 \times 0.75 = 14.25$	1.5	-3	-6
2	5	35	1.15	$19 \times 1.15 = 21.85$	1.15	-3	-3
3	8	5	0.40	$19 \times 0.40 = 7.6$	0.4	27	2
4	8	5	0.40	$19 \times 0.4 = 7.6$	0.4	-3	2

Detail *A*   Detail *B*

2×1=2[cm]

2 [cm] raft thickness

10 [kN/m]   10 [kN/m]

0.2 [m]

1.20 [m]   12 [kN/m²]   *A*   12 [kN/m²]

0.25 [m]

$20 \times 0.625 = 12.5$ [m] $20 \times 0.625 = 12.5$ [m]

Section

2×1=2[cm]

$16 \times 0.625 = 10.0$ [m]

a   a

Plan   Raft I   *B*   Raft II
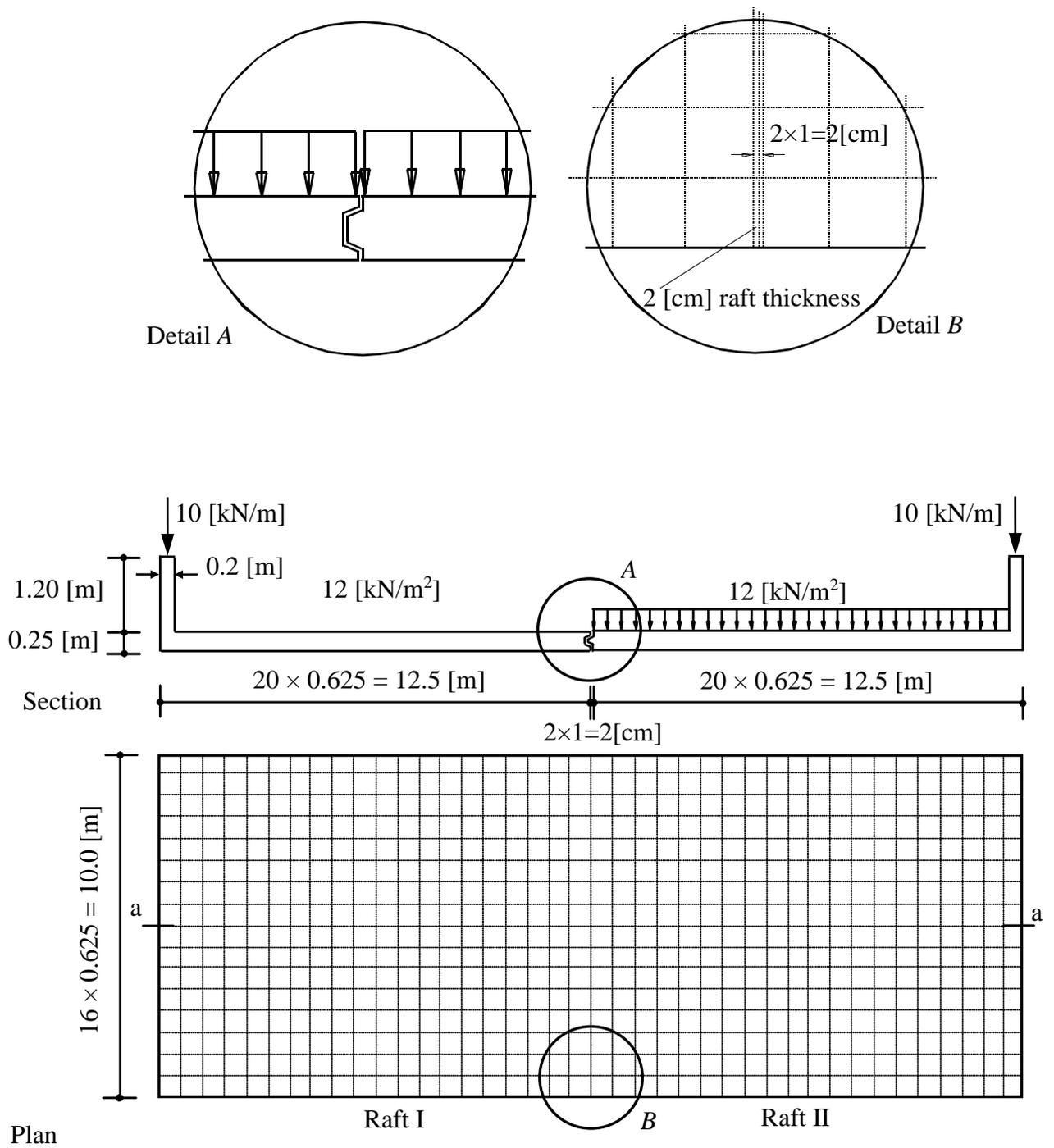
Figure 4.34   Rafts I and II are connected by a hinged joint (case 3)
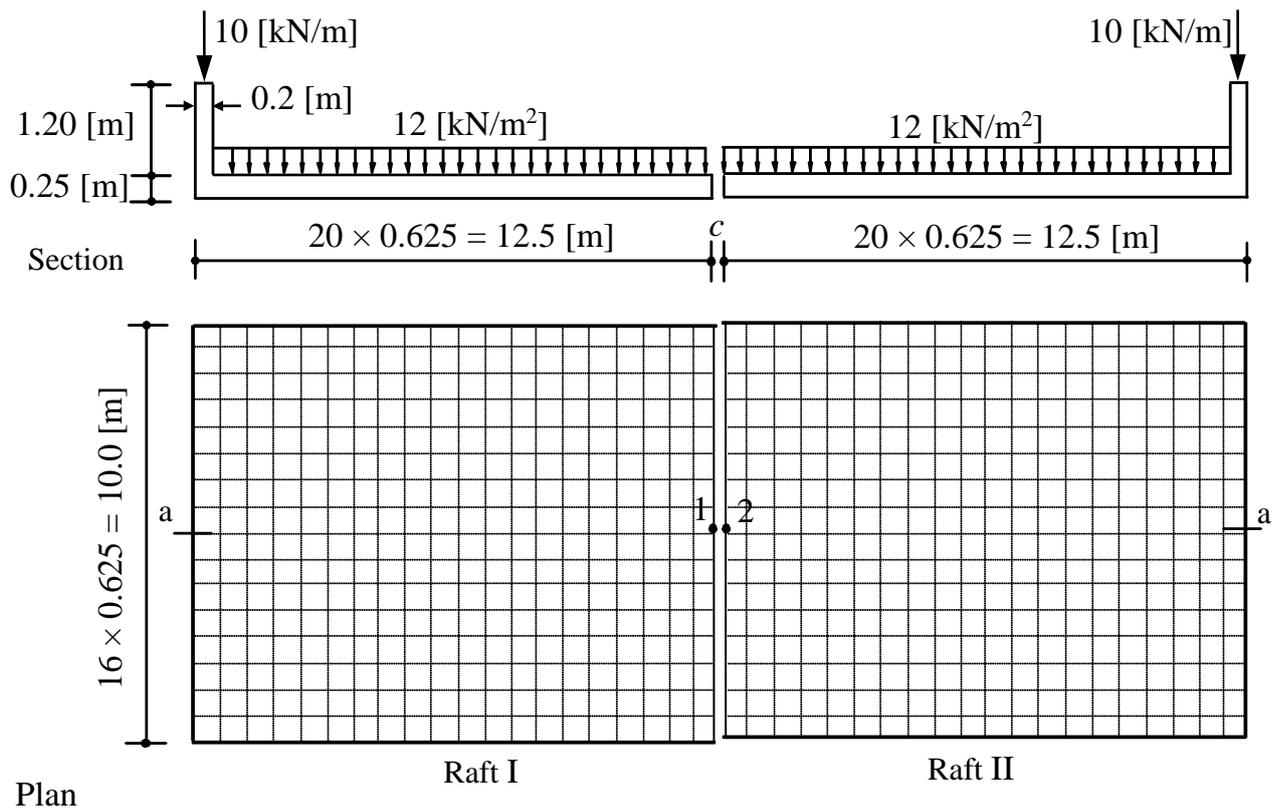
Figure 4.35   Rafts I and II are constructed side by side (cases 1 and 2)
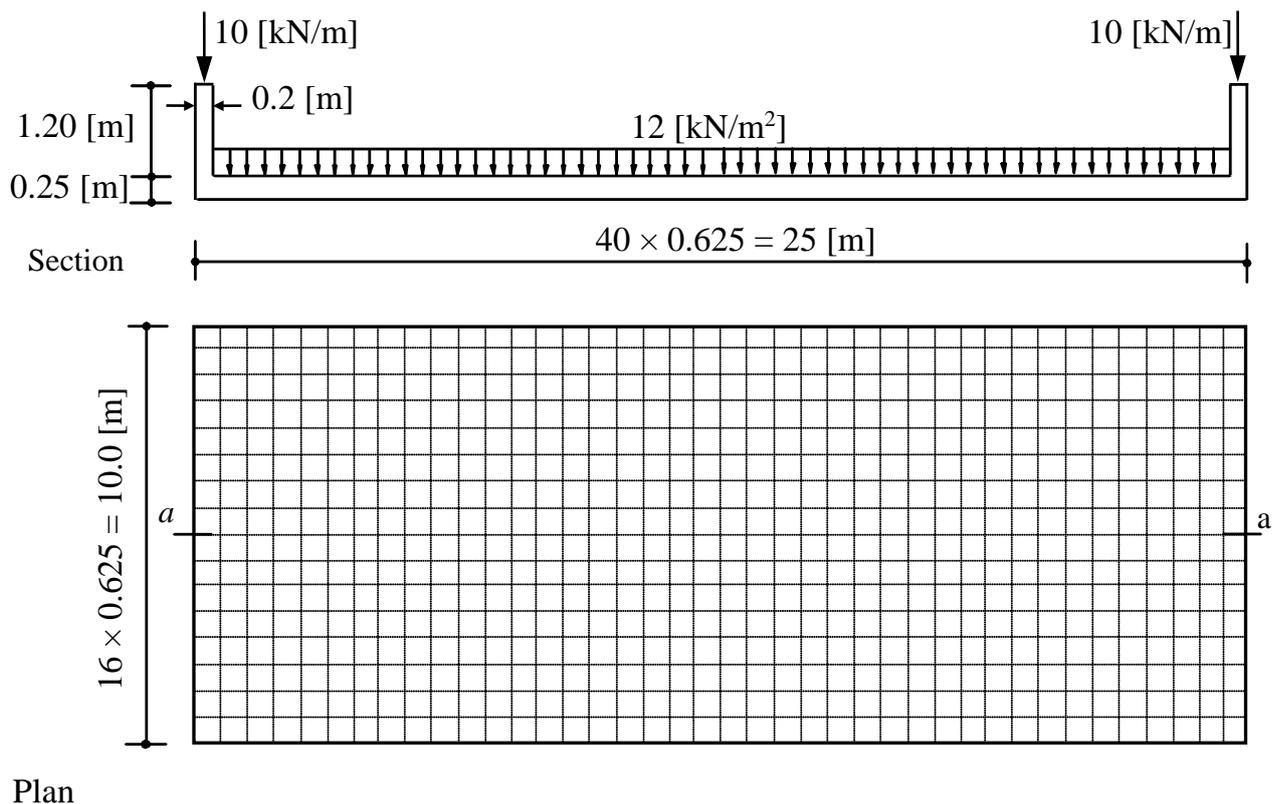
Figure 4.36   Rather than rafts I and II, only one raft is constructed (case 4)

6   Analysis
6.1   General

The rafts are subdivided into 640 square finite elements, each element has a side of 0.625 [m] as shown in Figures 4.34 to 4.36. The analysis of rafts in case 2 (analysis with interaction but without shearing forces) is carried out by using a net for the two rafts. The free distances between the rafts are carried out by inserting appropriate two very small elements between rafts. Each element has 1 [cm] width and 0.0 [cm] thickness. The very small widths of the elements keep the distance between the rafts nearly zero, while the zero thickness of the elements eliminates the raft rigidity at the joint.

To simulate a hinged joint between rafts in case 3 (analysis with interaction and with shearing forces), two very small elements are inserted between the rafts. Each element has 1 [cm] width and 2 [cm] thickness. The very small widths of the elements keep the distance between the rafts nearly zero, while the small thickness of the elements makes the raft rigidity at the joint very small. These boundary conditions allow interacting of only the vertical forces between rafts. Moments at hinged connection will be eliminated due to the very small rigidity of connection elements. For all cases of analyses, the horizontal forces due to water pressure or earth pressure are neglected.

## 6.2   Choice of the calculation method for studying the influence of the joint

A primary analysis was carried out by the modulus of compressibility method (method 7). It was found that this method maybe causes numerical problems; these problems also occur when applying the modulus of compressibility method using iteration (method 6). The numerical problems were due to the light loads distributed uniformly on the pool in addition to stiff edges as a result to edge walls. Consequently, negative contact pressures occur by applying the modulus of compressibility method. Therefore, all analyses of the pool were carried out by Modification of modulus of subgrade reaction by iteration (method 4). The iteration process of the method is repeated till the difference between the results of the step i and those of the step of $i +1$ are nearly the same. In this example 20 steps were sufficient for the analysis.

6.3   Choice of the calculation method for studying
the influence of the surrounding loading

The loads from filling around the swimming pool (21.85 [kN/m^2]) are higher than those acting on the swimming pool itself (12 [kN/m^2]). Therefore, it is expected great settlements on the swimming pool due to the filling. In this case, negative contact pressures will be expected on the swimming pool.

**6.4   Consideration of the irregularity of the subsoil material
         on the behavior of the swimming pool**

The available information about the subsoil under the swimming pool is five boring logs B1 to B5.
Each boring has four layers as shown in Figure 4.33 and Table 4.8. Arrangement of boring locations
is shown in Figure 4.37. In order to carry out the analysis of the swimming pool taking into account
the irregularity of the subsoil, the whole foundation area is subdivided into triangle zones as shown
in Figure 4.37. Then, the flexibility coefficients are determined by Interpolation method.

Zone type (I): Bilinear interpolation in the triangle area

Zone type (II): Linear interpolation between 2 boring logs
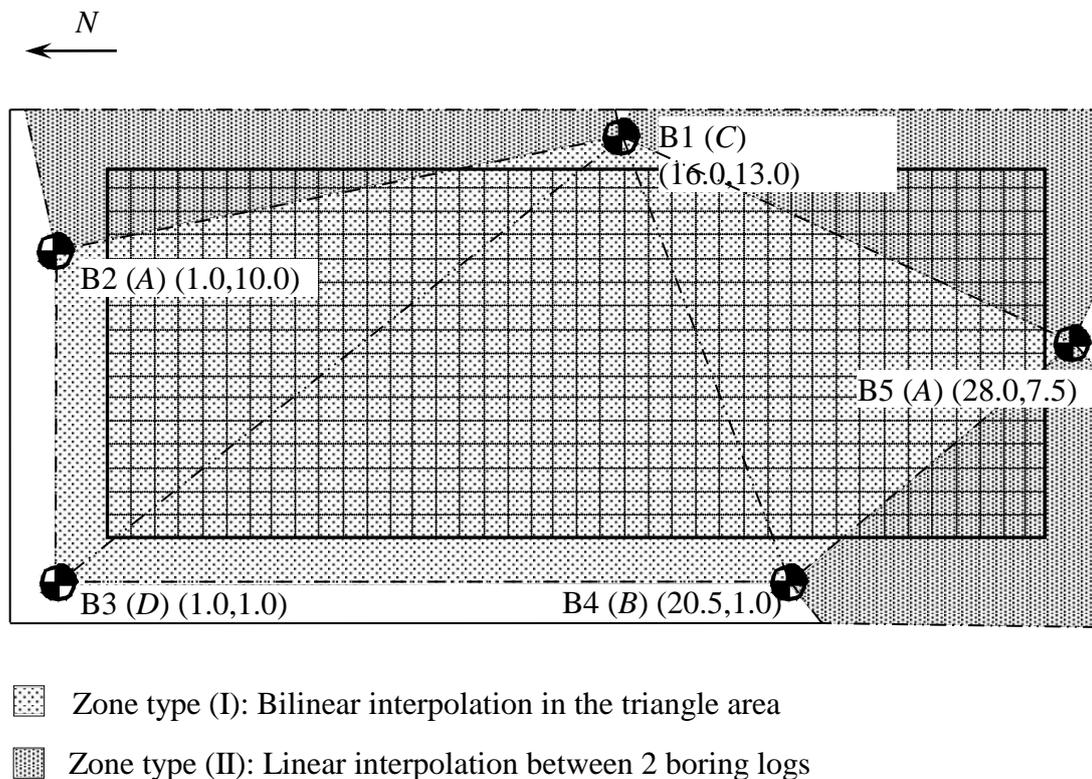
Figure 4.37   Locations of boring logs B1 to B5 with interpolation zones
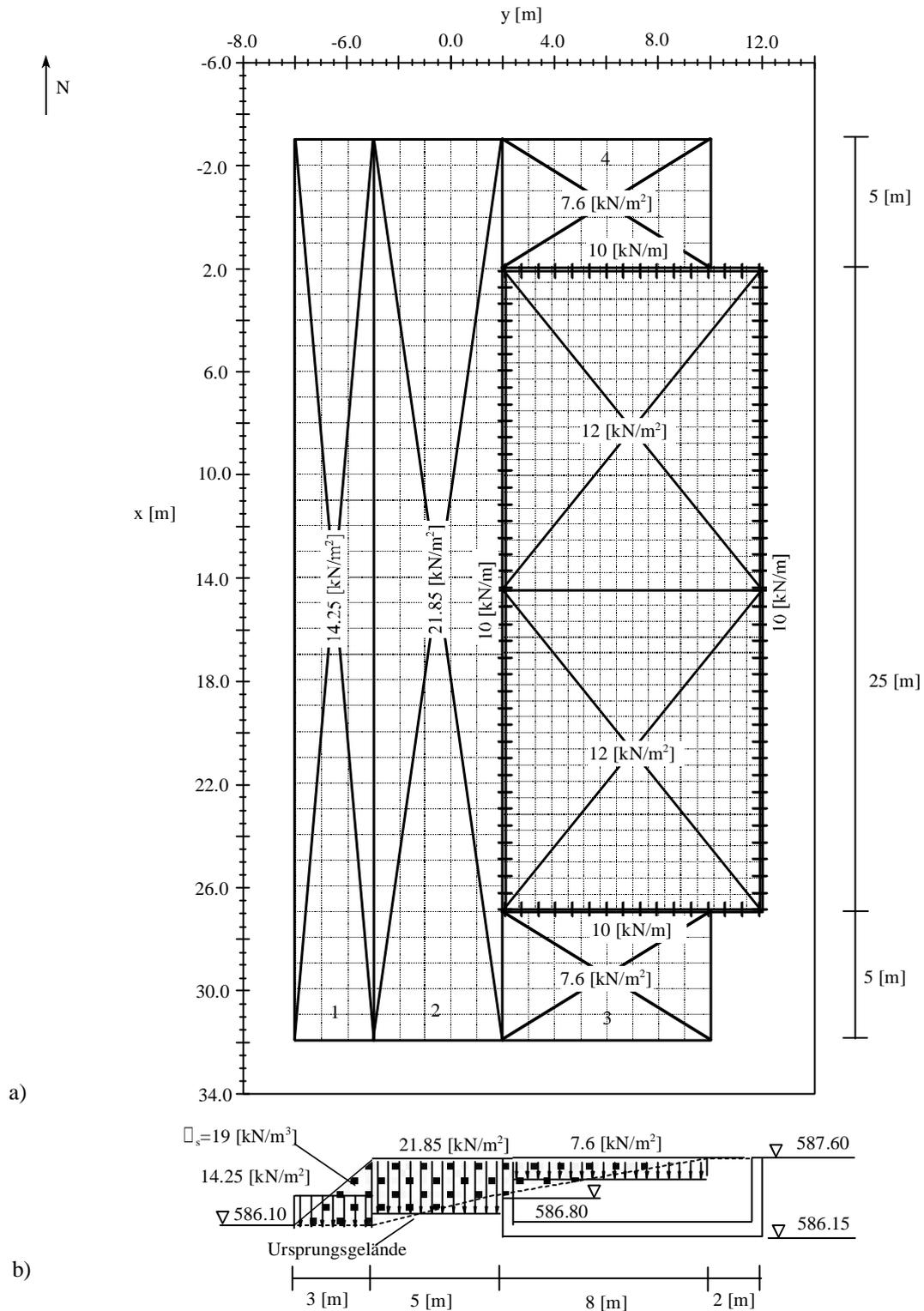
Figure 4.38   Swimming pool with loads and external loaded areas 1 to 4

Theory for the calculation of shallow foundations
Chapter 4
System of many Foundations

7   Results and discussion
7.1   Studying the influence of the joint

Figures 4.39 to 4.50 show the contour lines of settlements, isometric view of contact pressures, circular diagrams of moments for the four cases of analysis while Figure 4.51 shows settlements, contact pressures and moments at the middle section a-a. Figures 4.52 to 4.59 show the internal forces in the edge walls.

In general, it can be noticed from those figures that:

Settlements

-        Settlements at the edges (points 1 and 2) of the rafts with joints (cases 2 and 3) are greater than that without interaction (case 1) and without joint (case 4), Figure 4.51a

-        Settlements for rafts with joints (cases 2 and 3) are nearly similar (Figures 4.40, 4.41 and 4.51a)

-        If hinged joint between rafts is used (case 3), there will be continuation of settlement under the rafts (Figure 4.51a)

-        A continuation of settlement under the rafts with free joint (case 2) is also found, this related to the loads on both rafts are equal (Figure 4.51a)

-        The analysis of rafts with interaction showed that both rafts would lean toward each other (Figures 4.40 and 4.41)

Contact pressures

-        If hinged joint between rafts is used (case 3), there will be continuation of contact pressure under the rafts at the joint (Figures 4.45 and 4.51b)

-        Slight differences in contact pressures at the edges (points 1 and 2) of the rafts with free joint (case 2) occur (Figure 4.44)

Moments

-        Moments for rafts without interaction (case 1) and for the raft without joint (case 4) are much greater than that for rafts with joints (cases 2 and 3), Figures 4.47 to 4.50 and Figure 4.51c

-        For rafts with joints (cases 2 and 3), the positions of maximum moments are shifted to the center of the rafts (Figure 4.51c)

-        It is clear from Figure 4.51c for rafts with joints (cases 2 and 3) that the moment at the joints for the two rafts tends to zero

Internal forces in walls

-       Moments will be minimum if a raft with joint is used (cases 2 and 3), Figures 4.53 and 4.54. Moments and shear forces for rafts without interaction (case 1) is unreal (Figures 4.52 and 4.56)

-       For the raft without joint (case 4) a positive maximum moment at the position of connection is to be found (Figures 4.55), while for rafts with joints the moments are equal to zero at that position due to joints (Figures 4.53 and 4.54)

-       Moments and shear forces for the rafts with joints (cases 2 and 3) are nearly similar (Figures 4.53, 4.54, 4.57 and 4.58)

Finally, it can be concluded that:

-       Considerable differences will be expected in the results, if the analysis is carried out for rafts without and with interaction

-       The results for the rafts with free joint (case 2) and with hinged joint (case 3) are nearly similar in this example

-       If rafts with free joint (case 2) have equal loads, only slight differences will be expected at the position of joint connection. Therefore, both of the two types of joints (hinged or free) may be used in this example

-       Although the rafts with joints (cases 2 and 3) lead to higher settlements than that without joints (case 4), but give less internal forces

-       The suitable foundation system may be used in this example is the rafts with joints (case 2 or 3)

7.2   Studying the influence of surrounding loading

Figure 4.60 shows contour lines of the settlement under the swimming pool due to the surrounding loading only. As it is expected, the settlement at the edge of the swimming pool near the surrounding loading is about 2.5 [cm] greater than that due to the swimming pool itself (Figures 4.39 to 4.42) by application of the four cases of analysis concerning the joint. Figures 4.61 to 4.64 show the contour lines of settlement under the swimming pool due to both loads from filling and swimming pool itself. These figures show that the direction of the settlements is changed toward the surrounding loading. To overcome extreme results concerning the internal forces on the swimming pool in this case, it is recommended that most of the filling must be carried out before constructing the swimming pool.
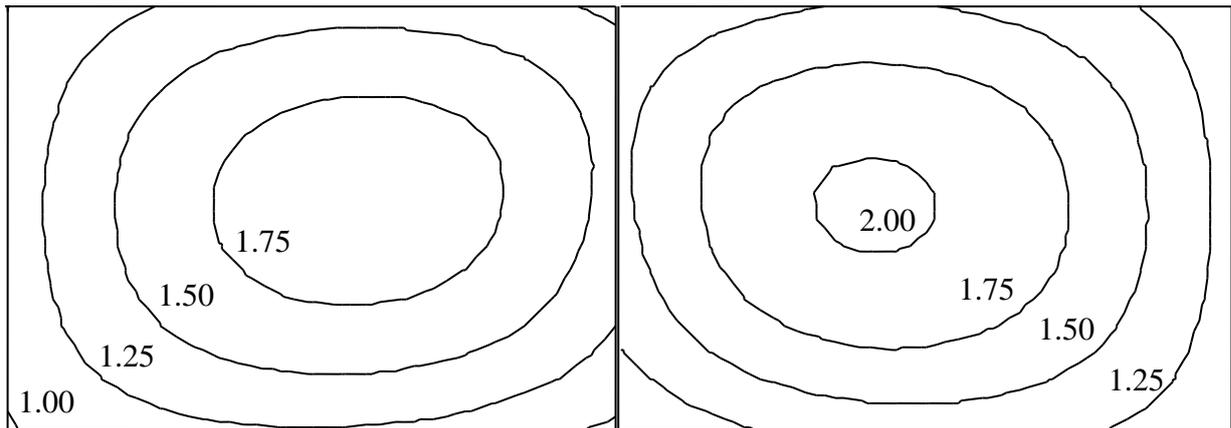
Figure 4.39   Contour lines of settlements *s* [cm]
   Analysis without interaction (case 1)
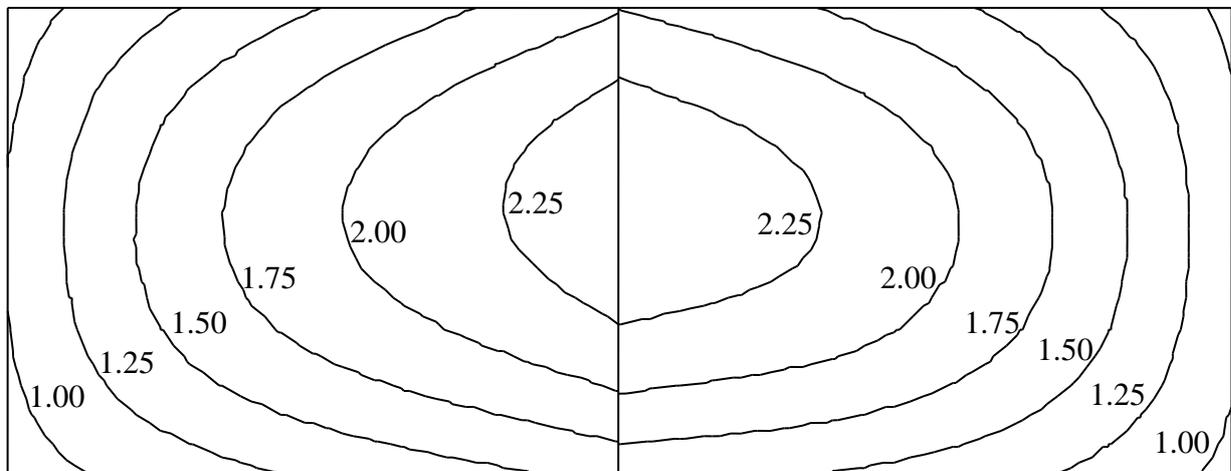
Figure 4.40   Contour lines of settlements *s* [cm]
                Analysis with interaction and without shearing forces (case 2)
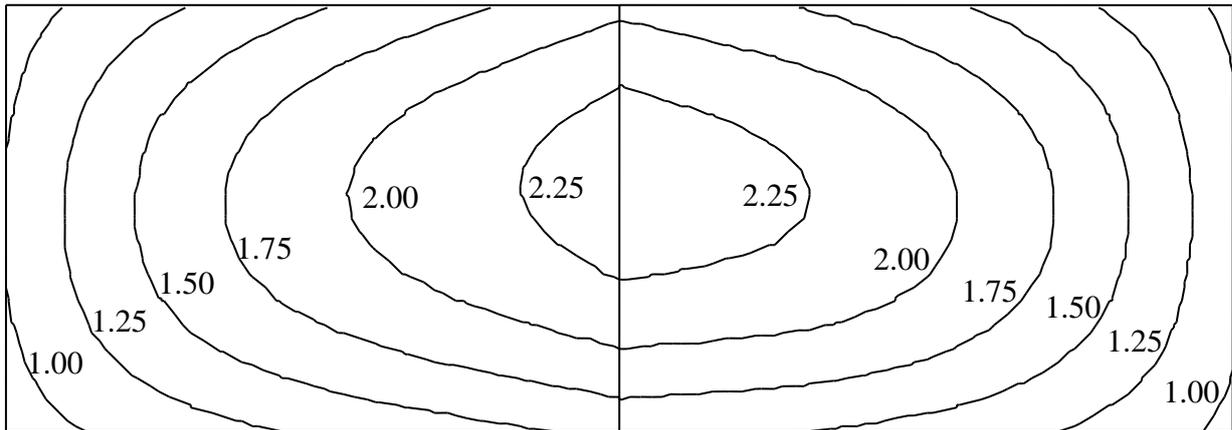
Figure 4.41   Contour lines of settlements *s* [cm]
   Analysis with interaction and with shearing forces (case 3)
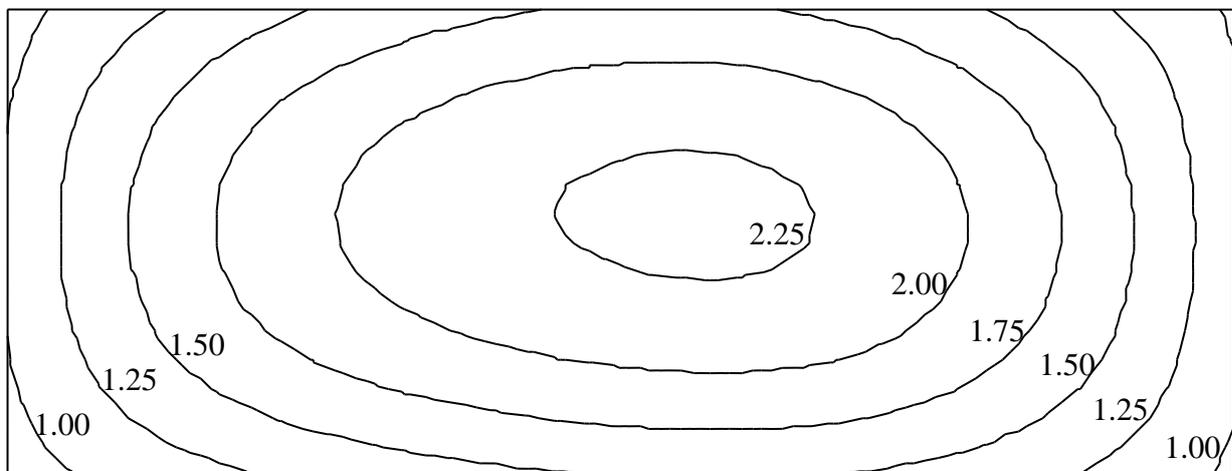
Figure 4.42   Contour lines of settlements *s* [cm]
   Analysis without joint (case 4)

0
100 [kN/m²]

545

521

380 433

548
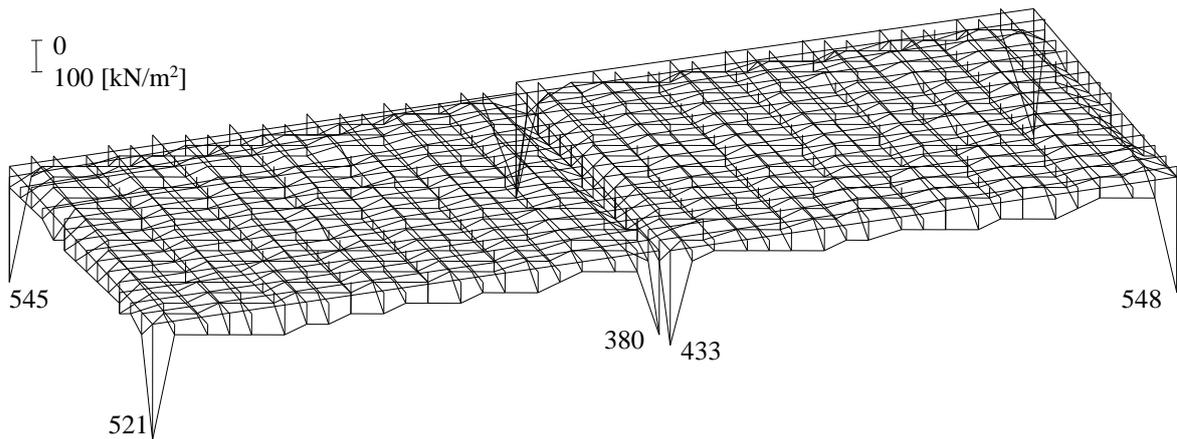
Figure 4.43   Isometric view of contact pressures q [kN/m²]
               Analysis without interaction (case 1)

0
100 [kN/m²]

466

458

151

486
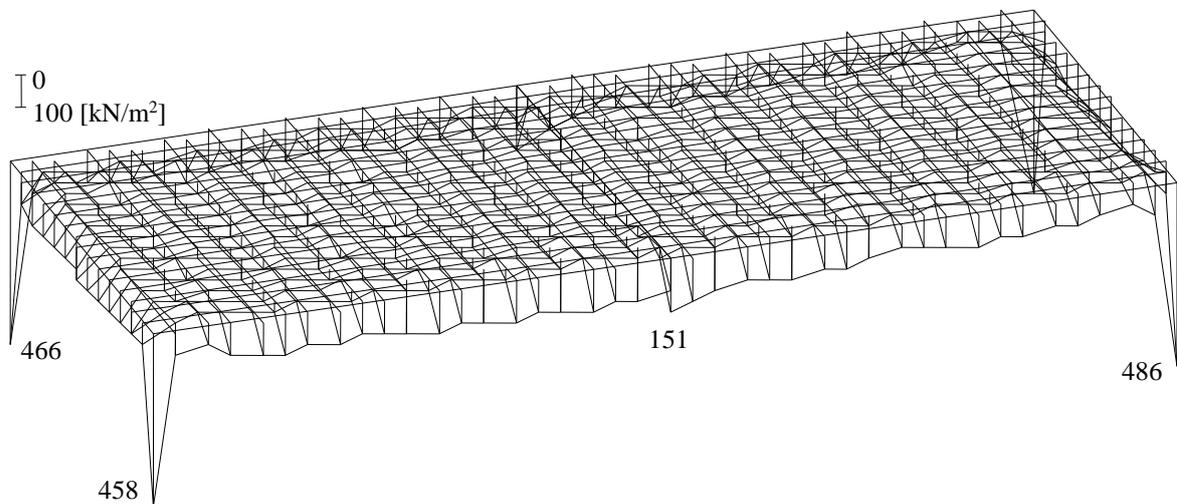
Figure 4.44   Isometric view of contact pressures q [kN/m²]
               Analysis with interaction and without shearing forces (case 2)

0
100 [kN/m²]

468   117   486

460
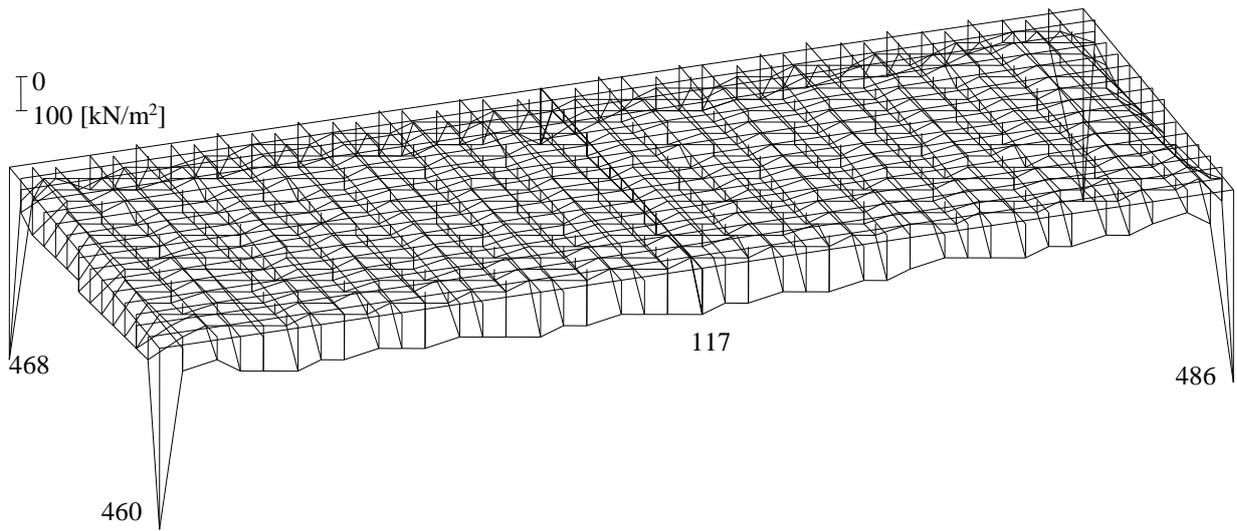
Figure 4.45   Isometric view of contact pressures q [kN/m²]
   Analysis with interaction and with shearing forces (case 3)

0
100 [kN/m²]

484   100   493

461
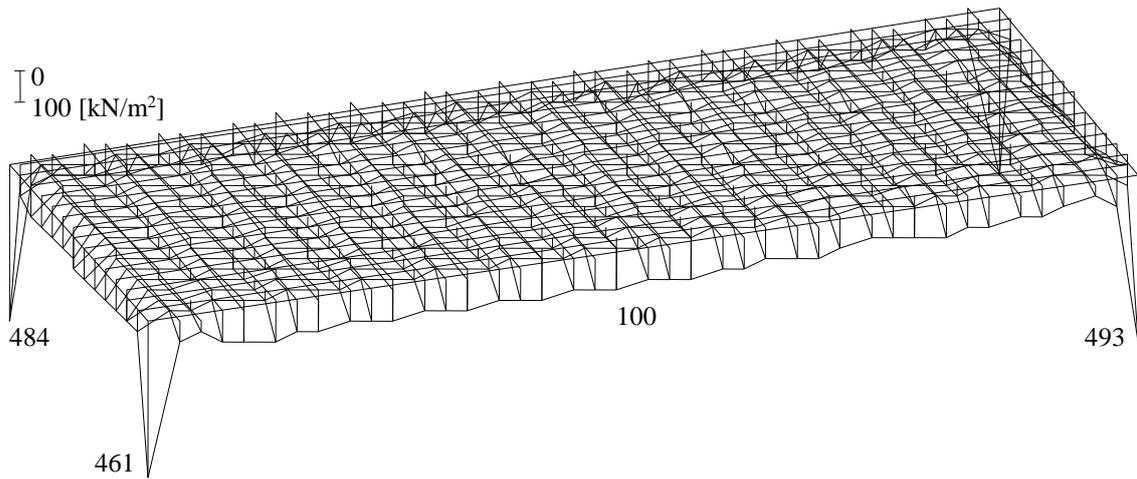
Figure 4.46   Isometric view of contact pressures q [kN/m²]
                Analysis without joint (case 4)

• 5 [kN.m/m]   • 10 [kN.m/m]   ● 15 [kN.m/m]   ● 20 [kN.m/m]
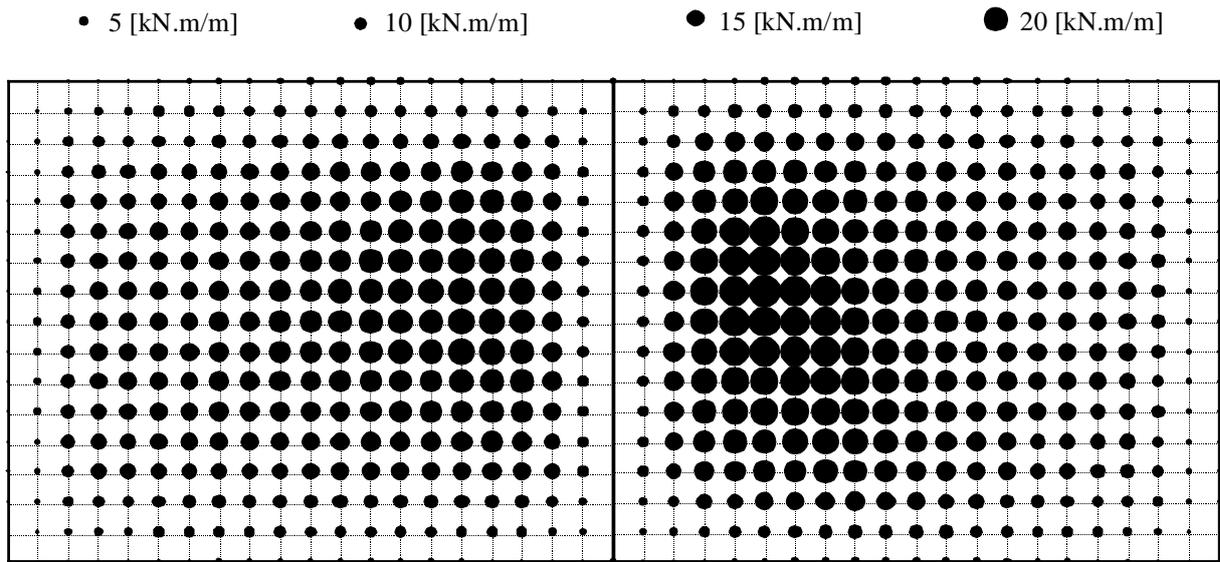
Figure 4.47   Circular diagrams of moments m_x [kN.m/m]
                 Analysis without interaction (case 1)

• 5 [kN.m/m]   • 10 [kN.m/m]   ● 15 [kN.m/m]   ● 20 [kN.m/m]
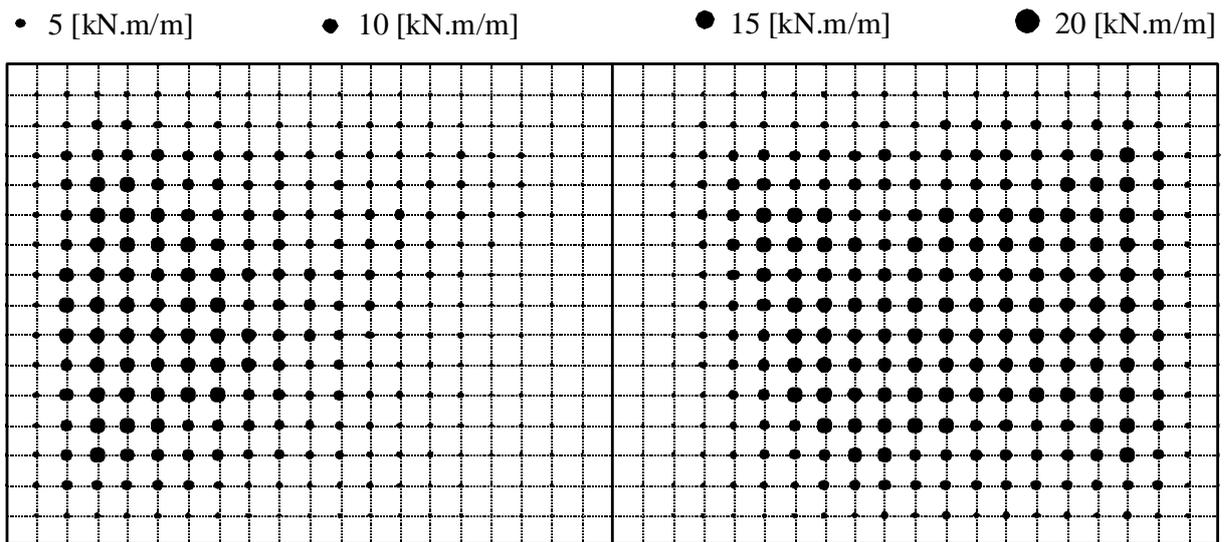
Figure 4.48   Circular diagrams of moments m_x [kN.m/m]
                 Analysis with interaction and without shearing forces (case 2)

• 5 [kN.m/m]   • 10 [kN.m/m]   ● 15 [kN.m/m]   ● 20 [kN.m/m]
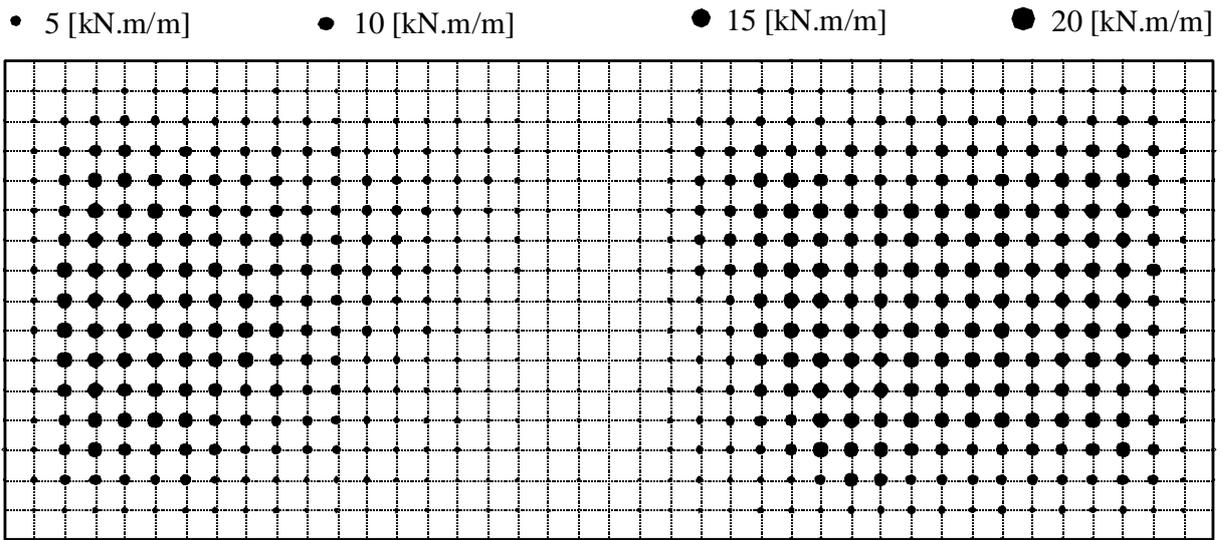
Figure 4.49   Circular diagrams of moments m_x [kN.m/m]
                      Analysis with interaction and with shearing forces (case 3)

• 5 [kN.m/m]   ● 10 [kN.m/m]   ● 15 [kN.m/m]   ● 20 [kN.m/m]
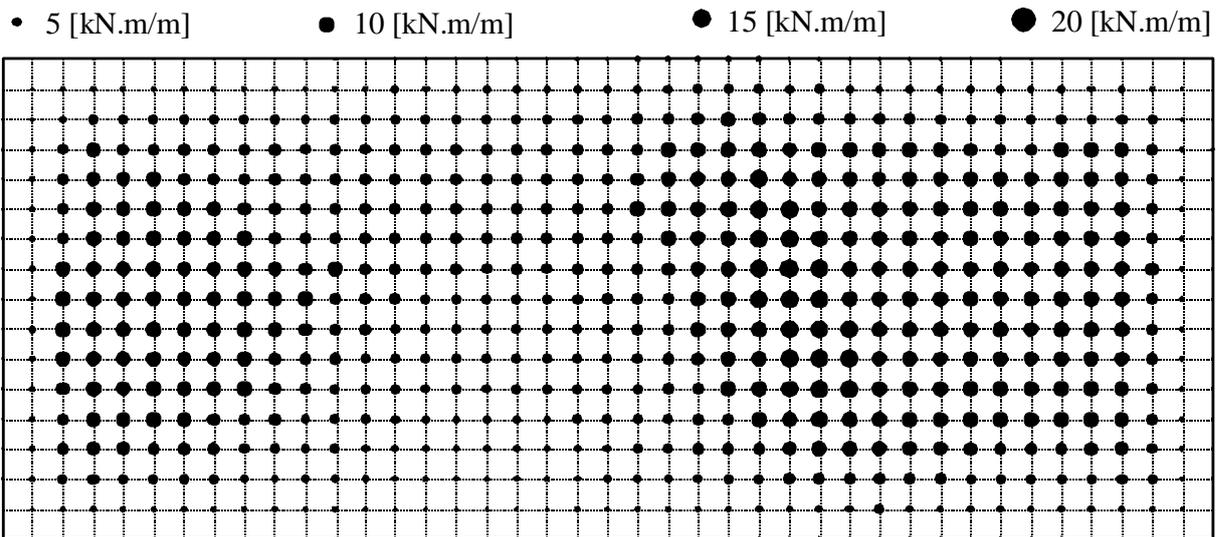
Figure 4.50   Circular diagrams of moments m_x [kN.m/m]
                      Analysis without joint (case 4)
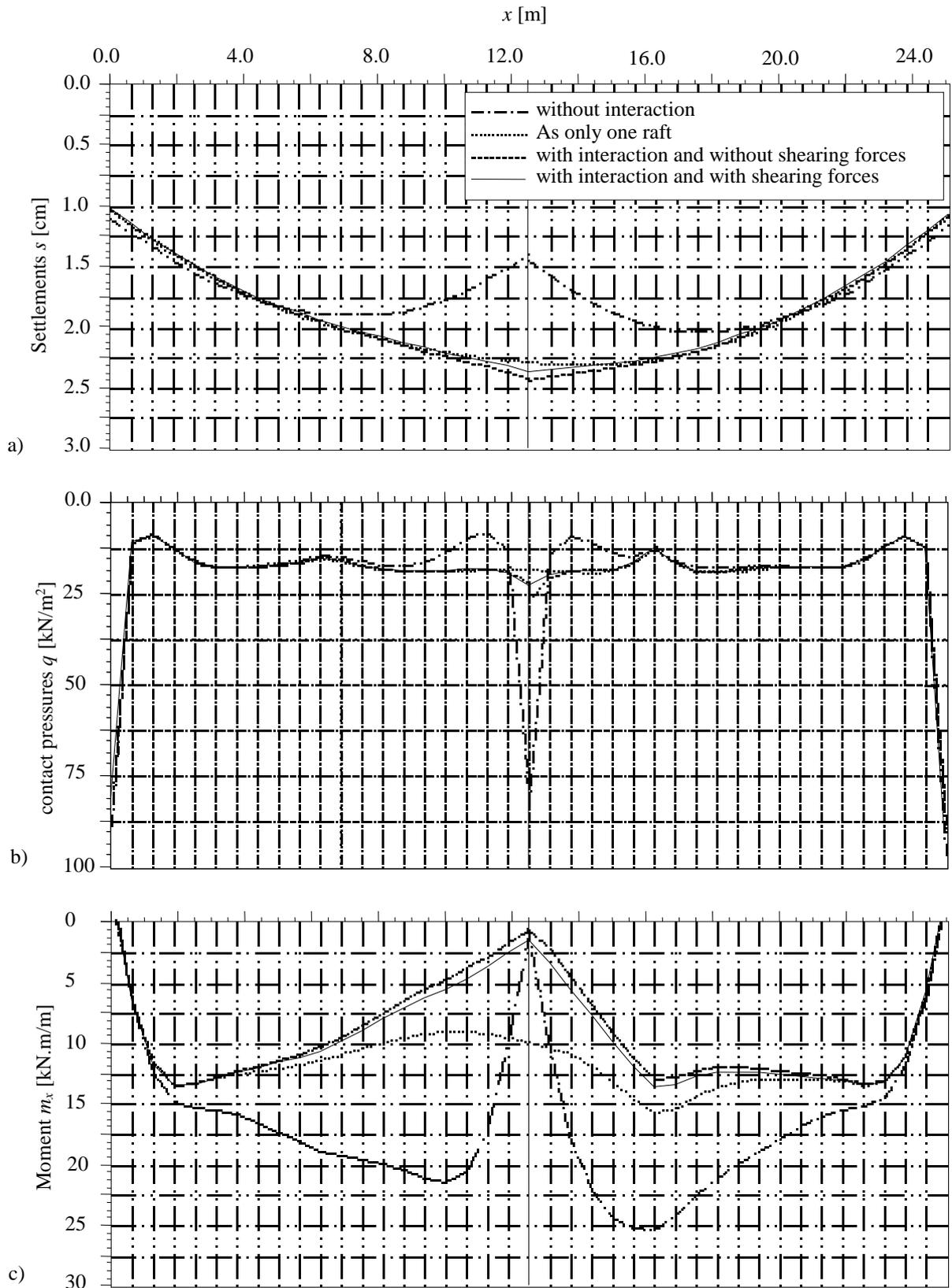
Figure 4.51   Settlements, contact pressures and moments at middle section of rafts I and II

50 [kN.m]
0

79

182

158

93

183

141
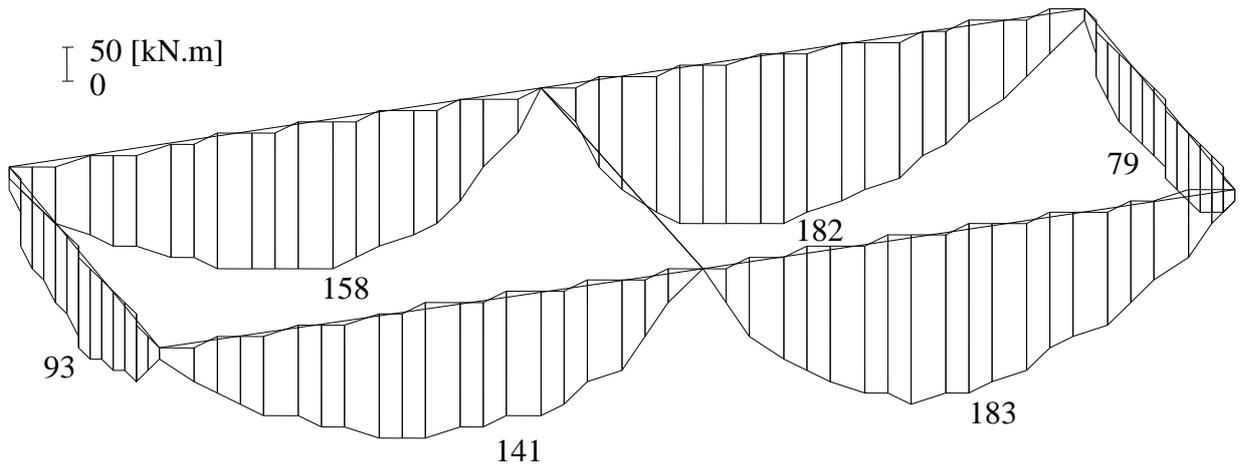
Figure 4.52   Beam-bending moments M_b [kN.m] at edge walls of the swimming pool
Analysis without interaction (case 1)

50 [kN.m]
0

65

99

48

81

113   50
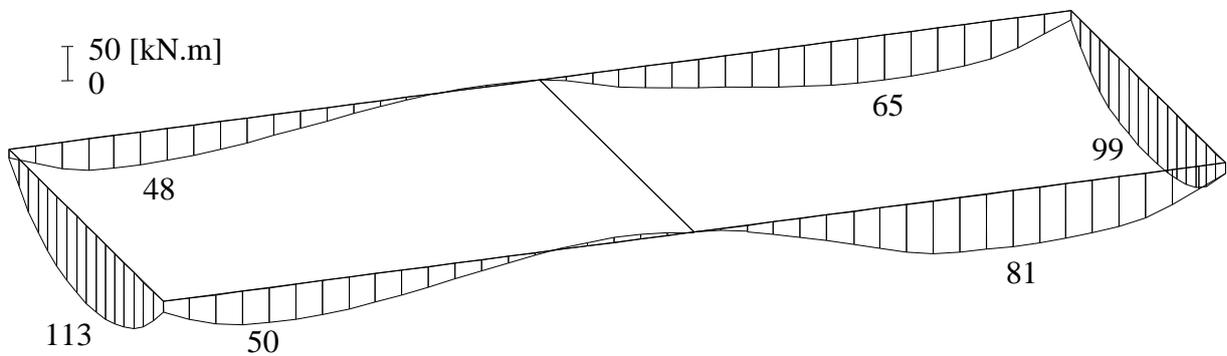
Figure 4.53   Beam-bending moments M_b [kN.m] at edge walls of the swimming pool
Analysis with interaction and without shearing forces (case 2)

50 [kN.m]
0

70

98

50

85

113   52
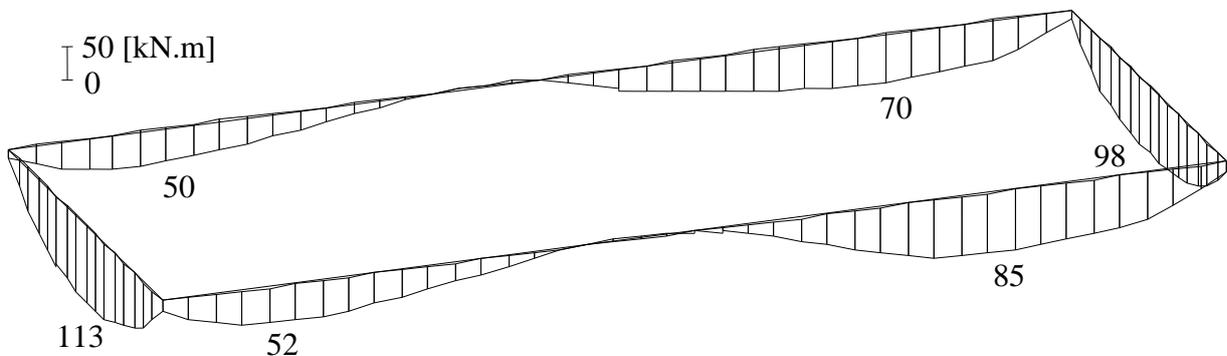
Figure 4.54   Beam-bending moments M_b [kN.m] at edge walls of the swimming pool
Analysis with interaction and with shearing forces (case 3)
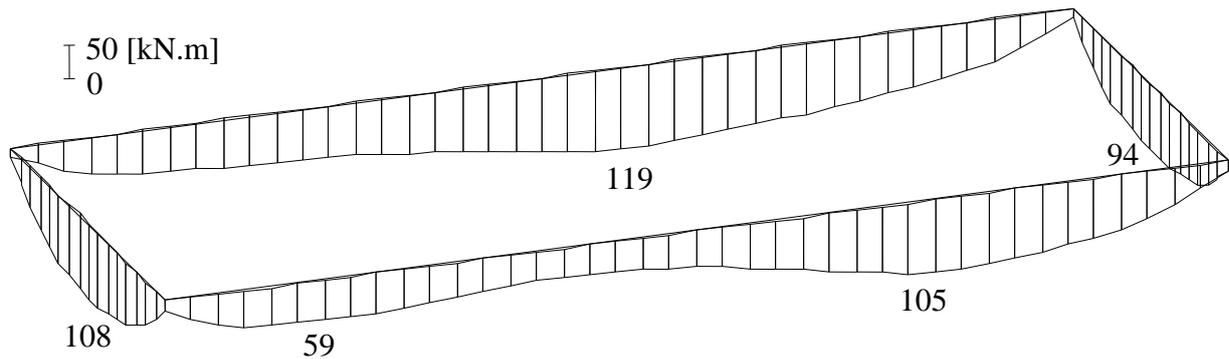
Figure 4.55   Beam-bending moments M_b [kN.m] at edge walls of the swimming pool
                Analysis without joint (case 4)
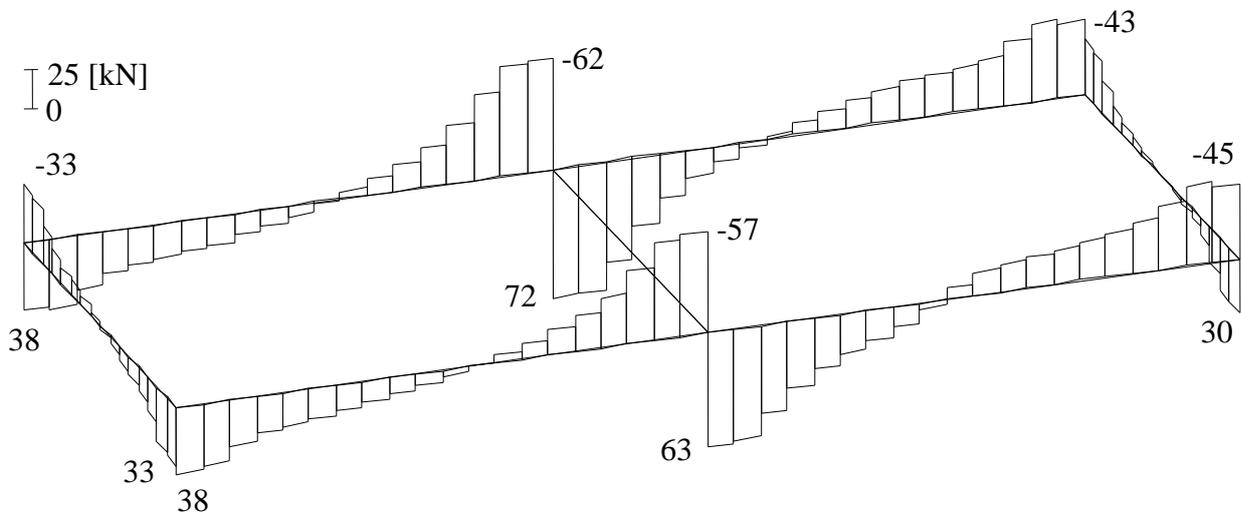
Figure 4.56   Beam-Shearing forces Q_s [kN] at edge walls of the swimming pool
                Analysis without interaction (case 1)
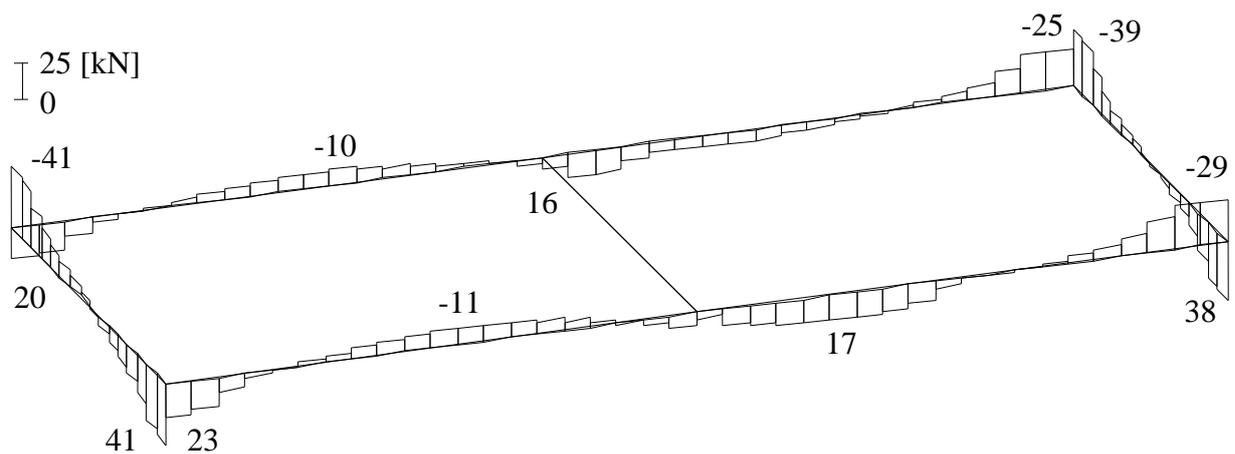
Figure 4.57   Beam-Shearing forces Q_s [kN] at edge walls of the swimming pool
   Analysis with interaction and without shearing forces (case 2)
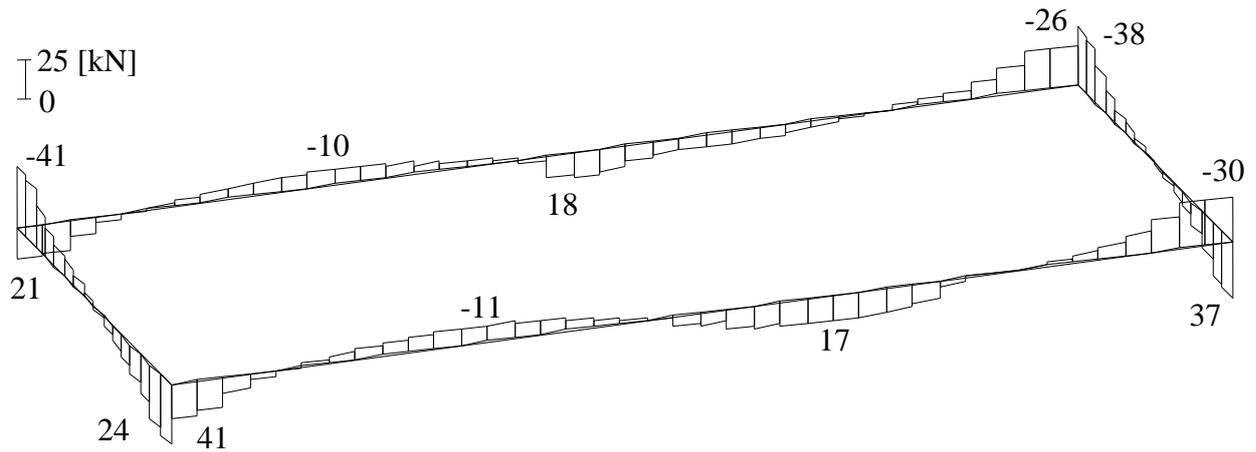
Figure 4.58   Beam-Shearing forces Q_s [kN] at edge walls of the swimming pool
Analysis with interaction and with shearing forces (case 3)
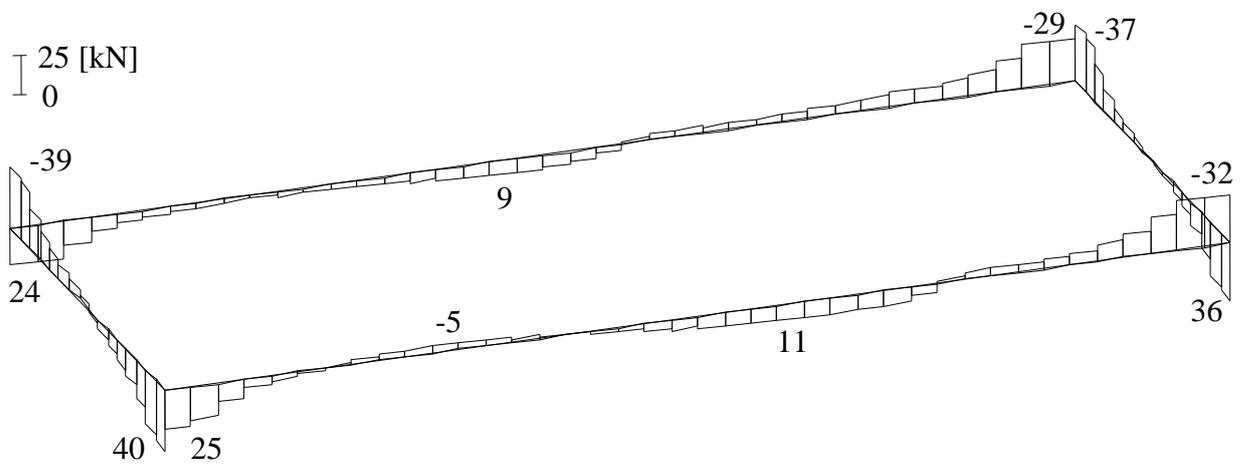
Figure 4.59   Beam-Shearing forces Q_s [kN] at edge walls of the swimming pool
Analysis without joint (case 4)
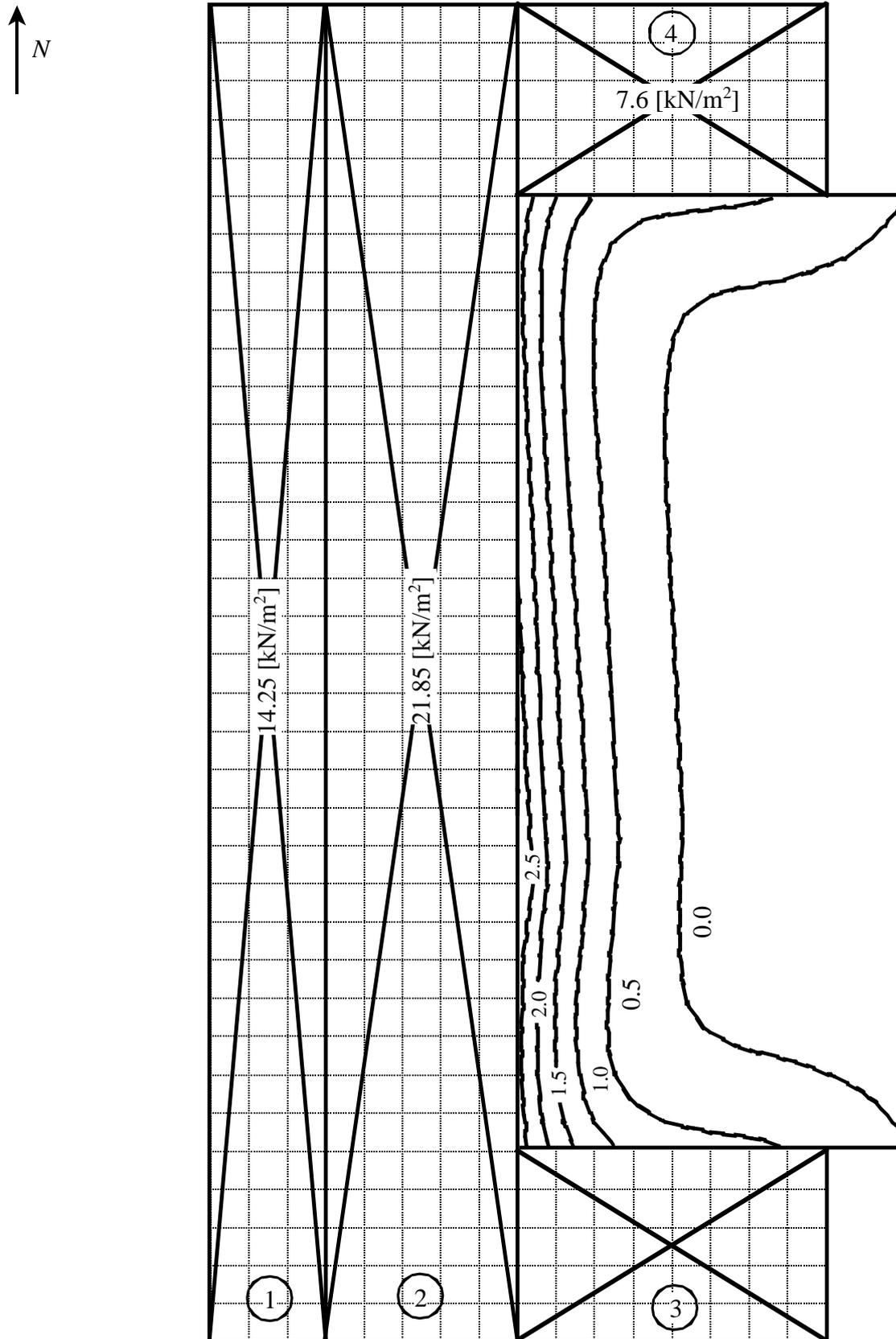
Figure 4.60   Contour lines of settlements under the swimming pool
               due to the filling around it
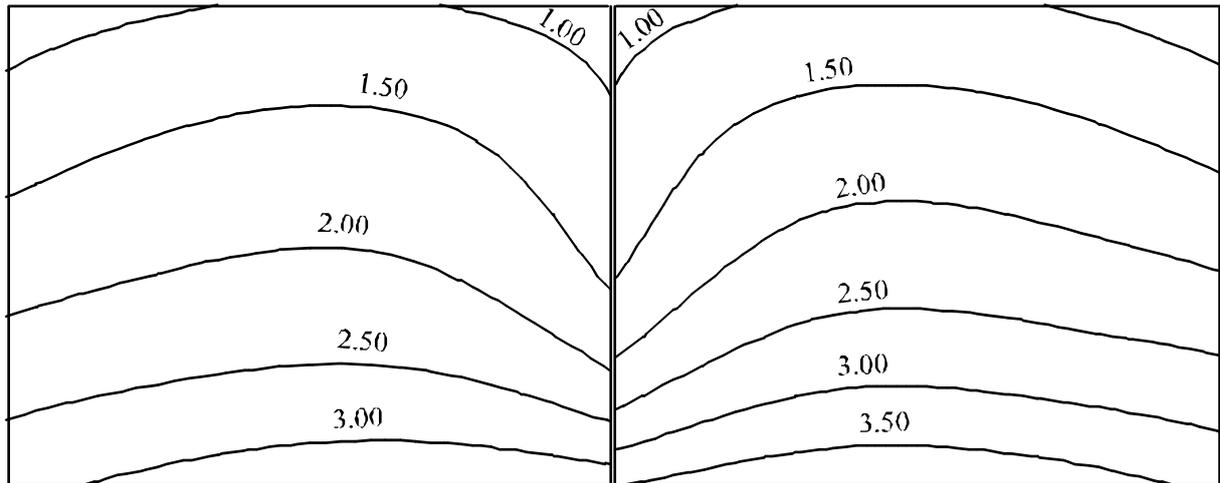
Figure 4.61   Contour lines of settlements s [cm]
               Analysis without interaction (case 1)
               With influence of surrounding loading
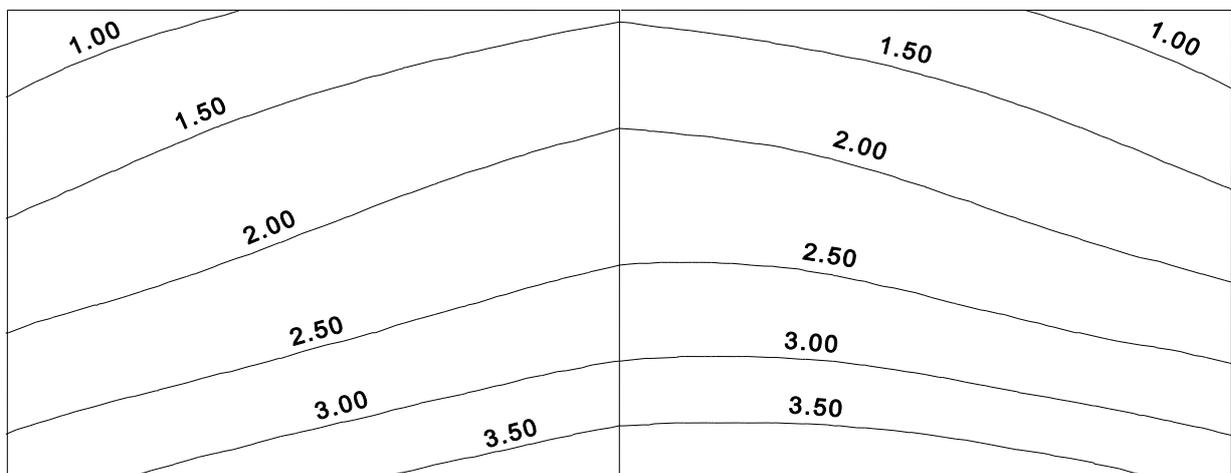
Figure 4.62   Contour lines of settlements s [cm]
               Analysis with interaction and without shearing forces (case 2)
               With influence of surrounding loading
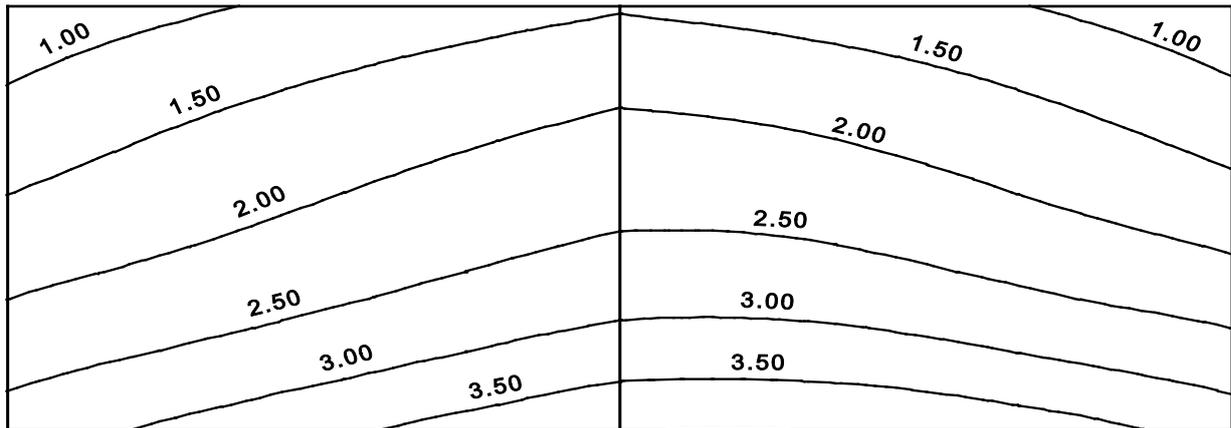
Figure 4.63   Contour lines of settlements *s* [cm]
               Analysis with interaction and with shearing forces (case 3)
               With influence of surrounding loading
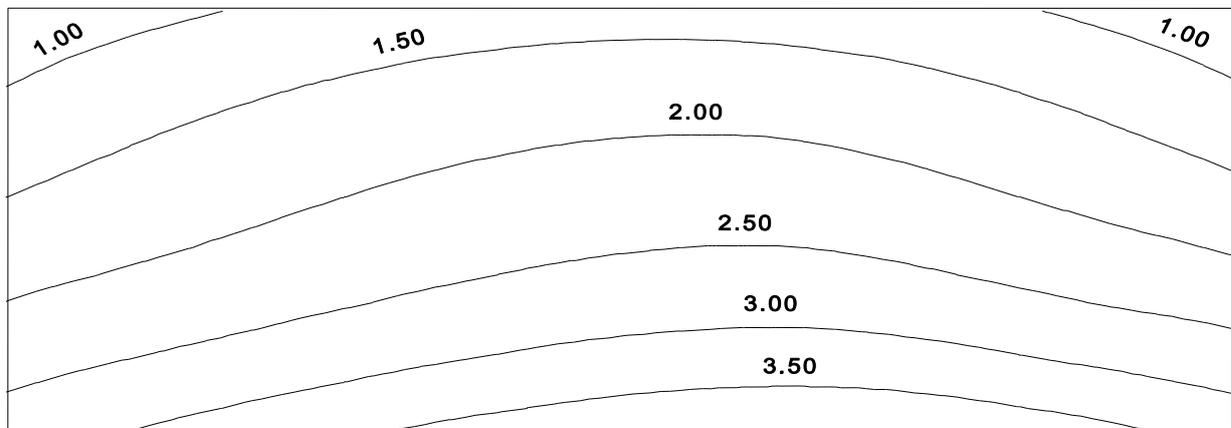
Figure 4.64   Contour lines of settlements *s* [cm]
               Analysis without joint (case 4)
               With influence of surrounding loading

Chapter 5

Foundation Rigidity

Contents

5.1   Introduction

The foundation is considered as rigid, elastic or flexible, depending on the ratio between the rigidity of the foundation and the soil. The oldest work for the analysis of foundation rigidity is that of *Borowicka* (1939). He analyzed the problem of distribution of contact stress under uniformly loaded strip and circular rigid foundations resting on semi-infinite elastic mass. The analysis showed that the distribution of contact stress, which is dependent on the relative stiffness of the soil-foundation system, k_B, is defined by

$$k_B = \frac{1}{6}\left(\frac{1-v_s^2}{1-v_b^2}\right)\left(\frac{E_b}{E_s}\right)\left(\frac{d}{b}\right)^3 \tag{5.1}$$

where:

v_b	*Poisson*'s ratios for foundation material	[-]
v_s	*Poisson*'s ratios for soil	[-]
E_b	*Young*'s modulus of foundation material	[kN/m^2]
E_s	Modulus of elasticity of the soil	[kN/m^2]
b	Half-width of the strip foundation or radius of the circular foundation	[m]
d	Thickness of foundation	[m]

$k_B = 0$ indicates a perfectly flexible foundation and $k_B = \infty$ means a perfectly rigid foundation.

After *Borowicka*'s analysis, many authors introduced formulae to find the foundation rigidity for plates resting on different subsoil models. For examples, *Gorbunov/ Posadov* (1959) introduced a formula for an elastic solid medium. *Cheung/ Zienkiewicz* (1965) introduced formulae for *Winkler* springs and isotropic elastic half-space model. *Vlazov/ Leontiv* (1966) introduced a formula for a two-parameter elastic medium. A good review for those formulae may be found in *Selvadurai* (1979).

Lately, based on great number of comparative computations for the modulus of compressibility method, *Graßhoff* (1987) proposed various degrees of system rigidity between foundation and the soil until case of practical rigidity using Equation 5.2. The equation is still used in many national standard specifications such as German standard (DIN 4018) and Egyptian Code of Practice (ECP 196-1995)

$$k_{st} = \frac{E_b}{E_s}\left(\frac{d}{l}\right)^3 \tag{5.2}$$

where:

E_b	*Young*'s modulus of the foundation material	[kN/m^2]
E_s	Modulus of elasticity of the soil	[kN/m^2]
d	Foundation thickness	[m]
l	Foundation length	[m]

$k_{st} \geq 2$ indicates a very rigid foundation, $k_{st} \leq 0.005$ indicates a flexible foundation and $0.005 < k_{st} > 2$ indicates a semi rigid foundation according to the Egyptian code of practice (ECP). While $k_{st} = 1$ indicates a rigid foundation, $k_{st} = 0.1$ indicates stiff foundation and $k_{st} = 0.01$ indicates flexible foundation according to *Graßhoff* (1987).

It is noticed, that most of the available formulae used to determine the foundation rigidity assume that the footings or rafts have regular shape, supporting simple load geometry. Besides the soil model is an isotropic elastic half-space soil model or soil model of a homogenous layer. This means that the practical application of those formulae is limited to certain problems. Figure 5.1 shows some practical problems where the use of traditional formulae may be not applicable for the analysis of foundation rigidity. Furthermore, the use of traditional formulae may be not acceptable if nonlinear analysis of the soil is considered, or if external influences such as the effect of tunneling, neighboring foundations are expected.

It is found that the foundation rigidity depends on the depth of the soil layers and their elastic properties, foundation geometry, foundation material, foundation thickness and the distribution of loading.

Recently, *El Gendy* (1998) and (1999) proposed accurate analysis to find the foundation rigidity, which can consider all the above factors. This analysis offers the possibility to find the rigidity of rafts having any shape considering holes, re-enter corners, variable thickness with different loading types and geometry and resting on irregular subsoil layers. The analysis deals with each foundation as an independent problem, in which two solutions are carried out, full flexible and full rigid, besides the elastic solution. Through those solutions, the system rigidity of foundation for any practical problem on a real subsoil model can be obtained for high accuracy. This analysis is described in the following section.


a) Foundation on irregular subsoil   b) Grid foundation or foundation with opening

c) Foundation with variable thickness   d) Ribbed foundation
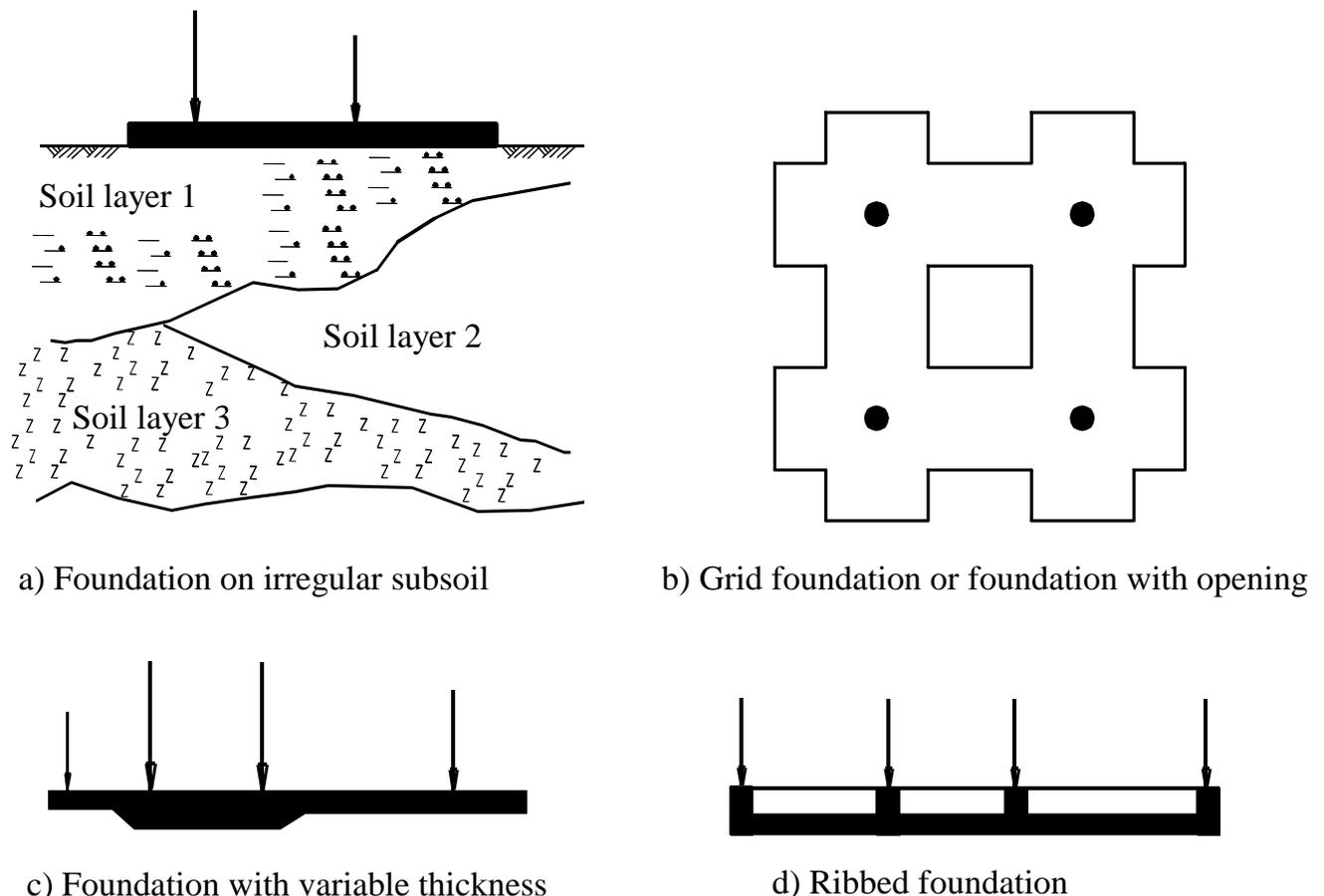
Figure 5.1   Some practical examples where traditioal formulae may be not applicable

5.2   Determination of foundation rigidity

Today, the finite element method is the most powerful procedure. It can be applied to nearly all engineering problems. In spite of the successful using of the finite element method in the analysis of foundations, it may cause numerical problems during the solution of the system of linear equations if the foundation is rigid enough. It can be drawn in this problem that the foundation (if it is sufficiently thick and without eccentricity about both axes) will be far stiffer than the soil, so the displacements beneath the foundation will mostly be the same at all points. Here, assuming the foundation is perfectly rigid is reasonable. Accordingly, the two solutions, full flexible and full rigid, besides the elastic solution by finite element method are used to estimate the foundation rigidity or the rigid thickness of the foundation.

5.2.1   Flexible solution

This solution represents a foundation with zero [%] degree of system rigidity. If the foundation is perfectly flexible (such as an embankment), then the contact stress will be equal to the gravity stress exerted by the foundation on the underlying soil.

For the set of grid points of the foundation, the soil settlements are given by

$$\{s\} = [c]\{Q\} \tag{5.3}$$

where:
$\{s\}$ Vector of soil settlements
$[c]$ Flexibility matrix of the soil
$\{Q\}$ Vector of contact forces

5.2.2   Rigid solution

This solution represents a foundation that has 100 [%] degree of system rigidity. If the foundation is completely rigid, two forms for foundation settlement are expected:

i)   If the foundation is subjected to a centric load, all points on the foundation will settle the same value w_o

ii)   If the foundation is subjected to an eccentric load, the foundation will rotate as a rigid body and there will be differential vertical movement between points on the foundation, but all points will remain in the same plane

For a completely unsymmetrical external loading, the unknowns of the interaction problem are the n contact pressures q_i, the rigid body translation of the foundation w_o and the rigid body rotations θ_{xo} and θ_{yo} of the foundation about the axes of the geometry centroid. Considering the n compatibility equations of rigid foundation translation and the settlement of subsoil at the n nodal points and the three equations of overall equilibrium gives the following equation

$$\{N\} = [X][k_s][X]^T \{\Delta\} \tag{5.4}$$

where:
$\{\Delta\}$ Vector of rigid body displacement w_o and the rigid body rotations θ_{xo} and θ_{yo} of the foundation
$[X]^T$ Coordinate matrix
$\{N\}$ Vector of the resultant forces and moments on the foundation
$[k_s]$ Soil stiffness matrix

5.2.3 Elastic solution

This solution represents a foundation with degree of system rigidity between > 0 [%] and < 100 [%]. The elastic solution considers the compatibility of deformations between the foundation and the soil medium. Here, the soil settlement s is equal to the foundation deflection w. The stiffness matrix of the whole foundation system is the sum of the foundation stiffness matrix $[k_p]$ and the soil stiffness $[k_s]$.

The following matrix equation expresses the equilibrium of the foundation-soil system

$$\left[[k_p] + [k_s] \right] \{\delta\} = \{P\} \tag{5.5}$$

where:
$\{P\}$ Vector of the known applied loads and moments on the foundation
$\{\delta\}$ Nodal displacements vector of the foundation. Each nodal displacement constitutes the foundation deflection w and the two rotations θ_x and θ_y about x- and y-axes, respectively

5.2.4 Parameter k_r

The main cofactor in Equations 5.3, 5.4 and 5.5 is the displacement w, which here is equal to the soil settlement s. Therefore, the definition of the rigid body movement is used to find the rigid thickness of the foundation. In fact, if the foundation is completely rigid, it will rotate as rigid body and it will be differential vertical movement between points on the foundation but all points will remain in the same plane. Therefore, Equation 5.4 gives easily the plan of translation, which can be defined only by three points. Consequently, the elastic settlements (= foundation deformations) of any three points on the foundation can define the whole foundation form if compared with those of rigid translations at the same three points.

The parameter k_r [%] at any three selected points at least on the foundation can be used to represent the foundation rigidity. This parameter is a function of the elastic settlement s and the rigid body translation w as given below

$$k_r = \left(1 - \frac{\Delta s_i}{w_i}\right) \times 100 \tag{5.6}$$

where:
s_i Settlement at point i
w_i Rigid body translation at point i
Δs_i Absolute difference between s_i and w_i at that point i

The foundation may be considered practically rigid at a thickness (or system rigidity) gives k_r more than 90 [%] for three selected points on it.

Example 5.1   Rigidity of a simple square raft

1   Description of problem

For comparison with complex foundation rigidity problems, no solution is yet available. Therefore, for judgment on the analysis of *El Gendy* (1998) to find the system rigidity of foundation, consider the simple example of raft foundation shown in Figure 5.2. The raft has dimensions of 12 [m] × 12 [m] and carries four symmetrical and equal loads, each of $P = 9000$ [kN]. The raft rests on a homogenous soil layer of thickness 20 [m]. *Young*'s modulus of the raft and soil materials is $E_b = 2 \times 10^7$ [kN/m^2] and $E_s = 10000$ [kN/m^2], respectively. *Poisson*'s ratio of the raft material is $v_b = 0.15$.
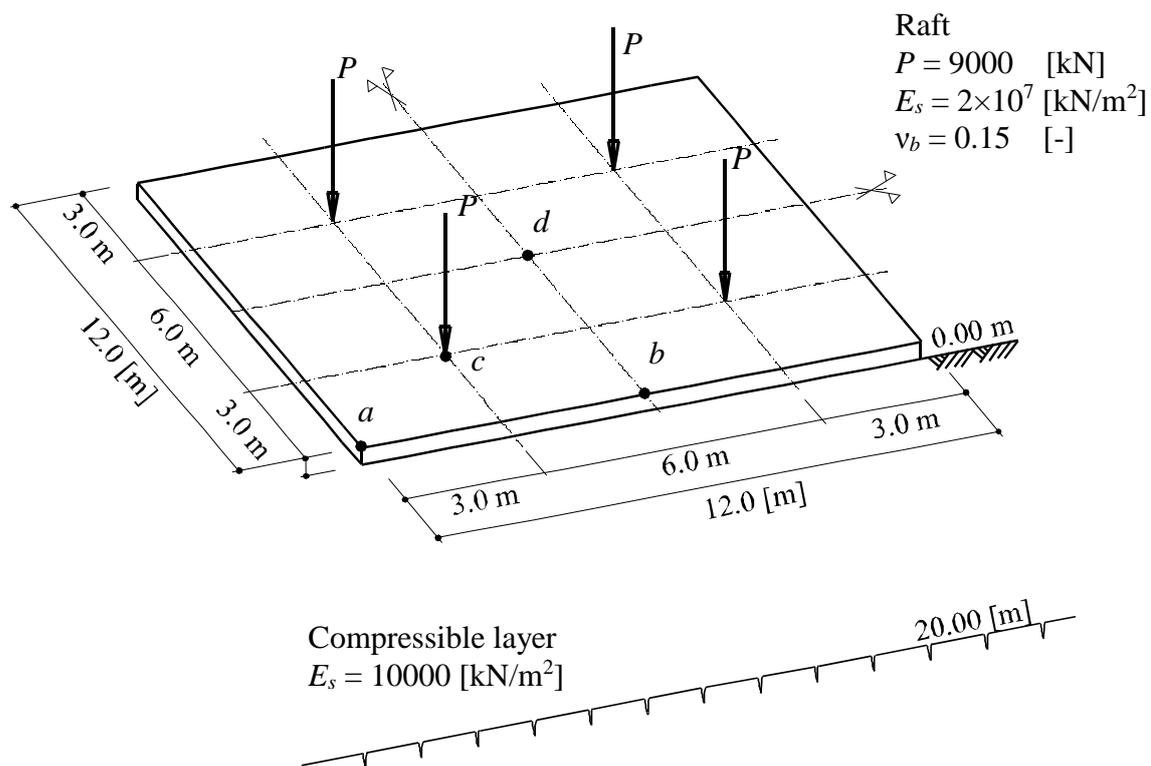
Figure 5.2   Raft dimensions, loads and subsoil

*Deninge*r (1964) studied the same example using the finite difference method by dividing the raft into 6 × 6 elements. Each element has dimensions of 2 [m] × 2 [m]. He examined the raft thickness for several values of 0.4, 0.5, 0.6, 0.8 and 2 [m].

The moment at any point on the raft foundation depends on the system rigidity of the foundation, external load values and load distributions. So, the moment m_x at the position of the concentrated load, independent of rigidity formulae, can be used to find the rigid thickness of the raft in this example. Here, the raft is considered rigid at a thickness gives moment m_x more than 90 [%] of the maximum moment that can occur at that point.

The raft in this example is considered rigid for thickness more than 0.85 [m] according to *Deninger*'s analysis. An application for Equation 5.2 to this example gives a system rigidity $k_{st} = 0.71$. So, the raft is considered very stiff according to system rigidity of *Graßhoff* (1987).

2   Analysis and discussion

Series of computations using the finite element method for several values of raft thickness are carried out. The moments and the settlements at some selected points are plotted against the raft thickness to describe the foundation rigidity.

First, the raft is subdivided first into 24×24 square elements. Each element has dimensions of 0.5 [m] $\times$ 0.5 [m]. Then, it is subdivided into 12×12 square elements. Each element has dimensions of 1 [m] $\times$ 1 [m] as shown in Figure 5.3. Taking advantage of the symmetry in shape, soil and load geometry about x- and y-axes, the analysis is carried out only for a quarter of the raft.
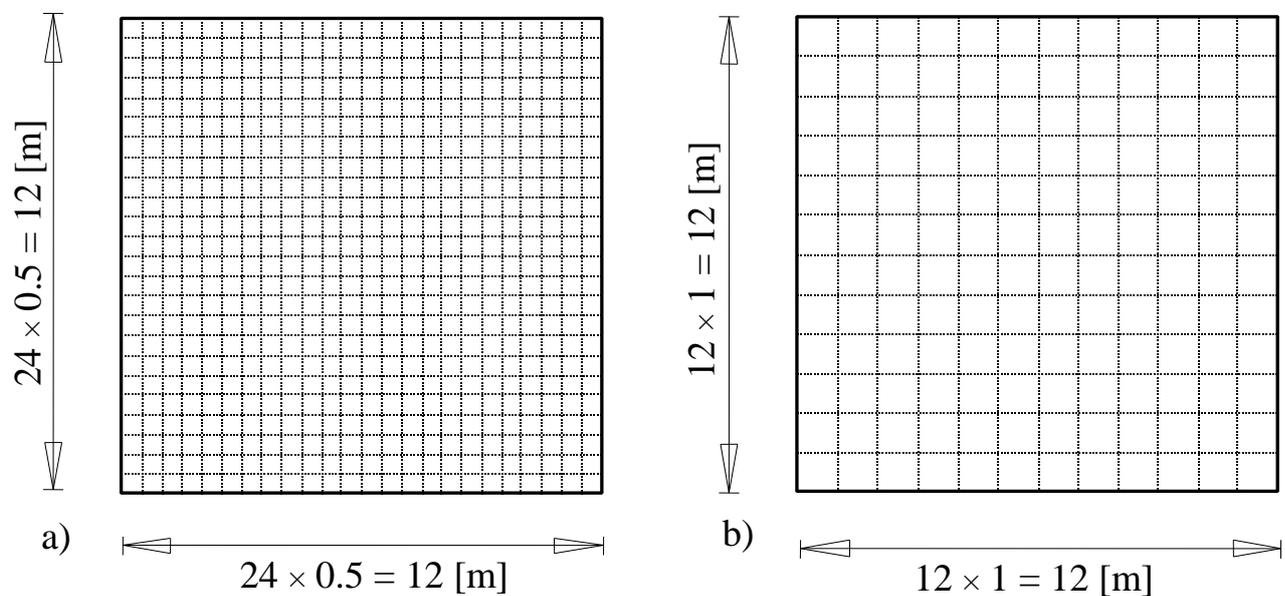
Figure 5.3   Finite element meshes of the raft

To show the convergence of the solution by finite element method and to verify the rigid thickness of the raft, the settlement s, at four characteristic points a, b, c and d on the raft and the rigid body translation w_o when the raft is perfectly rigid, are plotted against the raft thickness in Figure 5.4 and 5.5. In which

Point a Corner point of the raft
Point b Middle point of the raft edge
Point c Point under the load position
Point d Center point of the raft

Raft thickness d [m]
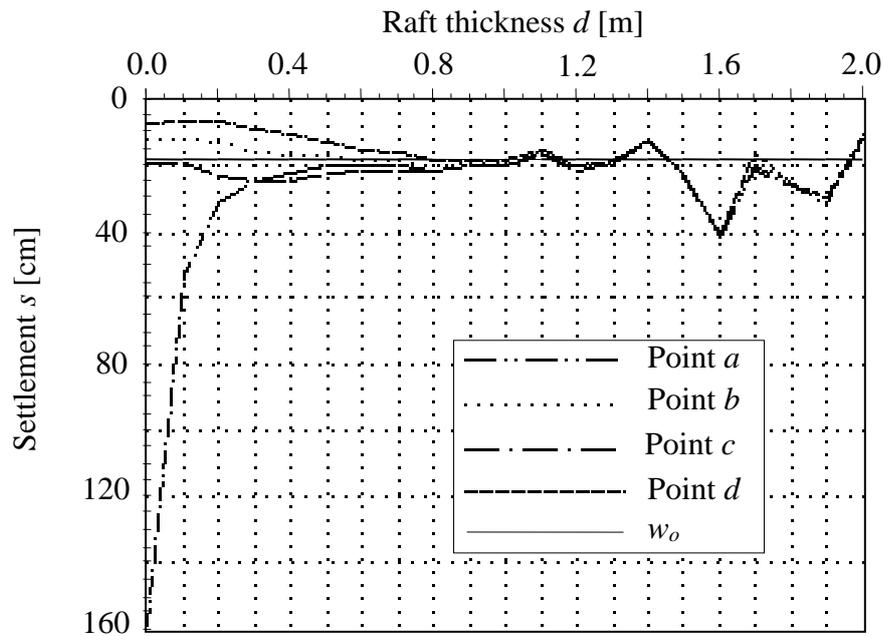
Figure 5.4   Settlement at the four characteristic points using a mesh of 24×24 elements

Raft thickness d [m]
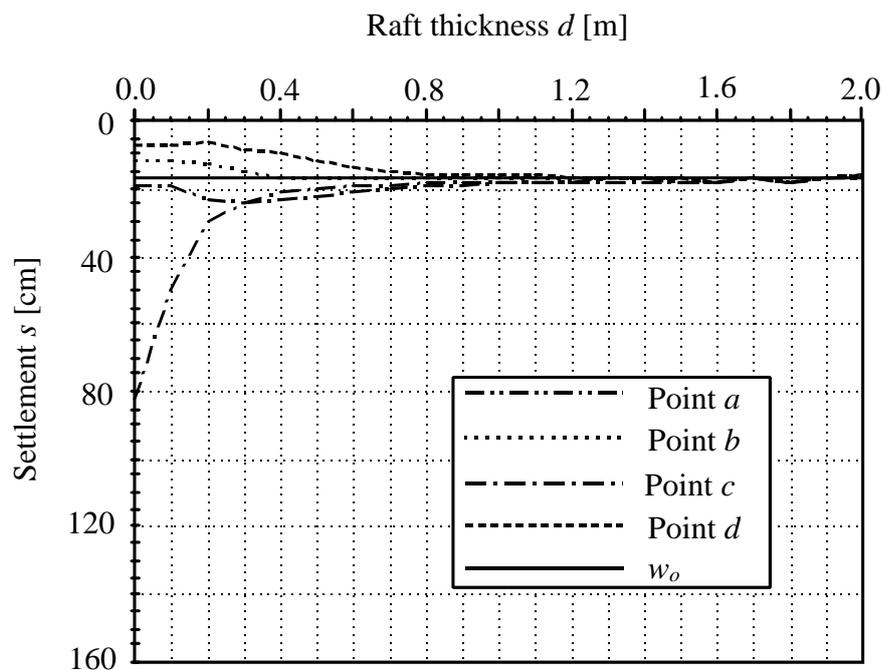
Figure 5.5   Settlement at the four characteristic points using a mesh of 12×12 elements

Figure 5.6 shows the moment m_x at point c under the concentrated load position using finite element mesh of 24×24 elements and 12×12 [m] elements, respectively.
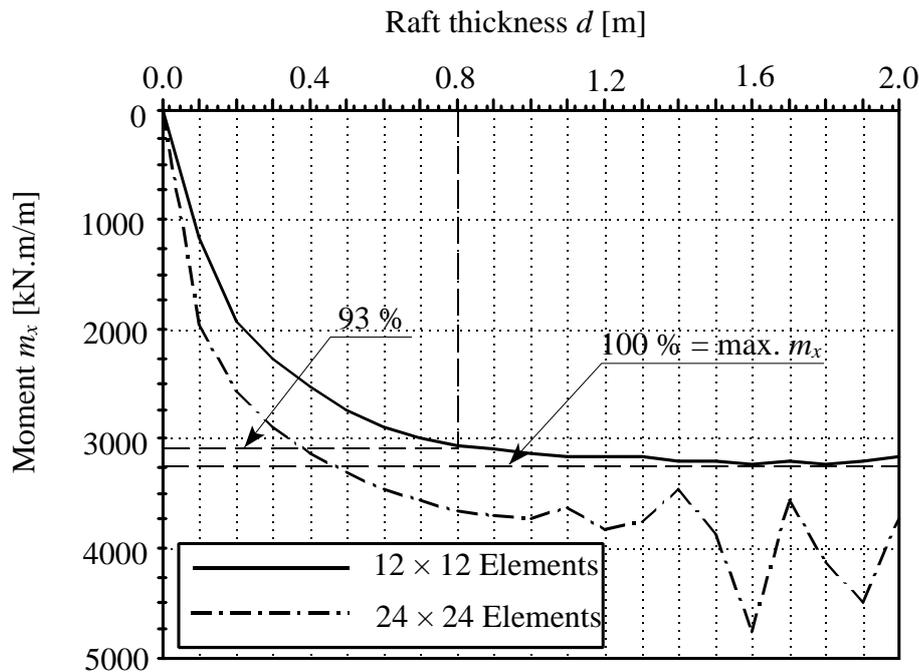
Raft thickness *d* [m]

Figure 5.6   Moment m_x at characteristic point *c*

Figure 5.4 indicates that, if a fine mesh of 24 × 24 elements is used, the solution for the raft thickness far 0.8 [m] will become divergence. In which no stability in the overall matrix occurs. As a result, if the foundation is rigid enough, the raft rotations will approach to zero and the raft will settle the same value of a displacement w_o. Therefore, the number of equations becomes greater than the number of unknowns. Another problem may be found that the relation between the plate element thickness and element size is limited by application of the finite element method using plate-bending elements.

Figure 5.5 shows that using a mesh of 12 × 12 elements gives good results. A comparison between Figure 5.4 and 5.5 indicates that, although the solution by using a fine mesh of 12 × 12 elements is divergence, the rigid thickness of the raft can be determined because the limit of rigid translation is known from the rigid solution.

Figure 5.6 shows that *Deninger*'s analysis cannot be used in case of using a fine mesh of 24 × 24 elements, to find the rigid thickness of the raft where the position of maximum moment at point *c* is not clear in the figure. Further, for a raft with complex load geometry or types, using this analysis is not practical, which represents the rigidity of the foundation only at the selected point.

Figure 5.7 shows the parameter k_r for the four characteristic points *a*, *b*, *c* and *d* of the raft. Figure 5.8 shows the parameter k_r for the same characteristic points if a uniform load of 250 [kN/m^2] replaces the external concentrated loads on the raft, which is equal to the average contact pressure, using also mesh of 12 × 12 elements.

The raft may be considered as rigid at thickness gives k_r more than 90 [%] for all characteristic points.

From Figure 5.7, the raft is considered rigid for thickness more than 0.80 [m]. The moment for this thickness m_x is 93 [%] from maximum moment at point c. This thickness also is different from that of *Deninger* (1964) by 5.6 [%] and makes the raft very stiff according to *Graßhoff* (1987).

According to this analysis, Figure 5.8 shows that the raft is considered rigid for thickness more than 0.7 [m] when it carries a uniform load of 250 [kN/m²]. This means that the type of loading has influence on the raft rigidity. Although the solution in this example is reported for a square raft, the approach can be also considered applicable for general problems.
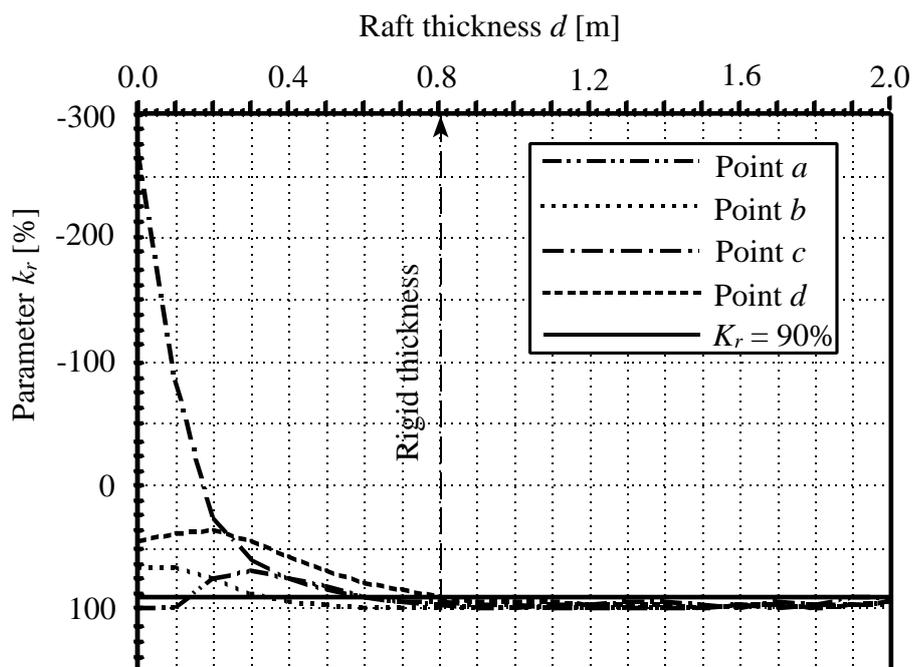
Figure 5.7   Parameter k_r for the characteristic points (raft carries concentrated loads)
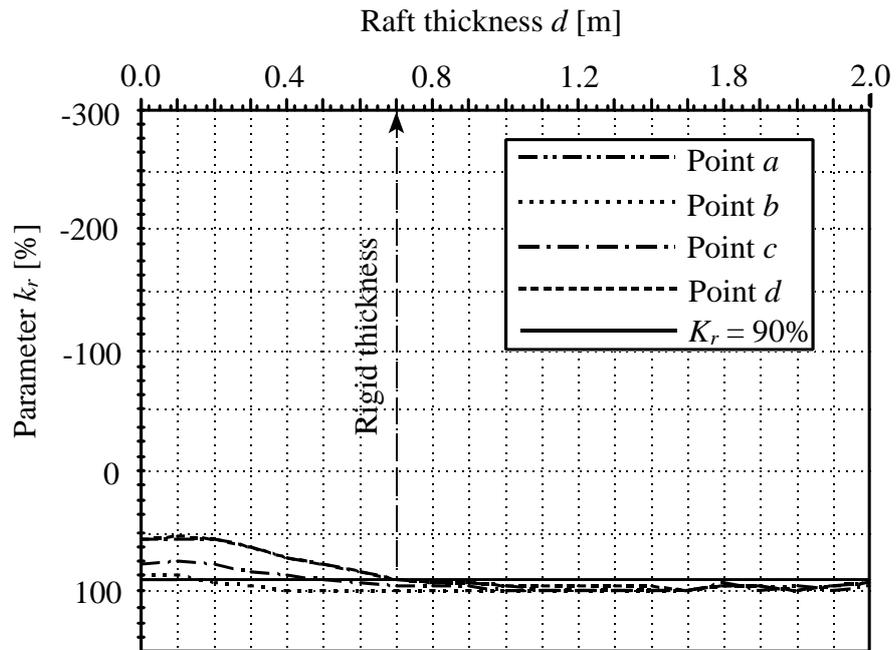
Figure 5.8   Parameter k_r for the characteristic points (raft carries a uniform load)

Example 5.2   Rigidity of irregular raft on irregular subsoil

1   Description of problem

A general numerical example is carried out to show the applicability of system rigidity analysis, proposed by *El Gendy* (1998), to find the rigid thickness of rafts of any shape considering re-entrant corner and opening within the rafts.

In one case the raft carries many types of external loads; concentrated loads, distributed load, line load and moments in *x*- and *y*-direction as shown in Figure 5.9. The raft parameters are *Young*'s modulus $E_b = 2 \times 107$ [kN/m2] and *Poisson*'s ratio $v_b = 0.25$. Level of foundation is $d_f = 2.7$ [m].
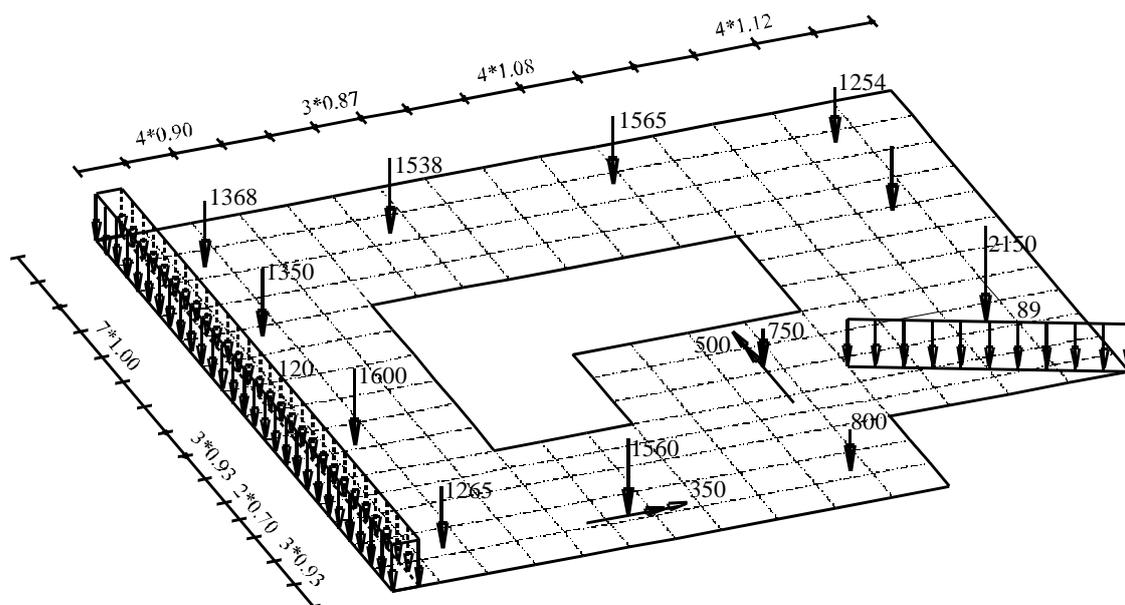
Figure 5.9   Raft dimensions, loads

The subsoil under the raft is characterized by three boring logs. Each has three layers with different materials. The moduli of compressibility of the three layers for loading are $E_{s1} = 9500$ [kN/m^2], $E_{s2} = 22000$ [kN/m^2] and $E_{s3} = 120000$ [kN/m^2] while for reloading are $W_{s1} = 26000$ [kN/m^2], $W_{s2} = 52000$ [kN/m^2] and $W_{s3} = 220000$ [kN/m^2]. *Poisson*'s ratio is assumed 0.3 and constant for all soil layers. The effect of reloading and water pressure is taken into account. Boring logs and locations are shown in Figure 5.10.

2   Analysis and discussion

The available solution from *Kany/ El Gendy* (1995) for the analysis of raft foundations on three-dimensional subsoil model using interpolation method is used here in the analysis of this general example. Four points on the raft are chosen to estimate the parameter k_r, which represent the whole foundation rigidity as shown in Figure 5.10a. Figure 5.11 shows the parameter k_r for these points. It can be seen that the raft is considered rigid for a thickness more than 1.01 [m].
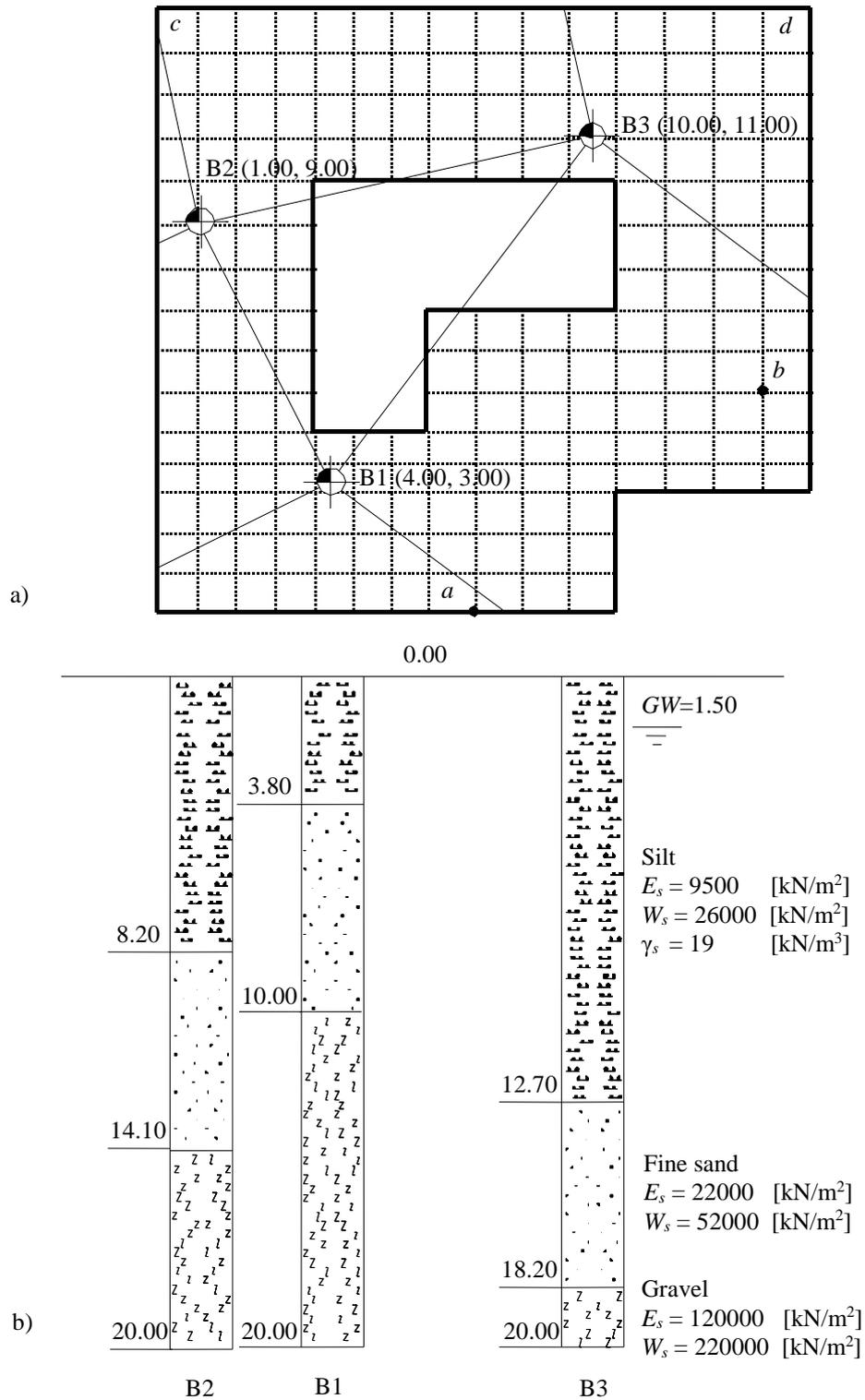
Figure 5.10   a) Boring locations and interpolation regions
               b) Boring logs B1 to B3
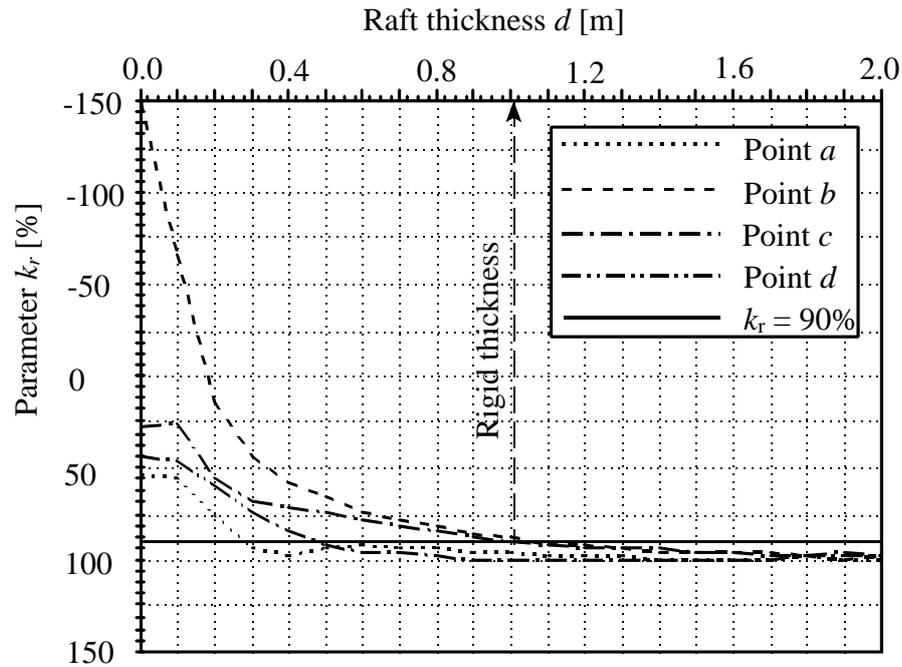
Raft thickness d [m]

Figure 5.11   Parameter k_r for the characteristic points a, b, c and d

Another parameter k'_r similar to k_r is obtained from the contact pressure shape. This parameter is plotted against raft thickness and for the 4 points in Figure 5.12. In which k'_r is given by

$$k'_r = \left(1 - \frac{\Delta q_i}{g_i}\right) \times 100 \qquad (5.7)$$

where:
q_i Contact pressure from elastic analysis at point i
g_i Contact pressure from rigid analysis at point i
Δq_i Absolute difference between q_i and g_i at that point i

Although Figure 5.12 gives a rigid thickness more than 1.05 [m] nearly as the same as that of Figure 5.11, but it is recommended to use k_r in which the rigid movement plane can be described only by three points.

To check the validity of the analysis for this example, the moments m_x and m_y at point b are plotted against raft thickness in Figure 5.13. The moments at a raft thickness of 1.01 [m] are compared with the maximum moments that may occur at that point. It is found that both moments m_x and m_y check closely, where the value of m_x is 92 [%] from maximum m_x while the value of m_y is equal to 95 [%] at the same point.

Although the raft in this example has a constant thickness, but it can determine the foundation rigidity when the thickness is variable. In this case, the rigidity of the foundation may be determined through plotting the parameter k_r against *Young*'s modulus of elasticity of the raft material E_b at several values of E_b.

Raft thickness d [m]
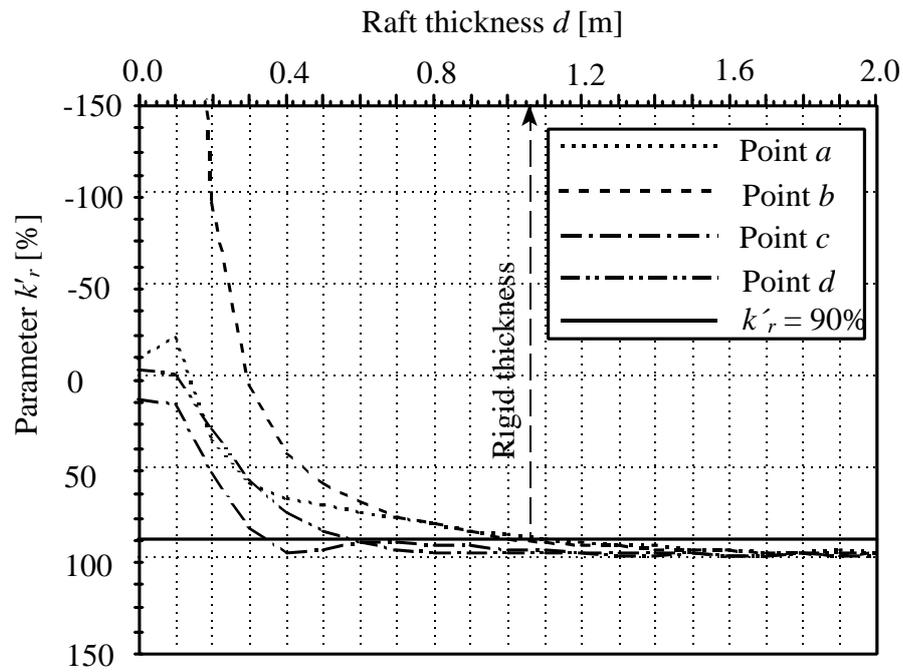
Figure 5.12   Parameter k'_r for the characteristic points a, b, c and d

Raft thickness d [m]
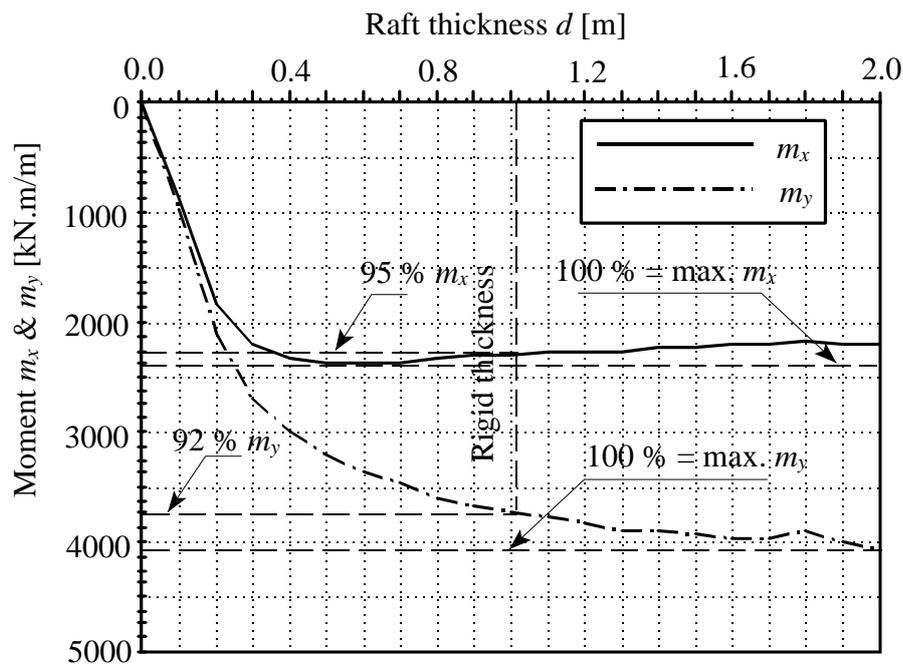
Figure 5.13   Moment m_x and m_y at characteristic point b

Chapter 6

Effect of Superstructure Rigidity on Foundation

Contents

6.1   Introduction

The presence of the structure on compressible subsoil causes settlements for the foundation and also for the structure itself. Values of settlements and settlement differences depend not only on the thickness of the compressible soil layer under the foundation, the value and distribution of structure loads, the foundation depth and contact pressure under the foundations but also on the flexural rigidity of the structure.

One of the properties with a considerable influence on the development of settlement is the rigidity of the superstructure. The more rigid structure has more uniform settlement and conversely, structure that is more flexible has greatest difference in settlement. The entire structure can be defined as the three media: superstructure, foundation and soil. The analysis of the entire structure as one unit is very important to find the deformations and internal forces. However, most of the practical analyses of structures neglect the interaction among the three media to avoid the three-dimensional analysis and modeling. The structure is designed on the assumption of non displaceable supports while the foundation is designed on the assumption that there is no connection between columns. Such accurate analysis of the entire structure is extremely complex.

The early studies for consideration the effect of the superstructure were by *Meyerhof* (1953) who suggested an approximate method to evaluate the equivalent stiffness that includes the combined effect of the superstructure and the strip beam foundation. *Kany* (1959) gave the flexural rigidity of a multi-storey frame structure by an empirical formulae. Also, *Kany* (1977) analyzed the structure with foundation using a direct method. *Demeneghi* (1981) used the stiffness method in the structural analysis. *Panayotounakos/ Spyropoulos/ Prassianakis* (1987) presented an exact matrix solution for the static analysis of a multi-storey and multi-column rectangular plexus frame on an elastic foundation in the most general case of response and loading.

At the analysis of foundations with considering the superstructure stiffness, it is required to distinguish between the analysis for plane structures (two-dimensional analysis) and that for space structures (three-dimensional analysis). Further, it is required to distinguish between approximation methods with closed form equations (*Kany* (1974), *Meyerhof* (1953), *Sommer* (1972)) and refined methods such as conventional plane or space frame analysis (*Kany* (1976)), Finite Elements (*Meyer* (1977), *Ellner/ Kany* (1976), *Zilch* (1993), *Kany/ El Gendy* (2000)) or Finite Differences (*Bowles* (1974), *Deninger* (1964)).

In addition, many analytical methods are reported for analysis of the entire structure as one unit by using the finite element. For examples:

Haddadin (1971) presented an explicit program for the analysis of the raft on *Winkler*'s foundation including the effects of superstructure rigidity.

Lee/ Brown (1972) analyzed a plane frame on a two-dimensional foundation.

Hain/ Lee (1974) employed the finite element method to analyze the flexural behavior of a flexible raft foundation taking into account stiffness effect of a framed superstructure. They proposed the use of substructure techniques with finite element formulation to model space frame raft soil systems. The supporting soil was represented by either of two types of soil models (*Winkler* and half space models).

Poulos (1975) formulated the interaction of superstructure and foundation by two sets of equations. The first set links the behavior of the structure and foundation in terms of the applied structural loads and the unknown foundation reactions. The second set links the behavior of the foundation and underlying soil in terms of the unknown foundation reactions.

Mikhaiel (1978) considered the effect of shear walls and floors rigidity on the foundation.

Bobe/ Hertwig/ Seiffert (1981) considered the plastic behavior of the soil with the effect of superstructure.

Lopes/ Gusmao (1991) analyzed the symmetrical vertical loading with the effect of the superstructure.

Jessberger/ Yuan/ Thaher/ Ming bao (1992) considered the effect of the superstructure in case of raft foundation on a group of piles.

Zilch (1993) proposed a method for interaction of superstructure and foundation via iteration.

Kany/ El Gendy (2000) proposed an iterative procedure to consider the effect of superstructure rigidity on the foundation. In the procedure, the stiffness of any substructure such as floor slab or foundation, connected by the columns can be represented by equivalent spring constants due to forces and moments at the connection nodes. Consequently the stiffness matrices of the slab floors, columns and foundation remain unaffected during the iteration process.

6.2   Simplified modeling of superstructure foundation soil system
6.2.1   Rigidity of the structure

Sometimes at the analysis of shallow foundations, examining the influence of the structure rigidity is imperative. Two rigidities concerning the rigidity of the structure are required to be computed. The first rigidity is the flexural rigidity of the structure that is independent of the deformation behavior of the subsoil. The second one is the system rigidity that expresses the ratio of the flexural rigidity of the structure to the stiffness of the subsoil.

In the analysis scope of shallow foundations, the following questions are required to be answered:

-        How flexural rigidity and system rigidity in a specific case are computed?
-        At which value of the system rigidity a structure can be described as practically rigid?
-        What is the influence of the flexural rigidity of the structure on the analysis results?

The presence of the superstructure on the foundation causes besides the stiffness of the foundation alone further stiffness on the system. This influence is great, when the ratio of the flexural rigidity of a structure to that of the foundation is great.

The flexural rigidities of the superstructure and foundation elements and the stiffness of the subsoil have been identified by many authors (*Brown/ Yu* (1986), *Lee/ Harrison* (1970) and *Meyerhof* (1953)). The absolute stiffness of superstructure K_B [kNm^2], foundation K_G [kNm^2] and subsoil K_s [kNm^2] or K_c [kNm^2] can be obtained as it is described in the following section.

6.2.1.1 Flexural rigidity of the superstructure

The flexural rigidity of the superstructure K_B [kNm^2] is expressed through the product of modulus of elasticity E_B [kN/m^2] of the superstructure material and the ideal moment of inertia I_B [m^4] of the entire superstructure system

$$K_B = E_B \, I_B \tag{6.1}$$

According to *Meyerhof* (1953), the flexural rigidity of the multi-storey superstructure composed of slabs and columns (or walls) running in the longitudinal direction of the bending axis can be obtained approximately as follows (Figure 6.1)
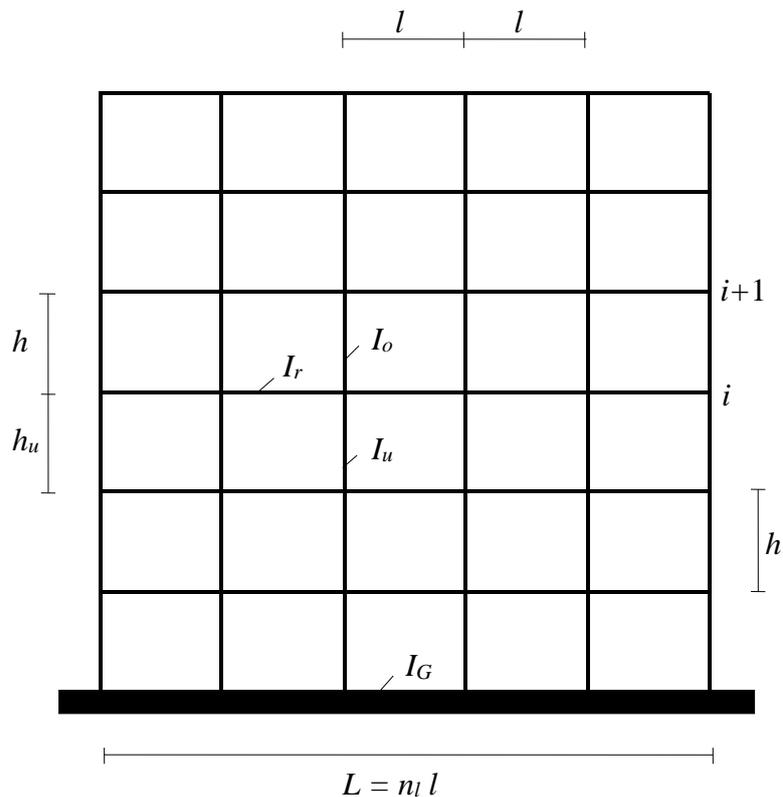
Figure 6.1   Details of multi-storey frame with foundation (*Meyerhof*'s formulae)

i)   The superstructure is open frame

In any storey *i* of an open multi-storey building frame with approximately equal bays, the flexural rigidity is given by

$$E_B \, I_i = E_B \, I_r \left\{ 1 + \left(\frac{K_u + K_o}{K_r + K_u + K_o} \right) \left(\frac{L^2}{l^2} \right) \right\} \tag{6.2}$$

where:

n_s	Total number of storeys	
L	Total length of the superstructure ($= n_s\, l$)	[m]
$K_r = I_r/l$	Average stiffness of floor	[m³]
I_r	Moment of inertia of floor	[m⁴]
l	Length of bay or floor beam	[m]
$K_u = I_u/h_u$	Average stiffness of lower columns	[m³]
I_u	Moment of inertia of lower columns	[m⁴]
h_u	Height of storey under the floor	[m]
$K_o = I_o/h_o$	Average stiffness of upper columns	[m³]
I_o	Moment of inertia of upper columns	[m⁴]
h_o	Height of storey upper the floor	[m]
I_i	Average moment of inertia of the storey i	[m⁴]

The total stiffness of the entire superstructure is then given by

$$K_B = E_B\, I_B = \sum_{i=1}^{n_s} E_B\, I_i \qquad\qquad (6.3)$$

ii)   The superstructure is an open frame with wall cladding

External building frames are generally stiffer than indicated above due to wall cladding. In this case the frame consists of solid panels between the beams and columns and only shearing stress can be transmitted from the frame to the panels. Therefore, in any storey i the flexural rigidity of Equation 6.2 is increased further as

$$K_B = E_B\, I_B = E_B\, I_i + \frac{E_f\, I_f\, L^2}{2\, h^2} \qquad\qquad (6.4)$$

where:

$E_f\, I_f = E_f\, t_w\, h^3/12$	Flexural rigidity of the panel (in vertical plane)	[kNm³]
I_f	Moment of inertia of wall	[m⁴]
E_f	Modulus of elasticity of the wall material	[kN/m²]
t_w	Wall thickness	[m]
h	Wall height	[m]

iii)   The superstructure is constructed as a deep beam

If the wall cladding is fully continuous so that the whole frame behaves like a solid deep beam, the flexural rigidity of the frame itself can frequently be ignored compared with that of the wall. Therefore, the flexural rigidity of the superstructure can be approximately obtained from

$$K_B = E_B\, I_B = \frac{E_B\, t_w\, H^3}{12} \qquad\qquad (6.5)$$

where:

H Height of wall or superstructure   [m]

With sufficiently great number of bays n_l, the following approximation Equation 6.6 for estimating the flexural rigidity of multi-storey open frames without wall cladding can be used

$$E_B\, I_B \approx E_B\, I_r\, n_s\, n_l^{\,2}\, \frac{2\,K_s}{K_r + 2\,K_s}$$

(6.6)

where:
$K_s = I_s/h$ Average stiffness of upper and lower columns   [m^3]
I_s Average moment of inertia of upper and lower columns   [m^4]

Equation 4.6 is derived from Equation 4.2,
when $K_s \approx K_u \approx K_o = $ constant and $n_l^2\, 2K_s/(K_r + 2K_s) \gg 1$

6.2.1.2 Flexural rigidity of the foundation

The flexural rigidity K_G [kNm^2] of a foundation of width B [m] and thickness d [m] is given by

$$K_G = E_G\, I_G = \frac{E_G\, B\, d^3}{12}$$

(6.7)

where:
I_G Moment of inertia of foundation   [m^4]
E_G Modulus of elasticity of the foundation material   [kN/m²]

Now, the total flexural rigidity of the entire structure $E_b\, I$ [kNm^2] can be defined as the sum of the flexural rigidities of the foundation K_G [kNm^2] and the superstructure K_B [kNm^2]

$$E_b\, I = E_G\, I_G + E_B\, I_B$$

(6.8)

where:
I Ideal moment of inertia for the entire structure   [m^4]
E_b Average modulus of elasticity for the entire structure   [kN/m²]

6.2.2   Stiffness of the subsoil

The stiffness of the subsoil for *Winkler*'s model depends on modulus of subgrade reaction k_s [kN/m^3] while for Continuum model depends on modulus of compressibility E_s [kN/m^2].

For a rectangular foundation of width B [m] and length L_f [m] the stiffness of the subsoil for *Winkler*'s model K_w [kNm^2] is given by

$$K_w = k_s\, L_f^{\,4}\, B$$

(6.9)

while for Continuum model K_k [kNm^2] is given by

$$K_k = E_s\, L_f^{\,3}\, B$$

(6.10)

6.2.3   System rigidities

The decision of whether a structure or foundation has to be considered as rigid, elastic or flexible depends on the ratio between the rigidity of the superstructure including the foundation and the stiffness of the subsoil.

If one neglects the superstructure, the system rigidity for *Winkler*'s model K_c [-] is given by

$$K_c = \frac{E_B\, I}{k_s\, L_f{}^4\, B} = \frac{E_B}{12\, k_s\, L_f} \left(\frac{d}{L_f} \right)^3 \tag{6.11}$$

while for Continuum model K_s [1] is given by

$$K_s = \frac{E_B\, I}{E_s\, L_f{}^3\, B} = \frac{E_B}{12\, E_s} \left(\frac{d}{L_f} \right)^3 \tag{6.12}$$

where:

K_c	System rigidity for *Winkler*'s model	[-]
K_s	System rigidity for Continuum model	[-]
E_B	Modulus of elasticity of foundation material	[kN/m²]
I	$B\, d^3/12$ = Moment of inertia of foundation section	[m⁴]

To consider the rigidity of the superstructure in Equations 6.11 and 6.12, the foundation thickness d [m] in the Equations is replaced by an ideal foundation thickness d_i [m]. The ideal foundation thickness d_i [m] is the thickness of a rectangular cross section which has the same ideal moment of inertia for the entire structure I [m⁴] and width B [m] according to Equation 6.8.

$$d_i = \sqrt[3]{\frac{12\, I}{B}} \tag{6.13}$$

In addition, to take the effect of the superstructure on the foundation, the analysis of the foundation shall be carried out with ideal thickness of the foundation d_i [m] instead of the original foundation thickness d [m].

According to experiences and based on great number of comparative computations, the values of the system rigidity between foundation and subsoil, at which the system can be considered as rigid, already exist (*Borowicka* (1939), *Graßhoff* (1987) and *Kany* (1974)). Table 6.1 shows a list of different values for the system rigidity according to the German Standard DIN 4018.

Table 6.1   Numerical values for different grade of system rigidity

Winkler's model $K_{be} = 12\,K_c$ [1]	Continuum model $K_{St} = 12\,K_s$ [1]	Description
$K_{Be} \geq 0.2$	$K_{St} \geq 1.0$	Rigid
$0.2 > K_{Be} \geq 0.08$	$1.0 > K_{St} \geq 0.4$	Very stiff
$0.08 > K_{Be} \geq 0.04$	$0.4 > K_{St} \geq 0.2$	Medium stiff
$0.04 > K_{Be} \geq 0.02$	$0.2 > K_{St} \geq 0.1$	Stiff
$0.02 > K_{Be} \geq 0.008$	$0.1 > K_{St} \geq 0.04$	Elastic
$0.008 > K_{Be} \geq 0.004$	$0.04 > K_{St} \geq 0.02$	Medium elastic
$0.004 > K_{Be} \geq 0.002$	$0.02 > K_{St} \geq 0.01$	Very elastic
$0.002 > K_{Be}$	$0.01 > K_{st}$	Flexible

Besides the practical meaning of the system rigidity for the decision of structure rigidity, it can be also used to choose the applicable numerical model for specific case according to the system rigidity. In case of rigid foundations (or rigid structures), it is expected simplification results by computing the contact pressure and soil settlement. Therefore, a simplified numerical model may be used here. For *Winkler*'s model, the distribution of contact pressure changes to simple distribution like that of the simple assumption model. For Continuum model, the contact pressure for a regular foundation can be obtained directly by the closed formulae of *Boussinesq*. In addition, the tables of *Kany* (1974) for obtaining the contact pressure under rigid foundations are applicable here. For flexible structures such as a group of footings, the loads on the foundations are known (statically determinate structure). Therefore, only the interaction of footings through the subsoil due to the overlap stress in soil may be taken into account at the analysis.

6.2.4   Modeling of wall-floor superstructure in the raft analysis

In most design applications, the only significant additional stiffness is provided by shear walls. Here, modeling the wall and its floor connections by beam elements joined to the raft in the plan positions of the wall is normally sufficient. According to evaluated measurements of settlements, considering only one or two storeys above the raft is usually necessary.

This stiffness can be determined approximately by defining the effective wall dimension. Guidelines for calculating effective flange width b_{eff} [m] according to *Hemsley* (1998) are given in Figure 6.2. Table 6.2 shows also effective flange widths for inner and edge walls. These effective flange widths depend on whether the floor slab is continuous on either sides of the wall or only on one side. Flange widths also depend on the wall spacing B_w [m] and span L_w [m]. In the analysis, the lowest of the three values of flange width b_{eff} [m] in Table 6.2 is used.

t_s ⊐		t_s ⊐
	t_w		t_w
d		d
	b_{eff}		b_{eff}
Inner wall		Edge wall
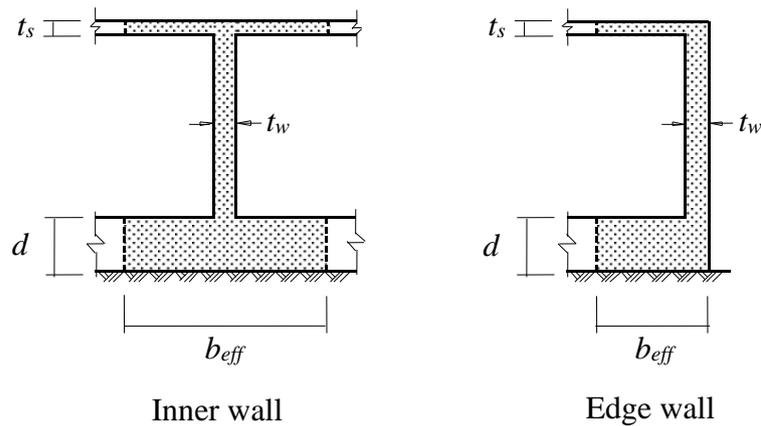
Figure 6.2   Effective flange widths for beams used to model wall-floor superstructure

Table 6.2   Effective flange width of the wall

Wall position	Effective flange width b_{eff} [m]		
Inner wall	$b_{eff} = t_w + 12\,t_s$	$b_{eff} = L_w/3$	$b_{eff} = B_w$
Edge wall	$b_{eff} = t_w + 4\,t_s$	$b_{eff} = L_w/6$	$b_{eff} = B_w/2$

where in Table 6.2 t_s [m] is the floor thickness.

6.2.5   Determination of replacement wall height h_{Ers}

To simulate the wall stiffness on the finite element mesh by using additional beam elements, the actual properties of the beam elements must be determined. The stiffness of the wall can be obtained through a replacement beam arranged in the center plane of the plate. The dimensions of the replacement beam can be taken as shown in Figure 6.3. This can be carried out by determining firstly the moment of inertia of the effective section of the wall I_{pb} [m^4] that contains two parts, flanges and web. Then, the replacement height of the web h_{Ers} [m] can be determined by equating the moment of inertia I_{pb} [m^4] to two equivalent moments of inertia. The first moment of inertia corresponds a rectangular flange I_p [m^4] while the second corresponds a rectangular web I_w [m^4]. The replacement height of the web h_{Ers} [m] must be higher than the sum of raft thickness d [m] and clear height of the wall h_w [m]. In the finite element model, the wall and floor flange are represented by beam element that has the property of t_w [m] and h_{Ers} [m] while the raft flange is already included in the plate finite element.

Inner wall I_{pd} = I_p + I_w

Edge wall I_{pd} = I_p + I_w
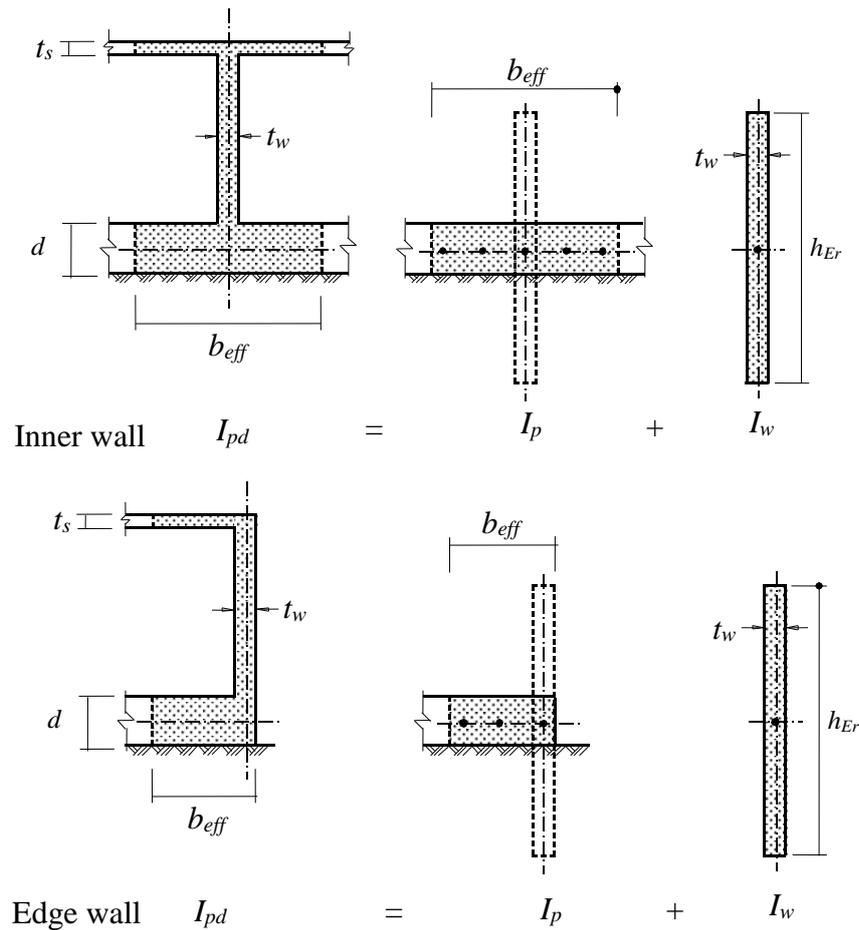
Figure 6.3   Determination of replacement height h_{Ers}

6.3   Direct modeling of superstructure-foundation-soil system

For modeling of the superstructure-foundation-soil system, the stiffness matrix for the entire structure must be derived from the summation of the stiffness matrices of superstructure, foundation and subsoil model. So, the three media can be treated as an integral unit. This can be applied by considering the compatibility of deformations between the superstructure, foundation and the soil medium, where the superstructure deformation is equal to the foundation deformation and the soil settlement is equal to the foundation deflection.

The equilibrium equation for the entire structure (superstructure foundation subsoil model) is written in matrix form as

$$[K_t]\{U\} = \{F\} \tag{6.14}$$

where:
[K_t]   Total stiffness matrix for the entire structure
{U}   Vector of nodal displacements for the entire structure
{F}   Vector of external nodal forces for the entire structure

The above system of linear equations can be solved using one of the following methods:

a)   *Gauss* elimination method. This method treats the total system of equations of the entire structure as one unit. Therefore, it requires large computer storage and long computation time

b)   Substructure technique, where the set of nodal displacements $\{U\}$ is divided into boundary displacements common to the superstructure and the supporting soil including the foundation displacements $\{U_b\}$ and interior displacements of the superstructure $\{U_i\}$. Corresponding to each of these displacement sets is a set of external forces $\{F_b\}$ and $\{F_i\}$, respectively. Then, the system of equations can be derived in two partitioned sets of equations. The boundary displacements $\{U_b\}$ can be calculated by solving the first set of equations, then the interior displacements of the superstructure $\{U_i\}$ can be obtained by performing back substitution of the internal nodes in which the boundary displacements $\{U_b\}$ are already obtained

c)   Iteration method allows less computer storage and short computation time. The iterative procedure available in program *ELPLA* to analyze the entire structure as one unit, developed by *Kany/ El Gendy* (2000), is described in the following section

6.4   Modeling of superstructure foundation soil system by iteration

Most of the methods for analysis of the entire structure as one unit were focused on the interaction analysis of open framed structures on linear elastic subsoil models. An actual modeling for structure may also be used, where the columns, walls, slabs and foundation are modeled as a three dimensional problem using plate element and frame element having six degrees of freedom at each node comprising 3 translations (u, v, w) and 3 rotations (θ_x, θ_y, θ_z). In spite of the success of this method in the analysis of structure, the analysis is time-consuming and requires large computer capacity. The use of such analysis leads to a great overall stiffness matrix of the structure. However, in many cases, the effects of some translation or rotation components may be ignored. For example, a structure carries vertical loading, due to the in-plane rigidity of the floors and foundation, has rigid body modes of displacements and no in-plane deformation is expected. That is why the in-plane stress and deformation can be neglected. In these cases the size of the stiffness matrix of structure will be considerably reduced, if a reasonable analysis is carried out. An example for this problem may be found in the analysis of common multi-storey buildings, where the degree of freedom at nodes of adjacent substructures is different.

In the raft foundation and floors each node has three degrees of freedom comprising one translation (w) and two rotations (θ_x, θ_y). In the superstructure components it has two translations (u, v) in the shear walls, three translations (u, v, w) and three rotations (θ_x, θ_y , θ_z) in a space frame. In the supporting soil it has only one translation w. One of the advantages of the iterative procedure of *Kany/ El Gendy* (2000) is to overcome the incompatibility in the degree of freedom at the different adjacent substructures by reflecting only the required translations and rotations during the iteration process. Thus, minimization of the calculation effort will take place.

The iterative procedure presents an accurate and rapid method for linear and nonlinear analysis of foundation supporting multi-storey buildings considering the effect of superstructure rigidity. Using this iterative procedure the computational time is significantly reduced compared with the traditional analysis of soil-structure problems.

To perform the entire active structure-foundation analysis two computer programs were developed, one for the analysis of floor and foundation slabs with or without girders, the second program for the analysis of a space frame. The two programs are standard finite element solution for plate element and space-beam element types.

6.4.1   Iterative procedure

To describe the iterative procedure, an idealized superstructure containing floor slabs and columns supported by a raft foundation is considered as a typical example shown in Figure 6.40. In the procedure the superstructure is partitioned into floor slabs and columns besides the foundation. The nodes are numbered for each substructure separately. To consider the effect of superstructure rigidity on the foundation an iterative procedure, Figure 6.4, can be described as follows:

(0) complete structure

(1) floors on fixed supports

(2) columns on fixed supports

(3) foundation under column reactions

(4) columns on elastic supports $\{k_f\}$

(5) floors on elastic supports $\{k_c\}$

(6) columns exposed to deformation $\{\delta_f\}$

(7) foundation under column reaction $\{V\}$

Convergence reached

No

Yes
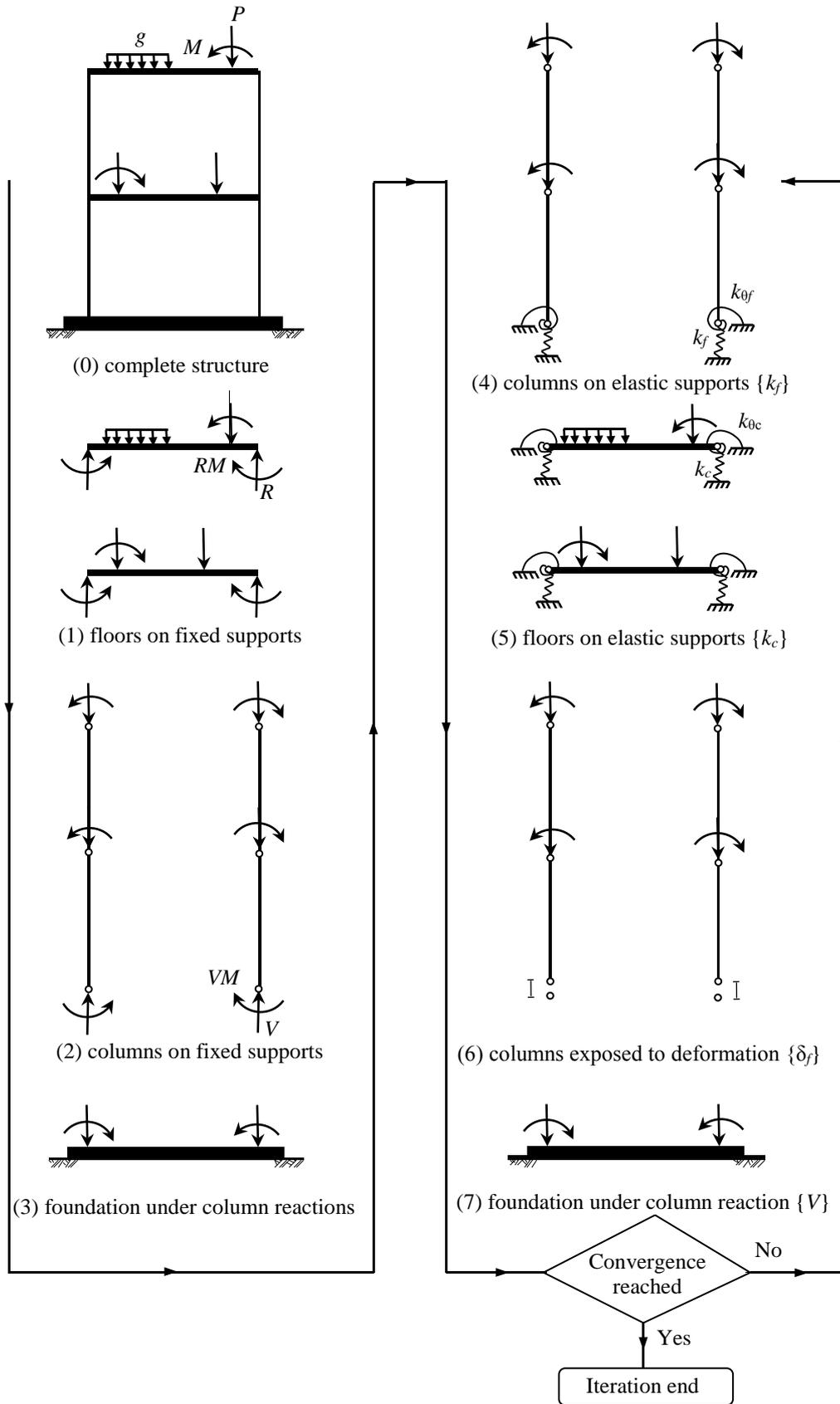
Iteration end

Figure 6.4   Interaction of superstructure and foundation via iteration

(1)   Each floor slab is analyzed separately as if it is rigidly attached to the columns (rotation = displacement = 0). Then, the support reactions $\{R\}$ at the position of the floor slabs attached to the columns are obtained

$$\{R\}_i = \{R_x, R_y, R_z, RM_x, RM_y, RM_z\}^T_i \qquad (6.15)$$

where $\{R\}_i$ is the vector of support reactions of the floor slab at node i attached to the column; R_x, R_y, R_z, RM_x, RM_y and RM_z are the support forces and moments in x-, y- and z-directions at that node

(2)   Support reactions $\{R\}$ from floor slabs are applied to the columns as external loads. Analyzing the frame of columns separately under these loads as if it is rigidly attached to the foundation (rotation = displacement = 0). Then, the end reactions of columns $\{V\}$ attached to the foundation are obtained

$$\{V\}_i = \{V_x, V_y, V_z, VM_x, VM_y, VM_z\}^T_i \qquad (6.16)$$

where $\{V\}_i$ is the vector of support reactions at the column base attached to the foundation at node i; V_x, V_y, V_z, VM_x, VM_y and VM_z are the support forces and moments in x-, y- and z-directions at that point

(3)   The end reactions at the column bases $\{V\}$ are applied to the foundation as external loads. The foundation is analyzed to obtain the deformations of the foundations $\{\delta_f\}$ at the column base positions

$$\{\delta_f\}_i = \{u_f, v_f, w_f, \theta_{xf}, \theta_{yf}, \theta_{zf}\}^T_i \qquad (6.17)$$

where $\{\delta_f\}_i$ is the vector of deformations of foundation at node i attached to the column base; u_f, v_f, w_f, θ_{xf}, θ_{yf} and θ_{zf} are the displacements and rotations in x-, y- and z-directions at that point

(4)   The above foundation deformations $\{\delta_f\}$ are used to obtain the foundation rigidity at the column bases. This is done by determining a set of spring constants $\{k_f\}$ to represent the foundation stiffness connections

$$\begin{aligned}
\{k_f\}_i &= \{k_{uf}, k_{vf}, k_{wf}, k_{\theta xf}, k_{\theta yf}, k_{\theta zf}\}^T_i \\
&= \left\{ \frac{V_x}{u_f}, \frac{V_y}{v_f}, \frac{V_z}{w_f}, \frac{VM_x}{\theta_{xf}}, \frac{VM_y}{\theta_{yf}}, \frac{VM_z}{\theta_{zf}} \right\}^T_i
\end{aligned} \qquad (6.18)$$

where k_{uf}, k_{vf}, k_{wf} are transitional spring stiffnesses due to forces in x-, y- and z-directions. $k_{\theta xf}$, $k_{\theta yf}$ and $k_{\theta zf}$ are rotational spring stiffnesses due to moments in x-, y- and z-directions

The analysis is performed on frame of columns separately under the previous loads $\{R\}$ as if it is resting on elastic supports having the spring constants $\{k_f\}$. Then, the column deformations $\{\delta_c\}$ at floor slab positions are obtained

$$\{\delta_c\}_i = \left\{ u_c, v_c, w_c, \theta_{xc}, \theta_{yc}, \theta_{zc} \right\}^T_i \tag{6.19}$$

where $\{\delta_c\}_i$ is the vector of column deformations at floor slab position at node i; u_c, v_c, w_c, θ_{xc}, θ_{yc} and θ_{zc} are the displacements and rotations in x-, y- and z-directions at that point

(5)   The previous column deformations $\{\delta_c\}$ are used to obtain the column rigidity at the floor slab positions. This is done by determining a set of spring constants $\{k_s\}$ to represent the column stiffness connections

$$\begin{aligned}\{k_c\}_i &= \left\{ k_{uc}, k_{vc}, k_{wc}, k_{\theta xc}, k_{\theta yc}, k_{\theta zc} \right\}^T_i \\ &= \left\{ \frac{R_x}{u_c}, \frac{R_y}{v_c}, \frac{R_z}{w_c}, \frac{RM_x}{\theta_{xc}}, \frac{RM_y}{\theta_{yc}}, \frac{RM_z}{\theta_{zc}} \right\}^T_i \end{aligned} \tag{6.20}$$

where k_{uc}, k_{vc}, k_{wc} are transitional spring stiffnesses due to forces in x-, y- and z-directions. $k_{\theta xc}$, $k_{\theta yc}$ and $k_{\theta zc}$ are rotational spring stiffnesses due to moments in x-, y- and z-directions

The analysis is performed on each floor slab separately as if it is resting on elastic supports having the spring constants $\{k_c\}$. Then, the floor slab deformations $\{\delta s\}$ at column positions are obtained

$$\{\delta_s\}_i = \left\{ u_s, v_s, w_s, \theta_{xs}, \theta_{ys}, \theta_{zs} \right\}^T_i \tag{6.21}$$

where $\{\delta_s\}_i$ is the vector of deformations of floor slab attached to column at node i; u_s, v_s, w_s, θ_{xs}, θ_{ys} and θ_{zs} are the displacements and rotations in x-, y- and z- directions at that node. Determination of the new support reactions $\{R\}$ of the floor slabs attached to the columns due to elastic supports

$$\begin{aligned}\{R\}_i &= \left\{ k_{uc}\, u_s, k_{vc}\, v_s, k_{wc}\, w_s, k_{\theta xc}\, \theta_{xs}, k_{\theta yc}\, \theta_{ys}, k_{\theta zc}\, \theta_{xs} \right\}^T_i \\ &= \left\{ R_x, R_y, R_z, RM_x, RM_y, RM_z \right\}^T_i \end{aligned} \tag{6.22}$$

(6)   The above foundation deformations $\{\delta_f\}$ are applied at the column bases. The analysis is performed on the frame of columns separately under the previous loads $\{R\}$. Then the end reactions of columns $\{V\}$ attached to the foundation are obtained

(7)   The end reactions at the column bases $\{V\}$ are applied to the foundation as external loads. The analysis is performed on the foundation to obtain the deformations of the foundations $\{\delta_f\}$ at the column base positions

The steps (4) to (7) have to be repeated until a sufficient compatibility of deformations between floor slabs and columns and between columns and foundation is reached at the connecting nodes.

6.4.2 Nonlinear mathematical soil model

A mathematical model for raft foundation resting on nonlinear soil medium for *Winkler*'s model was presented by *Baz* (1987) and *Hasnien* (1993). This model is selected here for the analysis of foundation considering the effect of superstructure rigidity. In the mathematical model, the soil medium was represented by springs with nonlinear relation between the contact pressure of an individual spring and corresponding settlement. The model represents the nonlinear behavior of the contact pressure-settlement at the raft-soil interface by Equation 6.23 analogous to the hyperbolic function that represents the stress-strain relationship of the soil

$$q_i = \frac{w_i}{\dfrac{1}{k_t} + \dfrac{w_i}{q_{ult}}}$$

(6.23)

where q_i [kN/m^3] is the contact pressure at node i on the foundation, w_i is the soil settlement at that node, k_t [kN/m^3] is the initial subgrade reaction and q_{ult} [kN/m^2] is the ultimate bearing capacity of the soil.

An extension for the above nonlinear soil medium for *Winkler*'s model is made in the procedure to represent the nonlinear behavior of foundation on Continuum model. In this case the initial subgrade reaction is variable from one node to the other and is obtained from the linear analysis of foundation on Continuum model, Equation 6.24

$$k_{ti} = \frac{q_{li}}{w_{li}}$$

(6.24)

where k_{ti} [kN/m^3] is the initial subgrade reaction at node i, q_{li} [kN/m^2] and w_{li} [m] are the linear contact pressure and soil settlement at that node respectively.

Now the nonlinear behavior of the soil for both *Winkler*'s and Continuum models can be introduced in the previous iterative procedure as follows, Figure 6.5:

-       At iteration cycle (j) the nonlinear contact pressure q_i at node i is

$$q_i^{(j)} = k_{si}^{(j)} w_i^{(j)}$$

(6.25)

       where k_{si} is the modulus of subgrade reaction at node i, and equal to the initial subgrade reaction k_{ti} at the first iteration cycle

-       For the next iteration cycle ($j + 1$) the modulus of subgrade reaction k_{si} is modified using Equation 6.23

$$k_{si}^{(j+1)} = \frac{1}{\dfrac{1}{k_{ti}} + \dfrac{w_i^{(j)}}{q_{ult}}}$$

(6.26)

These steps have to be repeated until a specified tolerance ε between the nonlinear contact pressure q_i calculated from iteration cycle (j) and that of the previous cycle (j - 1) is reached.
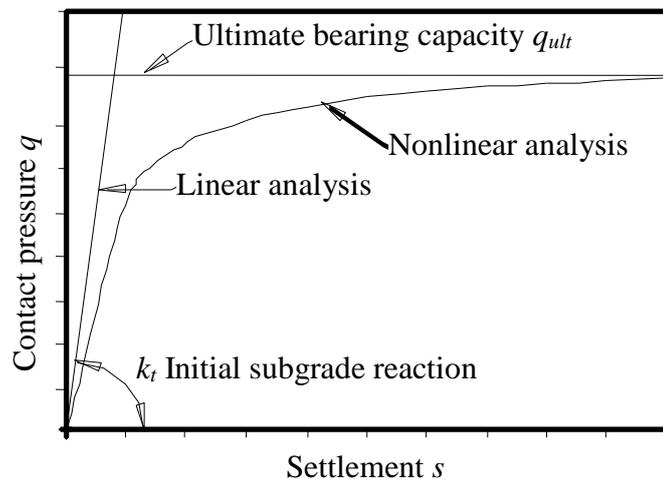
Figure 6.5   Contact pressure-settlement diagram, linear and nonlinear analysis

Example 6.1   Analysis of a raft for a high rise building

1   Description of the problem

This example was carried out to show the influence of flexure rigidity of the superstructure on the settlements and contact pressures for a raft of high rise building.

It is required to analyze a raft for the building shown in Figure 6.6 in three simplified sections. The building is a reinforced concrete skeleton structure and consists of a cellar and 13 storeys. The floor height is 3 [m] while the bay width is 3.6 [m]. The number of bays is 18. The total building length is 66 [m] while the total width of the cellar basement is 17.55 [m]. The raft thickness is 1.2 [m]. In the following study the raft is analyzed considering subsoil behavior. Also, an estimation of the superstructure deformations is carried out. In the analysis, settlements and contact pressures are determined in which a comparison is carried out in four cases as:

i)   For not stiffened raft
ii)   For compound system raft-cellar
iii)   For compound system raft-cellar-superstructure
iv)   For completely rigid raft

The stiffness of the structure system parallel to the long axis can be determined from the data given in Figures 6.6 and 6.7.

2   Soil properties

According to Figure 6.7, the subsoil layers consist of a sandy clay layer until 11.6 [m] depth under the ground surface with modulus of compressibility $E_s = 14\,000$ [kN/m^2]. Under the sandy clay layer exists in 11.60 [m] depth practically incompressible sandstone rock in great thickness. The settlement parts from the reloading of the soil are neglected. The foundation level under the original ground surface is 3.80 [m]. The modulus of compressibility method is used to analyze the foundation.

3   Material properties of concrete

The building material is reinforced concrete and has the following properties:

Young's modulus E_b $= 2 \times 10^7$ [kN/m^2]
Poisson's ratio ν_b $= 0.25$ [-]
Unit weight γ_b $= 0.0$ [kN/m^3]

Unit weight of the concrete is chosen $\gamma_b = 0.0$ to neglect the self-weight of the structure.

4   Loads

According to static calculation of the open frame assuming rigid supports, each column from the twice 17 columns of the external walls has a column load of 2700 [kN] while each column of the twice 17 internal columns has a column load of 2500 [kN]. The column load for the four corner columns is 1350 [kN] while for the four edge columns is 1250 [kN]. The loads with FE-Net of the raft are shown in Figure 6.8.

a) Longitudinal A-B

c) Cross-section C-D

b) Plan (section E-F)
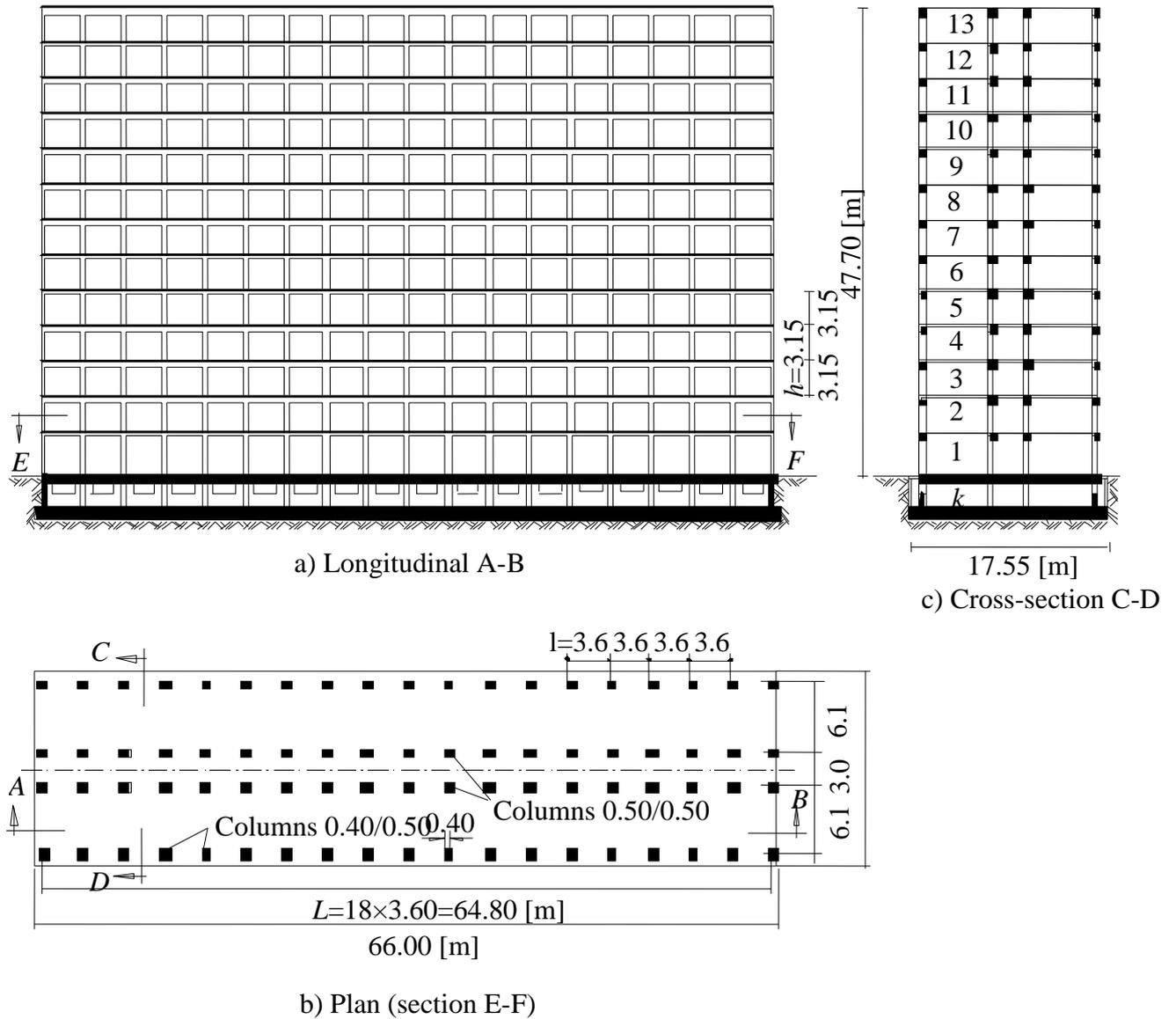
Figure 6.6   Details of the building

Figure 6.7   Subsoil and dimensions of the raft, floors and columns (cross-section)

$P_1 = 1250$ [kN]
$P_2 = 2500$ [kN]
$P_3 = 1350$ [kN]
$P_4 = 2700$ [kN]

2.75×24=66.00 [m]
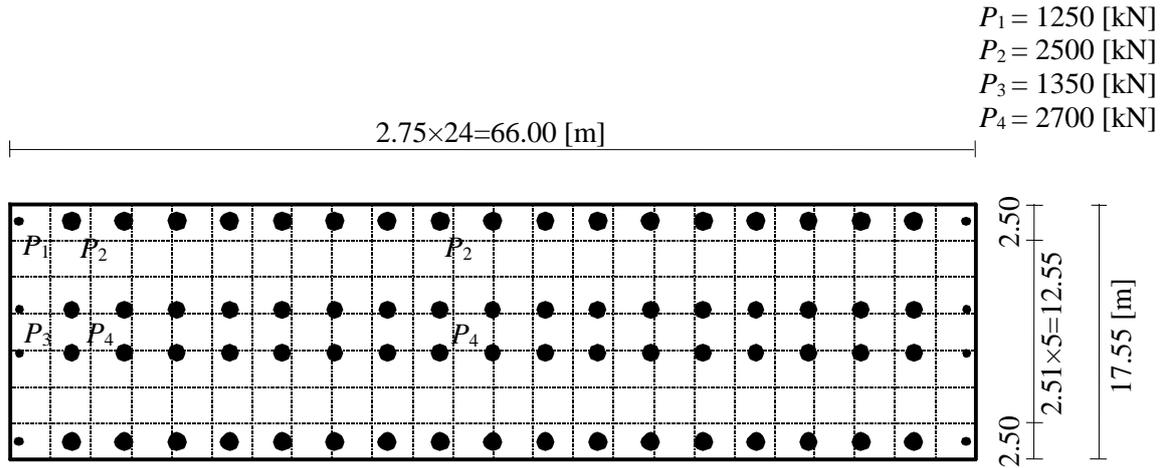
Figure 6.8   FE-Net of the raft with loads

5   Analysis of the structure
5.1   Analysis for not stiffened raft

At first, the settlements and contact pressures are determined under the assumption that except for the stiffness of the raft itself (thickness $d = 1.2$ [m]) no other rigidity is effective. So, the flexure rigidity of the raft K_G can be obtained from

$$K_G = E_G\, I_G = E_G\, \frac{B\, d^3}{12} = 2.1\times10^7\, \frac{17.55\,(1.2)^3}{12} = 5.31\times10^7\ [\text{kN/m}^3]$$

and system rigidity K_{st}

$$K_{st} = 12\, K_s = \frac{E_b}{E_s}\left(\frac{d}{L_f}\right)^3 = \frac{2.1\times10^7}{14000}\left(\frac{1.2}{66}\right)^3 = 0.009\,[\text{-}]$$

The raft is flexible according to Table 6.1, $(0.01 > K_{st})$.

5.2   Analysis for the compound system raft-cellar

From the assumption that the raft, the cellar walls and the cellar thickness represent combined flexure rigidity for the cross section, the cellar system with the raft must be connected rigidly through satisfied reinforcement. Considering the cross-section shown in Figure 6.7, the height x_s of the center of gravity of the system cellar-raft is given by

$$x_s = \frac{\sum F_i\, x_i}{\sum F_i} = \frac{(17.55\times1.2\times0.6)+(2\times0.5\times1.2\times1.8)+(0.4\times15.7\times3.8)}{(17.55\times1.2)+(2\times0.5\times1.2)+(0.4\times15.7)} = 1.36\,[\text{m}]$$

Then, the moment of inertia I_G of the foundation system according to *Steiner*'s law is given by

$$I_G = \left(\frac{17.55 \times (1.2)^3}{12} + 17.55 \times 1.2 \times (0.76)^2 \right) + 2 \left(\frac{0.5 \times (1.2)^3}{12} + 0.5 \times 1.2 \times (0.44)^2 \right)$$
$$+ \left(\frac{15.70 \times (0.4)^3}{12} + 15.7 \times 0.4 \times (2.44)^2 \right) = 52.54 \, [\text{m}^4]$$

The rigidity of the structure K_G is given by

$$K_G = E_G I_G = 2.1 \times 10^7 \times 52.4 = 110.33 \times 10^7 \, [\text{kN/m}^3]$$

Then, the ideal raft thickness d_i is given by

$$d_i = \sqrt[3]{\frac{12 \, I}{B}} = \sqrt[3]{\frac{12 \times 52.54}{17.55}} = 3.3 \, [\text{m}]$$

and system rigidity K_{st}

$$K_{st} = 12 \, K_s = \frac{E_b}{E_s} \left(\frac{d}{L_f} \right)^3 = \frac{2.1 \times 10^7}{14000} \left(\frac{3.3}{66} \right)^3 = 0.1875 \, [\text{-}]$$

The raft is stiff according to Table 6.1, $(0.2 > K_{St} \geq 0.1)$.

5.3   Analysis for the compound system raft-cellar-superstructure

In this case the structure system is considered as a raft, cellar and superstructure connected together as one unit. Here, the statical system of the structure may be taken as multi-storey open frame (13 storeys, 18 bays), which is statically indeterminate. The next calculation shows a simplificative way to estimate the rigidity of the overall structure on the foundation. In the calculation, it is assumed that only the rigidity of the open panels is taken into consideration where the contribution of filling walls on the structure rigidity is neglected.

Moment of inertia of the floor I_r

According to Beton-Kalender (1957), page 47 or *El Behairy* (1992), page 17 the moment of inertia can be obtained from

$$\frac{\sum b_o}{b} = \frac{2(0.3 + 0.5)}{15.7} = \frac{1.6}{15.7} = 0.102,$$
$$\frac{d}{d_o} = \frac{0.15}{0.5} = 0.3,$$
$$\mu = 0.0193$$
$$I_r = \mu \, b \, d_o^3 = 0.0193 \times 15.7 \times (0.5)^3 = 0.0379 \, [\text{m}^3]$$

Average stiffness of the floor K_r

$$K_r = \frac{I_r}{l} = \frac{0.0379}{3.6} = 0.01053 \, [\text{m}^3]$$

Moment of inertia of the columns I_s

The columns consist of two internal columns with cross-section of 0.5×0.5 [m] and two external columns with cross-section of 0.5×0.4 [m].

$$I_s = 2 \left(\frac{0.5 \times 0.5^3}{12} + \frac{0.5 \times 0.4^3}{12} \right) = 0.01575 \, [\text{m}^4]$$

Average stiffness of the columns K_s

$$K_s = \frac{I_s}{h} = \frac{0.01575}{3.15} = 0.005 \, [\text{m}^3]$$

Since all floors and columns are supposed to have similar cross-sections, the effective moment of inertia I_B of the multi-storey open frame according to *Meyerhof* (1953) can be given by

$$I_B = I_r \, n_s \, n_s^2 \, \frac{2 \, K_s}{K_r + 2 \, K_s} = 0.0379 \times 13 \times 18^2 \, \frac{2 \times 0.005}{0.01053 + 2 \times 0.005} = 77.76 \, [\text{m}^4]$$

Flexure rigidity of the superstructure K_B

$$K_B = E_B \, I_B = 2.1 \times 10^7 \times 77.76 = 163.29 \times 10^7 \, [\text{kN/m}^3]$$

Flexure rigidity of the entire structure K_b

$$K_b = K_G + K_B = 110.33 \times 10^7 + 163.29 \times 10^7 = 273.62 \times 10^7 \, [\text{kN/m}^3]$$

Ideal moment of inertia for the entire structure I

$$I = \frac{K_b}{E_b} = \frac{273.62 \times 10^7}{2.1 \times 10^7} = 130.3 \, [\text{m}^4]$$

Ideal raft thickness d_i

$$d_i = \sqrt[3]{\frac{12 \, I}{B}} = \sqrt[3]{\frac{12 \times 130.3}{17.55}} = 4.46 \, [\text{m}]$$

and system rigidity K_{st}

$$K_{st} = 12 \, K_s = \frac{E_b}{E_s} \left(\frac{d}{L_f} \right)^3 = \frac{2.1 \times 10^7}{14000} \left(\frac{4.46}{66} \right)^3 = 0.463 \, [\text{-}]$$

The raft is very stiff according Table 6.1, $(1.0 > K_{St} \geq 0.4)$.

5.4   Analysis for completely rigid raft

In this case both the superstructure and foundation are considered as an infinitely rigid structure. To determine the settlements and contact pressures in this extreme case, the modulus of compressibility method for the rigid raft is used. This method considers the raft is completely rigid. Rigid raft means a raft has a thickness of $d = \infty$ which also lead to a flexure rigidity of $K_G = \infty$.

Figures 6.9 and 6.10 show the settlements and contact pressures for the four cases of analyses. The settlements and contact pressures are determined with an ideal raft thickness d_i. Furthermore, the results of this example are represented in Table 6.3 in details, so that one can recognize the differences well.

6   Conclusions

This study shows that the results with and without the influence of the structure rigidity are different from one to other. Besides, the numerical example shows a way to how it can determine for more complicated structure systems the settlements and contact pressures taking into account the influence of the structure rigidity.

Table 6.3   Results of structure rigidity for the four different cases of analyses

Analysis	Moment of inertia I [m^4]	Flexure rigidity $K = E_b\, I$ [kN/m^3]	Ideal raft thickness d_i [m]	System rigidity K_{st} [1]	Grade of System rigidity
Not stiffened raft	2.53	5.31×10^7	1.20	0.009	Flexible $0.01 > K_{st}$
Compound system raft-cellar	52.54	110.33×10^7	3.30	0.1875	Stiff $0.2 > K_{St} \geq 0.1$
Compound system raft-cellar-superstructure	130.30	273.62×10^7	4.46	0.463	Very stiff $1.0 > K_{St} \geq 0.4$
Completely rigid raft	∞	∞	∞	∞	Rigid $K_{St} \geq 1.0$

x [m]
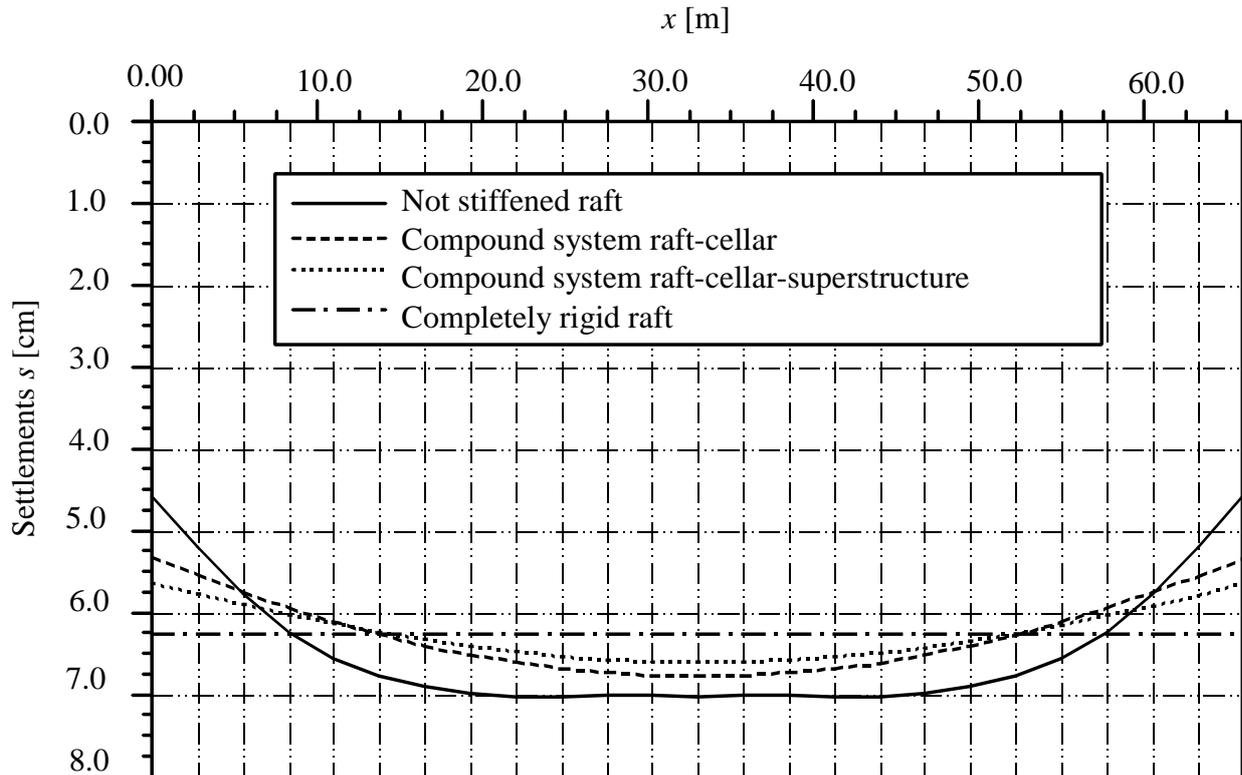
Figure 6.9   Settlements *s* [m] in longitudinal direction at the middle of the structure

x [m]
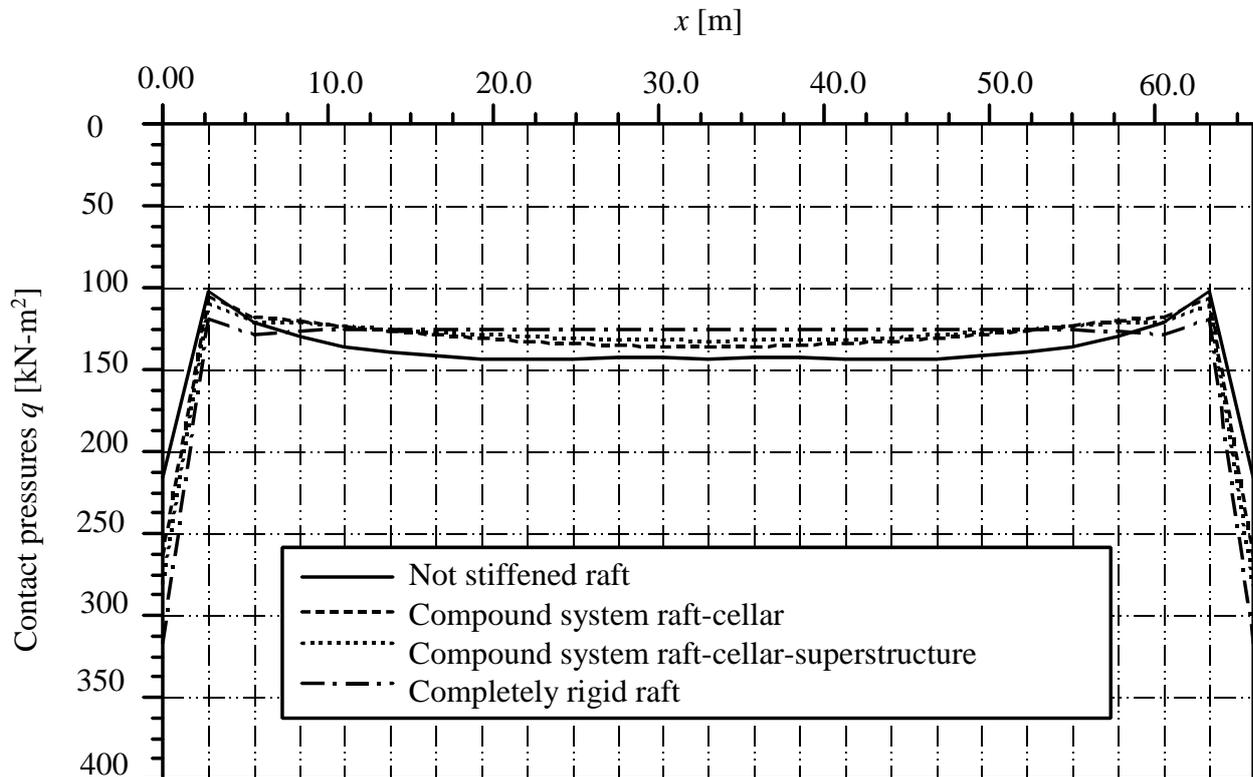
Figure 6.10   Contact pressures *q* [kN/m²] in longitudinal direction at the middle
                of the structure

Example 6.2   Verification of the iterative procedure

1   Description of problem

To verify the iterative procedure and evaluate its accuracy, a five-storey building resting on foundation through 36 columns is considered. The building is composed of five bays in both *x*- and *y*-directions, each bay is 5.0 [m] span. The height of the first storey is 4.0 [m] while the height of the other storeys is 3 [m]. The typical floor of the five storeys is chosen to be skew paneled beams as shown in Figure 6.11. The dimensions and loads of floor beams are shown in Table 6.4. The foundation is a grid type with 0.5 [m] thickness and 2.5 [m] breadth, Figure 6.12. The columns are square cross sections, the column models and dimensions for each storey are shown in Table 6.5.

The building material is reinforced concrete and has the following properties:

Young's modulus	E_b	$= 3 \times 107$	[kN/m^2]
Poisson's ratio	v_b	$= 0.15$	[-]
Shear modulus	G_b	$= 1.3 \times 10^7$	[kN/m^2]

The soil mass below the foundation is idealized as *Winkler*'s medium. The modulus of subgrade reaction of the soil k_s is 40000 [kN/m^3].

Table 6.4   Dimensions and loads of floor beams

Beam type	Dimensions		Load [kN/m]
	Depth [m]	Breadth [m]	
Exterior beam B1	0.50	0.25	15
Interior beam B2	0.70	0.25	30

Table 6.5   Column models and dimensions

Storey	Column dimensions [m × m]		
	Model C1	Model C2	Model C3
1st & 2nd storey	0.40 × 0.40	0.50 × 0.50	0.60 × 0.60
3rd & 4th storey	0.30 × 0.30	0.40 × 0.40	0.50 × 0.50
5th storey	0.25 × 0.25	0.30 × 0.30	0.40 × 0.40
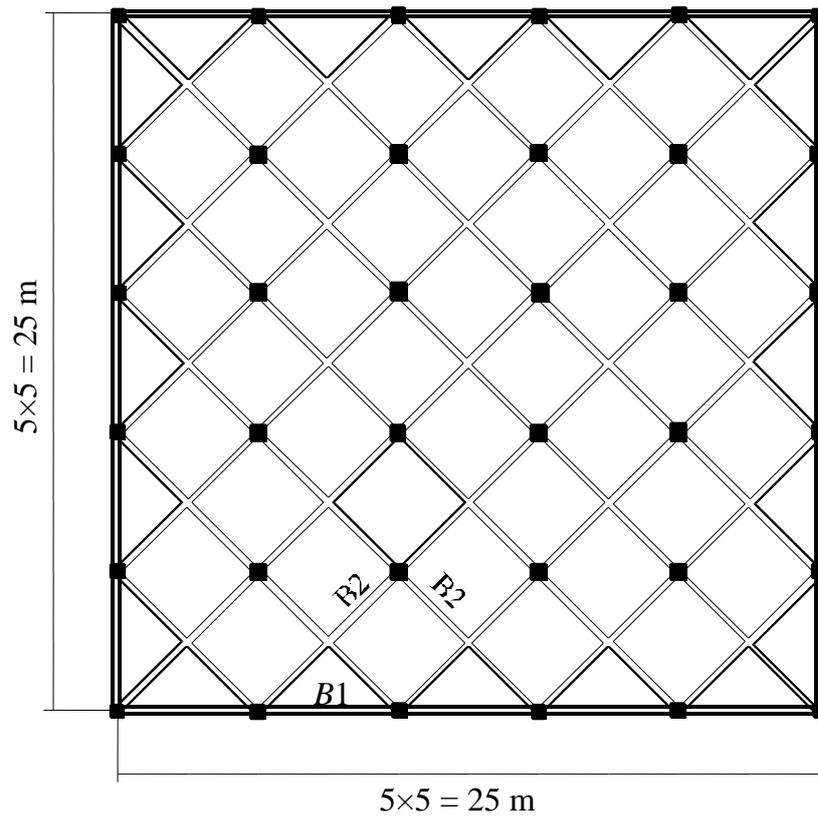
Figure 6.11   Typical floor in plan
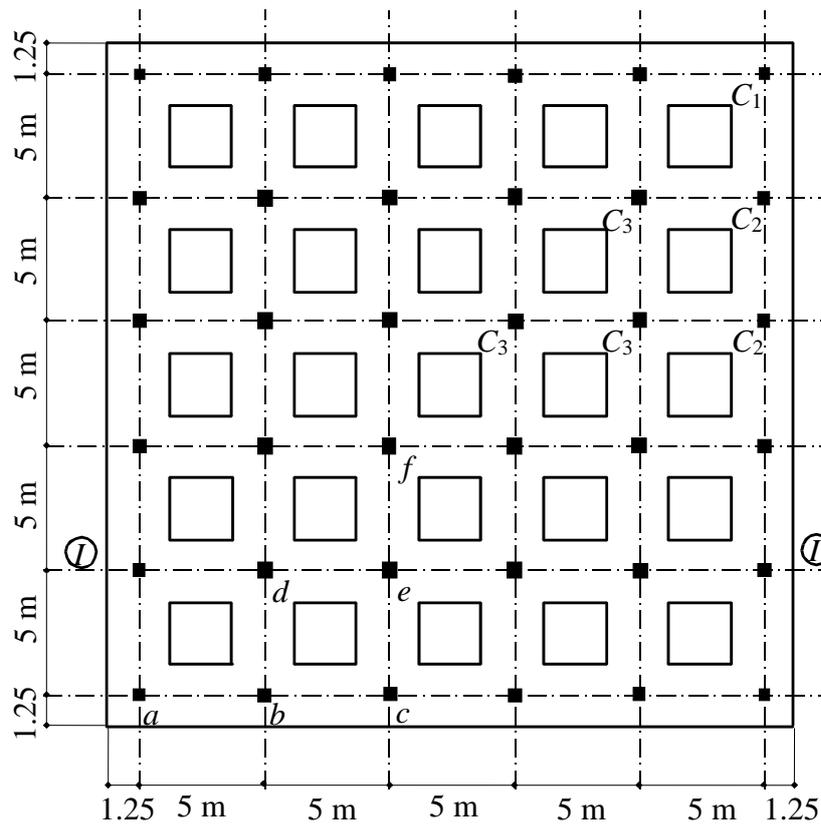
Figure 6.12   Foundation plan with column models

621

5 th floor □ (16.00)

551

4 th floor □ (13.00)

470

3 rd floor □ (10.00)

389

2 nd floor □ (7.00)

308

1 st floor □ (4.00)

227

Ground □ (0.00)

5×5 = 25 m

21

Y

X

Z

1

5×5 = 25 m
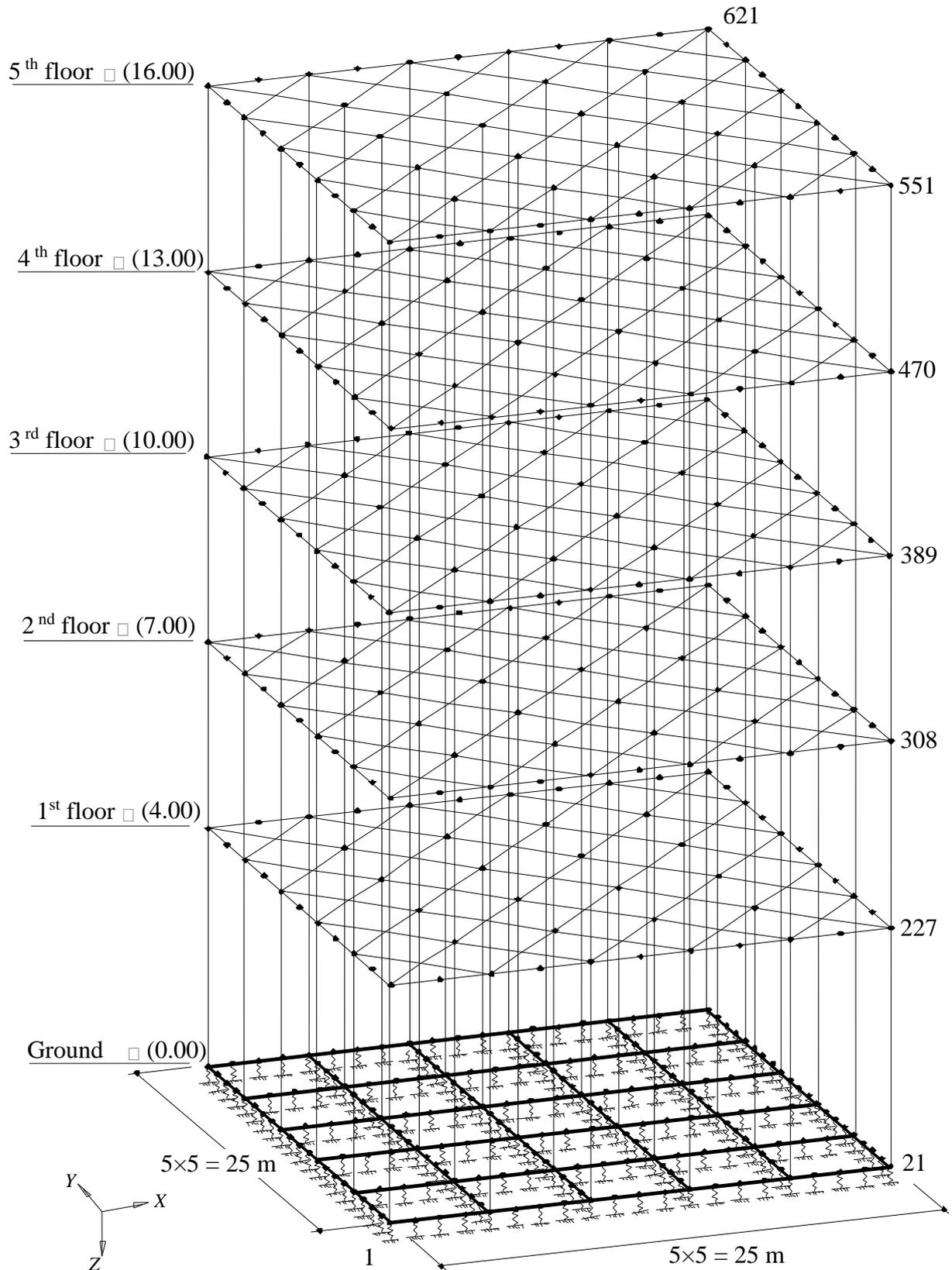
Figure 6.13   Statical system of space frame with foundation on elastic springs

2   Analysis

For the comparison between the results of building analysis using the proposed iterative procedure and that of traditional analysis without iteration, the building is modeled as a space frame supported by grid foundation resting on elastic springs. The element type for both the superstructure and foundation is a beam element as shown in Figure 6.13.

For the calculation based on the traditional analysis without iteration, the structure is divided into 1120 space frame elements yielding 621 nodes. Each node has six degree of freedom. This generates 3726 simultaneous equations. For the calculation based on the proposed iterative procedure, the structure is divided into three parts; floors, space frame (columns) and foundation. The number of elements is 140, 180 and 240, yielding 81, 216 and 216 nodes for floor, space frame and foundation, respectively. Because the structure subjects to symmetrical vertical loading, the effect of horizontal loads will be ignored. Therefore the horizontal translations (u, w) and stresses for the floors and foundation are not considered in the analysis.

For the calculation based on the traditional method, a three-dimensional space frame program is used to make the analysis of the structure. The horizontal translations and stresses in this case are ignored by assuming very small cross section areas for the floors and foundation elements. For the calculation based on the proposed iterative procedure, it is easy to use a two- or three-dimensional program whenever it is applicable to make the analysis of each part of the structure separately. A two-dimensional grid program is used to make the analysis of floors or foundation in order to omit the horizontal translations and stresses, and a three-dimensional space program is used to make the analysis of columns.

Due to symmetry in shape, dimensions, loading and supporting soil, it is possible to make the analysis for only one quarter of the structure. However, the analysis is carried out here for the whole structure and the conditions of symmetry are used to check the results.

3   Results and discussion

To verify the proposed iterative procedure, the results of deformations at six selected points (a) to (f) on the foundation are compared in Table 6.6 with those obtained by the traditional method without iteration.

Table 6.6   Comparison of deformations at selected points on the foundation obtained by iteration and those obtained by traditional method without iteration

Point	w [cm]		θ_x [-]		θ_y [-]	
	With iteration	Without iteration	With iteration	Without iteration	With iteration	Without iteration
a	0.214	0.213	0.00043	0.00042	-0.00043	-0.00042
b	0.229	0.229	0.00038	0.00037	0.00009	0.00008
c	0.219	0.219	0.00036	0.00035	-0.00003	-0.00003
d	0.308	0.308	-0.00011	-0.00009	0.00011	0.00009
e	0.291	0.291	-0.00011	-0.00009	-0.00004	-0.00003
f	0.269	0.270	0.00004	0.00004	-0.00004	-0.00004

The maximum difference between the vertical translations of floor slabs and columns and between those of columns and foundation at attached nodes is considered as an accuracy number

$$\varepsilon_w = \left(\frac{w_c - w_p}{w_c} \right) \times 100 \, [\%]$$

where ε_w is the accuracy number for vertical translation in percentage, w_c = vertical translation of column and w_p is the vertical translation of floor or foundation.

The accuracy number ε_w is 0.6 [%] for translation after four cycles. It can be concluded from the comparison that the results of the proposed iterative procedure are in good agreement with those obtained by the traditional method without iteration with accuracy $\varepsilon_w = 0.6$ [%] for the whole structure which yields maximum settlement error 0.47 [%] of the foundation.

The computation time required for the iteration process used in Pentium 100 computer with 64 MB RAM is 39 minutes, while that, required for solving the system of linear equations by the traditional method without iteration is 6.5 hours. The computation time required for solving the system of linear equations by the traditional analysis without iteration is 10 times more than required for the iteration process using the proposed iterative procedure for this example. Another analysis using the iterative procedure for the same example was carried out using a plate-beam element program for floors and foundation (see case example 4.2), indicated that the processing time was 43 minutes. That means, the long computation time for the traditional method is referred to solving the overall matrix of the complete structure in one time, which normally, in this case, has large band width.

Example 6.3   Analysis of structure on nonlinear soil medium

1   Description of problem

An application of the proposed iterative procedure is carried out to study the behavior of foundation resting on nonlinear soil medium with considering influence of the superstructure rigidity.

The previous example shown in Figures 6.11 and 6.12 is also chosen here to show the analysis of structure on nonlinear soil medium with some modification to be a practical problem.

The floor is chosen to be a slab of 22 [cm] thickness resting on skew paneled beams. The slab carries a uniform load of 11.8 [kN/m^2]. Foundation is considered as a raft foundation with openings. The dimensions of paneled beams, columns and foundation are the same as those of the previous example.

2   Soil properties

Two different types of soil models are considered in this case-study:

-        *Winkler*'s model that represents the subsoil by isolated springs
-        Layered model that considers the subsoil continuum medium

The foundation is resting on a soil layer of 10 [m], overlying a rigid base. The soil types are represented by the modulus of elasticity E_s, for layered model that yields modulus of subgrade reaction k_s, for *Winkler*'s model. Table 6.7 shows two different soil types examined in this study according to the soil properties E_s and k_s. The two soil types are selected to represent weak and stiff soil. *Poisson*'s ratio is taken $\nu_s = 0.3$ for the two soil types.

Table 6.7   Soil properties for two different soil types

Type of soil	k_s [kN/m^3]	E_s [kN/m^2]	q_{ult} [kN/m^2]
Weak soil	4000	18000	200
Stiff soil	40000	180000	400

3   Analysis

To show the difference between the results of linear and nonlinear analyses with and without interaction of superstructure for the two cases of soil models, the foundation is analyzed for both the two soil types four times as follows:

a)   As a plate resting on linear soil medium without the effect of superstructure rigidity
b)   As a plate resting on nonlinear soil medium without the effect of superstructure rigidity
c)   As a plate resting on linear soil medium with the effect of superstructure rigidity
d)   As a plate resting on nonlinear soil medium with the effect of superstructure rigidity

The raft foundation is divided into 504 square elements. Each element has the dimension of 1.25 [m] × 1.25 [m]. The typical floor is divided into 100 square plate elements. Each has dimensions of 1.0 [m] × 1.0 [m] to represent the floor slab. The plate elements are connected with 140 beam elements to represent the skew paneled beams.

For analyzing the foundation without interaction of the superstructure, the loads are obtained from floor reactions when analyzed as rested on fixed supports, Table 6.8.

Table 6.8   Loads on foundation without interaction of superstructure

Point	a	b	c	d	e	f
Load [kN]	480	1085	975	3000	2630	2270

The initial subgrade reactions k_{ti} for the continuum model are obtained from the linear analysis of foundation on Continuum model using Equation 6.24. For *Winkler*'s model, the initial subgrade reaction k_t is the same as that of the modulus of subgrade reaction k_s.

Because of the symmetry of structure in shape, load geometry and supporting soil about *x*- and *y*-axis, only one quarter of the structure is considered in the analysis.

4   **Results and discussion**

Figures 6.14 to 6.25 show the distribution of settlement, contact pressure and moment at section I for 16 cases of analysis. In general, it can be noticed from those figures for both models and types of soil that:

-        The settlement values from nonlinear analysis with or without interaction of superstructure are greater than those obtained from linear analysis at any node on the raft

-        The nonlinear analysis redistributes the contact pressure by decreasing its values under the columns and increasing the values at fields between columns. This makes the contact pressure approaches to the average pressure on the raft, especially for weak soil

-        According to the redistribution of the contact pressure on the raft due to nonlinear analysis, the column moment is increased, while the field moment is decreased

-        The maximum settlement, contact pressure and moment from the analysis with interaction of superstructure are less than those from the analysis without interaction
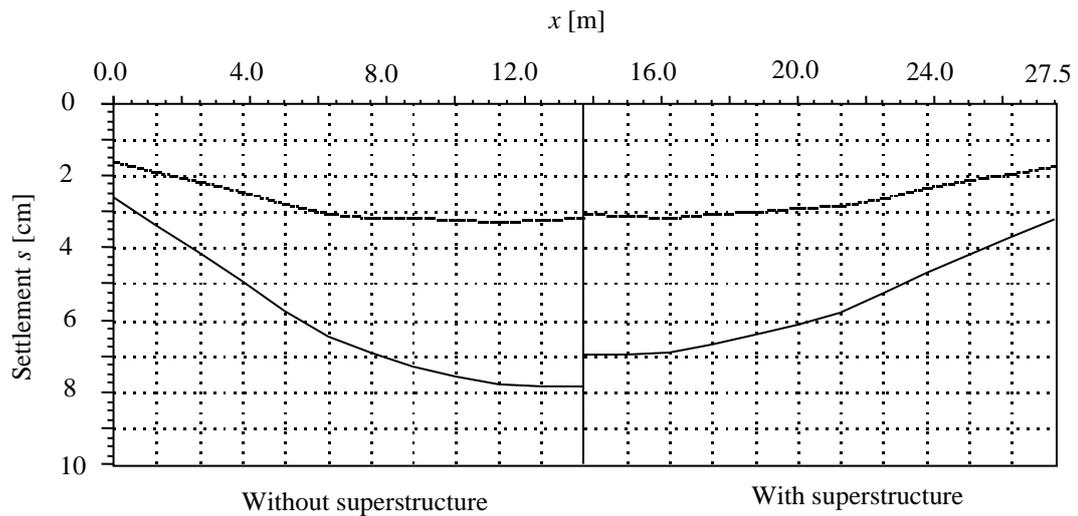
Figure 6.14   Settlement *s* [cm] at section I (*Winkler*'s model - weak soil)
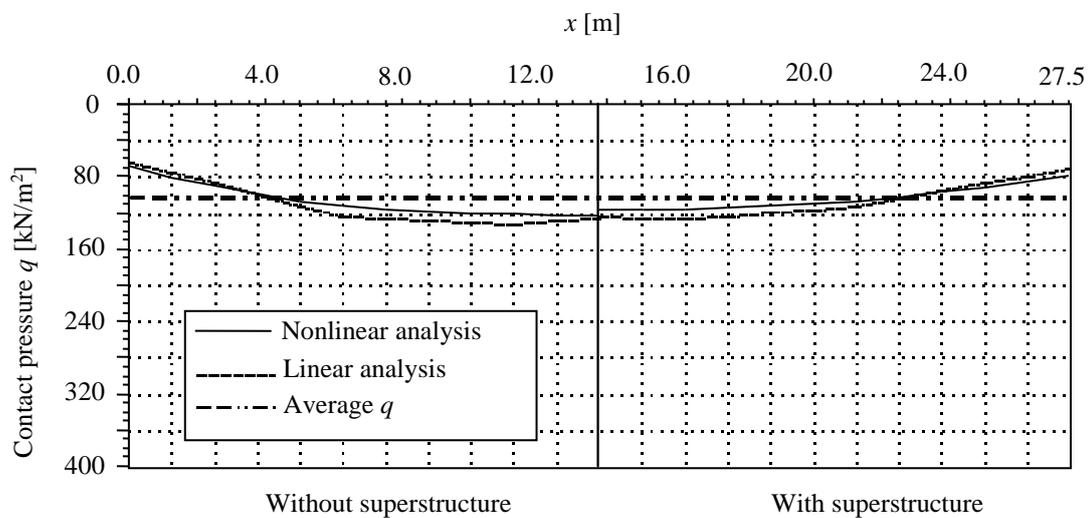
Figure 6.15   Contact pressure *q* [kN/m²] at section I (*Winkler*'s model - weak soil)
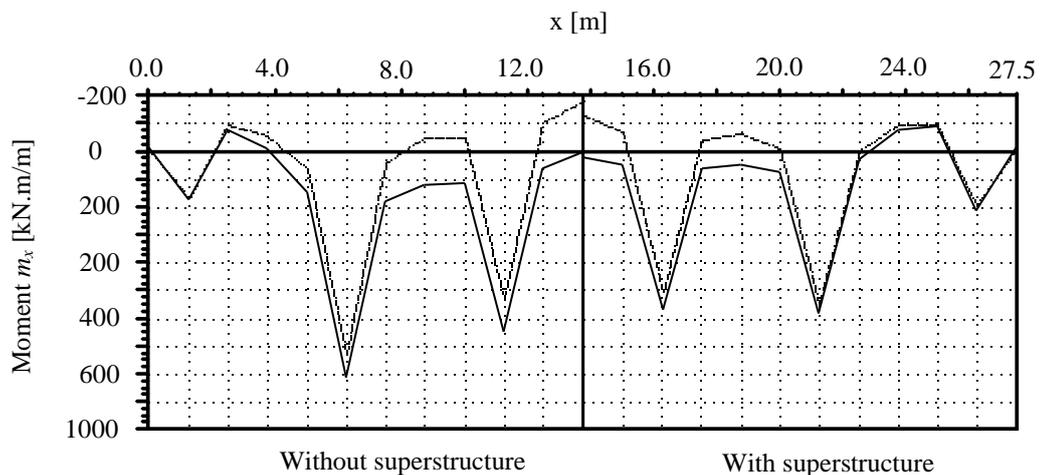
Figure 6.16   Moment m_x [kN.m/m] at section I (*Winkler*'s model - weak soil)
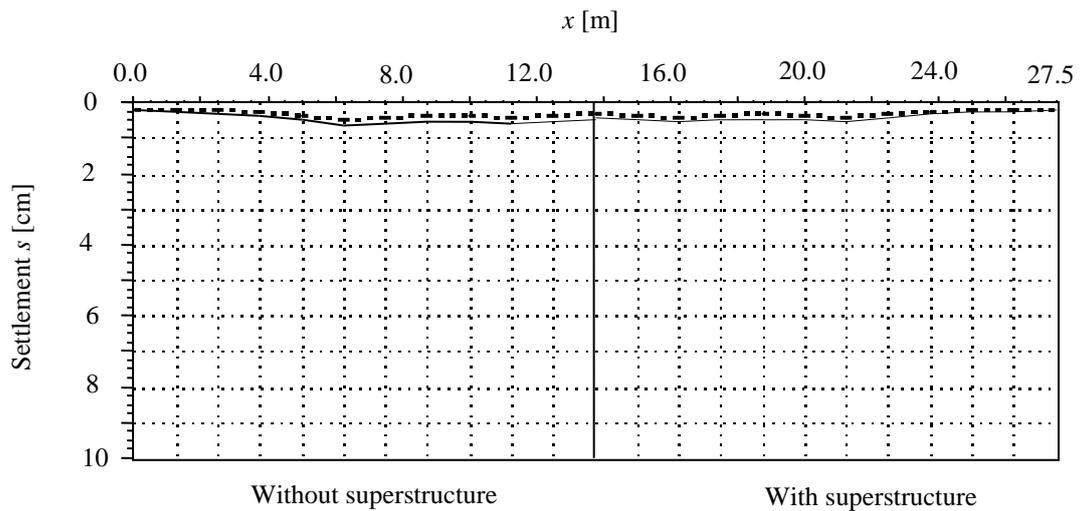
Figure 6.17   Settlement s [cm] at section I (*Winkler*'s model - stiff soil)
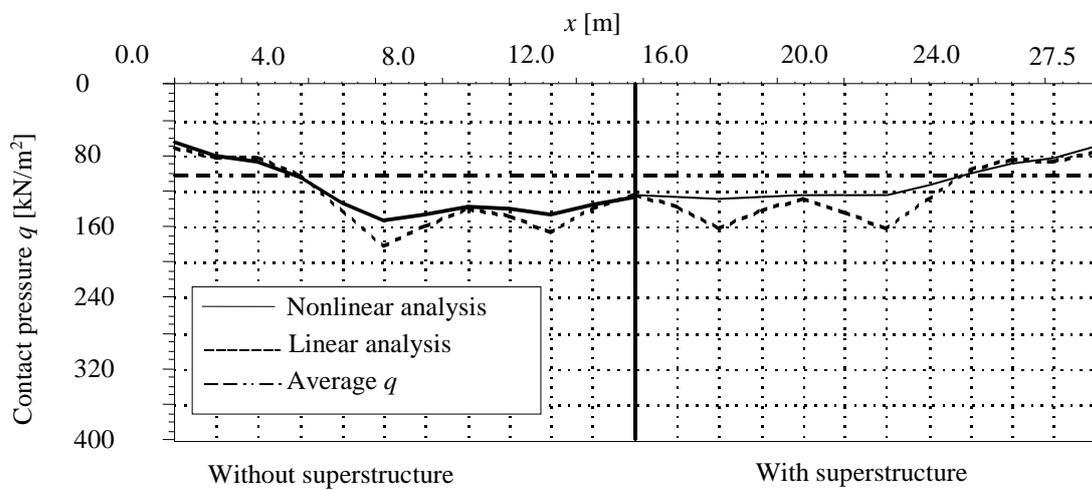
Figure 6.18   Contact pressure q [kN/m^2] at section I (*Winkler*'s model - stiff soil)
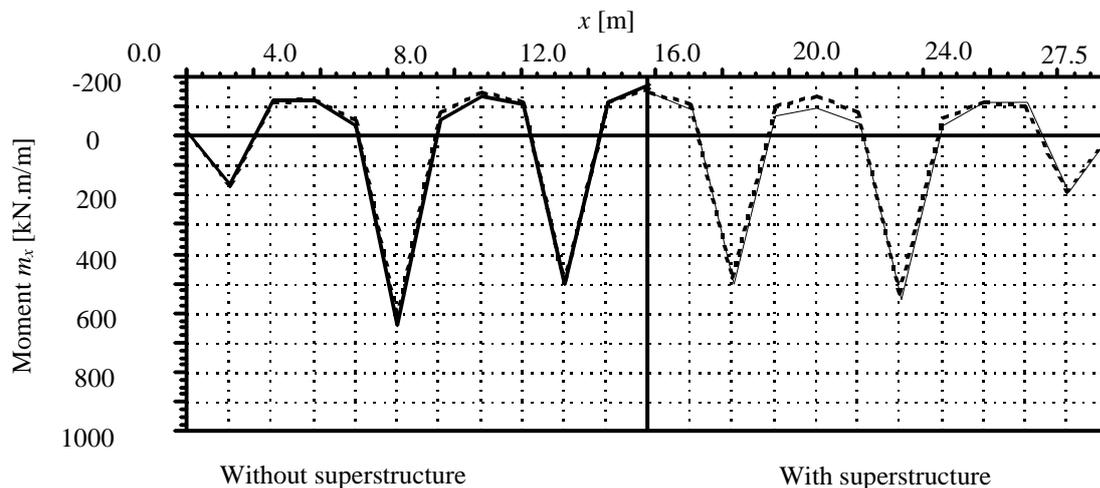
Figure 6.19   Moment m_x [kN.m/m] at section I (*Winkler*'s model - stiff soil)
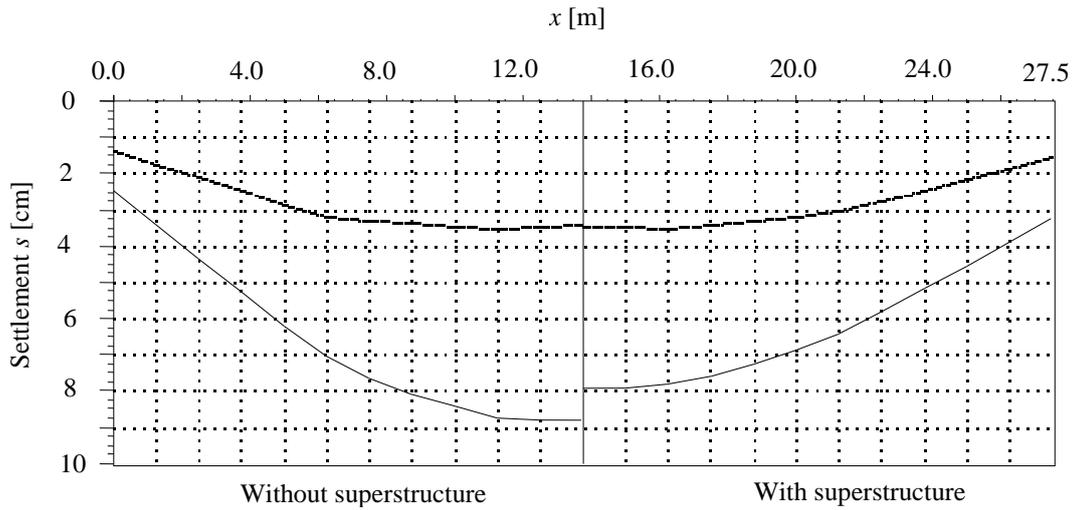
Figure 6.20   Settlement s [cm] at section I (layered model - weak soil)
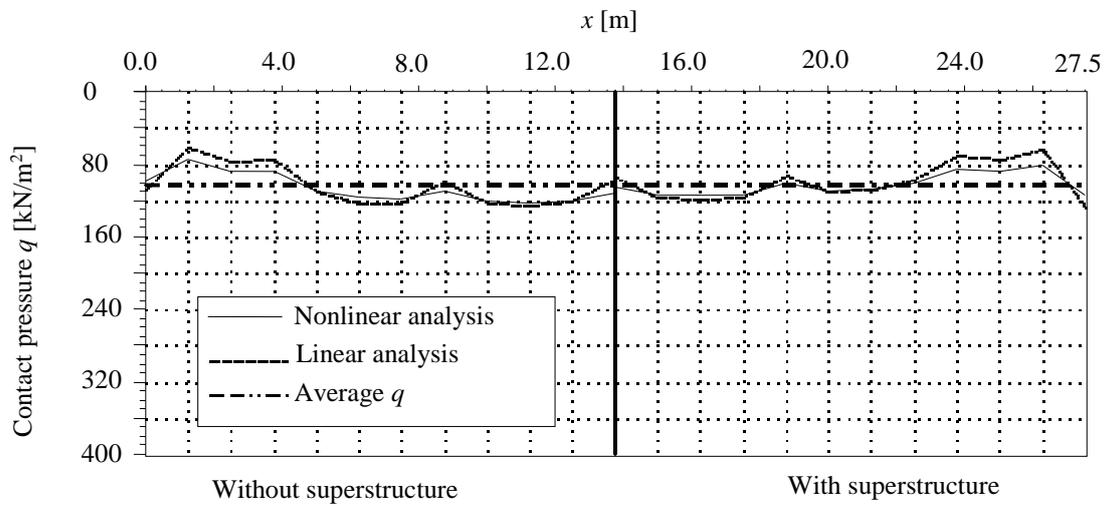
Figure 6.21   Contact pressure q [kN/m^2] at section I (layered model - weak soil)
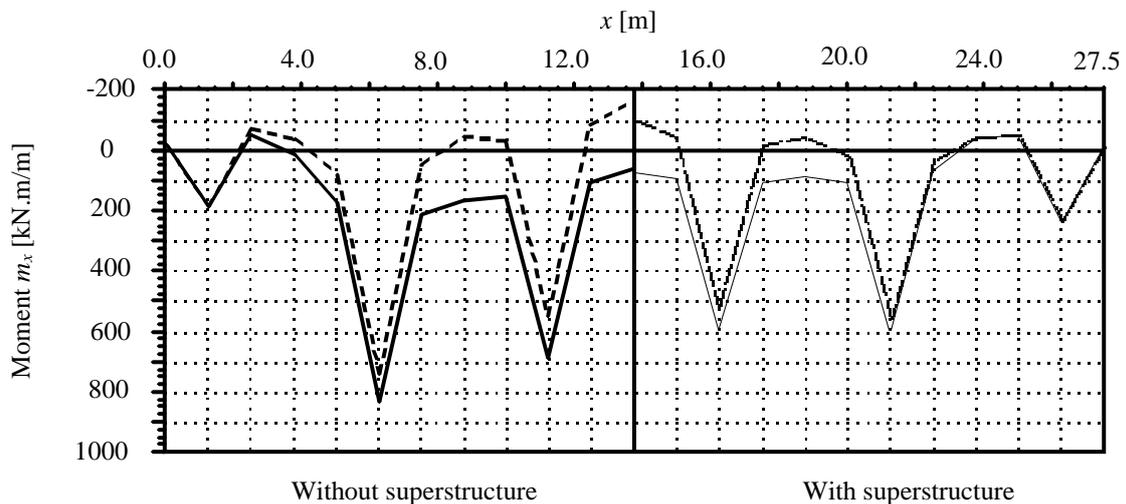
Figure 6.22   Moment m_x [kN.m/m] at section I (layered model - weak soil)
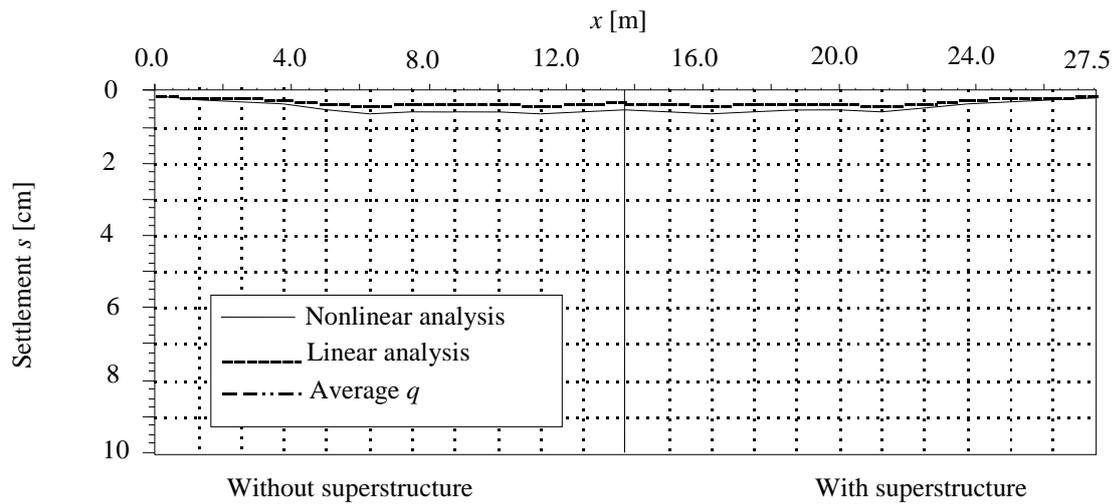
Figure 6.23   Settlement s [cm] at section I (layered model - stiff soil)
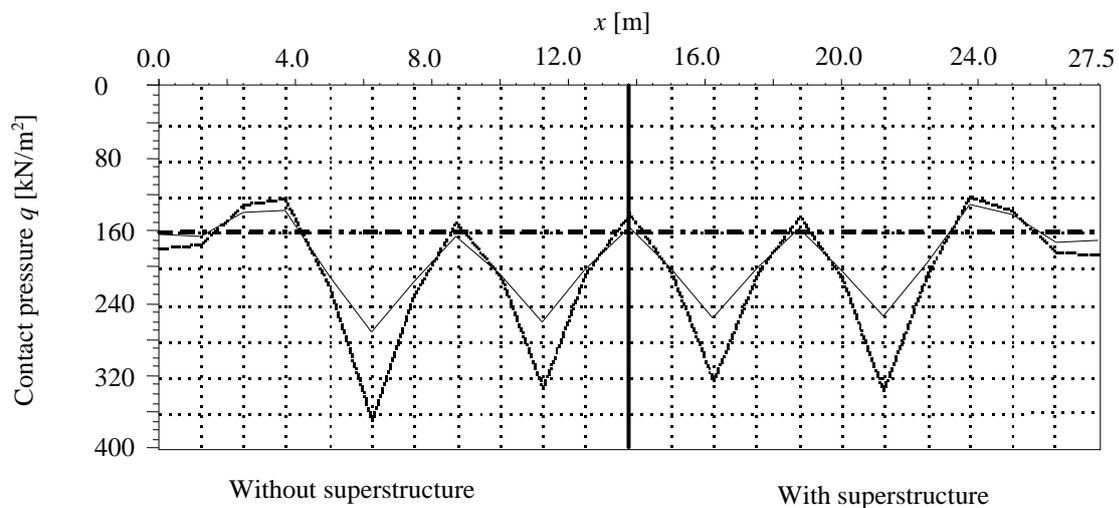
Figure 6.24   Contact pressure q [kN/m^2] at section I (layered model - stiff soil)
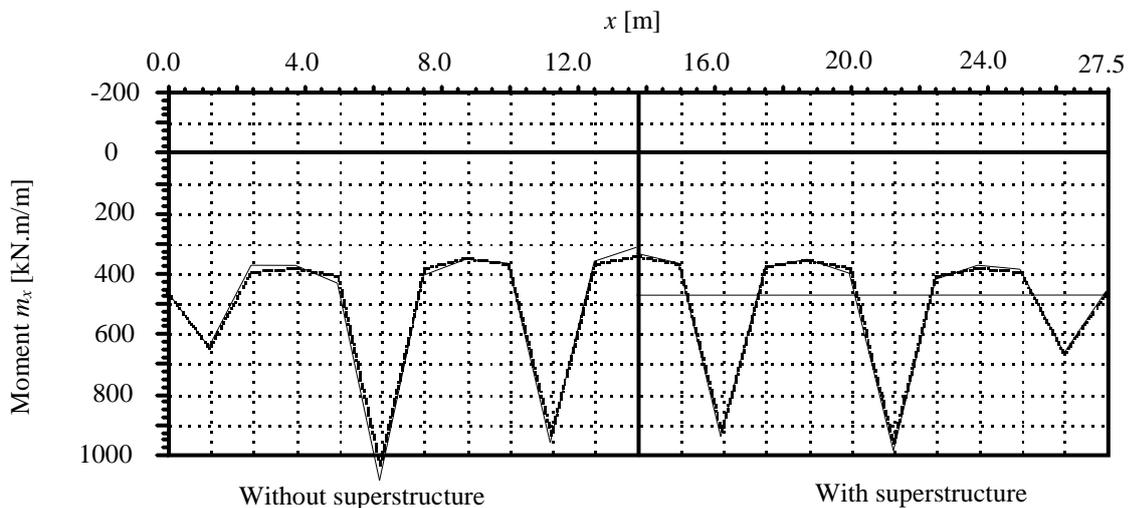
Figure 6.25   Moment m_x [kN.m/m] at section I (layered model - stiff soil)

The following Tables 6.9 to 6.12 show the maximum settlement, contact pressure under the columns, column moments and its differences Δ.

Table 6.9   Comparison of the maximum settlements max.s

Foundation-structure-interaction	Analysis of settlements	Settlements	weak soil $E_s = 18000$ [kN/m^2]		stiff soil $E_s = 180000$ [kN/m^2]	
			Winkler's model	Continuum model	*Winkler*'s model	Continuum model
without interaction	linear	s_{ln} [cm]	3.27	3.51	0.45	0.44
	nonlinear	s_{nl} [cm]	7.85	8.81	0.62	0.64
	$\Delta = 100 \times (s_{nl} - s_{ln}) / s_{ln}$ [%]		140	151	38	46
with interaction	linear	s_{ln} [cm]	3.15	3.50	0.41	0.42
	nonlinear	s_{nl} [cm]	6.94	7.93	0.54	0.58
	$\Delta = 100 \times (s_{nl} - s_{ln}) / s_{ln}$ [%]		120	126	32	38

Table 6.10   Comparison of the soil pressure q under the column

Foundation-structure-interaction	Analysis of settlements	Soil pressure	weak soil $E_s = 18000$ [kN/m^2]		stiff soil $E_s = 180000$ [kN/m^2]	
			Winkler's model	Continuum model	*Winkler*'s model	Continuum model
without interaction	linear	q_{ln} [kN/m^2]	131	126	182	310
	nonlinear	q_{nl} [kN/m^2]	122	122	152	212
	$\Delta = 100 \times (q_{nl} - q_{ln}) / q_{ln}$ [%]		-7	-3	-17	-32
with interaction	Linear	q_{ln} [kN/m^2]	126	119	163	276
	nonlinear	q_{nl} [kN/m^2]	115	114	139	196
	$\Delta = 100 \times (q_{nl} - q_{ln}) / q_{ln}$ [%]		-9	-4	-15	-29

Table 6.11   Comparison of the column moment m_x

Foundation-structure-interaction	Analysis of settlements	Column-moments	weak soil $E_s = 18000$ [kN/m^2]		stiff soil $E_s = 180000$ [kN/m^2]	
			Winkler's model	Continuum model	*Winkler*'s model	Continuum model
without interaction	linear	m_{ln} [kN.m/m]	725	742	609	557
	nonlinear	m_{nl} [kN.m/m]	812	836	638	613
	$\Delta = 100*(m_{nl} - m_{ln})/ m_{ln}$ [%]		12	13	5	10
with interaction	linear	m_{ln} [kN.m/m]	554	558	528	490
	nonlinear	m_{nl} [kN.m/m]	587	596	538	517
	$\Delta = 100*(m_{nl} - m_{ln})/ m_{ln}$ [%]		6	7	2	6

Table 6.12   Comparison of the field moment m_x

Foundation-structure-interaction	Analysis of settlements	Field-moments	weak soil $E_s = 18000$ [kN/m^2]		stiff soil $E_s = 180000$ [kN/m^2]	
			Winkler's model	Continuum model	*Winkler*'s model	Continuum model
without interaction	linear	m_{ln} [kN.m/m]	-184	-161	-162	-136
	nonlinear	m_{nl} [kN.m/m]	3.84	62	-178	-157
	$\Delta = 100\times(m_{nl} - m_{ln})/ m_{ln}$ [%]		102	139	10	15
with interaction	linear	m_{ln} [kN.m/m]	-125	-104	-153	-128
	nonlinear	m_{nl} [kN.m/m]	22	74	-159	-138
	$\Delta = 100\times(m_{nl} - m_{ln})/ m_{ln}$ [%]		118	171	4	9

Besides the above notes, the following results are reported (results are written without brackets for *Winkler*'s model, while in brackets ( ) for Continuum model):

Settlement (Table 6.9)

The maximum nonlinear settlement for weak soil exceeds maximum linear settlement by 140 [%] (151 [%]) and 120 [%] (126 [%]) for the analysis with and without interaction of superstructure, respectively, while for stiff soil by 38 [%] (46 [%]) and 32 [%] (38 [%]).

For both weak and stiff soil, the ratio between the maximum settlement from the analysis with interaction and that without interaction of superstructure is about 0.94 (0.97) for linear analysis, while this ratio decreases to 0.90 (0.90) for nonlinear analysis.

Contact pressure (Table 6.10)

The linear contact pressure for weak soil exceeds nonlinear contact pressure under the column by 8 [%] (4 [%]) for both analyses with and without interaction of superstructure, while for stiff soil by 16 [%] (31 [%]).

It is obvious that the contact pressure distribution patterns for *Winkler*'s model and Continuum model are not the same. The contact pressure under the columns for Continuum model are more than those of *Winkler*'s model by ratio of 1.7 for stiff soil. On the contrary to the case of stiff soil, this ratio is reduced to 0.95 for weak soil.

Moments (Tables 6.11 and 6.12)

For stiff soil, using either linear or nonlinear analysis the values of column moments are nearly the same. The difference between nonlinear and linear column moments does not exceed 5 [%] (10 [%]) and 2 [%] (6 [%]) for the analysis with and without interaction of superstructure respectively. This difference is slightly increased for field moments to 10 [%] (15 [%]) and 4 [%] (9 [%]).

For weak soil, there is also no significant change between linear and nonlinear column moments. But for field moments the difference between nonlinear and linear is 102 [%] (139 [%]) and 118 [%] (171 [%]) for the analysis with and without interaction of superstructure respectively. The results at section I also show that the field moment has changed from negative to positive at fields between columns due to the nonlinear analysis of the foundation.

Chapter 7

Nonlinear Analysis of Foundations

Contents

7.1   Nonlinear analysis of foundations for simple assumption model
7.1.1   Introduction

The simplest model for determination of the contact pressure under the foundation assumes a planar distribution of contact pressure on the bottom of the foundation (statically determined). In which the resultant of soil reactions coincides with the resultant of applied loads. If all contact pressures are compressive, the foundation system will be considered as linear and the contact pressure in this case is given directly by the following well-known formula

$$q_i = \frac{N}{A_f} + \frac{M_y\,I_x - M_x\,I_{xy}}{I_x\,I_y - I_{xy}^{\,2}}\,x_i + \frac{M_x\,I_y - M_y\,I_{xy}}{I_x\,I_y - I_{xy}^{\,2}}\,y_i \tag{7.1}$$

where:
N	Sum of vertical applied loads on the foundation	[kN]
q_i	Contact pressure at node i	[kN/m^2]
x_i	Coordinate of node i from the centroidal axis x	[m]
y_i	Coordinate of node i from the centroidal axis y	[m]
A_f	Foundation area	[m^2]
M_x	Moment due to N about the x-axis	[kN.m]
M_y	Moment due to N about the y-axis	[kN.m]
I_x	Moment of inertia of the foundation area about the x-axis	[m^4]
I_y	Moment of inertia of the foundation area about the y-axis	[m^4]
I_{xy}	Product of inertia	[m^4]

If the foundation subjects to big eccentricity, there will be negative contact pressures on some nodes on the foundation. Since the soil cannot resist negative stress, the foundation system becomes nonlinear and a resolution must be carried out to find the nonlinear contact pressures. The nonlinear analysis of foundation for the simple assumption model has been treated by many authors since a long time, where several analytical and graphical methods were available for the solution of this problem.

Pohl (1918) presented a table to determine the maximum corner pressure *max q_o* for arbitrary positions of the resultant *N*. *Hülsdünker* (1964) developed a diagram using the numerical values of this table from *Pohl* (1918) to determine the maximum corner pressure *max q_o*. For one corner detached footing, the closed form formulae cannot be used. Therefore, *Pohl* (1918) and *Mohr* (1918) proposed a method to estimate the neutral axis through the trial and error method. Besides tables and diagrams, *Graßhoff* (1978) introduced also influence line charts can be used to determine the contact pressure ordinates.

*Peck/ Hanso*n/ *Thornburn* (1974) indicated a trial and error method to obtain the neutral axis position for rectangular footing subjected to moments about both axes. *Jarquio/ Jarquio* (1983) proposed a direct method of proportioning a rectangular footing area subjected to biaxial bending. *Irles/ Irles* (1994) presented an analytical solution for rectangular footings with biaxial bending, which will lead to obtain explicit solutions for the corner pressures and neutral axis location.

The determination of the actual contact area and the maximum corner pressure *max q_o* under eccentric loaded foundation with irregular shape is very important. For T-shape foundation loaded eccentrically in the symmetry axis, *Kirschbaum* (1970) derived formulae to determine the maximum corner pressure *max q_o*. For some foundation areas with polygonal boundaries, *Dimitrov* (1977) gave formulae to determine the foundation kern and corner pressure *max q_o*. For the same purpose, *Miklos* (1964) developed diagrams. For general cases of foundation, *Opladen* (1958) presented graphical procedure.

Most of the analytical methods used to determine the contact area and corner pressures for eccentric loaded foundations are focused on regular foundations where irregular foundations can be analyzed only by graphical procedures. In this paper, an iteration procedure is presented to deal with nonlinear analysis of foundations for simple assumption model. The procedure can be applied for any arbitrary foundation shape and is suitable for computer programs as described in the following section.

7.1.2   Description of the procedure

In the procedure, the foundation is divided into rectangular finite elements. It is assumed that the contact pressure q_i can be replaced by equivalent force Q_i at the various nodal points. Consider the foundation shown in Figure 7.1 subjected to a big eccentricity. Then, the vector of contact pressures $\{Q\}^o$ obtained from the first analysis will contain some nodes with negative contact pressures. This vector can be rewritten in a form of separation vectors as

$$\{Q\}^{(o)} = \{Q_p\}^{(o)} + \{Q_n\}^{(o)} \tag{7.2}$$

where:
$\{Q_p\}^{(o)}$ Vector of positive contact pressures from the first analysis
$\{Q_n\}^{(o)}$ Vector of negative contact pressures from the first analysis

Now, instead of negative soil reactions $\{Q_n\}^{(o)}$ on the separation zone, equivalent reactions $\{\Delta Q\}^{(o)}$ over all foundation are to be found. This is achieved out in such a way that the resultant of soil reactions should equal and on the same line of action of the resultant of external loads. The iteration process to eliminate negative soil pressures for simple assumption model can be described in the following steps:

i   A new set of loads on the foundation are assumed where the vector $\{Q_n\}^{(o)}$
         represents these external applied loads at the same nodes

ii   Then, the vector $\{\Delta Q\}^{(o)}$ can be determined as the new soil reactions due to these
         applied loads using Equation 7.1

iii   The vector $\{\Delta Q\}^{(o)}$ is added to the vector of positive contact pressures $\{Q_p\}^{(o)}$
         to obtain the vector of redistributed contact pressures $\{Q\}^{(1)}$ as

$$\{Q\}^{(1)} = \{Q_p\}^{(o)} + \{\Delta Q\}^{(o)} \tag{7.3}$$

If new negative contact pressures appear, the above steps are repeated again until negative contact pressures no longer appear. Figure 7.1 shows the iteration cycle of the iteration process.

$$Q_i = q_i\, a_i\, b_i$$

Foundation with external load N

First analysis
$\{Q\}^{(o)} = \{Q_p\}^{(o)} + \{Q_n\}^{(o)}$

Foundation with external load $\{Q_n\}^{(o)}$

Equivalent reactions $\{\Delta Q\}^{(o)}$

Redistribution of Contact pressures
$\{Q\}^{(1)} = \{Q_p\}^{(o)} + \{\Delta Q\}^{(o)}$

New elimination

Check of negative pressure

Yes

No

Iteration end

(J) = Iteration cycle No.

i = Node No.
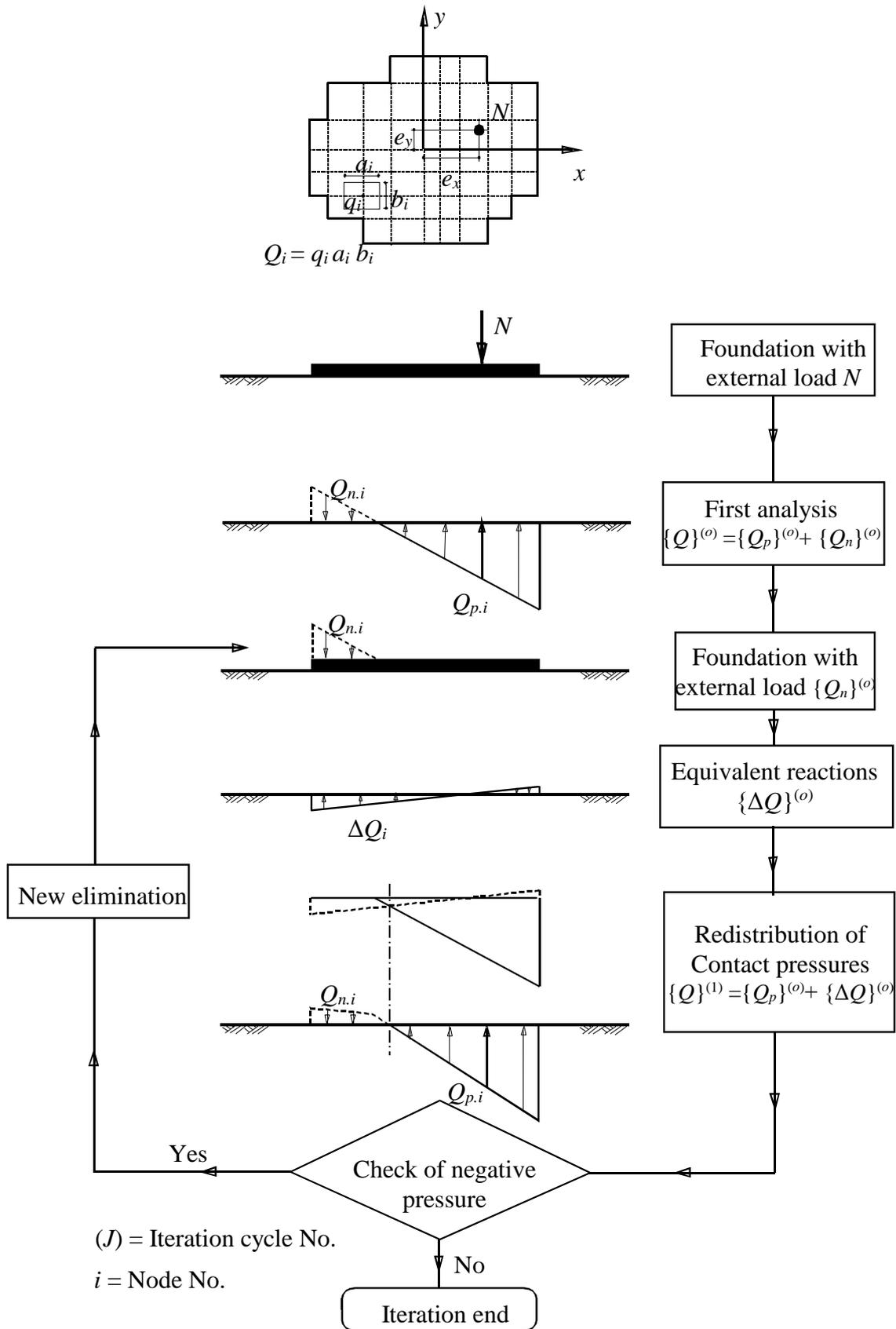
Figure 7.1   Iteration cycle of the iteration process

7.2   Nonlinear analysis of foundations for *Winkler*'s and Continuum models
7.2.1   Introduction

If the foundation carries heavy loads, there will be contact pressures on some nodes on the foundation much higher than the ultimate bearing capacity of the soil q_{ult}. Since the soil cannot resist such high pressure, the foundation system becomes nonlinear and a resolution must be carried out to find the nonlinear contact pressures. The nonlinear analysis of this problem for Continuum model was recorded by many authors, for example *Biedermann* (1981) and *Stark/ Majer* (1988). These methods based on specifying the maximum permissible contact pressure q^* in an iterative process during the analysis. The value of q^* is usually expressed as a proportion of the average applied pressure q_o on the foundation, typically $2q_o \leq q^* \leq 3\,q_o$ in practical applications. The first step in the analysis is to define the nodes that remain "elastic" and that become "plastic". Because the contact pressures of plastic nodes exceed the specified limit q^*, all the contact pressures in these nodes are reduced to q^*. Then, the foundation is analyzed again to obtain the modified contact pressures on the elastic nodes. If the new results show that the specified maximum contact pressure is exceeded at further nodes, then the entire procedure is repeated until convergence is reached.

A more realistic mathematical model for raft resting on nonlinear soil medium for *Winkler*'s model was presented by *Baz* (1987) and *Hasnien* (1993). In the mathematical model, the soil medium was represented by springs with nonlinear relation between the contact pressure of an individual spring and corresponding settlement. The model represents the nonlinear behavior of the contact pressure settlement at the raft soil interface by equation analogous to the hyperbolic function that represents the stress strain relationship of the soil.

*Kany/ El Gend*y (2000) developed this model for the analysis of foundation taking the effect of superstructure rigidity into account. Here, an extension for the nonlinear soil medium for *Winkler*'s model is made to represent the nonlinear behavior of elastic foundation on Continuum medium. In this case, the initial subgrade reaction is variable from one node to other and is obtained from the linear analysis of elastic foundation on Continuum medium.

In this study, a further extension for the above nonlinear soil medium for elastic foundation on Continuum medium is made to represent the nonlinear behavior of rigid foundation on Continuum medium. Also, an efficient method is presented to eliminate the negative contact pressures for elastic and rigid foundations on Continuum medium.

7.2.2   Description of the procedure

Elastoplastic analysis

The nonlinear analysis (Elastoplastic) for both *Winkler*'s and Continuum models based on a hyperbolic relation between contact pressures q_i and settlements s_i, which is given by

$$q_i = \frac{s_i}{\dfrac{1}{k_t} + \dfrac{s_i}{q_{ult}}} \tag{7.4}$$

where:

q_i	Contact pressure at node	[kN/m^2]
s_i	Soil settlement at node i	[cm]
k_t	Initial subgrade reaction	[kN/m^3]
q_{ult}	Ultimate bearing capacity of the soil	[kN/m^2]

The unknown parameters in Equation 7.4 are contact pressures q_i and settlements s_i. The initial subgrade reaction k_t for *Winkler*'s model is given for the problem and may be obtained directly from the elastic parameter of the soil. For either elastic or rigid foundation on Continuum medium, the initial subgrade reaction k_t is variable over all nodes and is obtained from the linear analysis of the problem as

$$k_{ti} = \frac{q_{li}}{s_{li}} \tag{7.5}$$

where:

k_{ti}	Initial subgrade reaction at node i	[kN/m^3]
s_{li}	Soil settlement at node i from linear analysis	[m]
q_{li}	Contact pressure at node i from linear analysis	[kN/m^2]

The ultimate bearing capacity of the soil q_{ult} in Equation 7.4 can be determined from Equation 7.6 according to DIN 4017 (1979)

$$q_{ult} = c\, N_c\, \nu_c + \gamma_1\, t_f\, N_d\, \nu_d + \gamma_2\, B\, N_b\, \nu_b \tag{7.6}$$

where:

t_f	Level of foundation under the ground surface	[m]
φ	Angle of internal friction of the soil	[°]
c	Cohesion of the soil	[kN/m^2]
γ_1	Unit weight of the soil above the foundation level	[kN/m^3]
γ_2	Unit weight of the soil under the foundation level	[kN/m^3]
B	Foundation width	[m]
A	Foundation length	[m]
N_c, N_d, N_b	Bearing capacity factors	[-]
	$N_d = e^{\pi\, tan\, \varphi}\, tan^2\, (45 + \varphi\,/\,2)$	
	$N_c = (N_d - 1)\, cot\, \varphi$	
	$N_b = (N_d - 1)\, tan\, \varphi$	
ν_c, ν_d, ν_b	Foundation shape factors	[-]
	$\nu_d = 1 + (B\,/\,A)\, sin\, \varphi$	
	$\nu_b = 1 - 0.3\, (B\,/\,A)$	
	$\nu_c = (\nu_d\, N_d - 1)\,/\,(N_d - 1)$	

For multi-soil system of n layers under the foundation level (Figure 7.2), the mean values of the soil constants φ_m, c_m and γ_m are determined by weighing the soil constant of the layer thickness h_i from n layers, in which the mean average values are given by

$$\varphi_m = \frac{\sum\limits_{i=1}^{n} \varphi_m\, h_i}{\sum\limits_{i=1}^{n} h_i}, c_m = \frac{\sum\limits_{i=1}^{n} c_m\, h_i}{\sum\limits_{i=1}^{n} h_i} \text{ und } \gamma_m = \frac{\sum\limits_{i=1}^{n} \gamma_i\, h_i}{\sum\limits_{i=1}^{n} h_i} \tag{7.7}$$

Here, a depth of the slide shape *max T_s* under the foundation dependent on φ_m is considered. Therefore, an iteration process is necessary. The iteration is repeated until the difference between the angle of internal friction which is determined from the iteration cycle i and that of the pervious cycle i - 1 is less than 0.1 [°]. According to DIN 4017 (1979), the mean values of the soil constants are only accepted, if the internal friction for each individual layer φ_i does not exceed the average value of the internal friction φ_{av} by 5 [°].
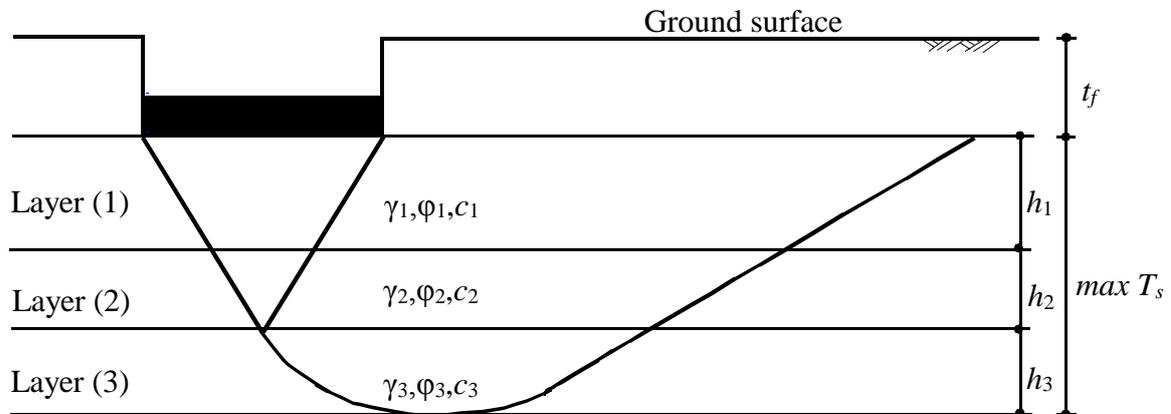
Figure 7.2   Ultimate bearing capacity for multi-layers system

For subsoil defined by number of boring logs, an interpolation among the ultimate bearing capacities of the boring logs may be carried out to take into account the irregularity of the soil in *x*- and *y*-directions.

Now the nonlinear behavior of the soil for both *Winkler*'s and Continuum models can be carried out as follows (Figure 7.3):

-        At an iteration cycle (j) the nonlinear contact pressure q_i at node i is

$$q_i^{(j)} = k_{si}^{(j)} s_i^{(j)} \qquad\qquad (7.8)$$

where k_{si} is the modulus of subgrade reaction at node i, and equal to the initial subgrade reaction k_{ti} at the first iteration cycle 1

-        For the next iteration cycle ($j + 1$) the modulus of subgrade reaction k_{si} is modified using Equation 7.9

$$k_{si}^{(j+1)} = \frac{1}{\dfrac{1}{k_{ti}} + \dfrac{s_i^{(j)}}{q_{ult}}} \qquad\qquad (7.9)$$

These steps have to be repeated until a specified tolerance ε between the nonlinear contact pressure q_i calculated from an iteration cycle (j) and that of the previous cycle ($j - 1$) is reached.
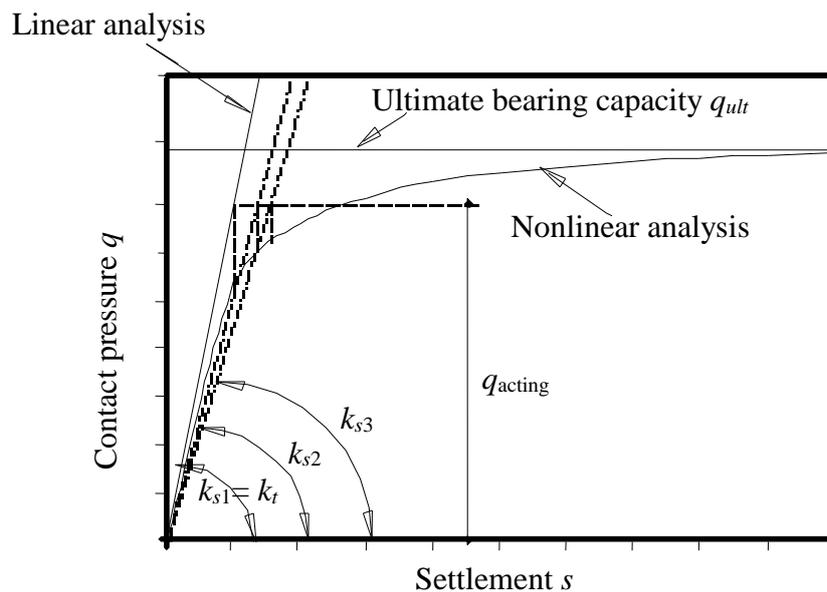
Figure 7.3   Nonlinear analysis procedure

Foundation separation analysis

In many cases for both elastic and elastoplastic analyses the results of foundation on either *Winkler*'s medium or Continuum medium include negative contact pressures. In practice, this means a separation between the foundation and the soil occurs. Therefore, it becomes necessary to continue the analysis to ensure that separation is allowed to occur, and that no contact pressures are at the separation zone.
For *Winkler*'s model, it is easy to eliminate the negative contact pressures by deleting the corresponding modulus of subgrade reaction k_s at nodes that have negative pressures. Then, the analysis is repeated until negative contact pressures no longer appear.

For elastic foundation on Continuum medium, *Cheung/ Nag* (1968) introduced an iterative procedure to eliminate the appropriate rows and columns in the flexibility matrix [c] and the solution is repeated using the modified stiffness matrix [k_s] until all contact pressures are compressive or zero. Thus the problem remains elastic but becomes nonlinear, as the compressive contact pressures are unknown. *El Gendy* (1994) applied the same procedure of *Cheung/ Nag* (1968) to rigid rafts on Continuum medium.

In this study, an efficient alternative method to eliminate the negative contact pressures is presented. The treatment of raft separation for either elastic or rigid raft on Continuum medium is similar to elastoplastic analysis. From the first analysis of the raft, the stiffness of the soil may be represented by individual springs of variable stiffness k_{si} through the known contact pressures and corresponding settlements. Then, it is easy to eliminate the negative contact pressures by deleting the soil stiffness k_{si} at the separated nodes. Then, the analysis of the raft on individual springs is repeated until negative contact pressures no longer appear.

As described before, in the nonlinear analysis (Elastoplastic and raft separation) for either elastic or rigid raft on Continuum medium, the subsoil on the nodes of the finite elements is represented by individual springs. Therefore, the system of linear equations in each iteration cycle is solved more efficiently as the soil stiffness matrix is a diagonal matrix, which in its original form is a full matrix. The solution is iterative, but convergence is usually rapid.

Example 7.1 Verification of nonlinear analysis for *Winkler*'s model

1   Description of the problem

To verify the nonlinear analysis of the program *ELPLA* for *Winkler*'s soil model, the results of a square footing resting on elastic springs obtained through nonlinear analysis by *Hasnien* (1993) are compared with those obtained by the program *ELPLA*.

A flexible square footing of 0.12 [m] thickness with dimensions of 2 [m] × 2 [m] is considered as shown in Figure 7.4.
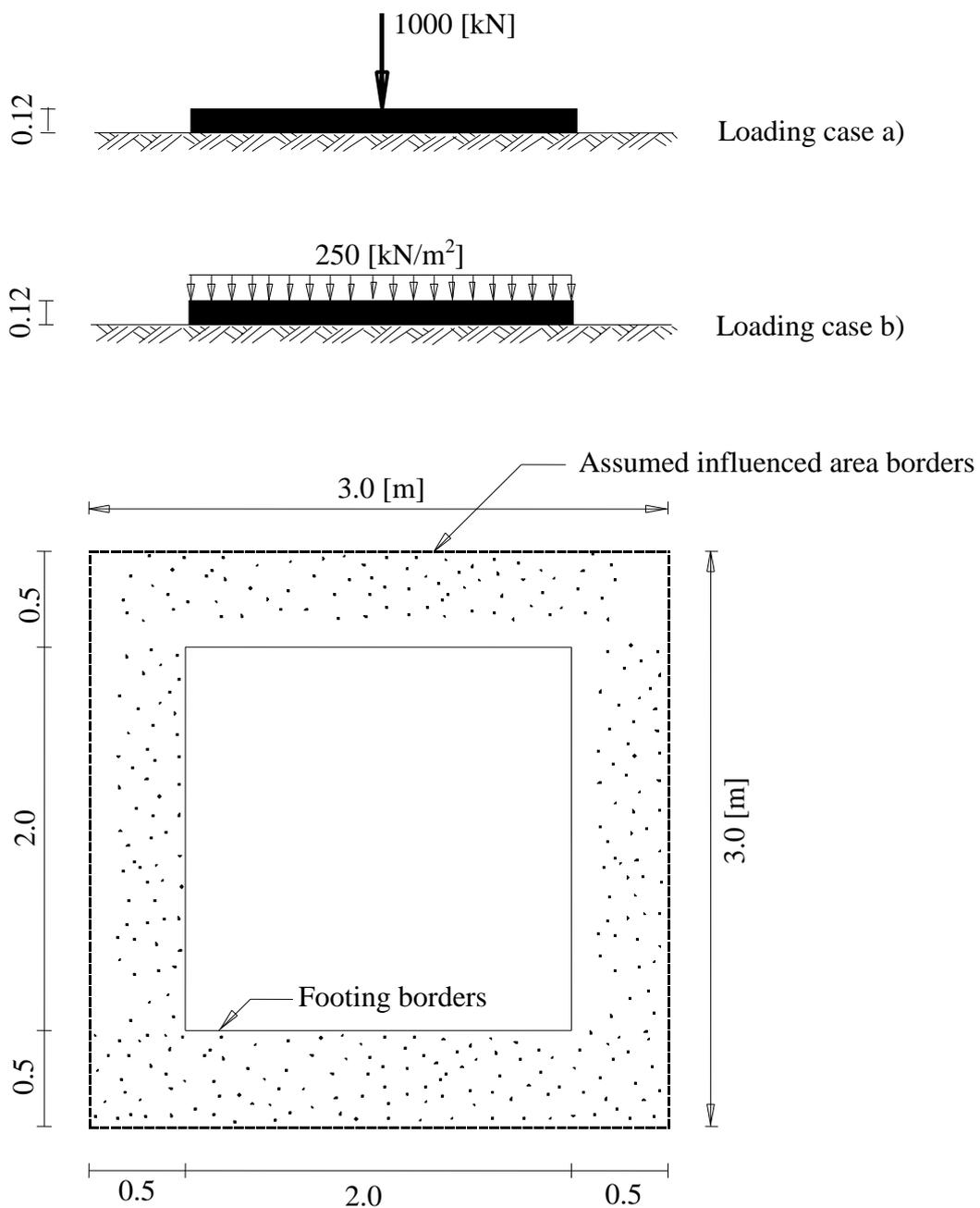
Figure 7.4   Footing geometry and loading

2   Soil properties

The soil under the footing has modulus of subgrade reaction $k_{st} = 30000$ [kN/m^3] and ultimate bearing capacity $q_{ult} = 600$ [kN/m^2].

3   Footing material

The footing material has the following parameters:

Young's modulus $E_b = 1.4 \times 10^7$ [kN/m^2]
Poisson's ratio $\nu_b = 0.15$ [-]
Unit weight $\gamma_b = 25$ [kN/m^3]

4   Analysis

Two cases of loading are studied:

a)   The footing carries a concentrated load of 1000   [kN]
b)   The footing carries a uniform load of 250   [kN/m^2]

To study the soil settlements outside the footing borders due to nonlinear analysis, imaginary surrounding elements of thickness 0.001 [m] are assumed to be around the footing. The footing and surrounding elements are subdivided into 144 square elements and each element has dimensions of 0.25 [m] × 0.25 [m].

5   Comparison

Tables 7.1 and 7.2 compare the results of settlements s, contact pressures q and moments m_x at the center of the footing obtained by *Hasnien* (1993) with those obtained by *ELPLA*. From these tables it can be seen that the results of both analyses are in good agreement.

Table 7.1   Comparison of the results at the center of the footing obtained by *Hasnien* (1993) and *ELPLA* (The footing carries a concentrated load of 1000 [kN])

Item	Type of analysis	*Hasnien* (1993)	*ELPLA*
Settlement s [cm]	Linear analysis	1.78	1.85
	Nonlinear analysis	2.55	2.58
Contact pressure q [kN/m^2]	Linear analysis	535	556
	Nonlinear analysis	337	338
Moment m_x [kN.m/m]	Linear analysis	213	272
	Nonlinear analysis	229	293

Table 7.2   Comparison of the results at the center of the footing obtained by *Hasnien* (1993) and *ELPLA* (The footing carries a uniform load of 250 [kN/m^2])

Item	Type of analysis	*Hasnien* (1993)	*ELPLA*
Settlement s [cm]	Linear analysis	0.78	0.81
	Nonlinear analysis	1.18	1.18
Contact pressure q [kN/m^2]	Linear analysis	232	242
	Nonlinear analysis	222	223
Moment m_x [kN.m/m]	Linear analysis	12	9
	Nonlinear analysis	13	12

Example 7.2   Rectangular foundation subjected to eccentric loading

1   Description of the problem

For comparison with complex foundation shape, no analytical solution is yet available. Therefore, for judgment on the nonlinear analysis of foundations for simple assumption model, consider the rectangular foundation shown in Figure 7.5. The foundation has the length $L = 8.0$ [m] and the width $B = 6.0$ [m]. The foundation carries an eccentric load of $N = 2000$ [kN]. Both of the x-axis and y-axis are main axes, which intersect in the center of gravity s of the foundation area. The position of resultant N is defined by the ordinates $x = e_x$ and $y = e_y$. Within the rectangle foundation area five zones are represented. It is found that the contact area and maximum corner pressure $max\ q_o$ depends on the position of the resultant N in these five zones (*Irles/ Irles* (1994)). In this example, the maximum corner pressure $max\ q_o$ is obtained using the program *ELPLA* for each zone and compared with other analytical salutations, which are available for rectangular foundation.
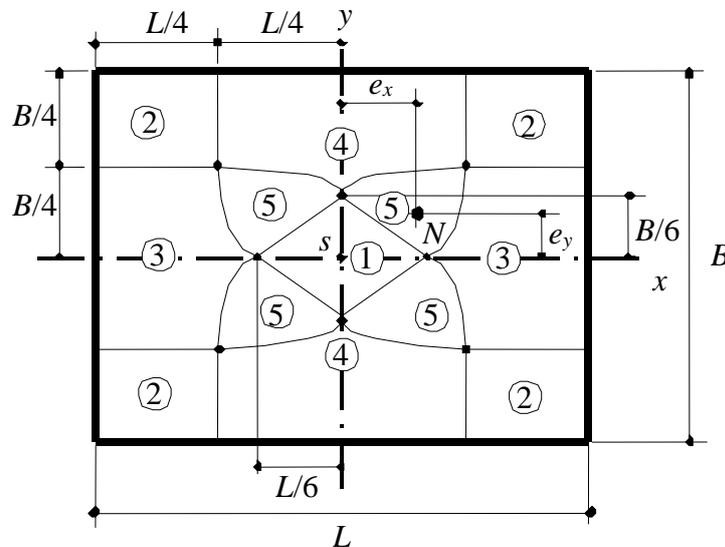
Figure 7.5   Division of the rectangular foundation in five zones
                according to the position of the resultant N

2   Hand calculation of the maximum corner pressure *max q_o*

The maximum corner pressure *max q_o* for the zone (1) can be obtained directly using Equation 7.1, where in this case the Resultant *N* lies in the foundation kern and no separation will occur. The maximum corner pressure *max q_o* for the other four zones can be obtained using available analytical solutions according to *Irles/ Irles* (1994), *Teng* (1962) and *Graßhoff/ Kany* (1997) as follows:

Zone (2)
Three corners detached (e_x = 3.0 [m], e_y = 2.25 [m])

The maximum corner pressure *max q_o* for zone (2), Figure 7.6a, can be given according to *Irles/ Irles* (1994) from the following equation

$$\max q_o = \frac{3\,N}{2\,(L - 2\,e_x)(B - 2\,e_y)}$$

$$\max q_o = \frac{3 \times 2000}{2\,(8 - 2 \times 3)(6 - 2 \times 2.25)} = 1000\,[\text{kN/m}^2]$$

Zone (3)
Two corners detached (e_x = 3.0 [m], e_y = 0.0 [m])

The maximum corner pressure *max q_o* for zone (3), Figure 7.6b, can be given according to *Teng* (1962) from the following equation

$$\max q_o = \frac{N}{L\,B}\left(\frac{4\,L}{3\,L - 6\,e_x}\right)$$

$$\max q_o = \frac{2000}{8 \times 6}\left(\frac{4 \times 8}{3 \times 8 - 6 \times 3}\right) = 222.22\,[\text{kN/m}^2]$$

Zone (4)
Two corners detached (e_x = 1.0 [m], e_y = 2.25 [m])

The maximum corner pressure *max q_o* for zone (4), Figure 7.6c, can be given according to *Graßhoff/ Kany* (1997) from the following equation

$$t = \frac{L}{12}\left(\frac{L}{e_x} + \sqrt{\frac{L^2}{e_x^{\,2}} - 12}\right) = \frac{8}{12}\left(\frac{8}{1.0} + \sqrt{\frac{8^2}{1.0^2} - 12}\right) = 10.141\,[\text{m}]$$

$$\tan\beta = \frac{3}{2}\left(\frac{B - 2\,e_x}{t + e_x}\right) = \frac{3}{2}\left(\frac{6 - 2 \times 2.25}{10.141 + 1.0}\right) = 0.202$$

$$\max q_o = \frac{12\,N}{L\,\tan\beta}\,\frac{L + 2\,t}{L^2 + 12\,t^2} = \frac{12 \times 2000}{8 \times 0.202}\,\frac{8 + 2 \times 10.141}{8^2 + 12 \times 10.141^2} = 323.58\,[\text{kN/m}^2]$$

Zone (5)
Only one corner detached ($e_x = 1.0$ [m], $e_y = 0.75$ [m])

The maximum corner pressure *max q_o* for zone (5), Figure 7.6d, can be given according to *Graßhoff/Kany* (1997) from the following equation

$$K = \frac{e_x}{L} + \frac{e_y}{B} = \frac{1.0}{8} + \frac{0.75}{6} = 0.25$$

$$\max q_o = \frac{N}{LB} K \left[12 - 3.9 \left(6K - 1\right)\left(1 - 2K\right)\left(2.3 - 2K\right)\right]$$

$$\max q_o = \frac{2000}{8 \times 6} K \left[12 - 3.9 \left(6 \times 0.25 - 1\right)\left(1 - 2 \times 0.25\right)\left(2.3 - 2 \times 0.25\right)\right]$$

$$\max q_o = 106.72 \, [\text{kN/m}^2]$$
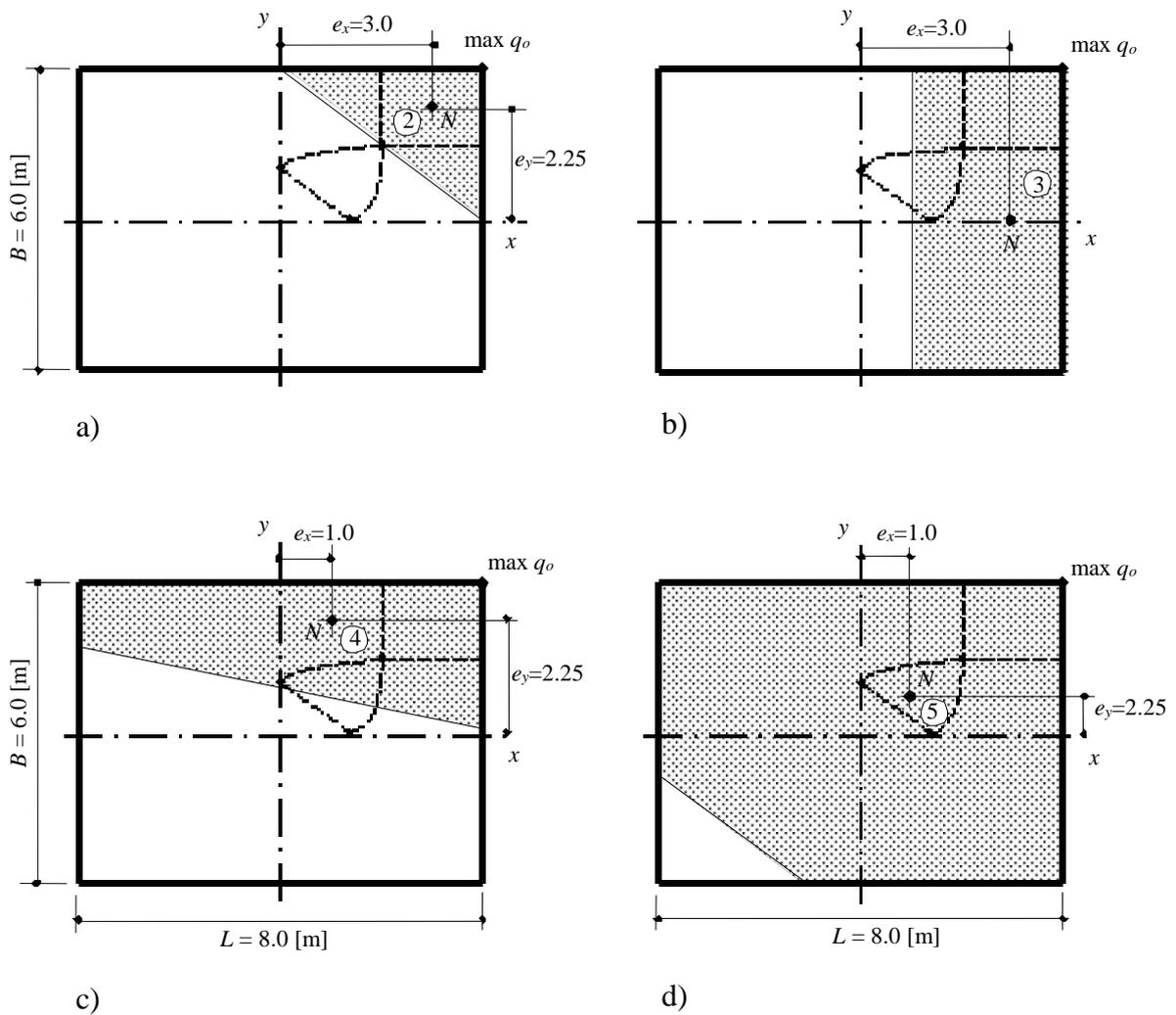
Figure 7.6   Resultant *N* lies in the four zones (2) to (5)

3   Determination of the maximum corner pressure *max q$_o$* by the program *ELPLA*

To achieve the comparison between the maximum corner pressure *max q$_o$* obtained from the program *ELPLA* and that obtained from the other available analytical solutions described above, the rectangular foundation is subdivided into refine mesh of square finite elements. Each element has a side of 0.1 [m]. The results obtained from the program *ELPLA* are compared with those obtained above in Table 7.3. It shows that the results of both the analytical and iteration methods are in a good agreement.

Table 7.3   Comparison between the maximum corner pressure *max q$_o$* [kN/m^2] obtained from program *ELPLA* and that obtained from the available analytical solutions

Zone No.	Zone (2)	Zone (3)	Zone (4)	Zone (5)
Available solutions	*Irles/ Irles* (1994)	*Teng* (1962)	*Graßhoff/ Kany* (1997)	
	1000	222	324	107
ELPLA	1017	223	325	106
Difference [%]	1.67	0.45	0.31	0.94

Example 7.3   Circular foundation subjected to eccentric loading

1   Description of the problem

Another example is considered to show the applicability of nonlinear analysis of foundations using the program *ELPLA* for simple assumption model to different foundation types. The results of nonlinear analysis for a circular raft calculated by *Teng* (1962) are compared with those obtained by the program *ELPLA*.

A circular raft of radius $r = 5$ [m] is considered as shown in Figure 7.7. The raft carries an eccentric load of $N = 2000$ [kN]. The position of the resultant N is defined by the ordinate e.
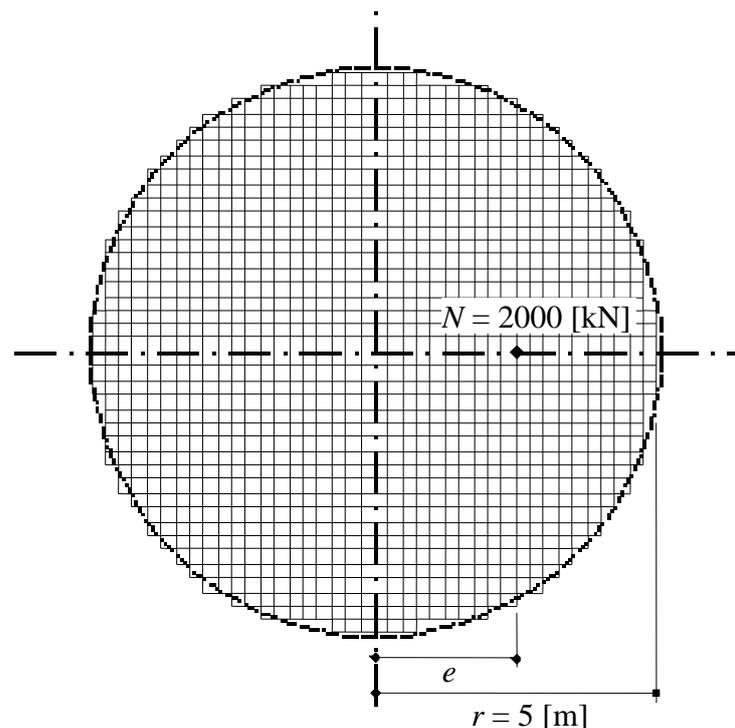
Figure 7.7   Plan of the circular raft with dimensions and FE-Net

2   Analysis
2.1   Simple assumption model

To carry out the comparison, the raft is subdivided into 1238 square elements. Each element has a side of 0.25 [m]. The contact pressures q under the middle of the raft are obtained in Figure 7.8 at different ratios e/r, which shows also the separation zones. The ratio e/r ranges from 0.25 to 0.75.
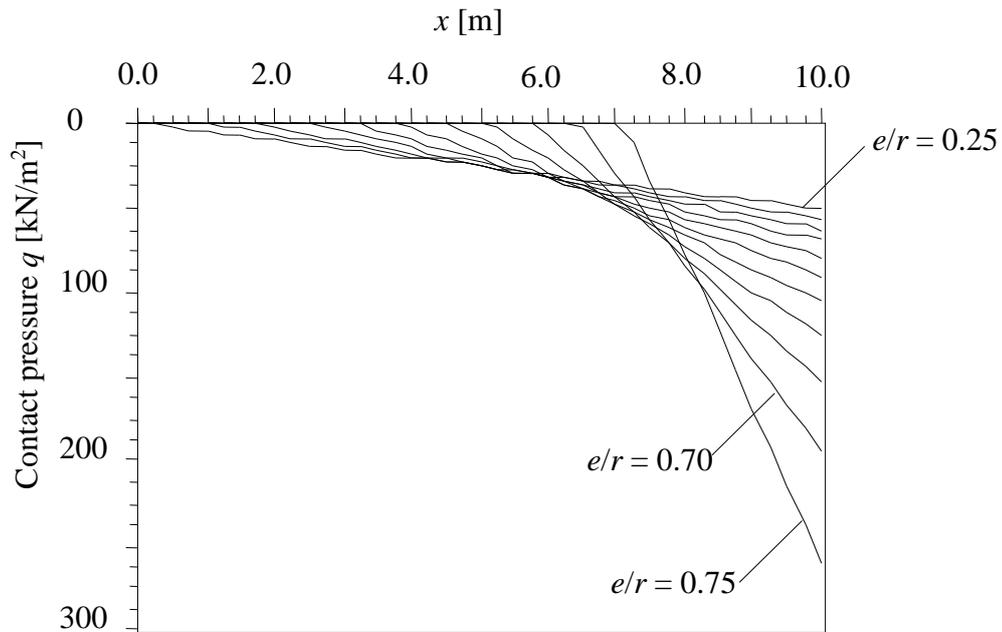
Figure 7.8   Contact pressures q [kN/m^2] under the circular raft at different values of e/r

The coefficient $k = max \, q_o \, \pi \, r^2/N$ at different ratios e/r obtained from the program *ELPLA* is plotted and compared with the results obtained by *Teng* (1962) in Figure 7.9. It can be concluded from this figure that the results of nonlinear analysis of the circular raft using the program *ELPLA* and those of *Teng* (1962) are in a good agreement.
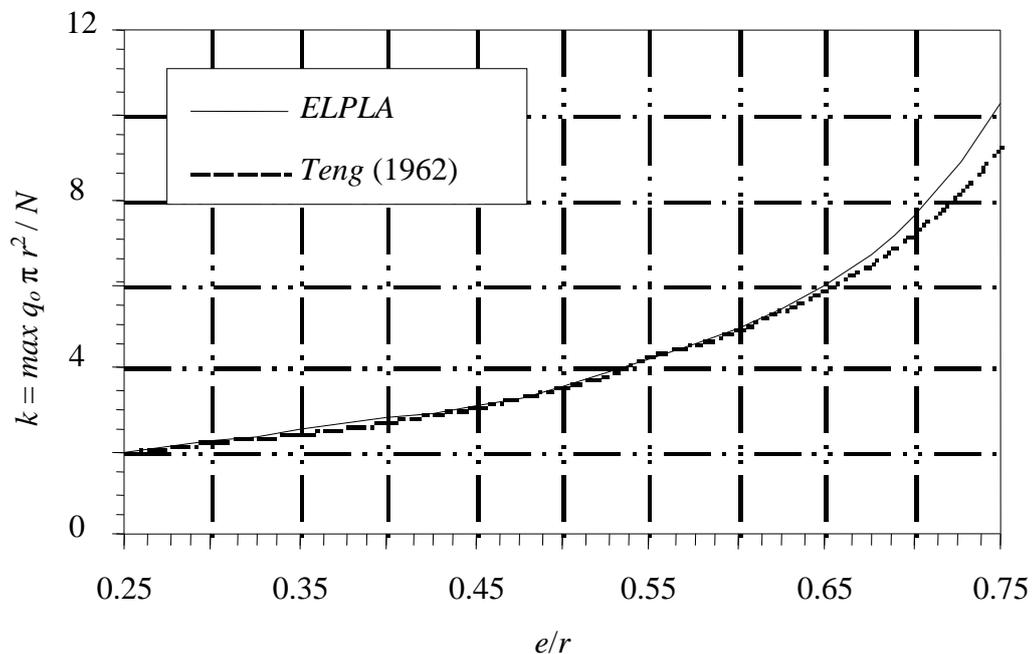
Figure 7.9   Coefficient $k = max \, q_o \, \pi \, r^2/N$ at different ratios e/r

2.2   Rigid raft on Continuum medium

Although it is easy to drive closed form equations for raft separation in case of regular rafts for simple assumption model, but it is difficult to drive such equations for circular rigid rafts. For this reason, the same circular raft is analyzed again for rigid raft on Continuum medium to show the applicability of the nonlinear analysis of foundations using the program *ELPLA* for different soil models. The subsoil under the raft is chosen to be a layer of sand, which has the following parameters:

Modulus of compressibility $E_s = 12\ 000$ [kN/m^2]
Poisson's ratio $\nu_s = 0.25$ [-]
Layer depth $z\ = 10$ [m]

The core of the circular raft, in which no separation occurs when the resultant *N* lies in it, takes a radius *r*/4 in case of simple assumption model, while in case of rigid raft on Continuum medium takes a radius *r*/3. Therefore, the rigid raft is analyzed for different ratios *e*/*r* from 0.35 to 0.75. Figure 7.10 shows the contact pressures *q* under the raft at different values of *e*/*r*, while Figure 7.11 shows the settlements *s*.
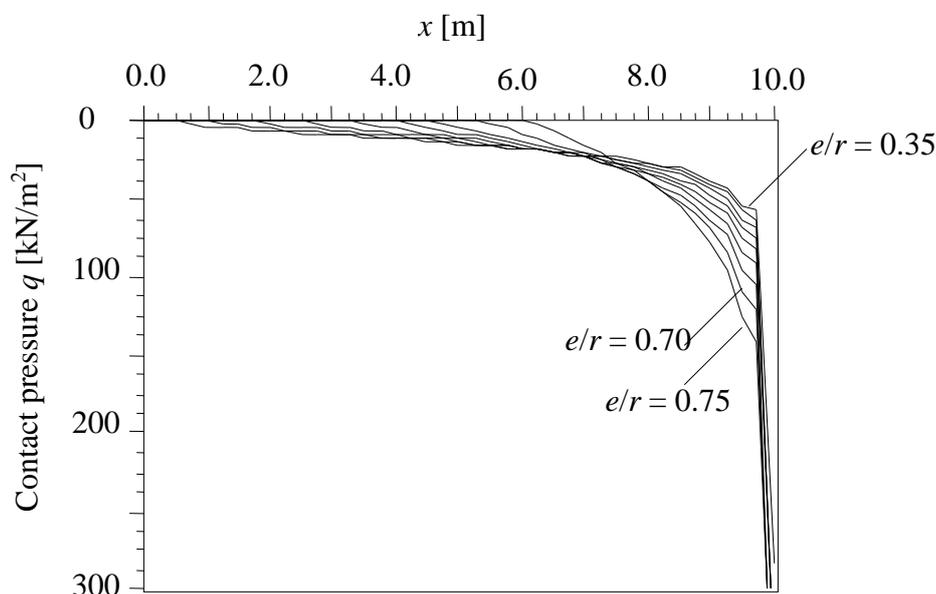
Figure 7.10   Contact pressures *q* [kN/m^2] under rigid circular raft at different values of *e*/*r*

A comparison between Figure 7.8 and Figure 7.10 shows that the effective contact area for the raft in case of simple assumption model is less than that of rigid raft on Continuum medium at the same corresponding ratio *e*/*r*. The effective contact area and effective width may be used to determine the ultimate load for the foundation, which carries eccentric loading. Figure 7.11 shows that the separation zones have upward settlements.

The effective contact width *c* for the circular raft is given in a non-dimensional form in Figure 7.12. Depending on the nature of the load eccentricity and the radius of the raft, once the magnitudes of the effective width and the effective area are determined, they can be used in Equation 7.6 to determine the ultimate load of the raft.
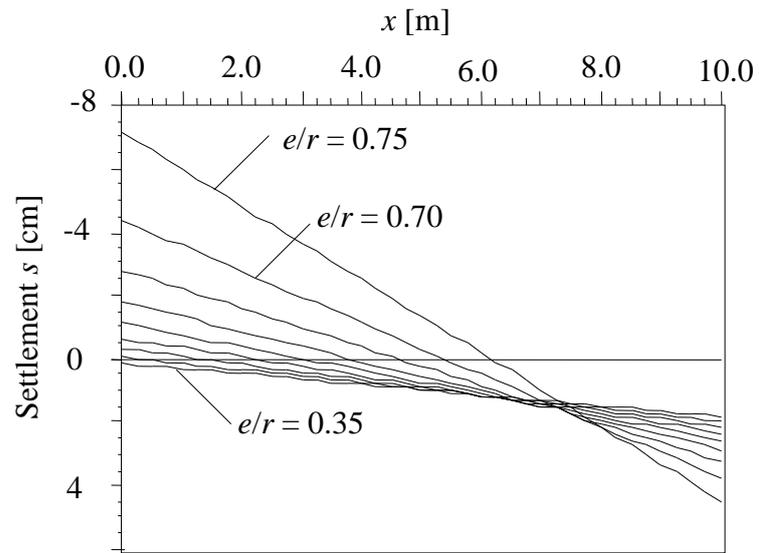
Figure 7.11   Settlements s [cm] under rigid circular raft at different values of e/r
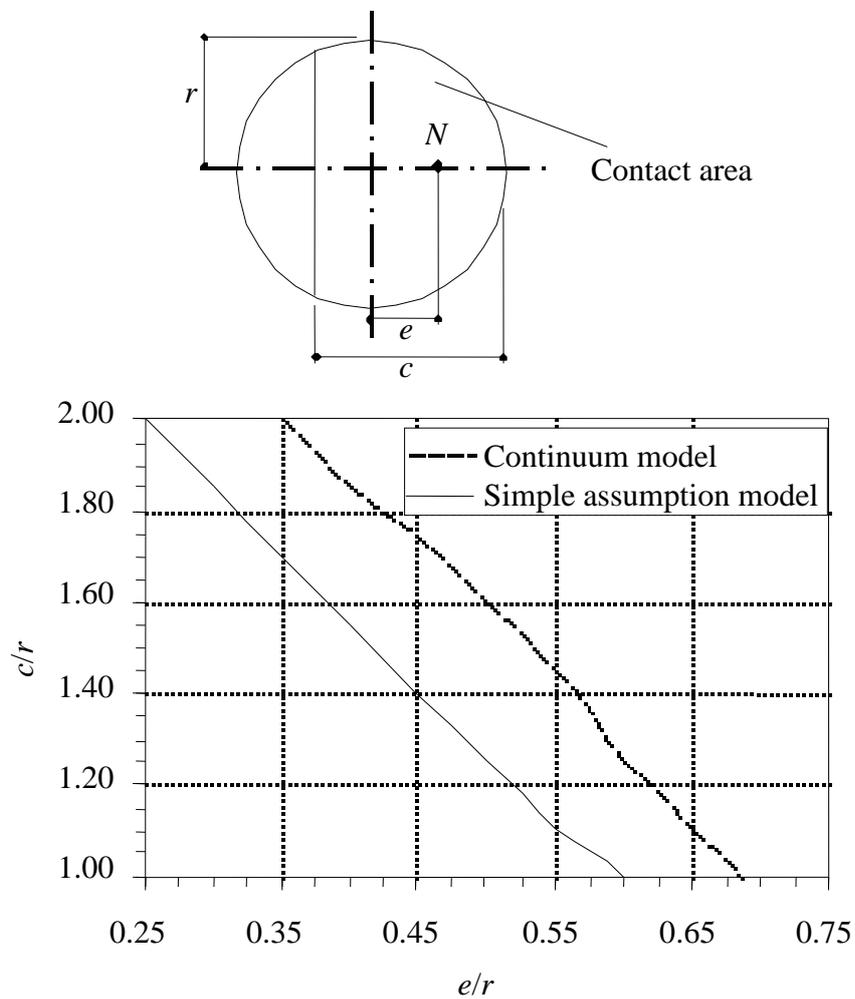
Figure 7.12   Diagram to determine the contact width c of the circular raft by eccentric loading

Example 7.4 Elastoplastic analysis of a raft resting on Continuum medium

1   Description of the problem

One of the difficulties by applying the Continuum model to practical problems is the appearance of the high contact pressures at the raft edges, especially when the raft carries heavy loads. The appearance of plastic zones at the raft edges is related to the traditional mathematical soil models used in the analysis, which depend on the theory of elasticity. Therefore, an application example is carried out to show the applicability of the developed nonlinear analysis to redistribute the high contact pressures at the edges of both elastic and rigid rafts.

A rectangular raft with dimensions of 8×16 [m^2] is chosen and subdivided into 512 square elements. Each element has a side of 0.5 [m] as shown in Figure 7.13. The raft carries a uniform load of 600 [kN/m^2].
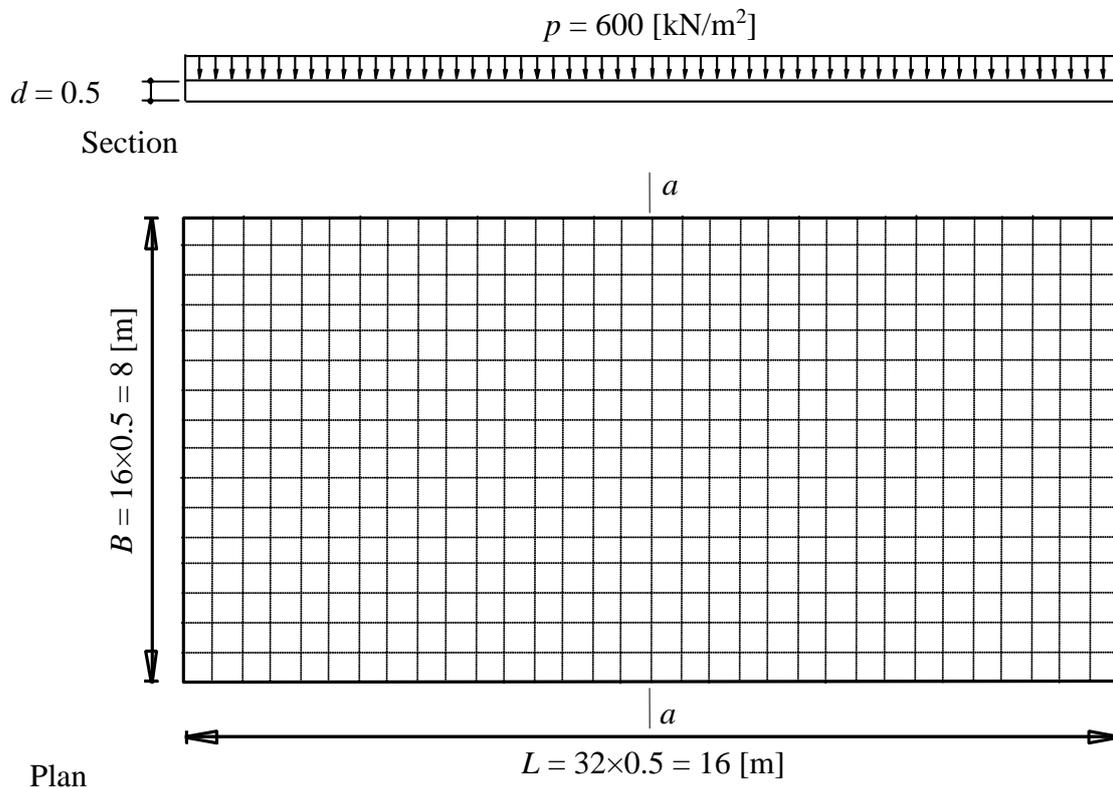
Figure 7.13   Raft geometry, loading and FE-Net

2   Soil properties

The raft rests on a homogeneous sand layer of thickness 10 [m], overlying a rigid base. The sand layer was supposed to have the following parameters:

Modulus of compressibility	$E_s = 12\ 000$	[kN/m^2]
Poisson's ratio	$\nu_s = 0.25$	[-]
Unit weight	$\gamma_s = 17.5$	[kN/m^3]
Angel of internal friction	$\varphi = 27.5$	[°]
Cohesion	$c = 0.0$	[kN/m^2]
Foundation depth under the ground surface	$t_f = 0.5$	[m]

3   Raft material and thickness

The raft material and thickness were supposed to have the following parameters:

Raft thickness	$d = 0.5$	[m]
Young's modulus	$E_b = 3 \times 10^7$	[kN/m^2]
Poisson's ratio	$\nu_b = 0.15$	[-]
Unit weight	$\gamma_b = 0.0$	[kN/m^3]

Unit weight of the raft is chosen $\gamma_b = 0.0$ [kN/m^3] to neglect the self-weight of the raft.

4   Analysis

The nonlinear analysis of the raft was carried out for both elastic and rigid rafts on Continuum medium. Two cases concerning the ultimate bearing capacity q_{ult} are considered as follows:

i)   The ultimate bearing capacity q_{ult} is uniform.
        Its value is obtained from Equation 7.6, $q_{ult} = 1603$ [kN/m^2]

ii)   The ultimate bearing capacity q_{ult} is variable.
        The ultimate bearing capacity q_{ult} at the raft edges is determined from the second term of Equation 7.6, $q_{ult} = \gamma_1\ t_f\ N_d\ \nu_d = 951$ [kN/m^2], while the ultimate bearing capacity q_{ult} at the raft center is determined from Equation 7.6 when the third term is doubled, $q_{ult} = \gamma_1\ t_f\ N_d\ \nu_d + 2\ \gamma_2\ B\ N_b\ \nu_b = 1753$ [kN/m^2]. Figure 7.14 shows the contour lines of the variable ultimate bearing capacity q_{ult}

B3 (0.0, 8.0)   a   B4 (16.0, 8.0)

B5 (4.0, 8.0)

B1 (0.0, 0.0)   a   B2 (16.0, 0.0)
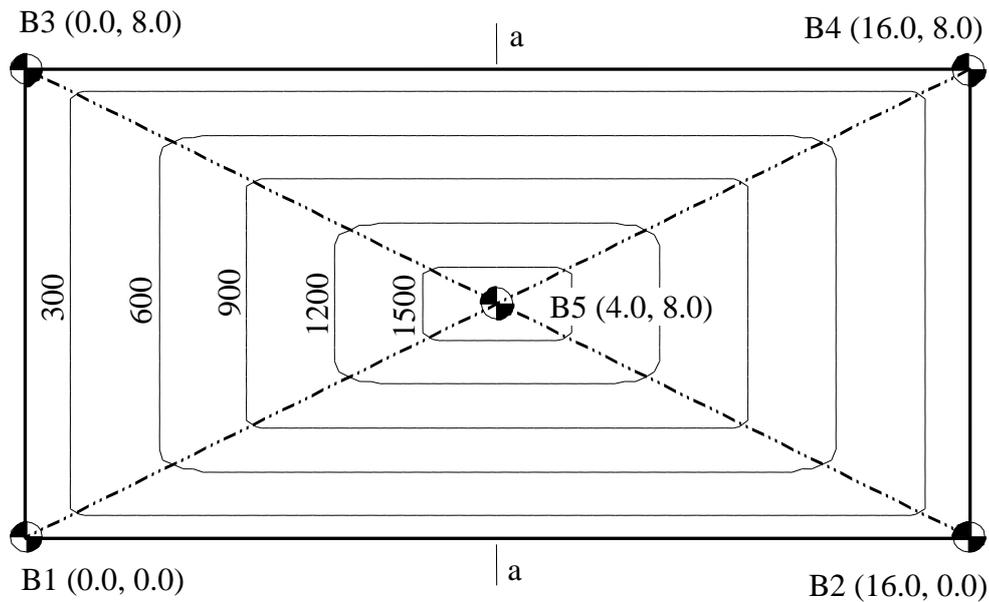
Figure 7.14   Contour lines of the variable ultimate bearing capacity q_{ult} [kN/m^2]

Unfortunately, until now there is no available method to determine the bearing capacity of the soil for irregular contact pressure, where the bearing capacity equations are derived for a uniform contact pressure under the foundation. In this example, the variability of q_{ult} under the raft is chosen according to the principle of equilibrium forces acting on the raft and the soil at the failure. In which, the part of ultimate bearing capacity from the second terms in Equation 7.6 is uniform. This part represents the influence of the applied pressure beside the foundation, $\gamma_1 \, t_f \, N_d \, v_d$. The part of ultimate bearing capacity from the third term in Equation 7.6 has a triangle cross-section at the middle of the raft (Figure 7.15). This part represents the influence of the foundation geometry, $\gamma_2 \, B \, N_b \, v_b$.
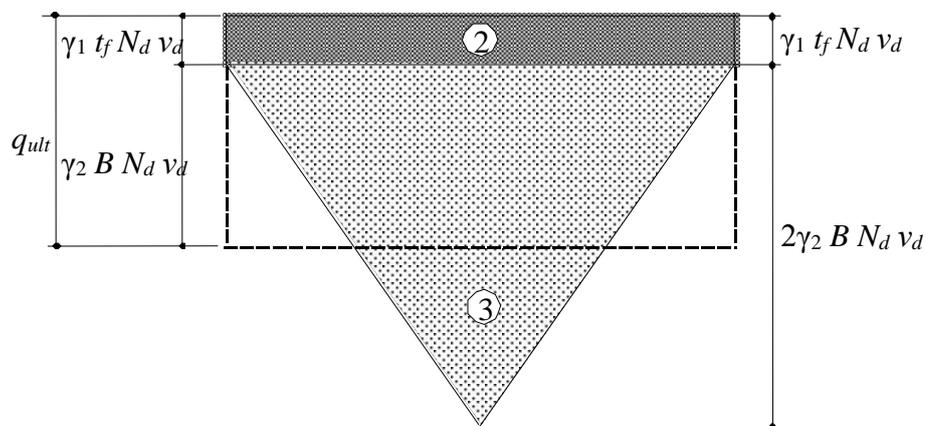
Figure 7.15   Ultimate bearing capacity at the soil failure (section a-a)

5   Results and discussions

The contact pressures q at section a-a of the raft in case of uniform q_{ult} are shown in Figures 7.16 and 7.17, while those in case of variable q_{ult} are shown in Figures 7.18 and 7.19. These figures show that the linear analysis of the both elastic and rigid rafts gives high contact pressures at the raft edges. As it is expected due to the nonlinear analysis, the contact pressures shift from the edges to the center of the raft, and this leads to a loss of the bearing capacity. Figures 7.16 and 7.17, which represent case of uniform q_{ult} show that although the contact pressures over all nodes on the raft are less than the ultimate bearing capacity limit, but the contact pressures at the raft edges still higher than those at the center. In contrast for case of variable q_{ult} the contact pressures take a form similar in shape to the limit line of q_{ult} (Figures 7.18 and 7.19).
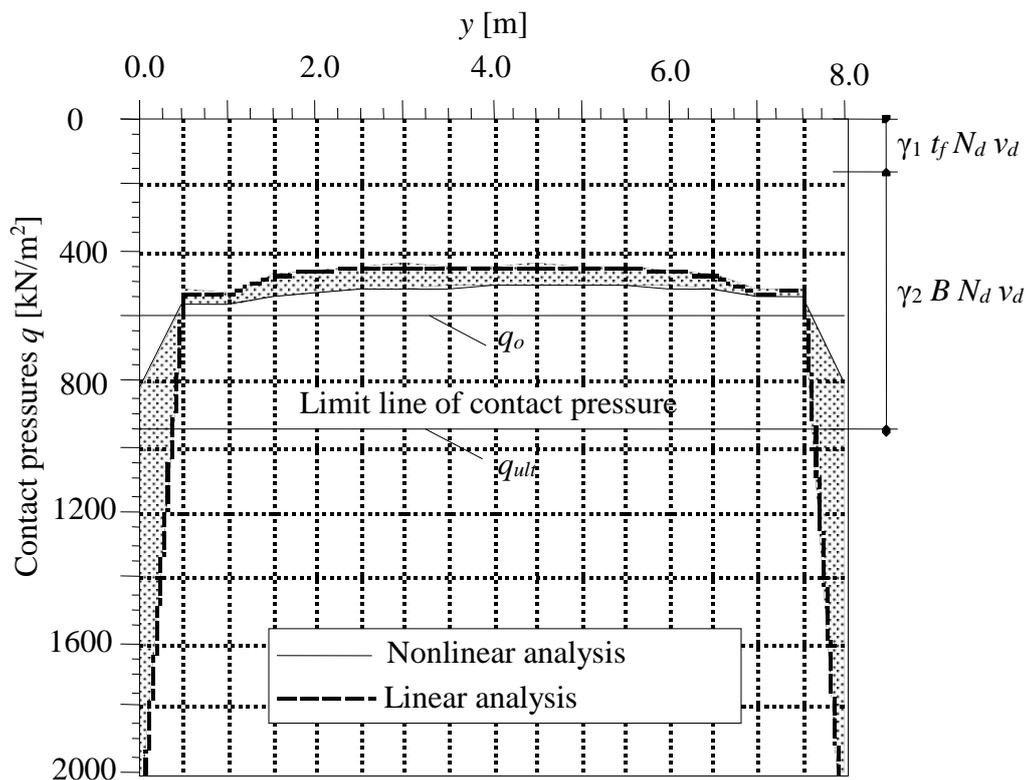
Figure 7.16   Contact pressures q [kN/m^2] at section a-a with and without limitation
(Elastic raft - uniform ultimate bearing capacity)
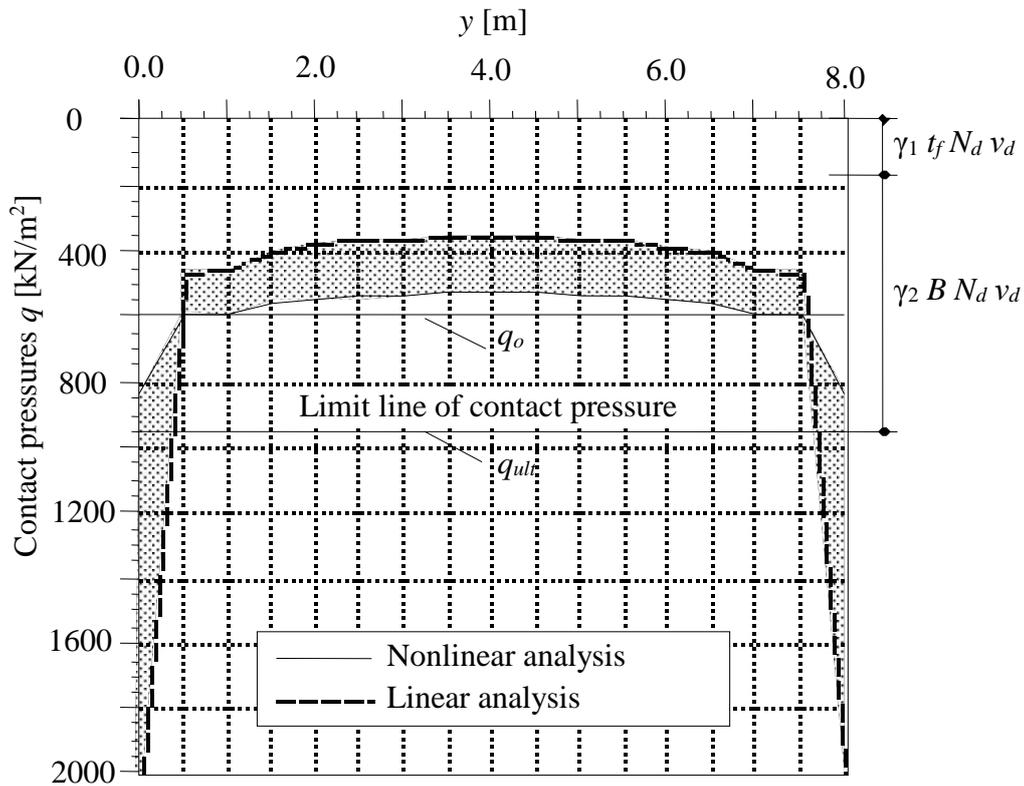
Figure 7.17   Contact pressures q [kN/m^2] at section a-a with and without limitation
(Rigid raft - uniform ultimate bearing capacity)
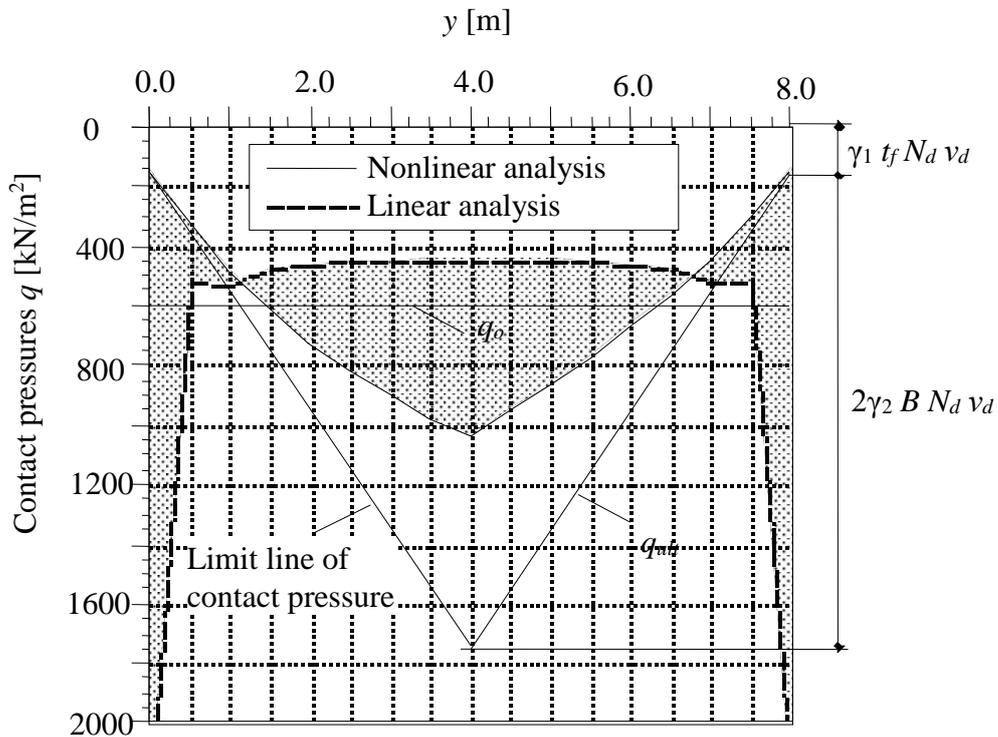
Figure 7.18   Contact pressures q [kN/m^2] at section a-a with and without limitation
(Elastic raft - variable ultimate bearing capacity)
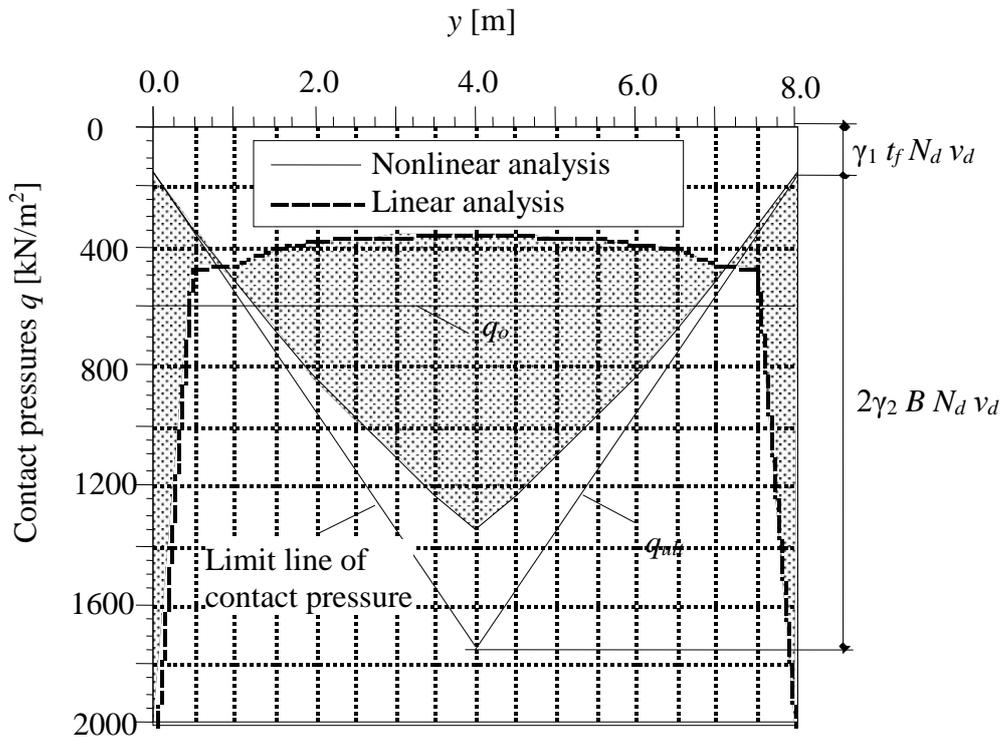
Figure 7.19   Contact pressures q [kN/m²] at section a-a with and without limitation
               (Rigid raft - variable ultimate bearing capacity)

The effect of redistribution of contact pressures on the moments m_y at section a-a of the raft is indicated in Figure 7.20 for case of uniform q_{ult} and in Figure 7.21 for case of variable q_{ult}. The Figures show that due to the redistribution of the contact pressures under the raft, the moments are considerably changed. In case of variable q_{ult}, not only the moments are changed but also the sign of moments. In case of uniform q_{ult}, the maximum moment m_y is reduced to 81 [%], while that in case of variable q_{ult} is reduced to more than double.
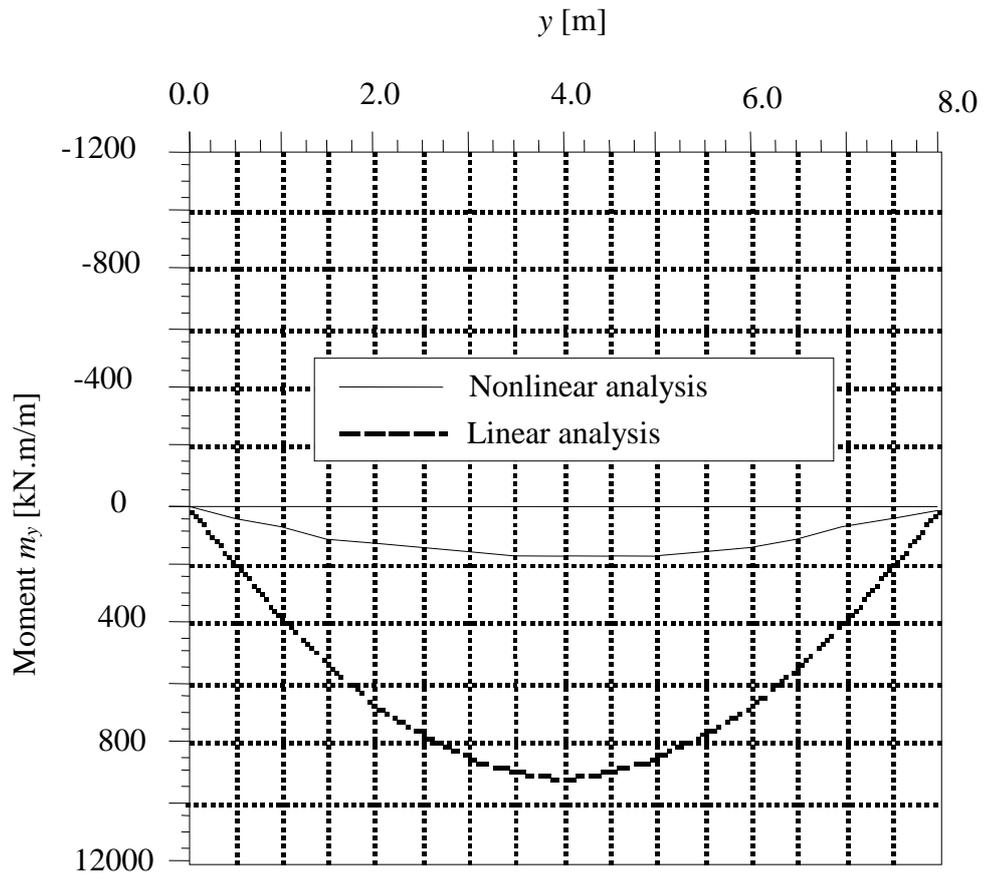
Figure 7.20   Moment m_y [kN.m/m] at section a-a with and without limitation
               (Elastic raft - uniform ultimate bearing capacity)
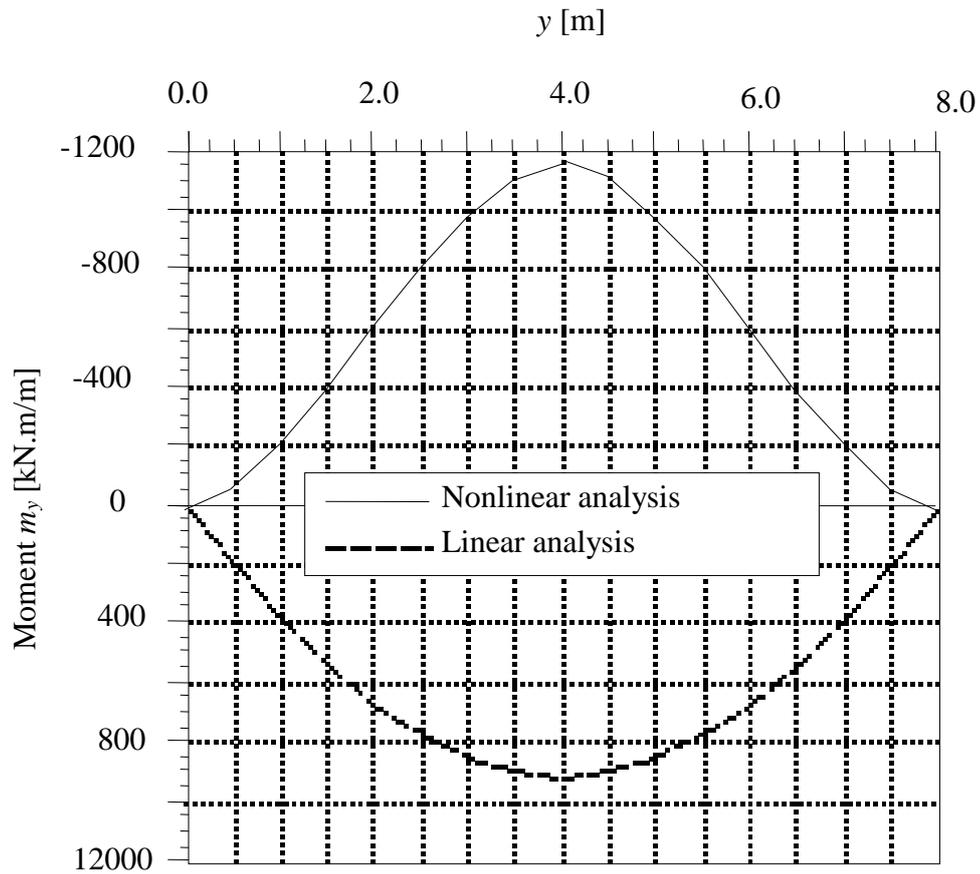
Figure 7.21   Moment m_y [kN.m/m] at section a-a with and without limitation
(Elastic raft - variable ultimate bearing capacity)

Chapter 8

Soil Properties and Parameters

Contents

8.1   *Poisson*'s ratio ν_s

Poisson's ratio ν_s for a soil is defined as the ratio of lateral strain to longitudinal strain. It can be evaluated from the Triaxial test. Here, *Poisson*'s ratio ν_s can be determined from at-rest earth pressure coefficient K_o as follows

$$\nu_s = \frac{K_o}{1 + K_o} \tag{8.1}$$

Some typical values for *Poisson*'s ratio are shown in Table 8.1 according to *Bowles* (1977). *Poisson*'s ratio in general ranges between 0 and 0.5.

Table 8.1   Typical range of values for *Poisson*'s ratio ν_s according to *Bowles* (1977)

Type of soil	*Poisson*'s ratio ν_s [-]
Clay, saturated	0.4 - 0.5
Clay, unsaturated	0.1 - 0.3
Sandy clay	0.2 - 0.3
Silt	0.3 - 0.35
Sand, dense	0.2 - 0.4
Sand, coarse (void ratio = 0.4 - 0.7)	0.15
Sand, fine grained (void ratio = 0.4 - 0.7)	0.25
Rock	0.1 - 0.4

8.2   Moduli of compressibility E_s and W_s and unit weight of the soil γ_s

The equations derived in chapter 1 for calculation of flexibility coefficients require either the moduli of compressibility for loading E_s and reloading W_s or moduli of elasticity for loading E and reloading W for the soil. The yielding of the soil is described by these elastic moduli. The moduli of compressibility E_s and W_s can be determined from the stress-strain curve through a confined compression test (for example Odometer test) as shown in Figure 8.1. In this case, the deformation will occur in the vertical direction only. Therefore, if the moduli of compressibility E_s and W_s are determined from a confined compression test, *Poisson*'s ratio will be taken $\nu_s = 0.0$. If the other moduli of elasticity E and W are used in the equations derived in chapter 1, *Poisson*'s ratio will be taken to be $\nu_s \neq 0$. In general, *Poisson*'s ratio ranges in the limits $0 < \nu_s < 0.5$.
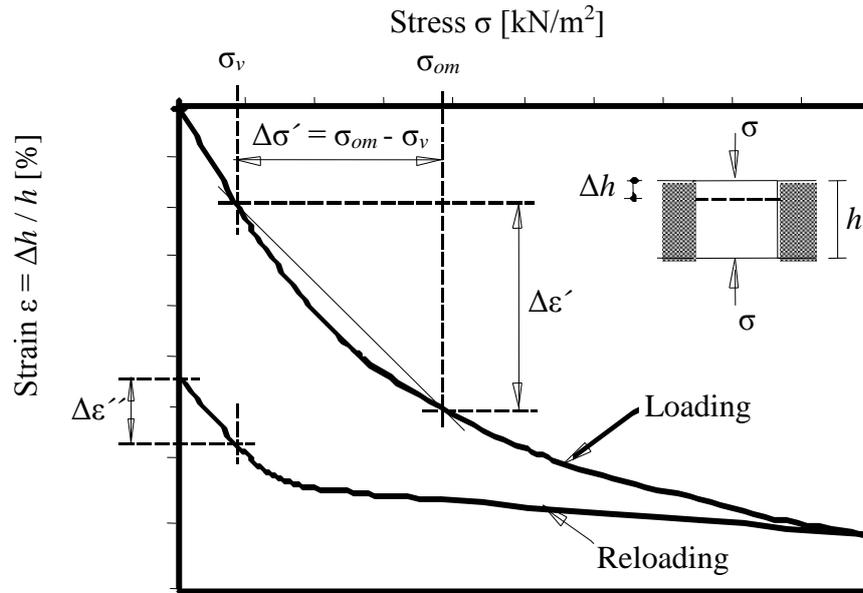
Figure 8.1   Stress-strain diagram from confined compression test (Oedometer test)

The modulus of compressibility E_s [kN/m^2] (or W_s [kN/m^2]) is defined as the ratio of the increase in stress $\Delta\sigma$ to decrease in strain $\Delta\varepsilon$ as (Figure 8.1)

$$\left.\begin{aligned} E_s &= \frac{\Delta\sigma'}{\Delta\varepsilon'} = \frac{\sigma_{om}-\sigma_v}{\Delta\varepsilon'} \\ W_s &= \frac{\Delta\sigma''}{\Delta\varepsilon''} = \frac{\sigma_v}{\Delta\varepsilon''} \end{aligned}\right\} \tag{8.2}$$

where:

$\Delta\sigma'$	Increase in stress from σ_v to σ_{om}	[kN/m^2]
σ_v	Stress equal to overburden pressure	[kN/m^2]
σ_{om}	Stress equal to expected average stress on the soil	[kN/m^2]
$\Delta\varepsilon'$	Decrease in strain due to stress from σ_v to σ_{om}	[-]
$\Delta\sigma''$	Increase in stress due to reloading	[kN/m^2]
$\Delta\varepsilon''$	Decrease in strain due to reloading	[-]

The moduli of compressibility may be expressed in terms of either void ratio or specimen thickness. For an increase in effective stress $\Delta\sigma$ to decrease in void ratio Δe, the moduli of compressibility E_s [kN/m2] and W_s [kN/m2] are then expressed as

$$\left.\begin{aligned} E_s &= \frac{1}{m_v'} = \frac{\Delta\sigma'(1+e_o')}{\Delta e'} \\ W_s &= \frac{1}{m_v''} = \frac{\Delta\sigma''(1+e_o'')}{\Delta e''} \end{aligned}\right\} \tag{8.3}$$

where:

$m´_v$	Coefficient of volume change for loading	[m^2/kN]
$m´´_v$	Coefficient of volume change for reloading	[m^2/kN]
$e´_o$	Initial void ratio for loading	[-]
$e´´_o$	Initial void ratio for reloading	[-]
$\Delta e´$	Decrease in void ratio due to loading	[-]
$\Delta e´´$	Decrease in void ratio due to reloading	[-]

The values of E_s and W_s for a particular soil are not constant but depend on the stress range over which they are calculated. Therefore, for linear analysis it is recommended to determine the modulus of compressibility for loading E_s at the stress range from σ_v to σ_{om}, while that for reloading W_s for a stress increment equal to the overburden pressure σ_v. On the other hand, since the modulus of compressibility increases with the depth of the soil, for more accurate analysis the modulus of compressibility may be taken increasing linearly with depth. Also, according to *Kany* (1976) the moduli of compressibility E_s and W_s may be taken depending on the stress on soil. In these two cases, the moduli of compressibility E_s and W_s can be defined in the analysis for several sub-layers instead of one layer of constants E_s and W_s.

As a rule, before the analysis the soil properties are defined through the tests of soil mechanics, particularly the moduli of compressibility E_s and W_s. For precalculations Table 8.2 for specification of the modulus of compressibility E_s can also be used.

According to *Kany* (1974), the values of W_s range between 3 to 10 times of E_s. From experience, the modulus of compressibility W_s for reloading can be taken 1.5 to 5 times as the modulus of compressibility E_s for loading.

For geologically strongly preloaded soil, the calculation is often carried out only with the modulus of compressibility for reloading W_s. In this case, the same values are defined for E_s and W_s.

Matching with the reality, satisfactory calculations of the settlements are to be expected only if the soil properties are determined exactly from the soil mechanical laboratory, field tests or back calculation of settlement measurements.

Table 8.2 shows mean moduli of compressibility E_s and the unit weight of the soil γ_s for various types of soil according to EAU (1990).

Table 8.2   Mean moduli of compressibility E_s and the unit weight of the soil γ_s
             for various types of soil

Type of soil	Unit weight γ_s [kN/m³]		Modulus of compressibility E_s [kN/m²]
	above water	under water	
Non-cohesive soil			
Sand, loose, round	18	10	20000 - 50000
Sand, loose, angular	18	10	40000 - 80000
Sand, medium dense, round	19	11	50000 - 100000
Sand, medium dense, angular	19	11	80000 - 150000
Gravel without sand	16	10	100000 - 200000
Coarse gravel, sharp edge	18	11	150000 - 300000
Cohesive soil			
Clay, semi-firm	19	9	5000 - 10000
Clay, stiff	18	8	2500 - 5000
Clay, soft	17	7	1000 - 2500
Boulder clay, solid	22	12	30000 - 100000
Loam, semi-firm	21	11	5000 - 20000
Loam, soft	19	9	4000 - 8000
Silt	18	8	3000 - 10000

8.3   Moduli of elasticity *E* and *W*

In the program *ELPLA*, the equations derived in chapter 1 to determine the flexibility coefficients are used with moduli of elasticity *E* and *W* for unconfined lateral strain with *Poisson*'s ratio $\nu_s \neq 0$. It must be pointed out that, when defining *Poisson*'s ratio by $\nu_s = 0$ (limit case), the moduli of compressibility E_s and W_s for confined lateral strain (for example from Odometer test) also can be used.

The modulus of elasticity is often determined from an unconfined Triaxial compression test, Figure 8.2. Plate loading tests may also be used to determine the in situ modulus of elasticity of the soil as elastic and isotropic.
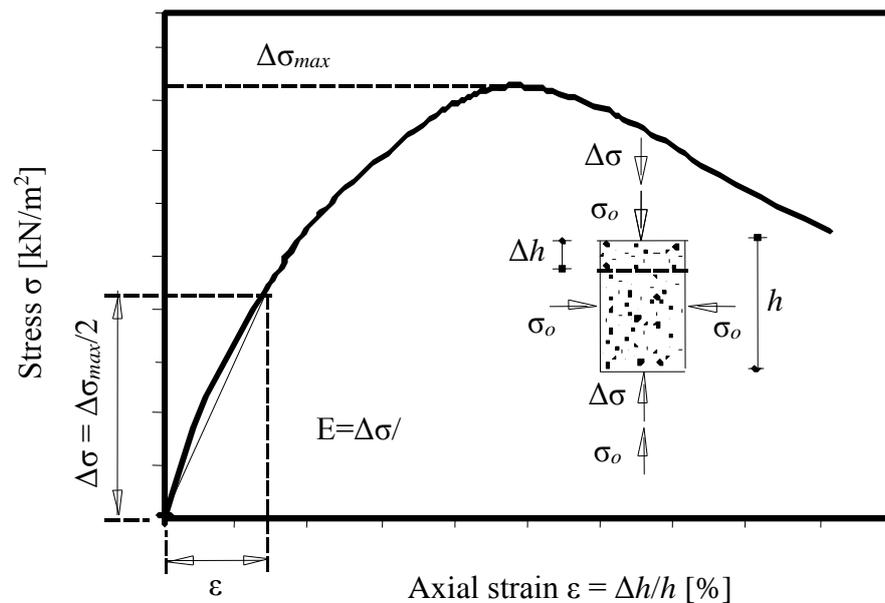
Figure 8.2   Modulus of elasticity *E* from Triaxial test

It is possible to obtain an expression for the moduli of elasticity *E* and *W* in terms of moduli of compressibility E_s, W_s and *Poisson*'s ratio ν_s for the soil as

$$\left. \begin{aligned} E = E_s \frac{1 - \nu_s - 2\nu_s^2}{1 - \nu_s} \\ W = W_s \frac{1 - \nu_s - 2\nu_s^2}{1 - \nu_s} \end{aligned} \right\}$$

(8.4)

Equation 8.4 shows that:

-       In the limit case $\nu_s = 0$ (deformation without lateral strain), the values of *E* and E_s (also *W* and W_s) are equal

-       In the other limit case $\nu_s = 0.5$ (deformation with constant volume), the moduli of elasticity will be $E = 0 \times E_s$ and $W = 0 \times W_s$. In this case, only the immediate settlement (lateral deformation with constant volume) can be determined. By the other way, the second term in *Steinbrenner*'s formula (1.51) will be omitted, if *Poisson*'s ratio $\nu_s = 0.5$ is used

Table 8.3 shows some typical values of modulus of elasticity according to *Bowles* (1977).

Table 8.3   Typical range of moduli of elasticity E for selected soils

Type of soil	Modulus of elasticity E [kN/m^2]	
Very soft clay	3000	- 3000
Soft clay	2000	- 4000
Medium clay	4500	- 9000
Hard clay	7000	- 20000
Sandy clay	30000	- 42500
Silt	2000	- 20000
Silty sand	5000	- 20000
Loose sand	10000	- 25000
Dense sand	50000	- 100000
Dense sand and gravel	80000	- 200000
Loose sand and gravel	50000	- 140000
Shale	140000	- 1400000

8.4 Compression index C_r und initial void ratio e_o

In case of clayey soil it is recommended to use the settlement parameters C_c, C_r and C_s to represent the elastic properties of the soil in the computation of consolidation settlements. These parameters or indices can be obtained directly from the consolidation test or indirect using some empirical equations such as Equations 8.7 and 8.8.

Compression index C_c from consolidation test

The typical relationship between the void ratio e and effective stress σ obtained from the consolidation test is shown in Figure 8.3. The slope of the end part of the e versus log σ curve is denoted as the Compression index Cc and computed as

$$C_c = \frac{\Delta e}{\log \dfrac{\sigma_2}{\sigma_1}} \tag{8.5}$$

By analogy, the other indices C_r and C_s can be obtained as shown in Figure 8.3 and Equation 8.6

$$C_r \text{ or } C_c = \frac{\Delta e}{\log \dfrac{\sigma_2}{\sigma_i}} \tag{8.6}$$

where:
C_r	Recompression index	[-]
C_s	Swell index	[-]
Δe	Change in void ratio between σ_i and σ_2	[-]
σ_i	Any pressure along the appropriate curve	[kN/m^2]
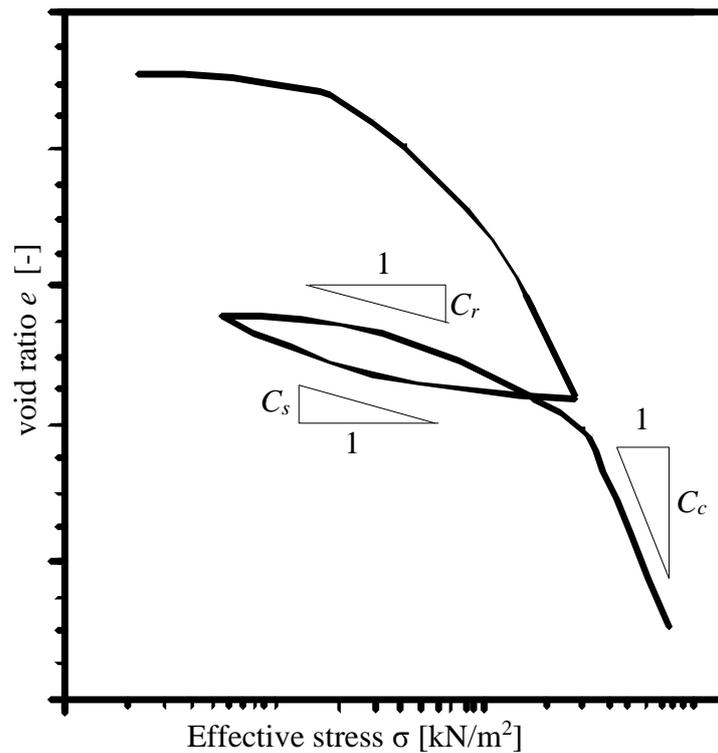
Figure 8.3   Relationship between void ratio and effective stress obtained from consolidation test

Compression index C_c from empirical equations

Because of the number of consolidation tests to obtain the compression indices for a given project is limited, it is often desirable to obtain approximate values by using other soil parameters which are more easily determined. Approximate values may be used for preliminary calculations or to check the laboratory data.

For normally consolidated clays *Terzaghi/ Peck* (1967), on the basis of research on undisturbed clays, proposed the following equation to obtain the Compression index C_c [-] from the liquid limit of the soil LL [%]

$$C_c = 0.009\,(LL - 10) \tag{8.7}$$

Azzouz (1976) lists several equations to obtain the compression index, one of them is given below to obtain the Compression index C_c [-] from the initial void ratio e_o [-] of the soil

$$C_c = 1.15\,(e_o - 0.35) \tag{8.8}$$

Typical values of compression and swell indices as well as the corresponding void ratio at stress $\sigma_o = 10$ [kN/m²] are presented in the following table according to *Gudehus* (1981). The compression index C_c is valid for loading while C_s is valid for both heaving and reloading.

Table 8.4   Compression and swell indices depending on the initial void ratio

Soil type	Compression index C_c [-]	Swell index C_s [-]	Initial void ratio e_o [-]
Gravely sand	0.001	0.0001	0.3
Fine sand, dense	0.005	0.0005	0.5
Fine sand, loose	0.01	0.001	0.7
Coarse silt	0.02	0.002	0.8
Clayey silt	0.03 - 0.6	0.01 - 0.02	0.9 - 1.2
Kaolin-Silt	0.1	0.03	1.5
Silt	0.1 - 0.3	0.03 - 0.1	1.2 - 2.5
Clay	0.5	0.4	5
Peat	1	0.3	10

8.5   Shear parameters φ and *c*

Angle of internal friction φ and cohesion *c* are physical soil properties for determining bearing capacity of the soil, they are called also shear parameters. The shear parameters φ and *c* can be obtained from shear test or Triaxial test. They are usually obtained for a certain soil by carrying out three shear tests with different stresses. The results of such series can be plotted as points in τ_f-σ diagram as shown in Figure 8.4.
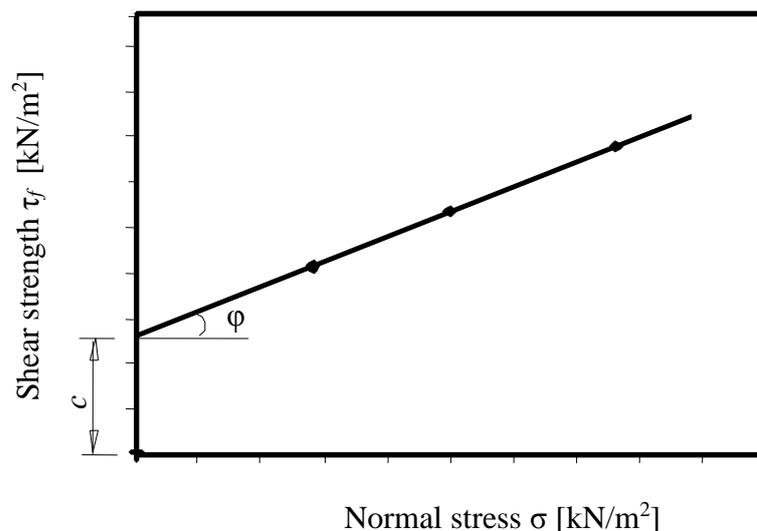
Figure 8.4   Shear strength at variable normal stress

For many soil types, the points lie quite exactly in a straight line. The intersection of the line with *y*-axis gives the value of cohesion *c*, while the inclination of the line gives the angle of internal friction φ. The straight line Equation 8.9 is called *Coulomb*'s friction law for shear strength

$$\tau_f = c + \sigma \ \tan \varphi \tag{8.9}$$

As known from the pore water pressure u that when the effective stress $\sigma' = \sigma - u$ is used instead of the normal stress σ, Equation 8.9 becomes

$$\tau_f = c' + \sigma' \tan \varphi' \qquad (8.10)$$

where:
c' Effective cohesion $[kN/m^2]$
φ' Effective angle of internal friction $[°]$

When the pore excess water pressure cannot drain, at least quickly, from the soil sample in the shear test, undrained condition occurs

$$\tau_f = c_u + \sigma \varphi_u \qquad (8.11)$$

where:
c_u Undrained cohesion $[kN/m^2]$
φ_u Undrained angle of shearing resistance $[°]$

In a fully saturated soil $\varphi_u = 0$.

You can write the shear parameters without the index u, if it is clear that the ultimate bearing capacity of the saturated soil is being without volume changes. The ultimate bearing capacity of the soil is often determined without considering the pore water pressure according to Figure 8.4 and Equation 8.9. Mean average values of the angle of internal friction φ and cohesion c for various types of soil are listed in Table 8.5 according to EAU (1990). These values are used only for preliminary calculation.

Table 8.5   Mean average values of shear parameters according to EAU (1990)

Type of soil	Angle of internal friction φ or φ' [°]	Cohesion	
		c' [kN/m²]	c_u [kN/m²]
Non-cohesive soil			
Sand, loose, round	30	-	-
Sand, loose, angular	32.5	-	-
Sand, medium dense, round	32.5	-	-
Sand, medium dense, angular	35	-	-
Gravel without sand	37.5	-	-
Coarse gravel, sharp edge	40	-	-
Cohesive soil			
Clay, semi-firm	25	25	50 - 100
Clay, stiff	20	20	25 - 50
Clay, soft	17.5	10	10 - 25
Boulder clay, solid	30	25	200 - 700
Loam, semi-firm	27.5	10	50 - 100
Loam, soft	27.5	-	10 - 25
Silt	27.5	-	10 - 50
Peat	15	5	-

Explanations about Table 8.5:

φ Actual angel of internal friction
φ' Effective angle of internal friction; for non-cohesive soil is $\varphi = \varphi'$
c' Effective cohesion referred to φ'
c_u Undrained apparent cohesion at zero friction for a saturated cohesive soil

8.6   Modulus of subgrade reaction k_s

It is important to say that the modulus of subgrade reaction k_s is not a soil constant, but it can be related to the elastic parameters E_s and ν_s of the soil.

It may be determined from in situ plate loading test. This test is generally performed using a circular steel plate (30 in diameter) thick enough so that the bottom plate will settle uniformly under a vertical load. The modulus of subgrade reaction k_s [kN/m³] is defined as the ratio between the soil pressure q [kN/m²] and corresponding settlement s [m], Equation 8.12

$$k_s = \frac{q}{s} \tag{8.12}$$

In practice the plate would not stress the same soil strata as the full size foundation. Therefore, the result from a plate loading test may give quite misleading results if the proposed foundation is very big. The soft layer of soil in Figure 8.5 is unaffected by the plate loading test but would be considerably stressed by the foundation. Therefore, it is recommended to evaluate the modulus k_s from the elastic parameters E_s and ν_s of the soil.
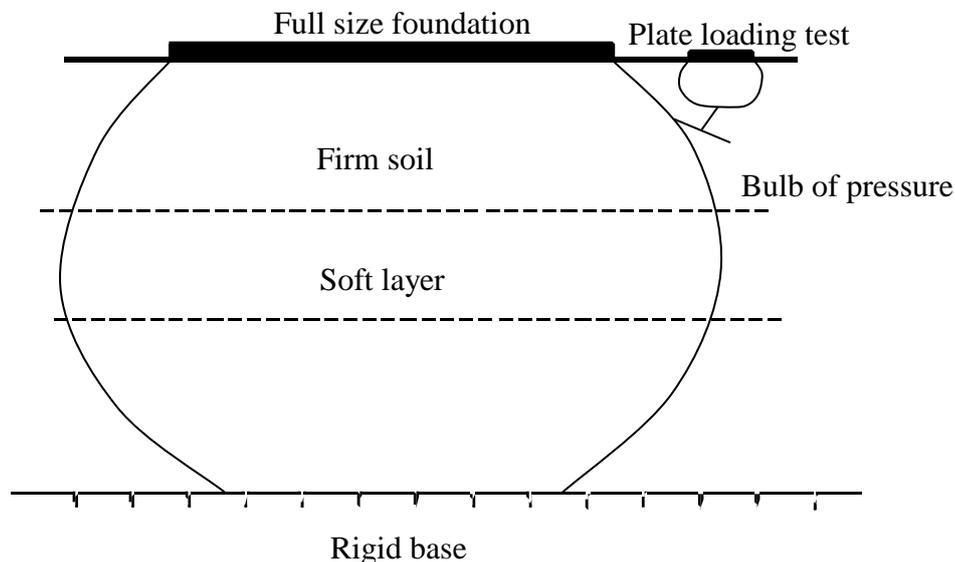
Figure 8.5   Illustration of how a plate loading test may give misleading results

A reasonable approximation of modulus of subgrade reaction k_s can be obtained from the allowable soil pressure q_{all} according to *Bowles* (1977). This way is presented on the assumption that the allowable soil pressure is based on some maximum amount of settlement s, including a factor of safety *FS*. Accordingly, the modulus of subgrade reaction k_s is given by

$$k_s = F\,S\,\frac{q_{all}}{S} \tag{8.13}$$

The modulus of subgrade reaction k_s [kN/m^3] for a settlement of $s = 0.0254$ [m] equal to $s = 1.0$ [m] and a factor of safety $FS = 3$ can be taken as

$$k_s = 3\,\frac{q_{all}}{0.0254} = 120\,q_{all} \tag{8.14}$$

In case of carrying out the analysis with constant modulus of subgrade reaction, it is recommended to determine the modulus of subgrade reaction from settlement calculation. More complicated analysis for irregular foundation on variable moduli of subgrade reactions is available in the program *ELPLA*. Furthermore, the moduli of subgrade reactions can be improved through the calculated contact pressures and settlements by iteration.

The following Table 8.6 shows the approximate average values of k_s according to *Wölfer* (1978). These values may be used only for primary calculation.

Table 8.6   Typical average values of moduli of subgrade reactions *ks* for selected soils

Type of soil	Modulus of subgrade reaction k_s [kN/m³]
Peat	5000 - 10000
Fill of sand and gravel	10000 - 20000
Wet clayey soil	20000 - 30000
Moistured clay	40000 - 50000
Dry clay	60000 - 80000
Hard dry clay	100000
Coarse sand	80000 - 100000
Coarse sand + small amount of gravel	80000 - 100000
Fine gravel + small amount of gravel	80000 - 100000
Middle size gravel + fine sand	100000 - 120000
Middle size gravel + coarse sand	120000 - 150000
Large size gravel + coarse sand	150000 - 200000

8.7   Allowable bearing capacity of the soil q_{all}

The value of allowable bearing capacity of the soil is based on theoretical as well as experimental investigation. Such a value usually includes a factor of safety of 3 ($q_{ult} = 3\, q_{all}$). This indicates that the design loads used in establishing the bearing capacity area of the foundation must be service loads with no reduction.

Approximate allowable bearing capacity q_{all} of common types of soils are listed in Table 8.7 according to *Bakhoum* (1986) and can be taken for primary calculations.

Table 8.7   Approximate allowable bearing capacity q_{ult} of common types of soils

Type of soil	Allowable bearing capacity q_{all} [kN/m²]
Noncohesive soil	
Loose sand	100
Medium sand	200
Dense sand	500
Hard rock	5000
Cohesive soil	
Soft-medium clay	90
Stiff clay	150
Very stiff clay	300
Hard clay	500

8.8   Settlement reduction factor α

As according to experience the real consolidation settlements are different from those calculated, the settlements *s* are multiplied by a factor α according to German standard DIN 4019, page No. 1. According to this standard the following reduction factors in Table 8.8 can be applied:

Table 8.8   Reduction factors α according to DIN 4019, page No. 1

soil type	α
Sand and silt	0.66
Normally and slightly over consolidated clay	1.0
Heavily over consolidated clay	0.5 - 1

In the program *ELPLA*, the moduli of compressibility E_s and W_s are divided by α as follows

$$\left.\begin{aligned}\overline{E}_s &= \frac{E_s}{\alpha} \\ \overline{W}_s &= \frac{W_s}{\alpha}\end{aligned}\right\} \tag{8.15}$$

In the final result, this process is equivalent to the following Equation 8.16

$$\overline{S} = \alpha\, S \tag{8.16}$$

Chapter 9

List of examples for the calculation
of foundations by the program *ELPLA*

Content

9   List of examples for the calculation of foundations by the program *ELPLA*
9.1   Introduction

When ordering package *ELPLA*, a CD is delivered. It contains the programs and 20 project data files for test purposes, which were described in this book. These data introduce some possibilities to analyze slab foundations by *ELPLA*.

Firstly, the numerical examples are carried out completely to show the influence of different subsoil models on the results. Furthermore, different calculation methods for the same subsoil model are applied to judge the computation basis and the accuracy of results. In some cases the influences of geological reloading, soil layers and also the structure rigidity are considered in the analysis.

For this purpose, the following numerical examples introduce some possibilities to analyze foundations. Many different foundations are chosen, which are considered as some practical cases may be happened in practice. All analyses of foundations are carried out by *ELPLA*, which was developed by *Kany/ El Gendy* (2007).

In the next pages, names of files of the numerical examples, content and short description of the examples are listed.

9.2   Examples of chapter 2

Example 2.1   A square raft on irregular subsoil

File name	Content
un1	Modulus of subgrade reaction - method 3 (Interpolation)
un2	Layered soil medium (elastic raft) - method 6 (Interpolation)
un3	Layered soil medium (rigid raft) - method 8 (Interpolation)
un4	Modulus of subgrade reaction - method 3 (Subareas method)
un5	Layered soil medium (elastic raft) - method 6 (Subareas method)
un6	Layered soil medium (rigid raft) - method 8 (Subareas method)
un7	Modulus of subgrade reaction - method 3 (regular layer)
un8	Layered soil medium (elastic raft) - method 6 (regular layer)
un9	Layered soil medium (rigid raft) - method 8 (regular layer)

Example 2.2   An irregular raft on irregular subsoil   9 - 4

File name	Content
gb1	Linear contact pressure - method 1
gb2	Constant modulus of subgrade reaction - method 2
gb3	Variable modulus of subgrade reaction - method 3
gb4	Modification of modulus of subgrade reaction by iteration - method 4
gb5	Isotopic elastic half-space soil medium - method 5
gb6	Layered soil medium by iteration (elastic raft) - method 6
gb7	Layered soil medium by elimination (elastic raft) - method 7
gb8	Layered soil medium (rigid raft) - method 8

Example 2.3   System of footings on irregular subsoil

File name	Content
foi	Footing i (i = 1 to 9)
Group	Group of footings
Dir: Interpolation	Analysis with limit depth using interpolation
Dir: LdrFooting3	Analysis with limit depth related to footing 3
Dir: LdrFooting5	Analysis with limit depth related to footing 5
Dir: Without LD	Analysis without limit depth

9.3   Examples of chapter 3

Example 3.1   Settlements outside the foundation

File name	Content
se1	Contact area I
se2	Contact areas II + III

Example 3.2   Influence of a new neighboring building on an old one

File name	Content
ei1	Only new building
ei2	New building + Old building

$E_b = 2 \times 10^7$ [kN/m²]
$\nu_b = 0.15$ [-]
$\gamma_b = 0.0$ [kN/ m³]

P_2 P_3 P_2 P_2 P_3 P_2

(0.00)

(1.50)

$d = 1.0$ m

Clay, stiff plastic

$E_s = 5000$ [kN/m²]
$W_s = 15000$ [kN/m²]
$\gamma_s = 18$ [kN/ m³]

(7.20)

Rock

a) Section *a-a*

New building II   Old building I

$P_1 = 500$ [kN]
$P_2 = 1000$ [kN]
$P_3 = 2000$ [kN]

P_1 P_2 P_1 P_1 P_2 P_1

$14 \times 0.72 = 10.08$ m

a P_3 P_3 P_3 P_3 P_3 P_3 a

P_1 P_2 P_1 P_1 P_2 P_1

$14 \times 0.72 = 10.08$ m $14 \times 0.72 = 10.08$ m

b) Plan

Example 3.3   Influence of ground lowering due to a tunnel on a building

File name	Content
tu1	Without tunnel
tu2	With tunnel

9.4   Examples of chapter 4

Example 4.1   Interaction of two circular rafts

File name	Content
ha1	Circular raft I
ha2	Circular raft II
h12	Circular raft I + Circular raft II

$P_1 = 1250$ [kN]
$P_2 = 1000$ [kN]

Example 4.2   Settlement behavior of four containers

File name	Content
sta	Circular raft A
stb	Circular raft B
stc	Circular raft C
std	Circular raft D
ste	Analysis of system of rigid circular rafts A + B

a)   b)

$F = 263$ [m^2]
$p = 352$ [kN/m^2]

Example 4.3   Interaction of two rafts considering two additional footings

File name	Content
sf1	Footing III
sf2	Footing IV
fl1	Flexible raft I
fl2	Flexible raft II
f12	Analysis of system of flexible rafts I + II
el1	Elastic raft I
el2	Elastic raft II
e12	Analysis of system of elastic rafts I + II + II
rg1	Rigid raft I
rg2	Rigid raft II
r12	Analysis of system of rigid rafts I + II

Example 4.4   Interaction of two square rafts constructed side by side

File name	Content
Rf1_sys	Raft system (raft I)
Rf2_sys	Raft system (raft II)
Rf1_2_sys	Raft system (rafts I + II)
Rf1	Without interaction (raft I)
Rf2	Without interaction (raft II)
Rf1_2_*cm	Case 1: (c = *cm)
Rf1_Nachbar_*cm	Case 2: raft I (c = *cm)
Rf2_Nachbar_*cm	Case 2: raft II (c = *cm)
Rf1_2	Case 3
Rf1_2_Fugen	Case 4

2×1=2 [cm]

2 [cm] raft thickness

Detail *A*   Detail *B*

400 [kN/m²]   A   200 [kN/m²]

Section   0.5 [m]

8×1.5 = 12 [m]   8×1.5 = 12 [m]

2×1=2 [cm]

8×1.5 = 12 [m]   *a*   *a*

Plan   Raft I   *B*   Raft II

Example 4.5   Analysis of a swimming pool

File name	Content
slr	Swimming pool left + right (without joint)
smt	Swimming pool left + right (with interaction and with shearing forces)
sol	Swimming pool left 5 (without interaction)
sor	Swimming pool right 5 (without interaction)
ssy	Swimming pool left + right 5 (with interaction and without shearing forces)
au*	Influence of the filling around Swimming pool (uniform load *)

Plan

Section A-A

9.5   Examples of chapter 5

Example 5.1   Rigidity of simple square raft

File name	Content
th*	Raft thickness from 0.0 to 0.9 [m]
t1*	Raft thickness from 1.0 to 2.0 [m]
txx	Rigid raft

Raft
$P = 9000$ [kN]
$E_s = 2{\times}10^7$ [kN/m²]
$v_b = 0.15$ [-]

0.00 m

3.0 m
6.0 m
12.0 [m]
3.0 m

P
P
P
P
a
b
c
d

3.0 m
6.0 m
12.0 [m]
3.0 m

Compressible layer
$E_s = 10000$ [kN/m²]   20.00 [m]

Example 5.2   Rigidity of irregular raft on irregular subsoil

File name	Content
g00	Raft thickness $d = 0.0$ [m]
gb*	Raft thickness from 0.1 to 0.9 [m]
g1*	Raft thickness from 1.0 to 1.9 [m]
g20	Raft thickness $d = 2.0$ [m]
gxx	Rigid raft

9.6   Examples of chapter 6

Example 6.1   Analysis of a raft for a high rise building

File name	Content
raft1	Only raft
raft2	Raft - cellar
raft3	Raft - cellar - superstructure
raftr	Rigid raft

a) Longitudinal *A-B*

c) Cross-section *C-D*

17.55 [m]

b) Plan (section *E-F*)

L=18×3.60=64.80 [m]

66.00 [m]

Columns 0.40/0.40   Columns 0.50/0.50

l=3.63.63.63.6

Example 6.2   Verification of the iterative procedure

File name	Content

Raft   Only raft
Raft1   Raft - cellar
Raft2   Raft - cellar - superstructure
Raft3   Rigid raft
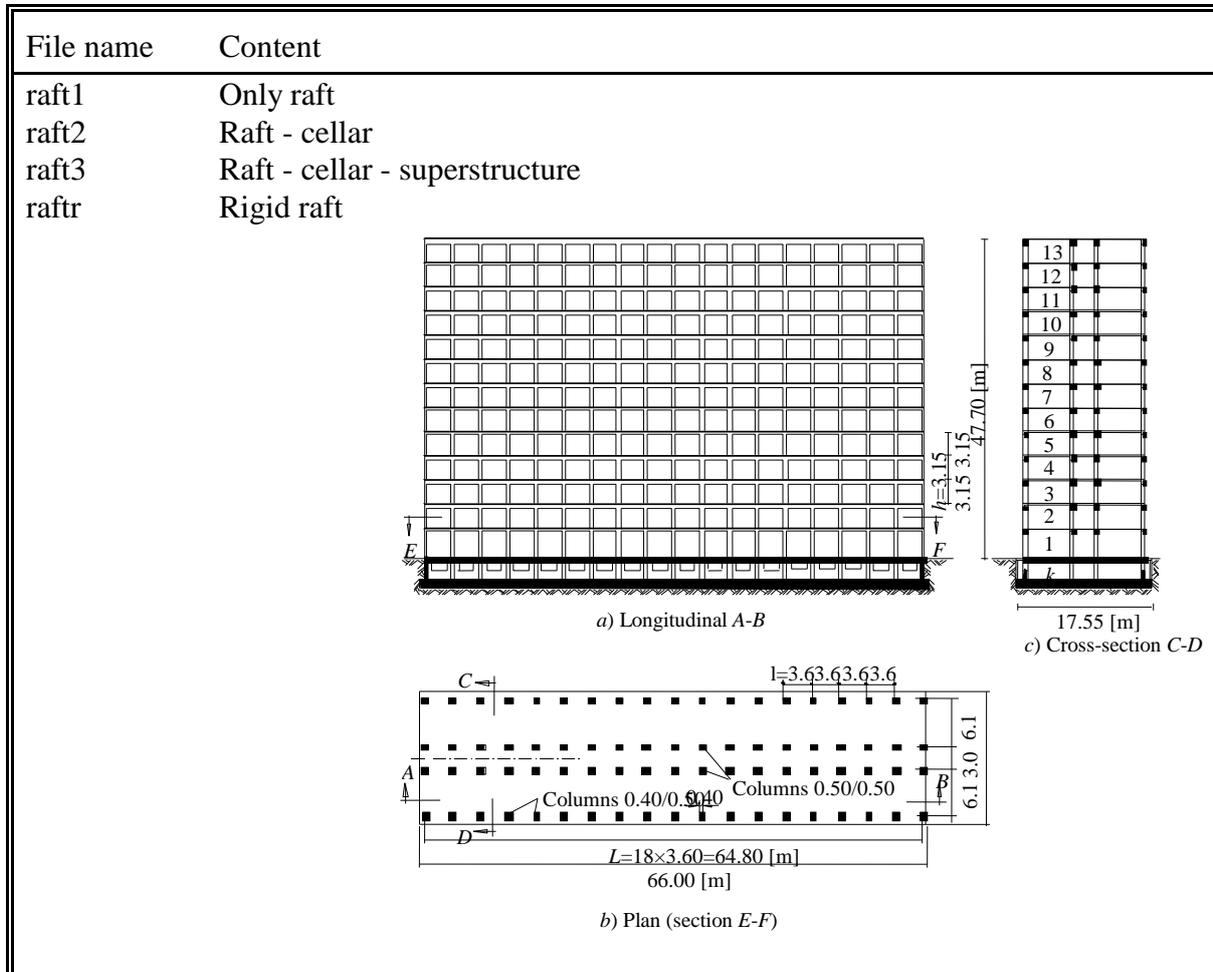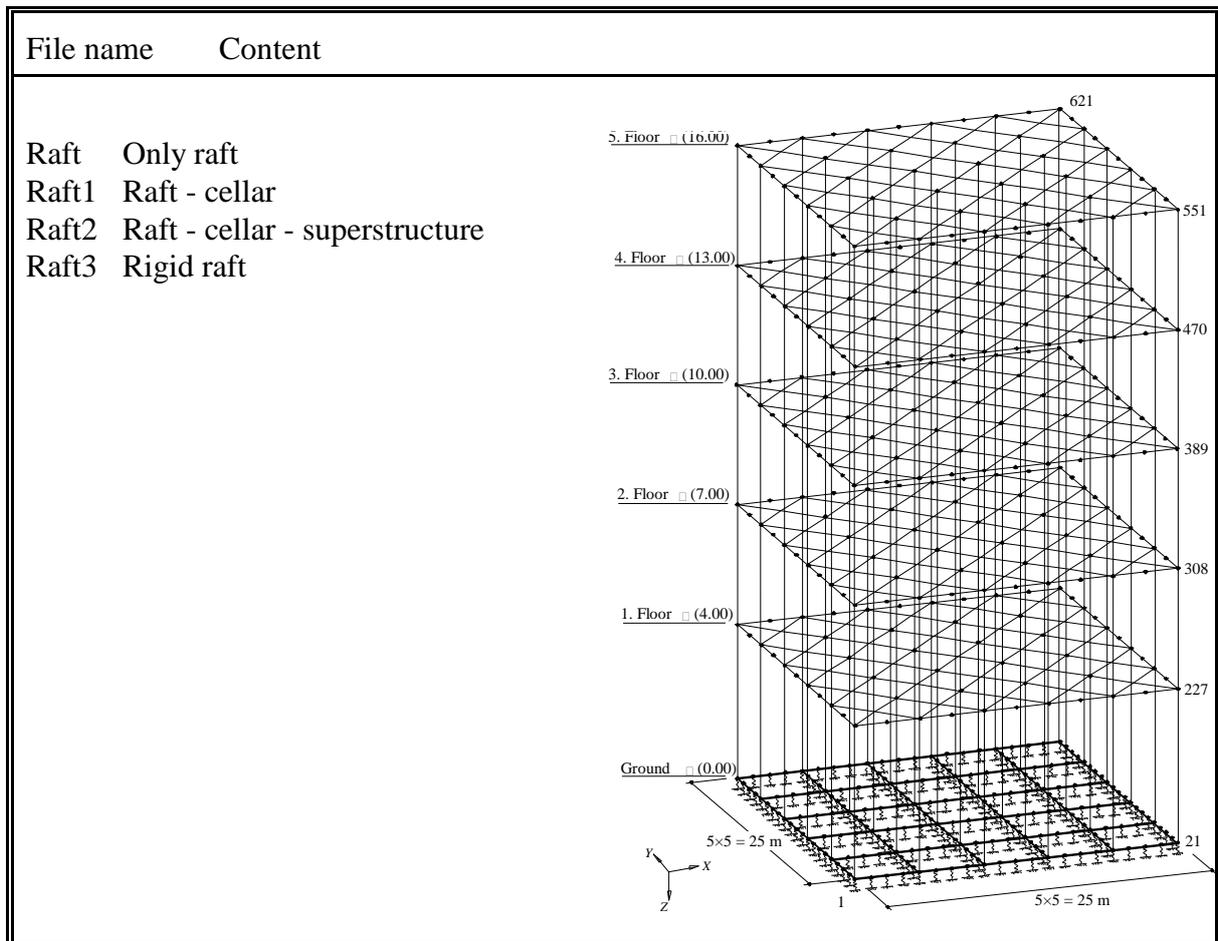
9.7   Examples of chapter 7

Example 7.1   Verification of nonlinear analysis for *Winkler*'s model

File name	Content
fc1	Point load (linear analysis)
fcn	Point load (non-linear analysis)
fu1	Uniform load (linear analysis)
fun	Uniform load (non-linear analysis)
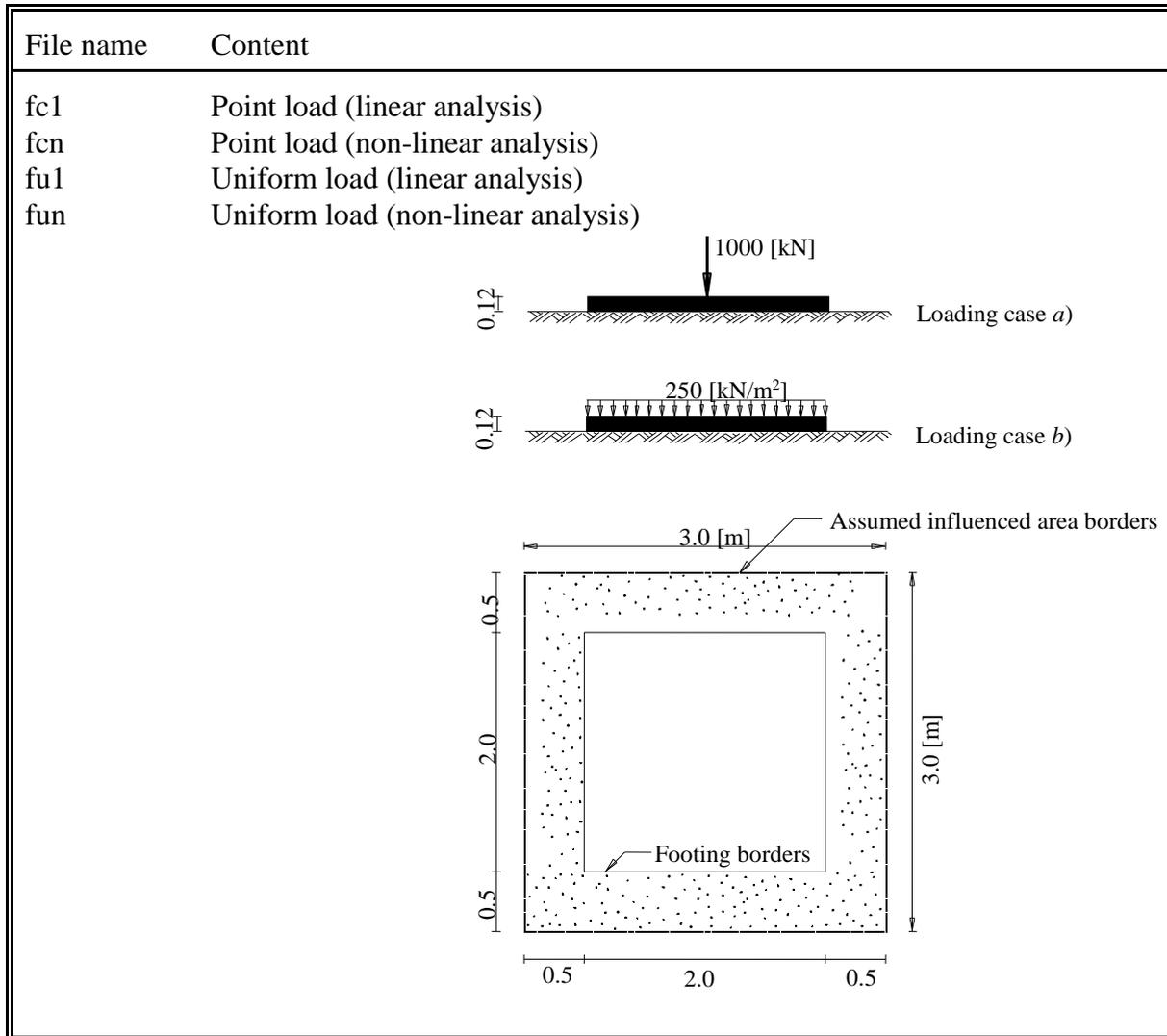
Example 7.2   Analysis of Rectangular foundation subjected to eccentric loading
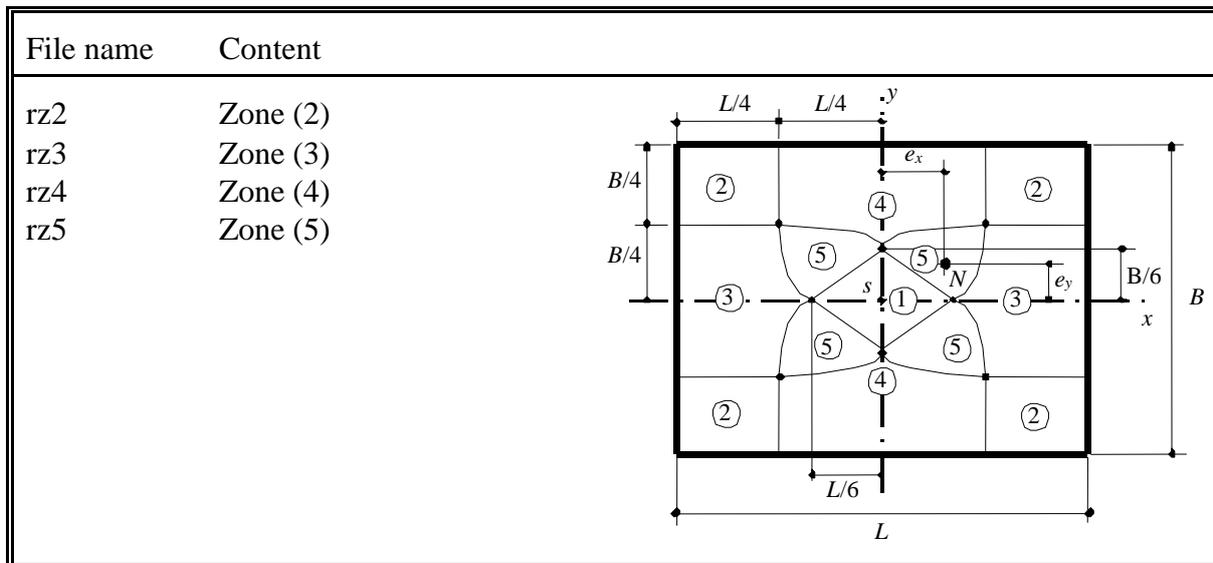
File name	Content
rz2	Zone (2)
rz3	Zone (3)
rz4	Zone (4)
rz5	Zone (5)

Example 7.3   Circular foundation subjected to eccentric loading

File name	Content
Cir-e=1.75	$e = 1.75$ [m]
Cir-e=2.00	$e = 2.00$ [m]
Cir-e=2.25	$e = 2.25$ [m]
Cir-e=2.50	$e = 2.50$ [m]
Cir-e=2.75	$e = 2.75$ [m]
Cir-e=3.00	$e = 3.00$ [m]
Cir-e=3.25	$e = 3.25$ [m]
Cir-e=3.50	$e = 3.50$ [m]
Cir-e=3.75	$e = 3.75$ [m]

Example 7.4   Elastoplastic analysis of a raft resting on Continuum medium

File name	Content
lin	Linear analysis
non	Non-linear analysis

$p = 600$ [kN/m^2]

$d = 0.5$

Section

a

$B = 16 \times 0.5 = 8$ [m]

a

$L = 32 \times 0.5 = 16$ [m]

Plan
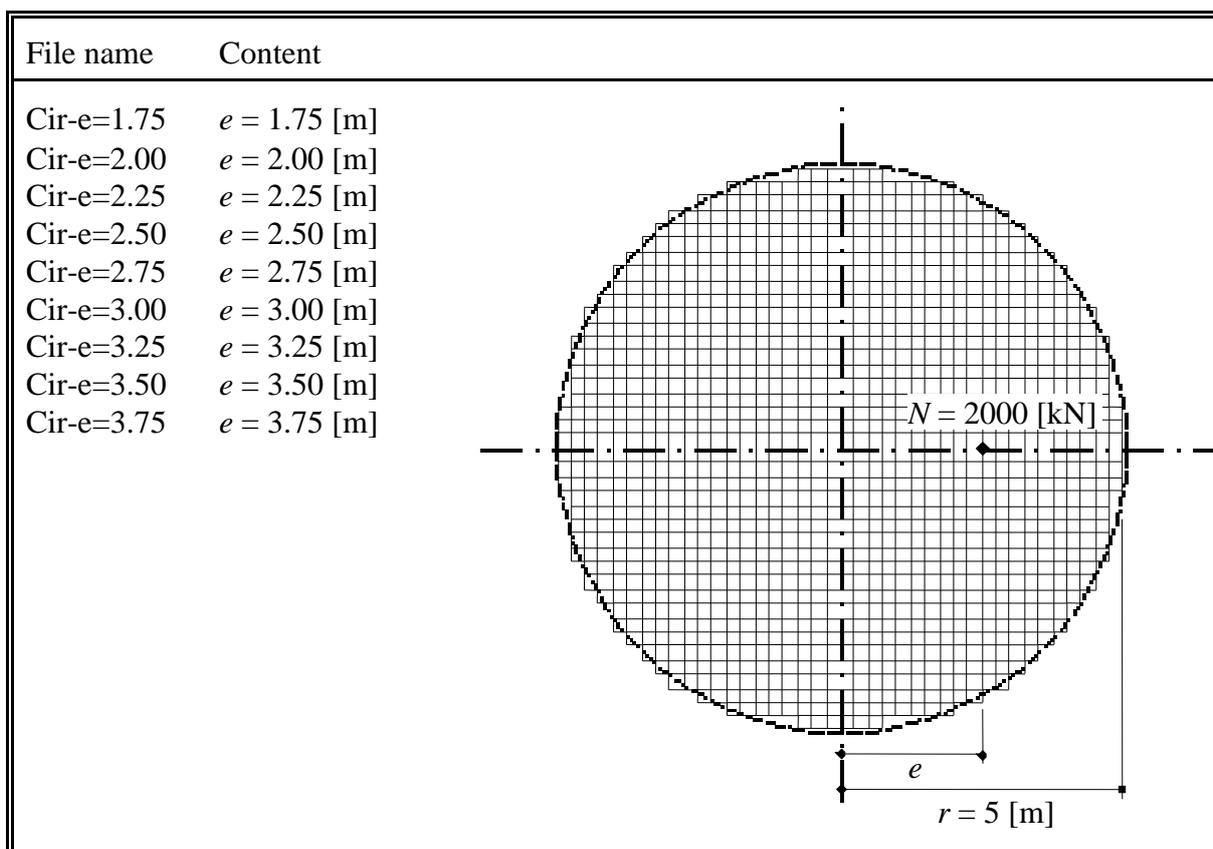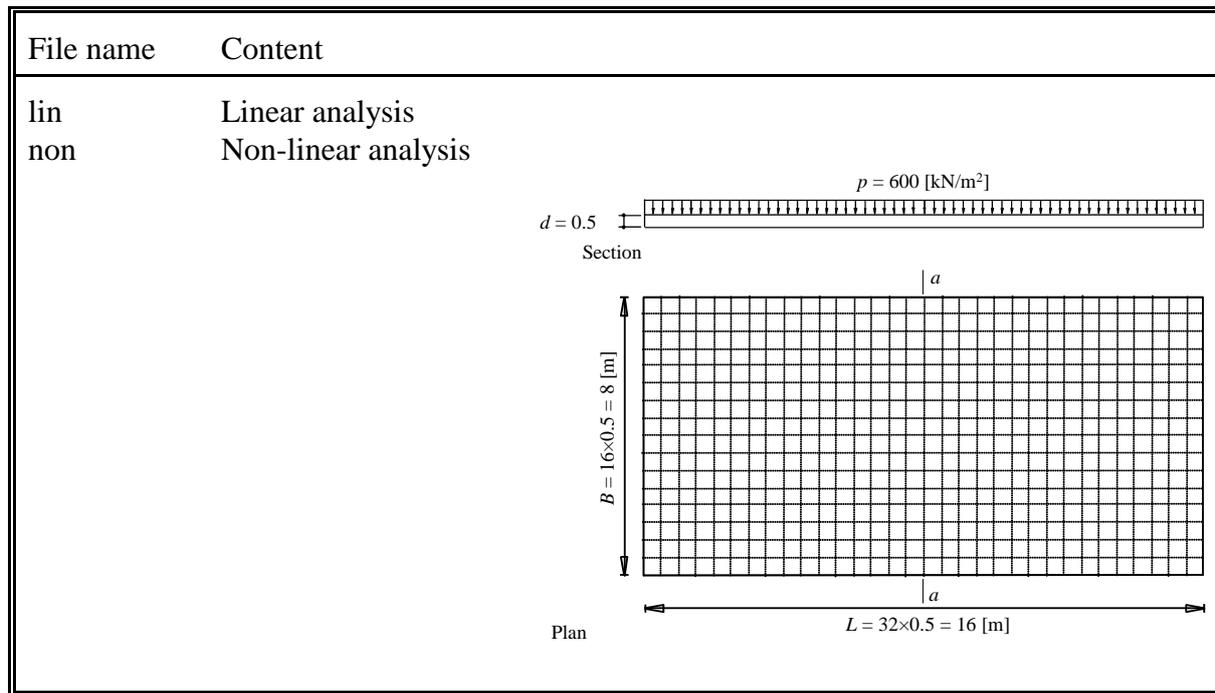
Chapter 10

References

Ahrens, *H./ Winselmann, D*. (1984): Eine iterative Berechnung von Flächengründungen nach dem Steifemodulverfahren. Finite Elemente Anwendungen in der Baupraxis
Verlag W. Ernst & Sohn, München

Amann, *P./ Breth, H*. (1972): Setzungsverhalten der Böden nach Messungen unter einem Frankfurter Hochhaus
Vorträge der Baugrundtagung Stuttgart

El Arabi, I./ El Gendy, M. (2001): On the Optimum Design of Foundation Systems
Suez Canal University, Faculty of Engineering, Port-Said
Port-Said Engineering Research Journal, November 2001

Azzouz, A./ Krizek, R./ Corotis, R. (1976): Regression Analysis of Soil Compressibility
Soil and foundations, Tokyo, vol. 16, no. 2, pp. 19-29

Bakhoum, A. (1986): An Investigation on the Analysis of Raft-Soil Interaction
M.Sc. Thesis, Cairo University, Egypt

Baz, M. (1987): Plates on Nonlinear Subgrade
M. Sc. Thesis, El Mansoura University, Faculty of Engineering, Egypt

Bazaraa, A./ Ghabrial, N./ Henedy, E. (1997): Effect of Boundary Retaining Walls on Raft Behaviour
The Third International Geotechnical Engineering Conference, Cairo University, Egypt

Bazaraa, A./ Shaheen, H./ Sabry, A./ Krem, A. (1991): Analysis of Tie-Beams Connecting Isolated Footing Resting on Soil
Proceeding of Fourth Arab Structural Engineering Conference, Cairo University, Egypt

El Behairy, S. (1992): Reinforced concrete design book
Ain Shams University, Cairo, Egypt

Beton-Kalender (1957)
Verlag W. Ernst & Sohn, Berlin/ München/ Düsseldorf

Biedermann, B. (1981): Der Einfluss plastischer Verformungen auf die Sohldruckverteilung
FBG, Dissertation, Heft 7, Technische Hochschule Aachen

Bobe, R./ Hertwig, G./ Seiffert H. (1981): Computing Foundation Slabs with Building Rigidity
Proc. Xth Intern. Conf. on Soil Mech. and Found. Engineering, Stockholm, 5/ 8, pp. 53-56

Borowicka, H. (1939): Druckverteilung unter elastischen Platten
Ingenieur-Archiv, Band 10, S. 113-125

Boussinesq, J. (1885): Applications des Potentiels a l'Etude de l'Equilibre et du Mouvement des Solides Elastiques
Gauthier-Villars, Paris

Bowles, J. E. (1974): Analytical and Computer Methods in Foundation Engineering
McGraw-Hill, New York

Bowles, J. (1977): Foundation analysis and design
McGraw-Hill, New York

Brown, P./ Yu, K. (1986): Load sequence and structure foundation interaction
J. Struct. Div. ASCE 112, 481-488

Cheung, M. (1978): A Simplified Finite Element Solution for the Plate on Elastic Foundation
Computers and Structures, Vol. 8, pp. 139-145, Pergamon

Cheung, Y./ Zienkiewicz, O. (1965): Plates and Tanks on Elastic Foundations - an Application
of Finite Element Method
International Journal of Solids Structures Vol. 1, pp. 451-461, Pergamon

Cheung, Y./ Nag, D. (1968): Plates and Beams on Elastic Foundation - Linear and Non-Linear
Behaviour
Géotechnique Vol. 18, pp. 250-260, London

Dememeghi, A. (1981): Analysis of Soil-Structure Interaction
Proc. Xth Intern. Conf. on Soil Mech. and Found. Engineering, Stockholm, 5/ 8, pp. 95-98

Deninger, A. (1964): Ein Verfahren zur Berechnung biegsamer und durch Wandscheiben
ausgesteifter rechteckiger Gründungsplatten
Dissertation, Karlsruhe

Dimitrov, N. (1977): Festigkeitslehre
Beton-Kalender, Teil I, S. 425-532
Verlag W. Ernst & Sohn, Berlin/ München/ Düsseldorf

DIN 4017 Teil 1 (1979): Baugrund. Grundbruchberechnungen von lotrecht mittig belasteten
Flachgründungen. Ausgabe August 1979
Beuth-Verlag GmbH, Berlin

DIN 4018 (1974): Baugrund. Berechnung der Sohldruckverteilung unter Flächengründungen
(mit Beiblatt 1: Erläuterungen und Berechnungsbeispiele)
Beuth-Verlag GmbH, Berlin

DIN 4019, Blatt 1 (1974): Baugrund. Setzungsberechnungen bei lotrechter, mittiger Belastung
Neufassung DIN V 4019-100 (1996). Mit Beiblatt
Beuth-Verlag GmbH, Berlin

DIN 18314 (1976): Baugrund. Untersuchung von Böden, Plattendruckversuch
Beuth-Verlag, Berlin/ Köln

EAU (1990): Empfehlungen des Arbeitsausschusses Ufereinfassungen, Seite 10
Berlin/ München/ Düsseldorf

ECP 464 (1989): The Egyptian Code of Practice, Design and Construction of Reinforced Concrete Structures (in Arabic)

ECP 196 (1995): Egyptian Code for Soil Mechanics, Design and Construction of Foundations Part 3, Shallow Foundations (in Arabic)

Ellner, A./ Kany, M. (1976): Berücksichtigung der aussteifenden Wirkung von Kellermauern und Decken bei der Berechnung von Sohlplatten mit der FE-Methode
Forschungsbericht Ka 282/6 an die DFG, Nürnberg

Empfehlungen EVB (1993): Verformungen des Baugrunds bei baulichen Anlagen - Erarbeitet durch den Arbeitskreis "Berechnnungsverfahren" der Deutschen Gesellschaft für Erd- und Grundbau e.V.
Verlag W. Ernst & Sohn, Berlin

EWB (2001): Empfehlung Wechselwirkung Baugrund/ Bauwerk
DIN-Arbeitsausschuss Berechnnungsverfahren
Verlag W. Ernst & Sohn, Berlin

El Gendy, *M.* (1994): Comparing examinations of the influence of calculation methods of basement slabs
Ph. D. Thesis, Suez Canal University, Egypt

El Gendy, M. (1998): An iteration method for design of slab on elastic foundation
Proceeding of the first International Conference on Civil Engineering, Helewan University, Cairo, Egypt

El Gendy, M. (1998): An Analysis for Determination of Foundation Rigidity
8th International Colloquium on Structural and Geotechnical Engineering
Ain Shams University, Egypt

El Gendy, M. (1999): Effect of Girders on the Raft Rigidity
1st International Conference for Advanced Trends in Engineering
Minia University, Egypt

Gorbunov-Posadov, M. (1959): Tables for Analysis of Thin Plates Resting on Elastic Foundations
Gosstroiizdat, Moscow (in Russian)

Graßhoff, H. (1955): Setzungsberechnungen starrer Fundamente mit Hilfe des kennzeichnenden Punktes
Der Bauingenieur, S. 53-54

Graßhoff, H. (1978): Einflußlinien für Flächengründungen
Verlag W. Ernst & Sohn, Berlin

Graßhoff, H. (1987): Systemsteifigkeit und Flächengründung
Ber. Nr. 6, Lehrgebiet Grundbau, Bodenmechanik und Unterird. Bauen, Berg. Universität GH Wuppertal

Graßhoff, H./ Kany, M. (1997): Berechnung von Flächengründungen
Grundbautaschenbuch Band 3, 5. Auflage
Verlag W. Ernst & Sohn, Berlin/ München

Gudehus, G. (1981): Bodenmechanik
Verlag Ferdinand Enke, Stuttgart

Haddadin, M. (1971): Mats and Combined Footings - Analysis by the Finite Element Method
Journal of the American Concrete Institute, Proceed. Vol. 68., pp. 945-949

Hahn, J. (1971): Durchlaufträger, Rahmen, Platten und Balken auf elastischer Bettung
11. Auflage; Werner-Verlag, Düsseldorf

Hain, S./ Lee, I. (1974): Rational Analysis of Raft Foundation
Journal of the Geotechnical Engineering Division, GT, pp. 843-860

Hasnien, M. (1993): Finite Element Analysis of Mat Resting on Nonlinear Elastic Medium
M. Sc. Thesis, Ain Shams University, Faculty of Engineering, Egypt

Haung, Y. (1974): Analysis of Symmetrically Loaded Slab on Elastic Solid
Transportation Engineering Journal of ASCE, Vol. 100 No. TE2, pp. 537-541

Haung, Y. (1974): Finite Element Analysis of Slabs on Elastic Solids
Transportation Engineering Journal of ASCE, Vol. 100 No. TE2, pp. 403-416

Hemsley, J. (1998): Elastic analysis of raft foundations
Tomas Telford, London

Hülsdünker, A. (1964): Maximale Bodenpressung unter rechteckigen Fundamenten bei Belastung mit Momenten in beiden Achsrichtungen
Bautechnik 41, H. 8, S. 269, Verlag W. Ernst & Sohn, Berlin

Irles, R./ Irles, F. (1994): Explicit Stresses under Rectangular Footings
Journal of Geotechnical Engineering, Vol. 120, No. 2, February 1994, pp. 444-450

Jarquio, R./ Jarquio, V. (1983): Design Footing Area with Biaxial Bending
Journal of Geotechnical Engineering, Vol. 109, No. 10, October 1983, pp. 1337-1341

Jessberger, H./ Yuan, H./ Thaher, M./ Ming-Bao, C. (1992): Superstructure- Foundation-Subsoil Interaction Analysis
Cooperation Research Project, Ruhr-University Bochum, Germany and Tongji University Shanghai, China

El Kadi, F. (1968): Die Statische Berechnung von Gründungsbalken und Gründungsplatten
Mitt. Inst. Verkehrswasserbau, Grundbau und Bodenmechanik der TH Aachen, VGB 42

Kany, M. (1954): Beitrag zur Berechnung von Gründungskörpern auf nachgiebiger Unterlage
Dissertation, Darmstadt
Kany, M. (1959): Berechnung von Flächengründungen, 1. Auflage
Verlag W. Ernst u. Sohn, Berlin

Kany, M. (1963): Sohldrücke und Setzungen der starren Platte
Europ. Baugrundtagung Wiesbaden, S. 401-409. Sonderdruck mit Ergänzungen in Heft 5 der
Veröffentl. des Grundbauinstitutes der LGA Bayern, Nürnberg

Kany, *M*. (1972): Berechnung von Systemen starrer Fundamentplatten mit beliebigem Grundriß
auf ungleich geschichtetem Baugrund
Grundbauinstitut der LGA Bayern, Nürnberg

Kany, M. (1973): Elektronische Berechnung von Fundamentgruppen mit wirtschaftlich optimaler
Bemessung
Veröffentl. des Grundbauinstitutes der LGA Bayern, Heft 24, Nürnberg

Kany, *M*. (1973): Einflüsse von Unregelmäßigkeiten im Baugrund und in der Bauwerksteifigkeit
auf die Biegebeanspruchung von Flächengründungen
Grundbauinstitut der LGA Bayern, Nürnberg

Kany, M. (1974): Berechnung von Flächengründungen, 2. Auflage
Verlag W. Ernst & Sohn, Berlin

Kany, M. (1976): Setzungsberechnung mit Verwendung Druckabhängiger Steifemoduln
Veröffentlichungen des Grundbauinstitutes der Landesgewerbeanstalt Bayern, Heft 24, Einzel-
beiträge, Nürnberg

Kany, M. (1976): Berechnung von Systemen elastischer Fundamentplatten auf beliebig
geschichtetem Baugrund
Benutzerhandbuch für das Programm *ELPLA*
Programmbibliothek des Grundbauinstitutes der LGA Bayern, Nürnberg

Kany, *M*. (1976): Berechnung der Sohldrücke und Setzungen von Systemen starrer Sohlplatten
nach dem Steifemodulverfahren von *Kany*
Benutzerhandbuch für das Programm *STAPLA*
Programmbibliothek des Grundbauinstitutes der LGA Bayern, Nürnberg

Kany, *M*. (1977): Method of analysis for structures on settling ground
Proc. IXth Intern. Conf. on Soil Mech. and Found. Engineering, Tokyo

Kany, M. (1980): Berechnung von Gründungsbalken auf beliebig geschichtetem Baugrund
Benutzerhandbuch für das Programm *ELBAL*
Programmbibliothek des Grundbauinstitutes der LGA Bayern, Nürnberg

Kany, *M.*/ *El Gendy, M.* (1995): Computing of beam and slab foundations on three dimensional layered model
Proc. VIth Intern. Conf. on Computing in Civil and Building Engineering, Berlin

Kany, M./ El Gendy, M. (1996): Benutzerhandbuch für das Programm *ELBAL*
Programmserie GEOTEC, Zirndorf

Kany, *M.*/ *El Gendy*, M. (1997): Analysis of System of Footing Resting on Irregular Soil
Proc. XIVth Intern. Conf. on Soil Mech. and Found. Engineering, Hamburg, Vol. 2, 995-998

Kany, *M.*/ *El Gendy*, *M.* (1999): Berechnung von großen Systemen starrer Sohlplatten
Bauingenieur, Band. 74, Nr. 11, Seite 471-478

Kany, M./ El Gendy, M. (2000): Einfluss der Bauwerkssteifigkeit auf das Fundamentsystem
2. Kolloquium Bauen in Boden und Fels, Technische Akademie Esslingen, Ostfildern, Germany

Kany, M./ El Gendy, M. (2007): Benutzerhandbuch für das Programm *ELPLA* 9
Zirndorf, Germany

Kézdi, A. (1964): Bodenmechanik (2 Bände)
VEB-Verlag für Bauwesen, Berlin

Kirschbaum, P. (1970): Nochmals: Ausmittig belastete T-förmige Fundamente
Bautechnik 47, H. 6, S. 214, Verlag W. Ernst & Sohn, Berlin

Landgraf, *K.*/ Quade, *J.* (1993): Bauwerk-Baugrund Wechselwirkung an biegsamen
Gründungsplatten und Platten bis zum Versagen
Zeitschrift Bauingenieur, S. 303

Lee, I./ Harrison H. (1970): Structure and foundation interaction theory
J. Struct. Div. ASCE 96, 177-197

Lee, I./ Brown P. (1972): Structure-Foundation Interaction Analysis
Journal of the Structural Division, Proc. of the American Society of Civil Engineers, St 11, pp. 2413-2431

Lopes, F./ Gusmão, A. (1991): On the Influence of Soil-Structure Interaction in the Distribution of Foundation Loads and Settlements
Proc. Xth Europ. Conf. on Soil Mech. and Found. Engineering, Florance, pp. 475-478

Matl, F. (1954): Zur Berechnung der Setzungen und Schiefstellungen des exzentrisch belasteten starren Plattenstreifens
Österr. Bauzeitschr., S. 65-70

Meyerhof, G. (1953): Some Recent Foundation Research and its Application to Design
The Structure Engineer, volume 13, pp. 151-167

Meyer, H. (1977): Beitrag zur Berechnung von Gründungsplatten mit Hilfe der Finte-Element-Methode
Bericht-Nr. F 77/2 der Forsch.- und Seminarberichte aus dem Bereich der Mech.
Techn. Univ. Hannover

Mikhaiel, S. (1978): Soil Structure Interaction in Multi-Story Buildings
Ph.D. Thesis, Cairo University, Egypt

Miklos, E. (1964): Ausmittig gedrückte symmetrische Trapez- und T-Querschnitte bei Ausschluß von Zugspannungen
Bautechnik 41, H. 10, S. 343, Verlag W. Ernst & Sohn, Berlin

Mohr, O. (1913): Abhandlungen aus dem Gebiet der Technischen Mechanik, II. Auflage, S. 66
Verlag W. Ernst & Sohn, Berlin

Ohde, J. (1942): Die Berechnung der Sohldruckverteilung unter Gründungskörpern
Der Bauingenieur, Heft 14/16, S. 99-107 - Heft 17/18 S. 122-127

Opladen, K. (1958): Spannungsnachweise bei schiefer Biegung mit und ohne Längskraft in beliebigen Querschnitten
Beton- und Stahlbetonbau 53, H. 11, S. 288

Panayotounakos, D./ Spyropoulos, C./ Prassianakis, J. (1987): Interaction of multi-story and multi-column rigid-jointed frames supported on an elastic foundation under static loading
Computer & Structure, Vol. 26, No. 5, pp. 855-869

Peck, R./ Hanson, W./ Thornburn, T. (1974): Foundation Engineering, 2nd Edition
John Wiley and Sons, New York

Pohl, K. (1918): Zahlentafeln zur Bestimmung der Nullinie und der größten Eckpressung im Rechteckquerschnitt bei Lastangriff außerhalb des Kerns und Ausschluss von Zugspannungen
Eisenbau 9, Nr. 10, S. 211
Auch: Beton-Kalender 1964, Bd. I, S. 194. Verlag W. Ernst & Sohn, Berlin/ München

Poulos, H. (1975): Settlement Analysis of Structural Foundation Systems
Proc. 4th South-East Asian Regional Conf. on Soil Eng., Kuala Lumpur, Malaysia, pp. 4.52-4.62

Poulos, H./ Davis, E. (1974): Elastic solution for soil and rock mechanics
Wiley, New York/ London/ Sydney/ Toronto

Schultze, E. (1953): Die Berechnung von Gründungsplatten
Arbeiten des AK "Berechnungsverfahren" DGEG-Baugrundtagung Hannover

Schwarz, H. (1984): Methode der finiten Elemente
Teubner-Verlag, Stuttgart

Selvadurai, A. (1979): Elastic Analysis of Soil-Foundation Interaction
Elsevier Scientific Publishing Company, Amsterdam/ Oxford/ New York

Selvadurai, A. (1983): Fundamental results concerning the settlement of a rigid foundation on an elastic medium due to an adjacent surface load
International Journal for Numerical and Analytical Methods in Geomechanics
John Wiley & Sons, Ltd

Sherif G./ König G. (1975): Platten und Balken auf nachgiebigem Baugrund
Springer Verlag, Berlin

Simmer, K. (1987): Grundbau 1, 18. Auflage
Verlag Teubner, Stuttgart

Smoltczyk, U./ Netzel, D./ Kany, M. (2001): Flachgründungen
Grundbautaschenbuch Teil 3, 6. Auflage
Verlag W. Ernst & Sohn, Berlin

Sommer, H. (1972): Bauwerkssteifigkeitsbeitrag aus dem Vergleich gemessener und berechneter Setzungen eines Hochhauses
Intern. Symposium Dresden. Schriftenreihe der Bauforsch., Reihe Ing.- und Tiefbau 47

Sowjetische Norm I - TU 6-48
(deutschsprachige Quelle: *Kézdi, A.* (1964): Handbuch der Bodenmechanik, Band 2, S. 141)

Stark, R. (1990): Beitrag zur numerischen Behandlung des Kontaktproblems beliebig orthogonal berandeter Fundamentplatten unter Einbeziehung von Grenzzuständen im Boden
Dissertation, Universität Innsbruck

Stark, R./ Majer, J. (1988): Soil-structure interaction - A possibility for elastic-plastic calculation of foundation slabs
Numerical Methods in Geomechanics, volume 2, pp. 1135-1141, Innsbruck

Steinbrenner, W. (1934): Tafeln zur Setzungsberechnung
Straße, S. 121-124

Szechy, D. (1965): Der Grundbau (3 Teile)
Springer-Verlag, Wien - New York

Teng, W. (1962): Foundation Design
Prentice-Hall, Inc. Englewood Cliffs, N. J., U.S.A

Terzaghi, K./ Peck, R. (1967): Soil Mechanics in Engineering Practice, 2nd Edition
Wiley, New York

Türke, H. (1990): Statik im Erdbau, 2. Auflage
Verlag W. Ernst & Sohn, Berlin

Winkler, E. (1867): Die Lehre von der Elasticitaet und Festigkeit
Dominicus, Prag

Wölfer, K. (1978): Elastisch gebettete Balken und Platten. Zylinderschalen
Bauverlag, Wiesbaden, Berlin

Zienkiewicz, O./ Cheung, Y. (1970): The Finite Element Method in Structural and Continuum Mechanics
McGraw-Hill, England

Zilch, K. (1993): Verfahren für die Berechnung der Interaktion von Baugrund und Bauwerk
Der Prüfingenieur, Heft 3